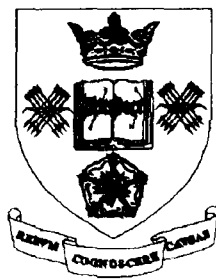


Properties of High Volume Fly Ash Concrete

Hsien-Hsin Hung

Thesis Submitted to the University of Sheffield
for the Degree of Doctor of Philosophy
in the Faculty of Engineering



Department of Mechanical Engineering

May 1997

“PROPERTIES OF HIGH VOLUME FLY ASH CONCRETE”

SUMMARY

This thesis presents a detailed investigation on the engineering properties and microstructural characteristics of concrete containing a high volume of fly ash (HVFA). The purpose of the project is to evaluate the concept of using relatively large volumes of fly ash in normal portland cement concrete, and hence enhance the beneficial use of fly ash in value-added products and construction.

A total of eight concrete mixtures with and without fly ash was investigated. The proportion of fly ash in all the HVFA concrete mixtures varied from 50 to 80 % by weight of the cementitious materials, with a constant water-to-cementitious ratio of 0.40 for all the mixtures. A high degree of workability was maintained by the use of a superplasticizer. To optimize the pozzolanic activity in the HVFA concrete, silica fume was used in some of the mixes. The total cementitious materials content was kept constant at 350 kg/m³ and 450 kg/m³ respectively. The influence of the different replacement materials and two curing regimes was studied.

The study consisted of two parts. The first part is an extensive study of the engineering properties such as strength development, modulus of elasticity, ultrasonic pulse velocity, swelling, and drying shrinkage at various ages up to 18 months. The depth of carbonation of HVFA concrete under different curing regimes was also investigated. A study of the microstructure of HVFA concretes forms the second part of the investigation. Pore structure, air permeability and water absorption of HVFA concretes with different replacement mixtures were studied. A detailed discussion dealing with the change of the morphological phase under different curing regimes is also presented.

The results show that HVFA concretes exhibit excellent mechanical properties with good long-term strength development. Compressive strength in the range of 40 to 60 MPa was achieved for all the HVFA concretes at the age of 90 days. The dynamic modulus of elasticity reached values of the order of 55 GPa at 90 days. Under similar conditions, concretes made with both fly ash and silica fume had engineering properties which were as good as those made with cement replaced by fly ash alone. The use of fly ash to replace both cement and sand has the advantage of mobilizing and combining the benefits and effects of

both separate replacements. The HVFA concretes also have low permeability and exhibit good potential characteristics to resist water penetration.

Reduction in the volume of large pores was observed with the progress of the pozzolanic reaction. Higher HVFA concrete strength was generally associated with a lower volume of large pores in the concrete. A decrease in the levels of calcium hydroxide was seen with progressive water curing and age in all the HVFA concretes, providing evidence of continued pozzolanic reactivity of the fly ashes.

Various empirical relationships and design equations are presented and conclusions are drawn at the end of each part. It is recommended that further research is required to determine the influence on HVFA concretes of extreme curing conditions such as high or low temperature and low moisture availability, and to improve the early strength properties of the HVFA concretes.

ACKNOWLEDGEMENTS

The author would like to express heartfelt gratitude to **Professor R. N. Swamy**, who gave kindly guidance and advice at all stages of the study, offered many helpful suggestions, and comments during this investigation. Many thanks are offered to **Him and Mrs. Swamy** for their thoughtful and frequent concern about the life of the author's family during the course of this study.

Thanks are also extended to **Professor J. H. Sharp**, Head of Department of Engineering materials, for permitting the use of Micromeritics Pore Size Analyser and X-ray Diffraction facilities.

The author also wishes to acknowledge the assistance of the technical staff, in particular **Mr. N. Morton, Mr. A. Smart**, of the Department of Mechanical Engineering ; and also from the Department of Civil and Structural Engineering, and the Department of Engineering Materials.

The author is indebted to his wife, **Chao-Chih**, for her most encouragement, and patient understanding throughout the research period, and the continuous concern and constant support from his **sisters and brothers**.

Table of Contents

SUMMARY	i
ACKNOWLEDGEMENTS	iii
TABLES OF CONTENTS	iv
LIST OF TABLES	ix
LIST OF FIGURES.....	xiii
NOTATIONS AND ABBREVIATIONS	xviii
CHAPTER ONE : INTRODUCTION.....	1
1-1. INTRODUCTION	1
1-2. BACKGROUND TO THE PROJECT.....	2
1-3. AIMS AND OBJECTIVES OF THE INVESTIGATION.....	2
1-4. THESIS LAYOUT.....	4
CHAPTER TWO : LITERATURE REVIEW	7
2-1. INTRODUCTION	7
2-2. THE CHEMICAL COMPOSITION AND PHYSICAL CHARACTERISTICS OF FLY ASH.....	9
2-3. CLASSIFICATION OF FLY ASH.....	11
2-4. HYDRATION AND POZZOLANIC REACTION	12
2-4-1. <i>Hydration of pure cement compounds</i>	12
2-4-2. <i>Mechanism of hydration between fly ash and portland cement</i>	16
2-5. CHARACTERISTICS OF FLY ASH ON FRESH CONCRETE	19
2-5-1. <i>Bleeding behaviour and setting time</i>	19
2-5-2. <i>Workability and fineness</i>	19
2-5-3. <i>Heat of hydration</i>	20
2-6. INFLUENCE OF FLY ASH ON HARDENED CONCRETE.....	21
2-6-1. <i>Compressive strength</i>	21
2-6-2. <i>Drying shrinkage</i>	23
2-6-3. <i>Creep</i>	23
2-6-4. <i>Modulus of elasticity</i>	24
2-7. INFLUENCE OF FLY ASH ON DURABILITY OF CONCRETE	24
2-7-1. <i>Permeability</i>	24

2-7-2. Sulphate resistance of concrete	26
2-7-3. Expansion due to alkali-aggregate reaction.....	27
2-7-4. Carbonation.....	28
2-7-5. Chloride penetration.....	28
2-8. INFLUENCE OF SILICA FUME IN CONCRETE	30
2-9. HIGH STRENGTH / HIGH PERFORMANCE CONCRETE AND HIGH VOLUME FLY ASH CONCRETE	31
CHAPTER THREE : EXPERIMENTAL PROGRAMME	38
3-1. INTRODUCTION	38
3-2. TEST PROGRAMME AND DETAILS OF CONCRETE MIXTURES	38
3-3. CHARACTERISTICS OF MATERIALS.....	40
3-4. CONCRETE MIXTURE DESIGN	43
3-5. MANUFACTURE OF TEST SPECIMENS AND CURING	44
3-6. DOSAGE OF SUPERPLASTICIZER (HRWR) AND SLUMP	45
3-7. TEST DETAILS	46
3-7-1. Flexural and compressive strength test.....	46
3-7-2. Dynamic modulus of elasticity	47
3-7-3. Ultrasonic pulse velocity.....	47
3-7-4. Swelling and drying shrinkage	49
3-7-5. Carbonation.....	49
CHAPTER FOUR : TEST RESULTS AND DISCUSSION OF PART I.....	51
4-1. INTRODUCTION	51
4-2. STRENGTH DEVELOPMENT	51
4-2-1. Effect of curing condition on compressive strength.....	52
4-2-2. Effect of curing condition on flexural strength.....	62
4-2-3. Relationship between flexural strength and compressive strength.....	68
4-2-4. Comparison with normal OPC concrete	71
4-2-5. Comparison with total binder content	74
4-3. COMPARISON OF STRENGTH DEVELOPMENT WITH PUBLISHED DATA.....	77
4-4. SWELLING OF HIGH VOLUME FLY ASH CONCRETE	77
4-5. DRYING SHRINKAGE OF HIGH VOLUME FLY ASH CONCRETE	83

4-5-1. <i>Effect of different mixes of drying shrinkage</i>	83
4-5-2. <i>Prediction of drying shrinkage on HVFA concrete</i>	91
4-5-3. <i>Comparison of drying shrinkage with published data</i>	93
4-6. DYNAMIC MODULUS OF ELASTICITY OF HVFA CONCRETE.....	95
4-6-1. <i>Effect of curing condition and different mixes on dynamic modulus of elasticity</i>	96
4-6-2. <i>Comparison with normal OPC concrete</i>	101
4-6-3. <i>Relationship between the dynamic modulus and compressive strength</i>	103
4-6-4. <i>Comparison of modulus elasticity prediction</i>	106
4-7. ULTRASONIC PULSE VELOCITY OF HVFA CONCRETE.....	108
4-7-1. <i>Effect of curing condition and different mixes on HVFA concrete</i>	109
4-7-2. <i>Comparison with normal OPC concrete</i>	115
4-7-3. <i>Relationship between the pulse velocity and the dynamic modulus elasticity</i>	116
4-8. CARBONATION OF HVFA CONCRETE.....	119
4-8-1. <i>Effect of curing condition and different replacement methods</i>	120
4-8-2. <i>Carbonation rate coefficient</i>	126
4-8-3. <i>Relationship between the carbonation depth and compressive strength</i>	128
4-8-4. <i>Comparison with published data</i>	130
4-9. CONCLUSIONS.....	131
CHAPTER FIVE : MICROSTRUCTURE OF HYDRATED CEMENT PASTES.....	134
5-1. INTRODUCTION.....	134
5-2. CLASSIFICATION OF PORE SIZE IN HYDRATED CEMENT PASTES.....	134
5-3. INFLUENCE OF POROSITY ON STRENGTH.....	137
5-4. INFLUENCE OF POROSITY ON DRYING SHRINKAGE.....	140
5-5. INFLUENCE OF POROSITY ON PERMEABILITY.....	140
5-6. INFLUENCE OF POROSITY ON ABSORPTION.....	142
5-7. MICROSTRUCTURE OF HARDENED CEMENT PASTE.....	143
5-7-1. <i>Calcium silicate hydrate gel (C-S-H gel)</i>	144

5-7-2. Calcium hydroxide (CH)	146
5-7-3. Calcium sulfoaluminate hydrates	147
5-7-4. Carbonates	148
CHAPTER SIX : EXPERIMENTAL PROGRAMME OF PART II.....	149
6-1. INTRODUCTION	149
6-2. CONCRETE MIXTURES AND CHARACTERISTICS OF MATERIAL.....	150
6-3. TEST PARAMETERS, PREPARATION OF TEST SPECIMENS	150
6-4. TEST DETAILS AND PROCEDURE	150
6-4-1. Mercury intrusion porosimetry study.....	150
6-4-2. Air permeability.....	157
6-4-3. Water absorption	158
6-4-4. X-ray diffraction.....	159
CHAPTER SEVEN : TEST RESULTS AND DISCUSSION OF PART II	162
7-1. INTRODUCTION	162
7-2. PORE SIZE DISTRIBUTION OF NORMAL OPC AND HVFA CONCRETE	163
7-2-1. Effect of different mixes and curing conditions on pore size distribution.....	163
7-2-2. Maximum continuous pore diameter of pore structure.....	171
7-2-3. Comparison with the total binder content on pore size distribution	179
7-2-4. Total, macro-pore and meso-pore volumes.....	186
7-2-5. Some relations between the pore structure and compressive strength	188
7-3. PERMEABILITY OF HVFA CONCRETE.....	192
7-3-1. Effect of curing condition on air permeability.....	192
7-3-2. Permeability and strength development of high volume fly ash concrete.....	198
7-3-3. Permeability-porosity relation in high volume fly ash concrete	200
7-4. WATER ABSORPTION OF HVFA CONCRETE	201
7-4-1. Effect of curing condition and different replacement methods.....	202
7-4-2. Absorption-permeability relation of HVFA concrete	206
7-5. SOLID PHASE ANALYSIS : X-RAY POWDER DIFFRACTION.....	208
7-5-1. X-ray diffraction of normal OPC and HVFA concretes with water	

<i>curing</i>	208
7-5-2. <i>Influence of air curing on X-ray diffraction</i>	217
7-6. CONCLUSION.....	220
CHAPTER EIGHT : CONCLUSIONS AND RECOMMENDATIONS FOR FUTURE RESEARCH	222
8-1. OVERALL CONCLUSIONS.....	222
8-2. RECOMMENDATIONS FOR FUTURE WORK.....	225
REFERENCES	227

List of Tables

Table 2-1 Chemical composition (%) of fly ash in various countries	10
Table 2-2. Relative proportions of hydration products in the solid portion of cement paste (assuming pure components).....	16
Table 2-3 Basic technical requirements of surface coatings.....	30
Table 2-4. Typical high compressive strength of fly ash concrete (Unit : MPa)	32
Table 2-5 Mix proportions and engineering properties of some HVFA concretes	36
Table 3-1 High volume fly ash concrete test parameters.....	39
Table 3-2 High volume fly ash concrete mixtures (Unit : kg/m ³).....	39
Table 3-3 Chemical composition of cements and mineral admixtures (Unit : %)	41
Table 3-4 Sieve analysis of fine aggregate and coarse aggregate.....	42
Table 3-5 Chemical compositions of fine aggregate and coarse aggregate	42
Table 3-6 High volume fly ash concrete mix proportions (Unit : kg/m ³)	43
Table 3-7 High volume fly ash concrete workability	45
Table 3-8 High volume fly ash concrete test details.....	48
Table 4-1 Compressive strength of HVFA concrete under water curing (Unit : MPa).....	55
Table 4-2 Rate of gain of compressive strength as a % of 28 days strength (Water curing) (Unit : %).....	56
Table 4-3 Compressive strength of HVFA concrete under air curing (Unit : MPa).....	58
Table 4-4 Rate of gain of compressive strength as a % of 28 days strength (Air curing) (Unit : %).....	59
Table 4-5 Influence of air curing on compressive strength-350 kg/m ³ binder content (Unit : %)	60
Table 4-6 Influence of air curing on compressive strength-450 kg/m ³ binder content (Unit : %)	60
Table 4-7 Flexural strength of HVFA concrete under water curing (Unit : MPa).....	63
Table 4-8 Rate of gain of flexural strength as a % of 28 day strength (Water curing) (Unit : %).....	64
Table 4-9 Flexural strength of HVFA concrete under air curing (Unit : MPa).....	65
Table 4-10 Rate of gain of flexural strength as a % of 28 days strength	

(Air curing) (Unit : %).....	66
Table 4-11 Influence of air curing on flexural strength-350 kg/m ³ binder content (Unit : %).....	67
Table 4-12 Influence of air curing on flexural strength-450 kg/m ³ binder content (Unit : %).....	67
Table 4-13 Strength development of normal OPC concrete.....	72
Table 4-14 Swelling strain of HVFA concrete (Water curing) (Unit : 10 ⁻⁶ m/m)	79
Table 4-15 Drying shrinkage strain of HVFA concrete (air curing) (Unit : 10 ⁻⁶ m/m)	84
Table 4-16 Typical % of mesopore of high volume fly ash concrete under air curing (Unit : %).....	88
Table 4-17 Comparison between measured and predicted drying shrinkage (Unit : 10 ⁻⁶ m/m)	93
Table 4-18 Comparison of drying shrinkage with published data	94
Table 4-19 Dynamic modulus of elasticity of HVFA concrete (Water curing) (Unit : GPa)	96
Table 4-20 Dynamic modulus of elasticity of HVFA concrete (Air curing) (Unit : GPa)	96
Table 4-21 Influence of air curing on dynamic modulus of elasticity (Unit : %) ...	100
Table 4-22 Dynamic modulus of elasticity of normal OPC concrete.....	101
Table 4-23 Rate of gain of modulus as a % of 28 day modulus (Water curing) (Unit : %).....	102
Table 4-24 Rate of gain of modulus as a % of 28 day modulus (Air curing) (Unit : %).....	102
Table 4-25 Comparison of predicting modulus of elasticity and published data under water curing (28 days).....	107
Table 4-26 Comparison of predicting modulus elasticity and published data under water curing (504 days).....	107
Table 4-27 Ultrasonic pulse velocity of HVFA concrete (Water curing) (Unit : km/sec)	110
Table 4-28 Ultrasonic pulse velocity of HVFA concrete (Air curing) (Unit : km/sec)	111
Table 4-29 Influence of air curing on pulse velocity (Unit : %).....	112

Table 4-30 Ultrasonic pulse velocity of normal OPC concrete.....	115
Table 4-31 Rate of gain of velocity as a % of 28 day pulse velocity (Water curing) (Unit : %).....	116
Table 4-32 Rate of gain of velocity as a % of 28 day pulse velocity (Air curing) (Unit : %).....	116
Table 4-33 Carbonation depth - 350 kg/m ³ mixes (Unit : mm).....	120
Table 4-34 Carbonation depth - 450 kg/m ³ mixes (Unit : mm).....	122
Table 4-35 Estimated parameters of equation $C = a + K\sqrt{t}$ (t = sec).....	126
Table 4-36 Comparison of carbonation depths with published data.....	130
Table 5-1 Classification of pore sizes in hydrated cement pastes.....	137
Table 6-1 A typical output of Micromeritics pore size analyses	154
Table 7-1 Total accessible pore volume of OPC and HVFA concrete (Water curing) (Unit : mL/g).....	168
Table 7-2 Total accessible pore volume of OPC and HVFA concrete (Air curing) (Unit : mL/g).....	168
Table 7-3 The porosity of OPC and HVFA concrete (Water curing) (Unit : %).....	169
Table 7-4 The porosity of OPC and HVFA concrete (Air curing) (Unit : %).....	169
Table 7-5 The max. dv/d (log d) and threshold diameter of OPC and HVFA concrete (Water curing).....	174
Table 7-6 The max. dv/d (log d) and threshold diameter of OPC and HVFA concrete (Air curing)	174
Table 7-7 The macropore and mesopore of OPC and HVFA concrete (Water curing) (Unit : %).....	187
Table 7-8 The macropore and mesopore of OPC and HVFA concrete (Air curing) (Unit : %).....	187
Table 7-9 High volume fly ash concrete permeability coefficient (Unit : 10 ⁻¹⁶ m ²).....	193
Table 7-10 Influence of air curing on permeability (Unit : %).....	196
Table 7-11 High volume fly ash concrete water absorption (Unit : %).....	203
Table 7-12 Influence of air curing on water absorption (Unit : %).....	205
Table 7-13 X-ray diffraction of OPC and HVFA concrete (Water curing) (28 days of hydration)	211
Table 7-14 X-ray diffraction of OPC and HVFA concrete (Water curing) (90days of hydration)	212

✓

Table 7-15 X-ray diffraction of HVFA concrete (Water curing) (18 months of hydration)	213
Table 7-16 X-ray diffraction of HVFA concrete (Air curing) (18 months of hydration)	218

List of Figures

Figure 4-1 Compressive strength of HVFA concrete-Water curing.....	55
Figure 4-2 Rate of compressive strength as % of 28 days strength-Water curing	56
Figure 4-3 Compressive strength of HVFA concrete-Air curing	58
Figure 4-4 Rate of compressive strength as % of 28 days strength-Air curing.....	59
Figure 4-5 Flexural strength of HVFA concrete-Water curing.....	63
Figure 4-6 Rate of flexural strength as % of 28 days strength-Water curing.....	64
Figure 4-7 Flexural strength of HVFA concrete-Air curing	65
Figure 4-8 Rate of flexural strength as % of 28 days strength-Air curing.....	66
Figure 4-9 Relationship between flexural strength and compressive strength of HVFA concrete-Water curing.....	69
Figure 4-10 Relationship between flexural strength and compressive strength of HVFA concrete-Air curing.....	69
Figure 4-11 Relationship between flexural strength and compressive strength of HVFA concrete.....	70
Figure 4-12 Effect of total binder content on compressive strength (Water Curing).....	75
Figure 4-13 Effect of total binder content on compressive strength (Air curing).....	75
Figure 4-14 Effect of total binder content on flexural strength (Water curing).....	76
Figure 4-15 Effect of total binder content on flexural strength (Air Curing).....	76
Figure 4-16 Variation of swelling of HVFA concrete-350 kg/m ³ mixes	80
Figure 4-17 Variation of swelling of HVFA concrete-450 kg/m ³ mixes	80
Figure 4-18 Effect of total binder content on swelling-350F/450F	81
Figure 4-19 Effect of total binder content on swelling-350SF/450SF.....	82
Figure 4-20 Effect of total binder content on swelling-350S/450S	82
Figure 4-21 Variation of drying shrinkage of HVFA concrete-350 kg/m ³ mixes	85
Figure 4-22 Variation of drying shrinkage of HVFA concrete-450 kg/m ³ mixes	85
Figure 4-23 Swelling / drying shrinkage characteristics-350 kg/m ³ mixes.....	87
Figure 4-24 Swelling / drying shrinkage characteristics-450 kg/m ³ mixes.....	87
Figure 4-25 Relationship between drying shrinkage and swelling.....	88
Figure 4-26 Effect of total binder content on drying shrinkage-350F/450F	89
Figure 4-27 Effect of total binder content on drying shrinkage-350SF/450SF.....	90
Figure 4-28 Effect of total binder content on drying shrinkage-350S/450S	90

Figure 4-29 The curve for determining the constants a and b (350 kg/m ³ mixes)....	92
Figure 4-30 The curve for determining the constants a and b (450 kg/m ³ mixes)....	92
Figure 4-31 Variation of dynamic modulus of HVFA concrete (Water curing)	98
Figure 4-32 Variation of dynamic modulus of HVFA concrete (Air curing).....	98
Figure 4-33 Effect of total binder content on dynamic modulus (Water curing)	99
Figure 4-34 Effect of total binder content on dynamic modulus (Air curing).....	99
Figure 4-35 Relationship between dynamic modulus of elasticity and compressive strength (Water curing).....	105
Figure 4-36 Relationship between dynamic modulus of elasticity and compressive strength (Air curing).....	105
Figure 4-37 Comparison of predicting modulus of elasticity and published data.....	108
Figure 4-38 Variation of pulse velocity of HVFA concrete under water curing.....	110
Figure 4-39 Variation of pulse velocity of HVFA concrete under air curing	112
Figure 4-40 Effect of total binder content on pulse velocity (Water curing).....	114
Figure 4-41 Effect of total binder content on pulse velocity (Air curing)	114
Figure 4-42 Relationship between pulse velocity and dynamic modulus of elasticity (Water curing)	117
Figure 4-43 Relationship between pulse velocity and dynamic modulus of elasticity (Air curing).....	118
Figure 4-44 Carbonation depth of concrete - 350 kg/m ³ mixes	121
Figure 4-45 Carbonation depth of concrete - 450 kg/m ³ mixes	123
Figure 4-46 Effect of total binder content on carbonation depth.....	123
Figure 4-47 Carbonation of specimens stored in the laboratory - 180 days	124
Figure 4-48 Carbonation of specimens stored in the laboratory - 540 days	124
Figure 4-49 Exposure period versus carbonation depth of concrete - 350 kg/m ³ mixes.....	127
Figure 4-50 Exposure period versus carbonation depth of concrete - 450 kg/m ³ mixes.....	127
Figure 4-51 Relationship between carbonation depth and compressive strength.....	129
Figure 5-1 Comparison of pore classifications.....	136
Figure 5-2 Relation between the compressive strength of mortar and gel / space ratio	139
Figure 5-3 Relation between compressive strength of mortar and of calculated from the volume of pores larger than 20 nm in diameter	139
Figure 5-4 The composition of the calcium silicate hydrates.....	145

Figure 6-1 Photograph of the Micromeritics Poresizer (Model 9320).....	152
Figure 6-2 A general view of “The Leeds Permeability Cells”.....	157
Figure 6-3 Correction factor related to the length of the specimen.....	159
Figure 7-1 Cumulative pore volume curves for the 350 kg/m ³ binder content OPC and HVFA concrete (Water curing).....	164
Figure 7-2 Cumulative pore volume curves for the 350 kg/m ³ binder content OPC and HVFA concrete (Air curing).....	165
Figure 7-3 Cumulative pore volume curves for the 450 kg/m ³ binder content OPC and HVFA concrete (Water curing).....	166
Figure 7-4 Cumulative pore volume curves for the 450 kg/m ³ binder content OPC and HVFA concrete (Air curing).....	167
Figure 7-5 Differential pore volume curves for the 350 kg/m ³ binder content OPC and HVFA concrete (Water curing).....	175
Figure 7-6 Differential pore volume curves for the 350 kg/m ³ binder content OPC and HVFA concrete (Air curing).....	176
Figure 7-7 Differential pore volume curves for the 450 kg/m ³ binder content OPC and HVFA concrete (Water curing).....	177
Figure 7-8 Differential pore volume curves for the 450 kg/m ³ binder content OPC and HVFA concrete (Air curing).....	178
Figure 7-9 Cumulative and differential pore volume of 350C/450C, 350F/450F (Water curing 28 day).....	180
Figure 7-10 Cumulative and differential pore volume of 350SF/450SF, 350S/450S (Water curing 28 day).....	180
Figure 7-11 Cumulative and differential pore volume 350C/450C, 350F/450F (Water curing 90 day).....	181
Figure 7-12 Cumulative and differential pore volume of 350SF/450SF, 350S/450S (Water curing 90 day).....	181
Figure 7-13 Cumulative and differential pore volume of 350F/450F (Water curing 540 day).....	182
Figure 7-14 Cumulative and differential pore volume of 350SF/450SF, 350S/450S (Water curing 540 day).....	182
Figure 7-15 Cumulative and differential pore volume of 350C/450C, 350F/450F (Air curing 28 day).....	183
Figure 7-16 Cumulative and differential pore volume of 350SF/450SF, 350S/450S (Air curing 28 day).....	183
Figure 7-17 Cumulative and differential pore volume of 350C/450C, 350F/450F	

(Air curing 90 day).....	184
Figure 7-18 Cumulative and differential pore volume of 350SF/450SF, 350S/450S (Air curing 90 day).....	184
Figure 7-19 Cumulative and differential pore volume of 350F/450F (Air curing 540 day).....	185
Figure 7-20 Cumulative and differential pore volume of 350SF/450SF, 350S/450S (Air curing 540 day).....	185
Figure 7-21 Relationship between compressive strength and porosity of OPC and HVFA concrete-Water curing	189
Figure 7-22 Relationship between compressive strength and porosity of OPC and HVFA concrete-Air curing.....	189
Figure 7-23 Relationship between compressive strength and porosity of OPC and HVFA concrete.....	191
Figure 7-24 Relationship between compressive strength and meso-pore of HVFA concrete.....	191
Figure 7-25 The permeability coefficient of HVFA concrete-water curing (350 kg/m ³ mixes).....	194
Figure 7-26 The permeability coefficient of HVFA concrete-water curing (450 kg/m ³ mixes).....	194
Figure 7-27 Relationship between permeability and compressive strength of HVFA concrete-water curing	199
Figure 7-28 Relationship between permeability and compressive strength of HVFA concrete-air curing.....	199
Figure 7-29 Relationship between permeability and meso-pore of HVFA concrete	201
Figure 7-30 The water absorption of HVFA concrete-water curing (350 kg/m ³ mixes).....	204
Figure 7-31 The water absorption of HVFA concrete-water curing (450 kg/m ³ mixes).....	204
Figure 7-32 Relationship between permeability and water absorption of HVFA concrete.....	207
Figure 7-33 X-ray diffractograms for OPC and HVFA concrete-Water curing (28 days hydration).....	214
Figure 7-34 X-ray diffractograms for OPC and HVFA concrete-Water curing (90 days hydration).....	215
Figure 7-35 X-ray diffractograms for HVFA concrete-Water curing	

(18 months hydration).....	216
Figure 7-36 X-ray diffractograms for HVFA concrete-Air curing	
(18 months hydration).....	219
Figure 8-1 Strategies of using fly ash in HVFA concrete construction.....	223

NOTATIONS AND ABBREVIATIONS

A. Cement Chemistry Shorthand Notations and Terminology

C = CaO	C \bar{C} = Calcite
S = SiO ₂	C ₄ AH ₁₃ = Tetracalcium Aluminate-13-hydrate
A = Al ₂ O ₃	C ₃ A = Tricalcium Aluminate
F = Fe ₂ O ₃	C ₄ AF = Tetracalcium Aluminoferrite
C-S-H = C-S-H gel	C \bar{S} = Anhydrite
\bar{S} = SO ₃	Alite = Impure form of C ₃ S
\bar{C} = CO ₂	Belite = Impure form of C ₂ S
H = H ₂ O	C ₄ A \bar{S} H ₁₂ = Monosulfoaluminate
CH = Calcium Hydroxide	C ₆ A \bar{S} ₃ H ₃₂ = Ettringite
C \bar{S} H ₂ = Gypsum	AFt = Al ₂ O ₃ -Fe ₂ O ₃ -trisulfate
C ₂ ASH ₈ = Gehlenite Hydrate	AFm = Al ₂ O ₃ -Fe ₂ O ₃ -monosulfate

B. Abbreviations

IL = Ignition Loss	MIP = Mercury Intrusion Porosimetry
OM = Optical Microscopy	SEM = Scanning Electron Microscopy
RT = Room Temperature (~ 25 °C)	OPC = Ordinary Portland Cement
T °C = Temperature in Celsius Scale	HVFA = High Volume Fly Ash Concrete
W / C = Water / Cement Ratio	XRD = X - Ray Diffraction
W / B = Water / Binder Ratio	MPa = Megapascal
ACI = American Concrete Institute	BSI = British Standards Institution
EPRI = Electric Power Research Institute	RILEM = International Union for Materials Testing Laboratories

C. Pore Classification by IUPAC

Unit (Diameter)	Å	nm
Macropores = Large Capillaries	> 500	>50
Mesopores = Small Capillaries	25 ~ 500	2.5 ~ 50
Micropores = Pores ; Intrinsic part of C-S-H	< 25	< 2.5

CHAPTER ONE

INTRODUCTION

1-1. INTRODUCTION

Pozzolanic materials, such as fly ash (FA), and cementitious materials such as ground granulated blast furnace slag (GGBFS), are by-products of industry. Pozzolanic materials have properties similar to those of cement, but are unable to undergo hydration alone ; thus, they are used as partial replacement of cement, or blended with portland cement [1,2,3,4]. In a study on synthetic fly ashes, it has been shown that the final products of fly ash - portland cement reaction are the same as those of portland cement alone i.e., C-S-H, C_4AH_{13} , C_8AFH_{26} and $C_4\bar{A}SH_{12}$ [5].

There are two major factors which influence the properties of fly ash concrete - its intrinsic variation in chemical and mineralogical composition, and the philosophy of mix proportioning adopted to produce the concrete incorporating fly ash [6]. In most of the studies reported so far, the amount of cement replacement by fly ash is of the order of 20 % to 30 %. Fly ash is the most abundant of all siliceous materials available throughout the world. Only a very small proportion of this available fly ash is used in concrete construction. The aim of this project is to explore the possibilities of extending the level of cement replacement to much higher amounts so that a much higher proportion of the available fly ash can be utilised in construction. The investigation aims to establish the engineering and microstructure properties of this high volume fly ash (HVFA) concrete, compared to that of conventional portland cement systems. It is hoped that this increased usage of fly ash would help to reduce disposal problems, and would also contribute, in a minor way, to a cleaner environment.

1-2. BACKGROUND TO THE PROJECT

During the 1950's, construction of both hydroelectric and thermal power stations was stepped up due to the sudden rise in demand for electricity. The production of fly ash as an industrial by-product from these power generating stations also gave rise to studies connected with the use of fly ash as a cement replacement material. The utilisation of fly ash in European countries began at about the 1960's, particularly in the USSR and Great Britain.

The advantages of incorporating a good quality fly ash in concrete include the improvement of the workability of the concrete, improvement of strength, water tightness and durability at later ages, reduction in the heat of hydration, and reduction of drying shrinkage. Probably, the foremost advantage of fly ash lies in the economy resulting from reduction of cement content and the production of better quality concrete. As shown in published literature, these advantages of fly ash compensate for much of the defects of portland cement, and the use of good quality fly ash as an essential ingredient of structural concrete is now widely accepted. From the point of view of using relatively large volumes of fly ash in portland cement concrete, this concept has many beneficial implications in terms of usage of waste materials, reduction of environmental pollution, and the conservation of material resources.

1-3. AIMS AND OBJECTIVES OF THE INVESTIGATION

As mentioned before, much of the earlier research on fly ash concrete concentrated on the development of concretes with about 20 ~ 30 % cement replacement. More recently, in the last couple of decades, a limited amount of research has been carried out on concretes incorporating higher amounts of fly ash, from 50 % to 60 % by mass of portland cement [7]. However, there is the need for much more information on such HVFA concrete to establish their properties reliably, and to give confidence to suppliers and users. In the present study, the proportion of fly ash in the total

cementitious materials varied from 50 to 80 %, while water and portland cement content were both kept at low levels.

The investigation is divided into two parts. Part I of the research deals with the basic characteristics of concrete containing high volume fly ash. The concrete was designed using different cementitious contents and replacement methods. In order to investigate changes in engineering properties, the concretes were cured under two different conditions, namely, prolonged water curing and prolonged air drying after an initial 7 day water curing. Silica fume was also incorporated in some of the mixes, and fly ash was used to replace both cement and fine aggregate. A superplasticizer was also incorporated to enhance workability, and to keep the water content low. In addition to the strength development of high volume fly ash concrete, several other concrete properties were also investigated. To complement the studies of engineering properties, Part II of the project concentrates on the hydration reaction and microstructure development of high volume fly ash concrete. Changes in pore structure and mineralogical composition were also investigated along with permeability, water absorption and the hydrate products in the pozzolanic reaction.

The main aim and objective of this project is to investigate the engineering properties, microstructural characteristics and the hydrate products of concrete containing high volume fly ash. The individual aims and objectives of each part are given below :

Part I : Engineering properties of high volume fly ash concrete

The aims and objectives of this part include :

1. To develop mix proportioning methods for the production of high performance fly ash concrete with a high level of replacement of portland cement with fly ash under different curing conditions. This is intended to include both cement and sand replacement by fly ash.
2. To study the short and long term strength development under different curing conditions and mixture parameters of high volume fly ash concrete.

3. To examine the engineering properties of concrete incorporating high volumes of fly ash by measuring changes in dynamic modulus of elasticity and ultrasonic pulse velocity.
4. To evaluate the effectiveness of moist and dry curing regimes on expansion and drying shrinkage behaviour of HVFA concrete.
5. To assess the effect of pozzolanic activity on the carbonation characteristics of concrete containing large quantities of fly ash.
6. To investigate the relationship between various engineering properties of concrete incorporating high volume fly ash.

Part II : Microstructure mechanism and hydration reaction of high volume fly ash concrete.

The aims and objectives Part II of the investigation are :

1. To study the relationship between microstructure and engineering properties of the resulting of high volume fly ash concrete.
2. To study the pore size distribution and porosity in relation to the engineering properties of high volume fly ash concrete.
3. To seek out the changes in calcium silicate hydrate (C-S-H gel), with curing ages in the hydration reaction of hardened HVFA concrete.
4. To investigate the mineralogical composition of calcium hydroxide, Ca(OH)_2 , crystals and the evidence of unhydrated concrete minerals such as gypsum, C_4AH_{13} and ettringite in concrete incorporating high volume fly ash.

1-4. Thesis layout

The thesis is divided into eight chapters which include both parts of the study. A brief outline of the thesis layout is given below.

The first chapter presents a general introduction to the background and advantages of fly ash incorporation in concrete, then describes the aims and the objectives of each part of the present study.

The second chapter contains a literature review on properties of concrete containing fly ash. The review begins with a brief outline of the basics of cement chemistry and hydrate reaction of the cement paste. This is followed by a detailed review of the influence of fly ash on engineering properties. A detailed review of high performance, high volume fly ash concrete characteristics is also presented.

In the third chapter, the experimental programme deals with the details of test parameters, concrete mixture design, specimen preparation and the experimental procedure. The characteristics and properties of the raw materials used in the experimental part of the research such as cement, fly ash, aggregate, superplasticizer and silica fume are also reported.

In chapter four, the experimental results of tests from Part I relating to the laboratory investigation of the engineering properties of high volume fly ash concrete are discussed. Long and short term strength development along with the dynamic modulus of elasticity and ultrasonic pulse velocity of different types of concrete are investigated. Other high volume fly ash concrete engineering properties such as swelling, and drying shrinkage are also presented. The effects of carbon dioxide from the atmosphere on the depth of carbonation in high volume fly ash concrete is also discussed in this section. The relationship between strength and other properties and cementitious content for different replacement methods is also presented.

Part II of the project is covered in chapters five, six, and seven. In chapter five, the review deals with a brief analysis of the pore structure of hydrated cement paste. This is followed by a detailed review of the influence of porosity and pore size distribution on the engineering properties. A detailed review of the hydrate products of hardened cement paste is also presented.

Chapter six deals with the test details, the preparation of test specimens and the tests conducted on the hydration and microstructure of high volume fly ash

concrete. The principal tests used included mercury intrusion porosimetry, air permeability, water absorption test and X-ray diffraction.

Chapter seven describes the results from the tests of Part II. This section looks into the microstructure mechanism in order to confirm the results from the engineering properties described in Chapter four of the thesis. This also contains a detailed discussion describing the changes in the mineralogical phase of different cementitious contents during the early and later periods of hydration of high volume fly ash concrete. It also presents a discussion on the mechanisms of pore size distribution.

Chapter eight summarizes the overall conclusions obtained from the two experimental projects along with some recommendations for future work towards the commercialisation of high volume fly ash concrete systems.

CHAPTER TWO

LITERATURE REVIEW

2-1. INTRODUCTION

There is a great deal of published literature on the properties of concrete containing fly ash. It is impossible to produce here a detailed critical review of all these publications. The aim here is to describe briefly those aspects of fly ash concrete which are important and relevant to this study.

The use of fly ash as a pozzolanic material in combination with portland cement for making fly ash concrete has been developed for nearly half a century. The term " fly ash " first appeared in literature in 1937 in a paper by Davis et al ; this paper presents results of extensive tests to determine the feasibility of using various types of portland cement with fly ash [8]. In 1948, the use of fly ash in Hungry Horse Dam gave an impetus, and exceptional progress has been made since in the techniques of collecting and producing fly ash all over the world. During the 1950's, the demand for electric power showed sudden growth, and along with this, there was great activity in constructing both hydroelectric and thermal power stations so that studies connected with fly ash were advanced. The standards on fly ash cement were gradually established (The United States ASTM Standard in 1954, Japan JIS Standard in 1958, France NF Standard in 1959).

The utilisation of fly ash in European countries came at about the 1960's. In the USSR and Great Britain, standards on fly ash were approved in 1963 and 1965 respectively. The first Australian Standard for fly ash in concrete was published in 1971. This was in the form of specified requirements of fly ash, and guidance for the use of fly ash in concrete. The Canada Centre for Mineral and Energy Technology (CANMET) began work in 1985 to develop structural concrete incorporating high

volumes of low calcium fly ash. In these investigations, an ASTM Class F fly ash was used in proportions of 50 to 60 percent of total cementitious material [7]. Low unit water content and a high degree of workability were obtained using high range water reducing admixtures. Full details of the study of high volume fly ash concrete were presented by EPRI (Electric Power Research Institute) in 1993 [9].

Fly Ash is a by-product of the combustion of pulverized coal in thermal power stations. It is removed by mechanical collectors or electrostatic precipitators as a fine particulate residue from the combustion gases before they are discharged to the atmosphere. Fly ash, besides being used as an admixture for cement and concrete, is also used in considerable quantities as an additive in cellular concrete, artificial lightweight aggregate, refractory materials, bricks, and in soil improvement. It is also used in asphalt as well as in abrasives, purifiers for polluted water and fertiliser. It is difficult to say how much fly ash is being used as an admixture for cement and concrete in various countries of the world, but it is estimated that some 800 m tonnes of fly ash are currently produced world-wide. In the UK alone some 15 to 20 m tonnes of fly ash are produced annually [10]. The annual consumption in recent years is around 1.5 m tonnes in the USA, and about 1 m tonne each in Japan, France and Germany.

The advantages of good quality fly ash are the improvement of workability of concrete, improvement of strength, water tightness and durability of concrete at advanced ages, alleviation of heat of hardening of concrete and reduction of drying shrinkage, although probably, the foremost advantage of fly ash lies in the economy resulting from the reduction of cement. When considering the fact that thermal power stations have to incur great expense in disposing of the material as waste, the advantages of utilising fly ash are even more marked.

2-2. THE CHEMICAL COMPOSITION AND PHYSICAL CHARACTERISTICS OF FLY ASH

Chemical composition of fly ash

The chemical composition of fly ash is determined by the coal used. More than 85 percent of most fly ashes comprise compounds and glasses formed from SiO_2 , Al_2O_3 , Fe_2O_3 , CaO and MgO . Kokubu [11] had tested the chemical composition of fly ash in various countries as shown in Table 2-1, which emphasizes the many differences in fly ash composition according to the country of production. The average values of the important oxides are 40 ~ 58 % for SiO_2 , 21 ~ 27 % for Al_2O_3 , 4 ~ 17 % for Fe_2O_3 and 4 ~ 6 % for CaO . These variations are largely due to the differences in the quality of coal used in the various countries.

Physical characteristics

In general, fly ash consists of glassy spheres of sizes varying from under 1 μm to as large as 150 μm , although typical particle size distribution shows that most of the material is under 20 μm [12]. The range of particle sizes in any given fly ash is largely determined by the dust collection equipment used. Table 2-1 gives the specific surface areas of fly ash in various countries. In this case also, a wide difference is seen between countries, the value ranging from 1220 to 8100 cm^2/g .

On the basis of optical and scanning electron micrograph observations, several morphological categories of fly ash occur, and these may be summarized as follows:

1. Most of the fly ash particles occur as solid glass spheres, which are mostly transparent but may be partially devitrified.
2. Irregular masses of large size may exist either as agglomerates of small silicate glass spheres or porous particles of incompletely burnt carbonaceous matter.
3. Magnetite and hematite occur as opaque spheres in high-iron fly ashes.

4. Sometimes low-calcium fly ashes may contain a small amount of hollow particles which are either completely empty (cenospheres) or packed inside with smaller spheres (plerospheres) [12].

Table 2-1 Chemical composition (%) of fly ash in various countries [11]

Country	Number of Composite Samples	Loss on Ignition	SiO ₂	Al ₂ O ₃	Fe ₂ O ₃	CaO	MgO	SO ₃	Na ₂ O	K ₂ O	Specific Surface (cm ² / g)
Japan	12										
Av.		0.73	57.96	25.86	4.31	3.98	1.58	0.34	1.49	2.15	3090
Max.		1.23	63.27	28.35	5.90	6.74	2.09	0.81	2.36	3.15	4150
Min.		0.06	53.41	22.88	2.82	1.04	1.00	0.02	0.88	1.73	1220
USA	34										
Av.		7.83	44.11	20.81	17.49	4.75	1.12	1.19	0.73	1.97	3673
Max.		18.00	51.90	28.30	31.30	12.0	1.40	2.80	2.10	2.98	4795
Min.		1.00	32.70	14.60	8.50	11.1	0.70	0.30	0.22	1.28	2430
UK	14										
Av.		3.86	46.16	26.99	10.44	3.06	1.96	1.59	0.90	3.26	5180
Max.		11.70	50.70	34.10	13.50	7.70	2.90	6.80	1.90	4.20	8100
Min.		0.60	41.40	23.90	6.40	1.70	1.40	0.60	0.20	1.80	2500
France	17										
Av.		3.72	48.45	25.89	8.07	5.95	2.36	1.01	0.64	3.94	---
Max.		15.15	54.05	33.40	15.30	38.7	4.45	7.00	0.85	6.00	---
Min.		0.30	29.90	10.80	5.80	1.48	1.10	0.10	0.15	0.70	---
Germany	9										
Av.		9.65	41.13	24.39	13.93	5.06	1.85	0.77	---	---	---
Max.		20.10	49.54	29.35	20.88	11.8	4.26	2.10	---	---	---
Min.		1.48	34.10	21.06	8.37	2.18	0.75	0.12	---	---	---
USSR	15										
Av.		---	55.08	25.97	7.83	5.08	1.81	1.63	---	---	---
Max.		---	62.08	37.15	12.01	10.6	2.90	3.78	---	---	---
Min.		---	47.90	20.71	3.08	1.10	0.28	0.20	---	---	---

2-3. CLASSIFICATION OF FLY ASH

From the standpoint of conspicuous differences in mineralogical composition and properties, fly ash can be divided into two categories, which differ from each other mainly in their calcium content. The first category, containing usually less than 5 percent analytical CaO is, generally, a product of combustion of anthracite and bituminous coals. The second category, containing usually 15 to 35 percent analytical CaO generally happens to be the product of combustion of lignite and sub-bituminous coals. The ASTM Standard Specification for Mineral Admixtures (C 618) does not differentiate fly ashes on the basis of calcium content, although this objective is achieved indirectly by requiring a minimum of 75 percent of the major non-calcium oxides (silica + alumina + iron oxide) for Class F fly ash, and 50 percent for Class C fly ash, since the latter is higher in calcium.

The low-calcium fly ashes, due to the high proportions of silica and alumina, consist principally of aluminosilicate glass. In the furnace very large spheres of molten glass may not get cooled rapidly and uniformly, thus crystallisation of aluminosilicates such as silica-alumina ($\text{Al}_2\text{O}_3 \cdot \text{SiO}_2$) and mullite ($3\text{Al}_2\text{O}_3 \cdot 2\text{SiO}_2$) as slender needles, takes place in the interior of the glassy sphere. This partial devitrification of glass in low-lime fly ashes, therefore, would account for the presence of crystalline aluminosilicates which are relatively non-reactive. In regard to high calcium fly ashes which may also contain significant amounts of magnesia, alkalis and sulphates, the situation is more complex than the low-calcium ashes from anthracite or bituminous coal. The chemical composition and reactivity of the non-crystalline or glassy phase is different from the glassy phase typically present in low-calcium fly ashes. Also, the principal crystalline mineral in high-calcium fly ash is generally C_3A , which is the most reactive mineral present in portland cement.

2-4. HYDRATION AND POZZOLANIC REACTION

2-4-1. Hydration of pure cement compounds

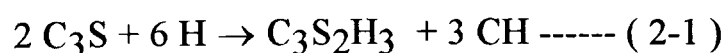
Portland cement is a hydraulic cement made by heating a mixture of limestone and clay to a temperature at which partial fusion occurs (1300°C ~ 1500°C). The clinker produced is ground usually to a fineness exceeding 1500 cm²/g and mixed with 2 ~ 4 % gypsum.

The cement consists essentially of crystalline compounds (minerals) of calcium combined with silica, alumina, iron oxide, and sulphate. Typically, the four principal crystalline phases are tri-calcium silicate (C₃S, 26 % ~ 53 %), di-calcium silicate (C₂S, 16 % ~ 54 %), tri-calcium aluminate (C₃A, 3 % ~ 15 %), and tetra-calcium alumino-ferrite (C₄AF, 8 % ~ 12 %). The relative percentages of these depend on the raw material used. In addition, many clinkers contain small amounts (less than 3 %) of free lime (CaO), periclase (MgO) and alkali sulphates. All the compounds present in portland cement clinker are anhydrous, but when brought into contact with water they are all attacked or decomposed, forming hydrate compounds. The main hydration reaction eventually develops the rigid matrix of hardened cement paste [12].

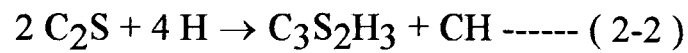
The chemistry of principal setting, hardening reaction and micromechanism may be presented as follows :

A : Reaction involving calcium silicates

The hydration reactions between tr-icalcium silicate, di-calcium silicate and water are as given below :



$$\text{Heat of Hydration } \Delta H = - 114 \text{ kJ / mol}$$



Heat of Hydration $\Delta\text{H} = - 43 \text{ kJ / mol}$

The principal hydration product is a colloidal calcium silicate hydrate gel (C-S-H gel) of colloidal dimensions. Calcium silicate hydrate occupies about 40 % to 70 % of the hardened cement paste volume. It is termed "gel" because its dimensions are in the colloid range (less than 100\AA), and it is poorly crystalline, being essentially amorphous. It possibly has a layer structure based on a degenerate structure of the calcium silicate hydrate mineral tobermorite , which has a structure analogous to that of common clay minerals , hence it has been called "tobermorite gel".

But in general the C / S ratio of C-S-H gel might be in the range between 1.0 ~ 2.0 with an average of 1.5. According to Young [13] the pore structure of a saturated paste is more open than previously thought and that the microporosity may only be created during drying.

The other product of hydration of the silicate minerals is about 20 to 25 percent calcium hydroxide (CH), which usually occurs as large hexagonal crystals, typically 0.01 ~ 1 mm. Crystals big enough to be seen with the naked eye can sometimes grow inside voids formed in concrete. Dehydration occurs rapidly at 400 ~ 500°C. Calcium hydroxide in cement paste may vary in morphology, being found as small equidimensional crystals ; large, thin, elongated crystals ; or variations of these forms. Calcium hydroxide crystals are not pure but contain significant amounts of silica as well as occluded C-S-H products, and therefore, it is better not to use values for the pure compound. Calcium hydroxide can limit the durability of cement paste because it is more soluble than C-S-H.

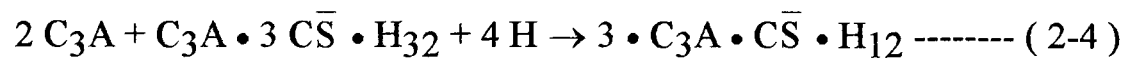
B : Reactions involving aluminate

(a) Tricalcium aluminate

The primary initial reaction of C_3A with water in the presence of a plentiful supply of gypsum is :



This calcium sulfoaluminate hydrate is commonly called "ettringite". Ettringite is a stable hydration product only while there is an ample supply of sulphate available. If the sulphate is all consumed before the C_3A has completely hydrated, then ettringite becomes unstable and converts to another calcium sulfoaluminate hydrate containing less sulphate.



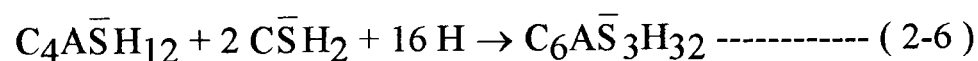
This second product is called monosulfoaluminate. The calcium sulfoaluminates are a relatively minor constituent of a cement paste, making up 10 to 20 percent by volume. Thus, they are generally ignored due to their correspondingly minor role in the microstructure of the hydrated cement paste. The morphology of ettringite can be "needle-like", "wall-like", or "amorphous" structure depending on time of curing and amount of ettringite formation. The morphology of hexagonal hydrates can be clusters of small, plate crystals instead of well formed hexagonal crystals.

The over reaction of C_3A can thus be represented by :



$$\text{Heat of Hydration } \Delta H = - 362 \text{ kJ / mol}$$

The monosulphate is a new source of sulphate ions from the solution, the ettringite can be formed once again :



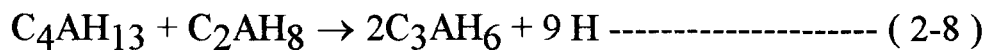
The more gypsum there is in the system, the longer the ettringite will remain stable.

In the absence of gypsum, the quantity of sulphate ions present in cement is insufficient, which can lead to flash set. As a consequence, the reaction takes place between C_3A and the water as following :



Heat of Hydration $\Delta H = - 340 \text{ kJ / mol}$

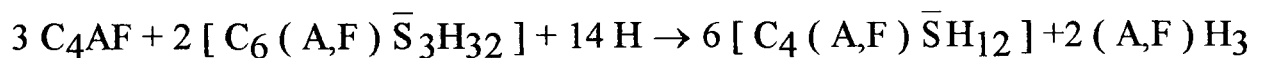
These calcium aluminate hydrates (C_2AH_8 and C_4AH_{13}), which are members of the AFm group and closely related structurally to monosulfate, are metastable phase and change gradually to another more stable cubic hydrate C_3AH_6 ; C_3AH_6 is a member of the hydrogarnet solid solution series.



(b) Tetra - calcium aluminoferrites (Ferrite phase) --- In this case, the A/F ratio is not the same as that of the parent compound.

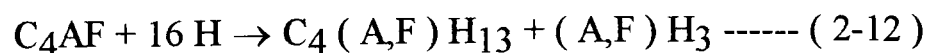
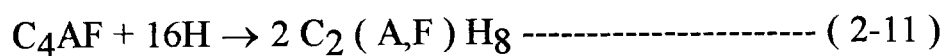
The hydration of tetra-calcium aluminoferrite is not as well comprehended but forms the same sequence of hydration products as does C_3A .

In the presence of gypsum, the reactions are slower and evolve less heat. The hydration between C_4AF and sulphate ions may be represented as :



----- (2-10)

In the absence of sulphate ions, sulphate-free AFm phase will be formed analogous to Eq 2-7. The thermodynamically stable phase is $C_4(A,F)H_6$,



The above equation such as (A,F) means that Al_2O_3 and Fe_2O_3 occur interchangeable in the compound.

The volume of the hydration products in a full hydrated and saturated paste is listed in Table 2-2.

Table 2-2. Relative proportions of hydration products in the solid portion of cement paste (assuming pure components) [13]

Compound	Hydration products	Volume in pure paste **	Volume in cement paste ***
C ₃ S	C-S-H gel	66%	32%
	CH	34%	16%
C ₂ S	C-S-H gel	87%	20%
	CH	13%	3%
C ₃ A	C ₃ AC \bar{S} H ₁₂ *	100%	19%
C ₄ AF	#	100%	8%
Minor oxides (as MgO)	Hydroxides	---	2%

Remarks :

- * Assumed stable phase in mature pastes.
- ** Expressed as percentage of solid products. A density of 2.25 g /cm³ was assumed for both CH and C-S-H gel.
- *** Assuming a typical composition Type I for portland cement.
- # Hydration of C₄AF assumed analogous to C₃A.

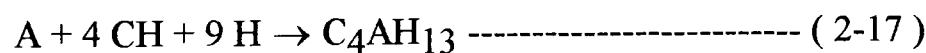
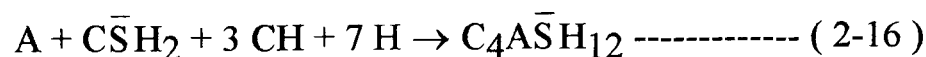
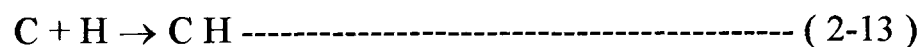
2-4-2. Mechanism of hydration between fly ash and portland cement

Fly ash is a pozzolanic material. According to ASTM C-595, a pozzolan is defined as "a siliceous or siliceous and aluminous material which in itself possesses little or no cementitious value but which will, in finely divided form and in the presence of moisture, chemically react with calcium hydroxide at ordinary temperature to form compounds possessing cementitious properties".

Pozzolans are rich in SiO₂ and poor in CaO, whereas the opposite holds for clinker and portland cement. Calcium hydroxide is produced from the excess CaO

during the hydration of cement constituents, and serves as the main source of alkalinity for the pozzolanic activity, i.e., for the conversion of the SiO_2 of the pozzolan into C-S-H. The pozzolanic reactions of various pozzolans have been examined in several investigations previously [11,14,15,16]. Guillaume [17] found a correlation between the decrease in calcium hydroxide, produced by hydration of cement, and the extent of pozzolanic reaction, which suggested that the pozzolanic reaction of fly ash starts at about 14 days. Bache et al [18] stated further that when fly ash absorbs calcium hydroxide, the absorbed calcium hydroxide appears to form a membrane over the fly ash particles and a film of water exists at the interface between the membrane and fly ash particles.

A study on synthetic fly ashes suggested that the initial reaction products appeared to be poorly-crystallized hydrates of calcium silicate or calcium aluminate. After one week of curing, a tetracalcium aluminate hydrate (C_4AH_x) was identified along with some fine needle-like crystals which were probably ettringite. After eight weeks, C-S-H was identified. The final products of fly ash reaction are the same those of portland cement. So, in very simplified terms, pozzolanic activity can be described by the following reactions [5][19] :



It is worth noticing that the reaction of fly ash in portland cement coincides with the reaction of portland cement. The main difference between the portland cement hydration reaction and the pozzolanic reaction lies in the former, where the entire quantity of each basic oxide of portland cement, i. e., of C, S, A and F, reacts in the form of the compounds, C_3S , C_2S , C_3A , and C_4AF , in which they occur in the clinker, whereas in the latter, only the amorphous forms of these pozzolanic oxides

may react with lime solution (CH). Another difference is that the pozzolanic reactions of fly ash may be initiated by the adsorption of calcium hydroxide, produced by cement hydration, on the surfaces of the fly ash particles. The adsorbed calcium hydroxide appears to form a membrane over the fly ash particles and a film of water exists at the interface between the membrane and fly ash particles [20].

It should be recognised that, because of the compositional heterogeneity of fly ashes and cements, and the heterogeneous nature of their pozzolanic reactions, reactivity is not a unique property of a fly ash. Even with a single cement, standard curing conditions and mix proportions, reactivity will probably vary with the progress of the reaction. Further, reactivity does depend on the intrinsic and extrinsic factors [6,21,22,23]. Intrinsic factors include the physical and chemical properties of the fly ash. Extrinsic factors include the properties of cement, curing conditions and environment, mix proportions, cement / fly ash ratio and water / cementitious ratio etc. In most studies, however, the relationships between the inorganic constituents of fly ash reactivity and hydrate reaction are still not well-defined, as will be apparent from this review.

2-5. CHARACTERISTICS OF FLY ASH ON FRESH CONCRETE

2-5-1. Bleeding behaviour and setting time

Hydration occurs right after the cementitious materials come into contact with water. The hydraulic cementitious reaction progresses to make the cementitious system harden and develop strength. Basically, setting behaviour is the result of cementitious grains dispersing and hydrating with water, and gradually forming a solid / liquid suspension of various size hydrates. As cement hydrates, the inner structure of the cementitious paste is further reinforced, and becomes a network structure which makes the cementitious material set and gain strength.

Bleeding is mainly due to the amount of mix water being greater than that required for complete cement hydration. The phenomenon is caused by the solid / liquid suspension being generated after the mixing of cement and water. Except for the adsorption of water due to the electrical double layer and diffusive water layer, the extra water escapes from the structural network of cementitious pastes, which explains the mechanism of bleeding. Concrete using fly ash is generally reported to show reduced segregation and bleeding, and to be more satisfactory when placed by pumping than plain concrete placed under the same circumstances.

2-5-2. Workability and fineness

The pozzolanic activity of fly ash has a close relationship with its fineness. The small size and the essentially spherical form of the particles comprising fly ash usually influence the rheological properties of cementitious pastes, causing a reduction in the amount of water required for a given degree of workability from that required for an equivalent paste without fly ash [24]. For a constant workability, the reduction in the water demand of concrete due to fly ash is usually between 5 and 15 % by

comparison with a portland cement only mix having the same cementitious material content. There are many reports confirming the workability and fineness characteristics of fly ash. As early as 1937, Davis et al made this clear in their paper [8]. Kokubu and Yamada [19] showed that unit water-content ratio was lowered with increasing fineness and that the unit water-content ratio exceeds 100 percent when specific surface area was lower than $2000 \text{ cm}^2/\text{g}$ with almost no effect on workability. Meanwhile, they cited the results from Homms et al, who collected 14 varieties of fly ash varying in fineness between $1000 \sim 4150 \text{ cm}^2/\text{g}$ from a thermal power plant and performed tests on mortar holding cement-fly ash quantities constant, replacing 25 percent of the cement with fly ash and determining unit water contents to obtain equal consistency. Cabrera and co-workers [25] have reported on measuring the effects of seven fly ash on concrete workability by using Tattersall Two Point Test. The test programme shows that fly ashes vary in their ability to improve concrete workability. There was no question that the fineness values of a fly ash affected the workability of the concrete. However, the standard value of fineness is significant in providing a criterion in planning fly ash collecting facilities. Table 2-1 also gives examples of the specific surface areas of fly ash in various countries.

2-5-3. Heat of hydration

Portland cement is in a high energy state because it is produced from clinkers in a burning process in a kiln at a high temperature. When it comes into contact with water, the clinker converts to a low energy state, and heat escapes during the hydration process. The heat of hydration of cement may be as high as 180 J / kg so that in structural concretes there might occur a temperature rise of 135°C if no heat were lost. Fortunately, in most concrete structures heat is lost to the environment almost as fast as it is generated so that no problems of thermal stresses result. In mass concrete, however, portions of the interior may remain in an essentially adiabatic state for a period of weeks after the concrete is placed [24]. The pozzolanic reaction of the aluminosilicates in fly ash with the calcium hydroxide liberated by the C_3S and

C_2S components of portland cement takes place more slowly than C_3S reaction and the approximate reaction rate of C_3S . This combined with the dilution of the portland cement component by fly ash results in a reduced rate of heat evolution, and reduced ultimate heat of hydration. Sturup et al [26] used a conduction calorimeter, and found that fly ash could be used successfully in lieu of both ASTM Type II and IV moderate and low-heat cements to control temperature rise and thermally induced cracking in mass concrete. The use of fly ash to reduce the heat of hydration of concrete is well established. The US Bureau of Reclamation (USBR) has conducted numerous experiments concerning heat of hardening of concrete containing fly ash. Malhotra et al also cited the results from Elfert who showed the effect of fly ash and a calcined diatomaceous shale on the temperature rise of mass concrete, and found that for a given total cementitious materials content, high volume fly ash concrete exhibits a substantially lower temperature rise than conventional concrete [24,27].

2-6. INFLUENCE OF FLY ASH ON HARDENED CONCRETE

2-6-1. Compressive strength

The factors affecting the development of concrete cementitious strength include its internal water content, curing condition, mix proportioning and admixtures. The particles of fly ash in a dry state often present a floc structure from the mutual attraction of the particles ; when concrete is mixed using fly ash which has a floc structure, or present as agglomerates, the particles of fly ash are flocculated and are difficult to disperse. Meanwhile, the contribution which fly ash makes to strength development of concrete is the result of pozzolanic reaction between the soluble silica and alumina from the glass phase of the fly ash, and lime, to form calcium silicate and calcium aluminate hydrates. Moreover, in addition to the effect of chemical reaction, fly ash has a physical effect of improving the microstructure of the hydrated cement paste. The main physical action is that of packing of the fly ash

particles at the interface of coarse aggregate particles. Much research has shown that proper percentage replacement of portland cement in concrete results in comparable strength between normal OPC and fly ash concrete [12,14,21,24,28]. In consideration of early strength fly ash concrete, it has been reported that concrete mixes with normal weight and lightweight aggregates containing 30 percent by weight of cement replacement of fly ash can be designed to have adequate early one-day strength for structure applications. Swamy et al [21] and Cripwell et al [29] have reported on compressive strengths when a part of normal portland cement is replaced with fly ash ; these studies show that the later-age strength development of fly ash concrete is higher than that of normal OPC concrete resulting in an 18 percent increase in compressive strength at 300 days. Thomas and Matthews [30] also have reported on investigating existing concrete structures built with fly ash concrete. The age of structures ranged from 2 to 33 years. The results indicated that in all cases the fly ash concrete has greater long term strength by comparison with the OPC concrete in the same structure. These effects of sand replacement on early age and long term fly ash concrete strength also suggests that the superior performance of these mixtures compared to normal OPC concrete mixtures is attributable to the densification of the paste structure due to pozzolanic action between the fly ash and calcium hydroxide liberated as a result of hydration of cement [31].

In recent years there has been considerable interest in the production and use of very high strength concrete (50 ~ 60 MPa) at 28 days. This type of concrete is a particular example of the combined practical use of fly ash and water-reducing admixtures [24]. An extensive scientific and engineering study (1990 ~ 1993) by EPRI (Electric Power Research Institute) has demonstrated the use of high volume fly ash (HVFA) concrete produced for structural applications. High volume fly ash concrete has adequate early age strength, and very good later age strength ; and, the ratio of the flexural to compressive strengths, and of splitting-tensile to compressive strength are comparable to the values for conventional portland cement concrete [9].

2-6-2. Drying shrinkage

The volume of a cementitious paste varies with its water content. Drying will cause a volume decrease, i. e., drying shrinkage (or shrinkage), and wetting causes volume increase, i. e., swelling. Consequently, the rate of removal of water from the cementitious paste controls the rate of shrinkage of the cementitious paste. All factors which affect drying, such as temperature, humidity, pressure and air movement, will also influence shrinkage. Also, the factors that affect the physical and chemical properties of the paste, such as cementitious composition, admixtures, curing temperature, and water / cementitious ratio, will also affect shrinkage.

2-6-3. Creep

Some studies have shown that fly ash increases the creep of concrete [28]. However, these investigations involved direct replacement of fly ash for cement, and produced lower strength at loading. Since creep is influenced by compressive strength and the modulus of elasticity of the concrete, higher creep strains were found in fly ash concrete at early age loading when strength was low, however the rate of creep decreased at later ages.

When similar 28 day strength is compared, creep of fly ash concrete is lower than its plain concrete equivalent. Investigations by Bamforth [32] on mass concrete showed that a reduction of 50 % in creep can be obtained when cement is replaced by about 30 % fly ash. Ross [33] had obtained 15 % reduction with 25 % fly ash replacement.

The high volume fly ash concrete appears to produce low creep strains compared to those of normal concretes. The low creep strains could be the result of a large portion of fly ash remaining unreacted in the concrete, and thus acting as fine aggregate, providing increased restraint against creep. The long-term creep behaviour of concrete containing high volume fly ash and superplasticizer has been described by

Cripwell et al [29]. The combined effect of high volume fly ash and superplasticizer is to decrease the creep of concrete stored in water or stored in air ; after 300 days of loading, creep was 50 % less than that in the case of portland cement concrete. Similar, long-term creep results by Alexander et al [34], showed that the creep of plain concrete specimens loaded at stress / strength ratio of 0.25 and 0.4 were found to be 50 % greater than that of fly ash concrete at 2 years, and the situation remained unchanged at 6 years.

2-6-4. Modulus of elasticity

Modulus of elasticity is very important from a design point of view in reinforced and prestressed concrete, since it can control concrete behaviour as much as compressive strength, particularly in structural elements subjected to flexure. The modulus of elasticity of concrete follows a pattern similar to compressive strength. Fly ash concrete is known to exhibit similar or slightly higher modulus of elasticity than portland cement concrete [12,24,26,35,36]. Long term, higher strength concrete can help to reduce deflections under load, and these can be anticipated when fly ash is used in concrete. A report by EPRI [9] on high volume fly ash concrete claims that, the generally high modulus of elasticity values of this concrete seems to be due to the densifying effect of the unhydrated fly ash particles acting as fine aggregate.

2-7. INFLUENCE OF FLY ASH ON DURABILITY OF CONCRETE

2-7-1. Permeability

Factors affecting permeability amongst others, include the presence of large voids in the hydrated cement, microcracks at the aggregate-cementitious paste transition

zone, water / cementitious ratio and curing efficiency. Unless curing conditions are especially poor, the impermeability of concrete containing fly ash is improved. The pozzolanic reaction of fly ash in concrete, which produces calcium silicate hydrate, tends to fill these unoccupied spaces to form a product with decreased permeability, which also results in improved corrosion resistance.

A number of investigations has been made on the influence of fly ash on relative permeability. Manmohan and Mehta [37] showed that the strength improvement as a result of pozzolanic reaction is accompanied by, and partly results from, a reduction in the volume of large pores, and found that in cements containing fly ash, the pore-size refinement and a drastic drop in permeability of the cement paste (from $11 \sim 13 \times 10^{-11}$ to 1×10^{-11} m/sec) occurred during the 28 to 90 days curing period. Kokubu [11] also cited results on concrete permeability which agrees with experimental data from Davis who compared permeability coefficients of concretes of unit cement contents of 225 kg/m^3 at the age of 6 months and stated that the coefficient of concrete with 30 % of cement replaced with fly ash was 1 / 5 of that of concrete without fly ash, while with 50 % replacement, the coefficient was reduced to 1 / 12. This is also consistent with the results of Davis, cited by Berry and Malhotra on permeability of a concrete pipe containing fly ash, which was higher than that of plain concrete at 28 days, and was substantially lower after 6 months of curing [24]. Subsequently, Malhotra [14] further added that the high performance, high volume fly ash concrete tests performed under uniaxial flow conditions under a pressure of 27 MPa indicated the permeability to be of the order of 10^{-13} m / sec. It is clear from these investigations that the permeability of the concrete is directly affected by hydration reaction, and that the low permeability of the concrete is due to the low porosity of the portland cement / fly ash system with gel pores being discontinuous.

2-7-2. Sulphate resistance of concrete

Most commonly, sulphate attack is a phenomenon in which the sulphates from the environment surrounding the concrete react with reactive calcium aluminate phases within the hardened concrete, resulting in internal expansion due to the formation of the crystalline compound ettringite, and yields a greater volume causing deterioration. The replacement of a portion of the portland cement with fly ash on the sulphate resistance of concrete can be conveniently explained in terms of two mechanisms. First, the pozzolanic reaction reduces the amount of calcium sulphate, which consequently decreases the amount of gypsum formed. The second mechanism, the concrete with fly ash in the mixture can decrease the proportion of the larger pores which results in a less porous matrix, and decreases the total amount of tricalcium aluminate (C_3A) content of the cement.

In recent years, several studies have tried to document the effect of fly ash on the sulphate resistance of concrete [35]. Mehta [38] and Carrasquillo et al [35] indicate that the effect of fly ash on the sulphate resistance of concrete is related to the composition of both the crystalline and amorphous phases. This phase dependent interaction can be used to expand on the R-value concept to reliably predict the effect of fly ash on the sulphate resistance of concrete. USBR (United States Bureau of Reclamation) guidelines include a resistance factor (R-value) defined as :

$$R = \frac{CaO\% - 5}{Fe_2O_3\%} \text{ ----- (2 - 18)}$$

and found that using cement replacement levels of 25 % fly ash with R-values less than 1.5 was found to improve the sulphate resistance of the concrete, and suggested that with the calcium oxide (CaO) content less than 5 % and low ferric oxide (Fe_2O_3) contents in the concrete, sulphate attack is reduced. Tikalsky and Carrasquillo [35,39] have given the same conclusion. In 1993, EPRI [9] reported the results of sulphate resistance by using 12 different power plant fly ashes on high volume fly ash concrete studies. From this work it was concluded that all of the fly ashes tested greatly improved sulphate resistance.

2-7-3. Expansion due to alkali-aggregate reaction

This undesirable expansion of concrete is due to reaction between the aggregate and hydroxyl and alkali ions in the pore solution forming a gelatinous alkali silicate, which is capable of absorbing large quantities of water. The consequent expansion disrupts the concrete and reduces both the strength and elasticity properties of concrete and the structural integrity of concrete structures [40,41,42]. Fly ash with siliceous constituents may react with alkalis in the cement to form products which take up water and swell, and can minimize or prevent the expansion [28]. The use of pozzolans to prevent alkali-aggregate reaction has been summarized from the results of Pepper and Mather by Plowman and Harrogate. They concluded that the effectiveness of different fly ashes in reducing long-term expansion varied widely, and suggested that the effectiveness may be dependent upon their alkali content or fineness [40].

Research at Canada Centre for Mineral and Energy Technology (CANMET) [9,43,44] has shown that the use of high volume fly ash concrete is highly effective in inhibiting the expansion due to alkali-aggregate reaction. The rationale for reduction in the expansion due to alkali-aggregate reaction is the extremely low permeability of the high-volume systems, and the reduced pH of the pore solution. Similar results by Alasali & Malhotra [45] showed that the expansion of the concrete incorporating 58 % fly ash, after 275 days of exposure under the various test conditions, is insignificant.

While it is clear that some fly ashes are effective in controlling alkali-aggregate expansion, it is questionable whether the strength losses caused by replacement of the cement by fly ash would be tolerable for more than a limited number of applications. The use of such large amounts of fly ash to reduce alkali-aggregate interaction, if required, would certainly demand reportioning of concrete if acceptable early strength were to be attained.

2-7-4. Carbonation

Carbonation is the process whereby carbon dioxide from the atmosphere penetrates the concrete, converting the hydroxides to carbonates and lowering the alkalinity of the protective concrete surrounding the steel, leading to dissolution of the protective oxide layer on the steel bars and to reinforcement corrosion [5,45]. There are a large number of factors that affect the rate and extent of carbonation, such as, the concentration of Ca(OH)_2 produced by the hydration of portland cement as well as C-S-H, which contains CaO. With concrete that contains portland cement and fly ash, there is a further increase in the number of carbonating variables when some of the cement is replaced by fly ash [46]. Browne [47] cited the results from Matthews, obtained at the Building Research Establishment, who showed that after 10 years, fly ash concrete carbonates approximately to the same extent as normal OPC concrete, with the rate of carbonation found to be related to the strength of the concrete. Langley et al [27] carried out tests on large concrete blocks containing high volumes of low-calcium fly ash and showed that, for concretes of similar 730 days strength, fly ash concrete carbonates to a lesser depth than the OPC concrete. After 7.5 years cores of high volume fly ash concrete examined showed average carbonation depth less than 8 mm [44].

Contradicting results have been reported by Papadakis et al [5] and Kawamura & Haque [48] ; they indicated higher rates of carbonation in fly ash concrete than that of the control normal OPC concrete. As both concretes had the same value of water-to-binder ratio, a pozzolanic cement concrete had significantly higher carbonation depth due to its greater porosity, and also due to the smaller concentration of carbonatable constituents.

2-7-5. Chloride penetration

The main cause of reinforcement corrosion is the loss of efficiency of the concrete cover, which protects the steel and keeps it in a passive state. Chloride ions have the

special ability to destroy the passive oxide film of steel. The chloride ions which penetrate into the concrete arise either from internal mix constituents or external sources. Internal mix constituents include CaCl_2 added as an accelerating admixture and other admixture compositions. External sources are contact with sea water, de-icing salts and structures exposed to the splash zone and marine environment.

The paths that allow chloride ions to intrude depend upon the pore structure of the concrete. The intrusion process of chloride ions occurs by external hydraulic pressure that bring the ions through the pores into concrete. The amount of chloride required to initiate corrosion depends on the pH of the solution in contact with the steel, and comparatively small quantities are needed to offset the basicity of portland cement [13]. Even at high alkalinities, the intrusion of chloride will be accompanied by a chemical reaction with the tricalcium aluminate to form calcium-chloroaluminate hydrate. There are several strategies that have been developed to prevent corrosion of reinforcing steel, based largely on studies carried out on bridge-decks. The possible strategies can be divided into several categories such as reduction of permeability of concrete, protective coatings on the concrete, protective coatings on the steel, and suppression of the electrochemical process. Swamy and Tanikawa [49] have given recommendations for the selection criteria of surface coatings, as shown in Table 2-3. The effect of using fly ash in concrete is to reduce the amount of chloride intrusion which can arise due to a lower porosity and high tortuosity of the pore channels inhibiting ionic diffusion. Dhir et al [50] found that it is not the fly ash quality that effects chloride diffusion but the quantity of fly ash in the concrete. Haque, Kayyali, and Gopalan [51] also observed that the presence of fly ash significantly reduced the concentration of free Cl^- ions in concrete when the chloride ingress is from the surrounding sodium chloride solution. The rapid chloride-ion diffusion tests performed on HVFA concrete indicated very low chloride-ion diffusion at 1 year, ranging from 119 to 179 coulombs confirming the excellent resistance of HVFA concrete to chloride-ion penetration [9].

Table 2-3 Basic technical requirements of surface coatings [49]

Characteristics of properties	Descriptions
Chemical resistance	<ul style="list-style-type: none"> • Resistance to salt (salt spray, dry / wet salt spraycycle, immersion in sea water). • Acid resistance.
Weathering resistance	<ul style="list-style-type: none"> • Outdoor exposure (ultra violet light, ozone variable temp / humidity). • Heat resistance. • Resistance to water permeability.
Resistance to expansive force	<ul style="list-style-type: none"> • Freezing and thawing. • Alkali silica reaction.
Engineering properties	<ul style="list-style-type: none"> • Crack bridging ability. • Adequate elastic / fatigue resistance (to resist crack opening / closing). • Strain capacity - stress - strain behaviour. • Adhesion strength (film continuity). • Abrasion Resistance. • Thermal Compatibility.
Diffusion resistance	<ul style="list-style-type: none"> • Water, air (oxygen, carbon dioxide), chloride ions, water vapour). • Air diffusion at high pressure.
Economic requirements	<ul style="list-style-type: none"> • Ease of application. • Long service life. • Pleasant appearance.

2-8. INFLUENCE OF SILICA FUME IN CONCRETE

Silica fume is the by-product of electric arc furnaces during the production of silicon metal or ferrosilicon alloys. Ferrosilicon alloys containing 50 ~ 70 % Si are the most important alloys of silicon. The raw materials used for the production of ferrosilicon are usually 3 ~ 6 inch pieces of crushed quartz, coke, and iron ore pure silicon metal is produced at temperatures of the order of 2000°C, in the areas between electrodes submerged in the charge. About 10 ~ 15 % quartz in the charge is lost in the form of Si and SiO vapours, which react with air to form SiO₂. The fine particles are collected by filtering gases escaping from the arc furnace. The chemical compositions of the condensed silica fume from the ferrosilicon industry corresponds, generally, to 85 ~ 92 % SiO₂, 0.5 ~ 3 % Fe₂O₃, 1 ~ 3 % alkalis, 1 ~ 2 % carbon, and minor

amounts of Al_2O_3 , CaO , and MgO [52]. These percentage compositions depend on what is being produced in the furnace. The particle size analyses show individual spherical particle shape with a number of primary agglomerates, and amorphous particles range from 0.01 to 0.3 μm , with about 70 % < 0.1 μm . Nitrogen adsorption measurements show 15 ~ 20 m^2/g surface area of the material.

Areas of application where silica fume has shown particular advantage, and some of the results from these investigations have been recently published in a comprehensive review [15,43,53,54,55,56]. There is strong evidence that the use of silica fume increases the homogeneity and decreases the number of large pores in cement paste, and results in a denser interface between cement paste and coarse aggregate. These studies have demonstrated that the pozzolanic activity effect of silica fume in concrete is faster than ordinary portland cement, because of its high surface area, and the high amount content of amorphous silica in silica fume. Many authors foresee a wide-ranging application of silica fume if it is used as a strength accelerator in portland cement concrete containing fly ash [52].

2-9. HIGH STRENGTH / HIGH PERFORMANCE CONCRETE AND HIGH VOLUME FLY ASH CONCRETE

The factors affecting the development of cement paste strength include its internal water content, voids in the matrix, and interface organisation. Reducing water content and voids as well as compressing the interface may produce high strength / high performance concrete. Concrete is commonly used in constructing building frames. Recent developments in high strength / high performance concrete have extended its use to tall buildings [57].

The name “high strength / high performance concrete” implies that, in many cases, it is high durability that is the required property, although, in others, it is high strength, either very early, or at 28 days, or even later. In some applications, a high modulus of elasticity is the property sought.

Although both properties of high strength and low permeability are not necessarily concomitant, high strength requires a low volume of pores, especially of the large capillary pores. The way to have a low volume of pores is, in general, achieved by the use of mineral admixtures, such as fly ash, slag or silica fume, which fills the space between the cement particles and between the aggregate and the cement particles.

Indeed, high strength / high performance concrete can be said to be a logical development of concrete containing different mineral admixtures which change the internal structure of concrete. While there exists no standard, or even typical, mix proportion of high strength / high performance concrete, it is useful to present information on several successful mixes, and this is shown in Table 2-4 [58]. Several of these mixes contain, in addition to portland cement and fly ash, other cementitious materials. There is an economic advantage in using these various cementitious materials, partly because they are more effective than portland cement, but also because they allow a reduction in the quantity of cement.

**Table 2-4. Typical high compressive strength of fly ash concrete [58]
(Unit : MPa)**

Mixture Type kg/m ³	Age (days)	Wet	7 day wet / air	Air
350 OPC	28	55.7	57.9	52.9
	90	60.8	63.2	59.6
	260	68.5	71.5	62.2
300 OPC + 20 SF + 30 FA	28	60.1	63.6	60.1
	90	75.5	77.3	71.1
	260	78.3	80.1	73.0
250 OPC + 20 SF + 80 FA	28	59.4	64.0	57.1
	90	67.8	72.7	61.0
	260	71.4	76.2	63.0
250 OPC + 20 SF + 80 slag	28	67.9	70.9	61.7
	90	74.8	78.4	67.5
	260	84.4	88.0	70.1

The importance of fly ash cannot be exaggerated ; it is no longer a cheap substitute for cement, nor an extension or an addition to the mix. The variability of the properties of fly ash was mentioned in the preceeding section. The effects of fly ash are activated by the pozzolanic reaction when portland cement is used with it. Moreover, in addition to the effect of chemical reactions, fly ash has a physical effect of improving the microstructure of the hydrated cement paste.

Concrete containing high volume low-calcium fly ash (ASTM Class F) has been used in various parts of the world during the last 10 years. The first use of this type of HVFA concrete is believed to have been in roller compacted dams and highway base courses. Roller compacted concrete has very low unit water content, and lacks the workability required for placement as structural concrete.

It was mentioned before that structural concrete incorporating high volumes of low-calcium fly ash was developed at CANMET in 1985 [7]. The initial research focused on developing a HVFA concrete mixture suitable for ready-mixed operation, having a relativity low temperature rise, for use in massive unreinforced structural elements. Extensive testing has shown that the above type of HVFA concrete made with ASTM Type II cement has high unit weight, satisfactory early-age compressive strength, high modulus of elasticity, and high later-age strength. In this type of HVFA concrete, cement content is kept at about 150 kg/m^3 and the ratio of fly ash to total cementitious material content is increased to about 55 %. As the water content of these mixtures is less than 120 kg/m^3 , the workability is achieved by using large dosages of superplasticizers.

Swamy and Mahmud [59] also introduced such HVFA concrete at the international symposium on the Fly Ash, Slag, Silica Fume and Natural Pozzolans in Concrete of 1986. Subsequently, W. S. Langley and Association limited, Halifax, Nova Sotia undertook in a large HVFA concrete block, $3.05 \times 3.05 \times 3.05 \text{ m}$, to monitor the long-term strength development of HVFA concrete. The water-to-cementitious material ratio of these HVFA concrete ranged from 0.27 to 0.49, and their total cementitious material content ranged from 400 to 225 kg/m^3 . Test results were presented in 1989 and 1992 respectively [27,60]. The test data on strength

properties, modulus of elasticity, drying shrinkage, creep, and freeze-thaw durability indicate that concrete incorporating low cement content and high volume of fly ash compares favourably to normal portland cement concrete. Also, limited tests performed to date indicate that the permeability of concrete incorporating high volumes of fly ash is also very low.

An investigation undertaken on HVFA concrete made with a combination of fly ash and silica fume was reported by Giaccio and Malhotra [61]. From the test results, it was concluded that HVFA concrete has excellent mechanical properties and satisfactory resistance to repeated cycles of freezing and thawing.

Xu and Sarkar [62] investigated the microstructure of HVFA concrete, and suggested that both CH and C-S-H phases precipitate on their surface, consequently leading to a more homogeneous distribution of hydration products. Most obvious was the reduction in the amount and size of CH crystals at later ages. A study dealing with the role of concrete incorporating high volume of fly ash in controlling the expansion due to alkali aggregate reactions was reported by Malhotra and Alasali, who indicated that the fly ash was highly effective in inhibiting the alkali-silica reaction [45]. Similar results were presented by Malhotra et al, and they indicated very low chloride-ion diffusion in HVFA concrete at 91 days, ranging from 197 to 973 coulombs [63].

In 1990, CANMET undertook to develop an engineering data base on HVFA concrete. Eight fly ashes, covering a wide range of mineralogical and chemical compositions, and two portland cements from different sources were selected for the study. The investigation was carried out for the Electric Power Research Institute (EPRI), Palo Alto, California, under a subcontract with Radian Canada Inc. [9]. Briefly, in this HVFA concrete, the water and cement contents are kept low at about 115 and 155 kg/m³ of concrete, respectively, and the proportion of fly ash in the total cementitious materials content ranged from 55 to 60 percent. The results have shown excellent mechanical properties at both early and late ages, with compressive strengths reaching as high as 50 MPa at 91 days. Values of Young's modulus of elasticity of the order of 40 GPa at 91 days were achieved for the HVFA concretes

investigated. The creep and drying shrinkage of the HVFA concretes investigated were relatively low.

Some research data on engineering properties from investigations of HVFA concrete mixtures are presented in Table 2-5.

A mix of particular interest is Malhotra et al of the Table 2-5 with a water / cementitious ratio of 0.30, and a total content of cementitious material of 340 kg/m³. The compressive strength at 1 day was 0.6 MPa but it reached 79 MPa at the age of 1 year. It should be emphasized that experimental production of HVFA concrete necessitates a very strict and consistent quality control.

Table 2-5 Mix proportions and engineering properties of some HVFA concretes

Ingredient (kg/m ³)	Swamy & Mahmud [59]			Giaccio & Malhotra [61]	Malhotra et al [60]				
	266	348	466		375.7	400	340	340	225
Total cementitious content	266	348	466	375.7	400	340	340	225	340
Portland cement	133	174	233	154	180	150	150	100	150
Fly ash	133	174	233	211	220	190	190	125	190
Silica fume	—	—	—	10.7	—	—	—	—	—
Water / Cementitious	0.615	0.420	0.320	0.31	0.28	0.30	0.33	0.49	0.35
SP % of total cementitious	1.7%	1.8%	1.8%	1.13%	—	—	—	—	—
Slump (mm)	—	—	—	—	120	200	100	100	210
Compressive strength (MPa) at age (days)	100mm cubes	100mm cubes	100mm cubes	102×203 mm cylinders	150×300 mm cylinders	150×300 mm cylinders	150×300 mm cylinders	150×300 mm cylinders	150×300 mm cylinders
1	4.4	11.8	21.8	9.3	13.7	0.6	10.2	4.0	2.7
7	13	31.3	43.3	17.6	34.2	26	25.8	12.1	20.5
28	23.7	46.6	63.3	32.5	57.1	49.1	46.1	23.0	37.5
91	46.8	70.0	88.8	41.2	75.2	63.0	61.8	37.9	53.0
365	49.5	75.6	92.5	—	—	79.0	—	—	69.0
Flexural strength (MPa) at age (days)	100×100 ×500mm prisms	100×100 ×500mm prisms	100×100 ×500mm prisms	76×102×40 6mm	150×300 mm cylinders	150×300 mm cylinders	150×300 mm cylinders	150×300 mm cylinders	150×300 mm cylinders
1	0.78	1.92	3.12	—	—	—	—	—	—
7	1.80	3.12	3.92	—	—	—	—	—	—
28	2.56	4.56	4.52	4.9	—	6.9	—	—	6.0
91	4.88	6.64	7.64	—	9.6	—	8.9	—	—
365	4.70	5.80	7.52	—	—	9.0	—	—	7.5
Modulus of elasticity (GPa) at age (days)	100×100 ×500mm prisms	100×100 ×500mm prisms	100×100 ×500mm prisms	152×305mm cylinders	150×300 mm cylinders	150×300 mm cylinders	150×300 mm cylinders	150×300 mm cylinders	150×300 mm cylinders
28	35.6	41.7	46.9	35.5	36.1	35.1	33.8	27.9	—
Drying shrinkage (microstrain) at age (days)	100×100 ×500mm prisms	100×100 ×500mm prisms	100×100 ×500mm prisms	—	—	—	—	—	—
7	169	163	187	—	—	—	—	—	—
28	365	319	325	—	—	—	—	—	—
91	430	405	413	—	—	—	—	—	—
365	478	452	468	—	—	—	—	—	—
730	485	460	475	—	—	—	—	—	—

Table 2-5 (Contd./)

Ingredient (kg/m ³)	V. Sivasundaram et al [63]				Langley et al [27]		Georges Carette et al [43]		
Total cementitious content	545	520	363	360	380	225	363	365	363
Portland cement	229	219	153	152	180	100	152	153	152
Fly ash	316	301	210	208	200	125	211	212	211
Water / Cementitious	0.21	0.22	0.31	0.32	0.27	0.49	0.33	0.33	0.33
Slump (mm)	200	200	200	200	200	110	140	110	190
Compressive strength (MPa) at age (days)	152×305 mm cylinders	152×305 mm cylinders	152×305 mm cylinders	152×305 mm cylinders	152×305 mm cylinders	152×305 mm cylinders	152×305 mm cylinders	152×305 mm cylinders	152×305 mm cylinders
1	—	—	2.8	—	—	—	5.6	10.3	5.8
7	—	—	17.8	15.6	27.5	—	18.8	24.9	18.2
28	55.4	48.2	28.2	27.2	44.0	22.1	28.8	39.3	27.8
91	—	—	35.9	32.9	59.7	35.5	39.7	50.9	39.5
365	—	—	39.1	36.6	67.3	—	52.0	57.9	54.7
730	—	—	—	—	73.3	—	58.4	65.2	55.0
Flexural strength (MPa) at age (days)	—	—	—	—	75×100× 400mm prisms	75×100× 400mm prisms	75×102× 406mm prisms	75×102× 406mm prisms	75×102× 406mm prisms
14	—	—	—	—	—	—	3.7	4.8	3.4
91	—	—	—	—	7.2	5.6	5.2	6.5	5.4
365	—	—	—	—	7.5	6.3	—	—	—
730	—	—	—	—	—	—	6.2	6.5	6.0
Modulus of elasticity (GPa) at age (days)	152×305 mm cylinders	152×305 mm cylinders	152×305 mm cylinders	152×305 mm cylinders	152×305 mm cylinders	152×305 mm cylinders	152×305 mm cylinders	152×305 mm cylinders	152×305 mm cylinders
28	41	37.9	—	—	30.1	27.9	33	35.8	32.8
91	—	—	—	—	—	—	39.2	41.0	40.4
125	45.2	44.5	—	—	—	—	—	—	—
365	—	—	—	—	41.3	—	42.4	42.6	43.6
Drying shrinkage (microstrain) at age (days)	—	—	—	—	—	—	76×102× 390mm prisms	76×102× 390mm prisms	76×102× 390mm prisms
7	—	—	—	—	—	—	139	245	192
28	—	—	—	—	—	—	341	422	326
56	—	—	—	—	—	—	389	493	369
112	—	—	—	—	—	—	380	536	426
224	—	—	—	—	—	—	418	582	461
448	—	—	—	—	—	—	433	589	454
Chloride-ion penetration (Charge in coulombs) at age (days)	φ100×50 mm cores	φ100×50 mm cores	φ100×50 mm cores	φ100×50 mm cores	—	—	102×203 mm cylinders	102×203 mm cylinders	102×203 mm cylinders
7	—	—	8484	7821	—	—	—	—	—
28	—	—	2130	935	—	—	1804	815	1743
91	—	—	—	539	—	—	585	297	635
365	—	—	—	—	—	—	136	127	156
Pulse velocity (km/sec) at age (days)	—	—	—	—	152×305 mm cylinders	152×305 mm cylinders	—	—	—
7	—	—	—	—	4.22	—	—	—	—
42	—	—	—	—	4.76	4.22	—	—	—
365	—	—	—	—	4.78	4.47	—	—	—
730	—	—	—	—	4.84	4.60	—	—	—

CHAPTER THREE

EXPERIMENTAL PROGRAMME

3-1. INTRODUCTION

In order to understand the role of fly ash in concrete, and to develop a good method of mixture proportioning of high volume fly ash concrete (HVFA), several mixtures were tested and the results analysed. The development of strength in high volume fly ash concrete is intimately related to mix proportioning, and the method of mix proportioning will influence the properties of such concrete. The underlying principle of the method used here is to produce high performance concrete for structural applications. The first stage of this research consists in the development of several mixtures of high volume fly ash concrete and the details are presented below.

3-2. TEST PROGRAMME AND DETAILS OF CONCRETE MIXTURES

Several methods of mixture proportioning of fly ash concrete have been developed over the years. Basically, fly ash has been used as partial replacement of cement, fine aggregate, or cement and fine aggregate. This method of mixture design has been used extensively in many studies, and is also adopted for use in this research. The mix parameters and proportions of the cement replacement mixtures are summarized in Table 3-1 and Table 3-2.

All experimental work was performed in a laboratory environment, i.e., at room temperature, and pressure, except when otherwise specified. A high range

water reducer (HRWR) was used in all the mixes, and the dosage of this superplasticizer was adjusted to give a slump of 150 ~ 200 mm.

Table 3-1 High volume fly ash concrete test parameters

Parameter	Range of variables
Type of mixture	(OPC Mixes) Mix-350C, Mix-450C (HVFA Mixes) Mix-350F, Mix-350SF, Mix-350S Mix-450F, Mix-450SF, Mix-450S
Total binder content (kg / m ³)	350 and 450
Method of replacement	<ul style="list-style-type: none"> • Partial replacement of cement • Partial replacement of sand
Water / binder ratio	0.40
Size of specimen (mm)	100 × 100 × 500
Curing condition	<ul style="list-style-type: none"> • Wet curing continuous in water • 7 days water curing + continuous air curing
Slump (mm)	150 ~ 200

Table 3-2 High volume fly ash concrete mixtures (Unit : kg/m³)

Type of mixture and identification	Total cementitious content	Cement	Fly ash	Silica fume
350C	350	350	---	---
350F	350	150	200	---
350SF	350	150	180	20
350S	350	150	180	20
450C	450	450	---	---
450F	450	200	250	---
450SF	450	200	230	20
450S	450	200	230	20

Remarks : Mix-350S and Mix-450S had both cement and sand replacement with fly ash.

3-3. CHARACTERISTICS OF MATERIALS

Cement

The cement used was ordinary portland cement (OPC) conforming to British Standard obtained from Castle Cement Limited, Lancashire. The specific surface area of this cement was 345 m²/kg.

Fly ash

A Class F fly ash with the ASTM designation C618 was used in this investigation. The fly ash used in this concrete was obtained from Boral Pozzolan Ltd, Herts. The MgO content of 1.62%, satisfies to the BS 3892 : Part 1 : 1981 “Pulverized-fuel ash for use as a cementitious component in structural concrete”, which restricts the MgO content to less than 4 %.

Silica fume

A silica fume slurry containing 50 % by weight of water was used. The silica fume was supplied by Elkem Materials Limited in slurry form. Its specific gravity is 2.2. The chemical composition of the portland cement and mineral admixtures are shown in Table 3-3.

High Range Water Reducer

A superplasticizer was used in this programme ; a concrete plasticiser P6 obtained from W. R. Grace Ltd. Cormix Division. This high range water reducer was used to provide an effective means of producing low water-binder ratio concrete combined with good workability. For the same workability of a concrete mix, the mix incorporating a superplasticizer would need less water, leading to a lower water/cementitious ratio, with a high workability.

Normal Aggregate

The fine and coarse aggregates were obtained from the Redlands quarry. A sieve analysis was carried out on representative samples in accordance with BS 812 : Part 103.1: 1985 “Sieve tests”. The sieve analysis results of the aggregates are given

in Table 3-4. The fine aggregate had a water absorption coefficient of 2.1 %, and a bulk specific gravity 2.62, in saturated surface dry condition. The coarse aggregate consisted of a mixture of rounded and crushed gravel with 10 mm maximum particle size. The coarse aggregate water absorption was 0.3 % and bulk specific gravity 2.62, in saturated surface dry condition. Chemical analysis (XRF method) of the aggregates was provided by the aggregate supplier. The results of these tests are shown in Table 3-5.

**Table 3-3 Chemical composition of cements and mineral admixtures
(Unit : %)**

Chemical composition	OPC	Fly ash	Silica fume
SiO ₂	20.4	51.4	97.0
Al ₂ O ₃	5.70	28.1	-
Fe ₂ O ₃	2.10	11.1	-
CaO	65.3	1.38	-
MgO	1.10	1.62	-
SO ₃	3.20	-	-
Na ₂ O	0.20	1.32	-
K ₂ O	0.59	4.08	-
TiO ₂	-	0.77	-
C ₃ S	54.3	-	-
C ₂ S	17.6	-	-
C ₃ A	11.6	-	-
C ₄ AF	6.40	-	-
Fe	-	-	0.09
Al	-	-	0.09
Ca	-	-	0.11
Mg	-	-	0.09
K	-	-	0.30
Na	-	-	0.09
H ₂ O	-	-	0.50
Loss of Ignition	1.00	3.50	1.10
Specific surface (m ² / kg)	345	370 ~ 400	-

Table 3-4 Sieve analysis of fine aggregate and coarse aggregate

Sieve size (mm)	Fine aggregate		Coarse aggregate	
	Passing (%)	BS 882: (%)	Passing (%)	BS 882:(%)
13.2			100	100
9.5			96	85 ~ 100
4.75			20	0 ~ 25
2.36			3	0 ~ 5
9.5	100	100		
4.75	93	89 ~ 100		
2.36	84	60 ~ 100		
1.18	80	30 ~ 100		
0.6	77	15 ~ 100		
0.3	39	5 ~ 70		
0.15	6	0 ~ 15		
F.M.	2.21		1.81	

Table 3-5 Chemical compositions of fine aggregate and coarse aggregate

Chemical composition	Content (%)	
	Fine aggregate	Coarse aggregate
SiO ₂	91.72	92.57
TiO ₂	0.13	0.25
Al ₂ O ₃	3.86	2.22
Fe ₂ O ₃	0.96	1.28
CaO	0.50	1.53
MgO	0.34	0.98
Na ₂ O	N / A	0.00
K ₂ O	2.18	0.93
Cr ₂ O ₃	0.025	0.03
Mn ₃ O ₄	0.005	0.009
P ₂ O ₅	0.02	--
BaO	0.04	0.02
V ₂ O ₅	0.007	--
Loss of Ignition	0.95	1.98

3-4. CONCRETE MIXTURE DESIGN

The total cementitious content was kept constant in all the specimens at 350 kg/m³ and 450 kg/m³ respectively. The water / binder ratio of all the specimens was also kept constant at 0.40. The aggregate / binder ratio was 5.2 / 1 for 350 kg/m³ mixes , 4.04 / 1 for 450 kg/m³ mixes and the percentage of fine aggregate in the total was 35 % for the total aggregate. In the mixes studied in this project in addition to cement replacement, a proportion of the fine aggregate, amounting to 25 %, was also replaced by fly ash for Mix-350S and Mix-450S. The final mix proportions of high volume fly ash concrete considered in this study are listed in Table 3-6.

Table 3-6 High volume fly ash concrete mix proportions (Unit : kg/m³)

Type of mixture and identification	Total binder content	Cement	Fly ash	SF	Water	Coarse aggregate	Fine aggregate
350C	350	350	---	---	140	1183	637
350F	350	150	200	---	140	1183	637
350SF	350	150	180	20	140	1183	637
350S	350	150	180 (340)*	20	140	1183	160(Fly ash) 477(Sand)
450C	450	450	---	---	180	1183	637
450F	450	200	250	---	180	1183	637
450SF	450	200	230	20	180	1183	637
450S	450	200	230 (390)*	20	180	1183	160(Fly ash) 477(Sand)

Remarks:

1. Total cementitious : Aggregate = 1 : 5.2 for 350 kg/m³ mixes, 1 : 4.04 for 450 kg/m³ mixes
2. 35 % Total aggregate = Fine aggregate
3. SF = Silica fume
4. Mix-350S and Mix-450S had both cement and sand replacement with fly ash
5. * : Total fly ash content

3-5. MANUFACTURE OF TEST SPECIMENS AND CURING

The fine and coarse aggregates were used in an air dry condition. Water content was checked and adjusted before mixing. Due to very low water / binder ratio, different methods of combining the constituents were tried and the following method was found to obtain a homogenous mix and without bleeding.

1. The coarse aggregates were first placed in the mixer and half the quantity of water was then added and the mixer was spun for about a minute.
2. The cement and mineral admixture with the fine aggregates were added, then mixed 30 seconds.
3. Added remaining 1 / 2 of mixing water, then mixed for 90 seconds.
4. Superplasticizer was then added directly to the mixer and mixed for a further minute.
5. Slumps of the mixes were performed after superplasticizer addition.

All specimens were cast in steel moulds which had been lightly oiled. After casting, all the specimens were covered by polythene sheet and left in the laboratory. The specimens were demoulded after 24 hours, and then cured in water for 7 days. Curing was then continued either in water or in a drying environment. Eight batches were cast for all the concrete mixtures. Each batch contained six prisms, three prisms for water curing, and three for curing in a drying environment respectively.

Only one geometry of test specimen was used in the Part I of this research study, namely, 100 × 100 × 500 mm prisms. The advantage of using 100 × 100 × 500 mm prisms test specimens for this part of the study is that with a single test geometry, the essential properties of the concrete can be established, thus reducing the amount of time and effort required for casting various sizes of specimens.

3-6. DOSAGE OF SUPERPLASTICIZER (HRWR) AND SLUMP

From an engineering application point of view of the high volume fly ash concrete, the mixture proportioning should produce a concrete with adequate flow characteristics, so that the concrete can be easily placed and compacted. To achieve this purpose, a relatively large variation in the superplasticizer dosage requirement was needed, the quantities ranging from 0.9 to 2.5 percent of the total cementitious content for the different concrete mixtures. The difference in the dosage of the superplasticizer was mainly due to the different cementitious contents of the high volume fly ash concrete mixes.

The workability in these studies was determined by the slump test. All the mixes appeared to have good cohesiveness and no bleeding was detected. With structural concrete, the aim is to produce a specified workability and 28 day normally cured strength. The mixes in this study were designed to have a slump of 150 to 180 mm, and the results are shown in Table 3-7.

Table 3-7 High volume fly ash concrete workability

Type of mixture and identification	Total cementitious content	Superplasticizer (%) of Cementitious material	Slump (mm)
350C	350	2.2	165
350F	350	0.9	165
350SF	350	1.1	165
350S	350	1.6	165
450C	450	2.5	165
450F	450	1.2	160
450SF	450	1.3	165
450S	450	1.8	165

The normal portland cement concrete mixes had the highest demand of HRWR of 2.2 % to 2.5 % of the cement content. Mix-350F had the most workable concrete with the lowest dosage of the superplasticizer. The dosages required for

concrete made with Mix-450F, Mix-350SF, and Mix-450SF were also quite low. Mix-350S and Mix-450S had the highest water demand of all concretes with mineral admixtures, and consequently, higher superplasticizer dosages of 1.6 % ~ 1.8 % of total cementitious material were required. The high water demand of Mix-350S and Mix-450S is most likely due to the higher fly ash content, and the presence of a high proportion of fine material.

3-7. TEST DETAILS

The eight batches of specimens were used for determining the ultrasonic pulse velocity, dynamic modulus of elasticity, drying shrinkage and expansion at various ages up to 18 months. At each specific age, the batches were also used for the determination of air permeability, water absorption, carbonation and compressive strength following the flexural strength test. After the flexural strength test, each broken prism was used for a modified cube compressive strength test. The carbonation test followed the compressive strength test. For each test, three prisms were used. Table 3-8 shows the details of the tests and the test specimen size used. The tests are described in detail below.

3-7-1. Flexural and compressive strength test

One of the objectives of this study was to establish whether the incorporation of silica fume in a high volume fly ash content was beneficial to the early strength development. Accordingly, flexural and compressive strength tests were carried out for all of the concretes at 1, 3, 7, 28, 90, 180, 360 days and 18 months after moist or air curing. At each testing age, three specimens were tested ; they were removed from water one hour before testing. For flexural strength, the test procedure was according to BS 1881 : Part 118 :1983 “Method of determination of flexural strength”.

The compressive strength of the concrete was found by using portions of prisms broken in the flexural tests (equivalent cube method). The equivalent cube method of determining the compressive strength of concrete consists of applying the load through 100×100 mm square auxiliary platens, equal to the nominal cross-sectioned dimensions of the prism. The test was carried out according to BS 1881 : Part 119 :1983, "Method for determination of compressive strength using portion of beams broken in flexure".

3-7-2. Dynamic modulus of elasticity

The dynamic modulus of elasticity of concrete is related to the structural stiffness and deformation process of concrete structures. The test was determined by the "Resonant Frequency Tester", made by C N S Electronics Ltd. The instrument consisted of an "Erudite" electromagnetic exciter unit, an electromagnetic pick-up unit, a digital counter unit, a variable frequency oscillator and a cathode ray oscilloscope. The test was conducted by placing the electromagnetic exciter unit and the pick-up unit, along the longitudinal axis, at the centre of the specimen, against the 100×100 mm sides with a path length of 500 mm for each prism. Tests were performed on the same specimens at intervals of 7 days. The test principle, procedure and calculation of the value were all according to BS 1881 : Part 209 : 1990, "Recommendations for the measurement of dynamic modulus of elasticity".

3-7-3. Ultrasonic pulse velocity

The purpose of the ultrasonic pulse velocity tests was to look into the effects of the two different curing conditions with time, and to monitor the development of the internal structure and microcracking of the high volume fly ash concrete.

The ultrasonic pulse velocity tester used in the present study was the PUNDIT, manufactured by C.N.S. Electronics Ltd. 54 kHz transducers of 50 mm diameter were used. The measurements were taken at the two 100 × 100 mm sides, along the longitudinal axis of the prisms. The measurement intervals at which the ultrasonic pulse velocity was recorded were the same as for the dynamic modulus of elasticity test. The test method was in accordance with BS 1881 : Part 203 : 1986, "Recommendation for measurement of velocity of ultrasonic pulse in concrete".

Table 3-8 High volume fly ash concrete test details

Type of testing	Specimen size (mm)	Standard
Flexural strength	100 × 100 × 500	• BS 1881 : Part 118 : 1983 "Method of determination of flexural strength".
Modified cube compressive strength	100 × 100 × 500	• BS 1881 : Part 119 : 1983 "Method for determination of compressive strength using portion of beams broken in flexure". • BS 1881 : Part 116 : 1983 "Method for determination of compressive strength of concrete cubes".
Dynamic modulus of elasticity	100 × 100 × 500	• BS 1881 : part 209 : 1990, "Recommendations for the measurement of dynamic modulus of elasticity".
Ultrasonic pulse velocity	100 × 100 × 500	• BS 1881 : Part 203 : 1986, "Recommendation for measurement of velocity of ultrasonic pulse in concrete".
Swelling	100 × 100 × 500	• BS 1881 : Part 5 : 1970, "Determination of changes in length on drying and wetting".
Drying shrinkage	100 × 100 × 500	• BS 6073 : Part 1 : 1981, "Specification for precast concrete masonry units " Appendix D " Determination of drying shrinkage".
Carbonation (Phenolphthalein Test)	100 × 100 × 500	• The depth of carbonation is measured using phenolphthalein solution. "Measurement of hardened concrete carbonation depth" [64].
Air permeability	50 × 30 cylinder	• "A new gas permeameter for measuring the permeability of mortar and concrete".
Water absorption	75 × 100 cylinder	• BS 1881 : Part 122 : 1983 "Method for determination of water absorption".

3-7-4. Swelling and drying shrinkage

The volume of a concrete varies with its water content. Drying will cause a volume decrease, i.e., drying shrinkage, and wetting will cause a volume increase, i.e., swelling. Consequently, the rate of removal of water from concrete controls the rate of shrinkage of the concrete. Reasonably, all factors which affect drying, for example : temperature, humidity, pressure, air movement, etc., will actually control the shrinkage.

To study the swelling and drying shrinkage characteristics of high volume fly ash concrete, water curing and air curing were chosen. After demoulding, all the specimens had two locating discs bonded to the concrete over a 200 mm gauge length in the longitudinal direction in the middle of each of the four sides. Initial readings were taken within an hour of fixing the discs. The measurements were taken over a period of 18 months at regular intervals of 7 days. For each curing condition, three specimens were tested, the results are thus the average of twelve readings. The demec gauge can be read accurately to 8×10^{-6} strain. The swelling and drying shrinkage were measured according to BS 6073 : Part 1 : 1981, "Specification for precast concrete masonry units", Appendix D, "Determination of drying shrinkage".

3-7-5. Carbonation

Carbon dioxide which penetrates the surface of concrete can react with alkaline components in the concrete, mainly Ca(OH)_2 . This process leads to a reduction of the pH value of the pore solution. The depth of carbonation is measured using phenolphthalein solution [64].

At the specific age of the flexural strength test, the broken surface was immediately cleaned of dust and loose particles after breaking. Carbonation tests were carried out on the freshly broken surface by spraying with phenolphthalein solution. The depth of the carbonation layer from the external surface of concrete to

the start of the coloration of the concrete was measured as depth of carbonation. Eight measurements were made on each of the faces of each broken prism, therefore, the depth of carbonation reported is the average result of 24 readings.

CHAPTER FOUR

TEST RESULTS AND DISCUSSION OF PART I

4-1. INTRODUCTION

A series of concrete mixtures involving two different curing conditions, with and without fly ash and / or silica fume, with total cementitious contents of 350 kg/m^3 and 450 kg/m^3 , were designed. All the HVFA concrete mixes were made with a water / binder ratio of 0.4. Because of the very low water content used, large dosages of a superplasticizer had to be used to obtain the required workability.

In this chapter, the results of the effect of pozzolanic reaction on the engineering properties of concrete such as compressive and flexural strength, dynamics modulus of elasticity, ultrasonic pulse velocity, swelling and drying shrinkage are reported at various ages up to 18 months. The effect of fly ash on carbonation is also presented and discussed.

4-2. STRENGTH DEVELOPMENT

The strength of a concrete is its most important property because, after all, concrete is a construction material. The hardening of the concrete is the result of the hydration reaction, the subsequent development of bonds in the hydration products, and gradual increase of the internal strength. Nevertheless, strength usually gives an overall picture of the quality of concrete, because strength is directly related to the structure of the hydrated cement paste. Moreover, the strength of concrete is almost invariably a vital element of structural design, and is specified for compliance purposes.

This section presents the results of the strength properties of high volume fly ash concrete in its hardened form. For purpose of comparison, the strength properties of normal portland cement concrete are also discussed .

The flexural and compressive strength tests were carried out for all of the concretes at 1, 3, 7, 28, 90, 360 days and 18 months of moist curing and air curing. Three specimens were tested at each age, and the results are thus the average of three measurements. The compressive strength of the concrete was found by the modified cube test.

4-2-1. Effect of curing condition on compressive strength

The data on the compressive strength development under both curing conditions are presented in Tables 4-1 and 4-3 and illustrated in Figs 4-1 and 4-3.

The compressive strength expressed as a percentage of the 28 day values under both curing conditions is given in Tables 4-2 and 4-4, and Figs 4-2 and 4-4. The strength development pattern is quite different for the two curing conditions, and cementitious contents, and these are therefore discussed separately.

Water curing on compressive strength development

Early strength development is a matter of great importance to the construction industry, and closely related both to the performance and economics of concrete at early ages [6].

The compressive strength development of high volume fly ash concrete under water curing is shown in Table 4-1 and compared in Fig 4-1.

It can be seen from the table that, the early age compressive strength of concrete incorporating both fly ash and silica fume, i.e. of, Mix-350SF and Mix-450SF, is higher in comparison with those of concrete with cement replaced partially by fly ash alone i.e., Mix-350F, Mix-450F, but lower than the strength of mixes

containing fly ash as partial replacement of both sand and cement. The increased gain in strength at early ages of concrete incorporating fly ash and silica fume may suggest an early start of the pozzolanic reaction due to the use of silica fume, although this may also be partially accounted for by the filler effect of silica fume resulting in a denser matrix structure [65].

The data in Table 4-1 show that the compressive strength generally increased with age for all the HVFA concretes, producing high compressive strength in the range of 60 to 68 MPa at the age of 18 months. The data also show that the presence of silica fume had very little effect on the long-term strength of the HVFA concrete.

There are two possible reasons for the higher strength of Mix-350SF and Mix-450SF concretes at early ages. First, because of its small particle size, silica fume can act as a filler in the spaces between cement grains. This results in a reduction in the size of the individual pores and voids in the concrete, although the total porosity is not affected. Since pores are discontinuities in the cement concrete matrix, reduced pore sizes require a higher stress to initiate a crack ; thus, the strength is increased [54]. A second reason for the early high strength of the 350SF, 450SF concrete is due to the pozzolanic nature of silica fume, which also explains why the 350SF, 450SF concretes become progressively stronger with time relative to the concretes containing fly ash only.

Mix-350S and Mix-450S containing fly ash as both cement and sand replacement showed slightly higher strength at all ages than the mixes without and with silica fume. As mentioned before, early fly ash concrete mixes were based on low percentage of cement replacements ; these methods are suitable for mass concrete where early strength development is not a criterion, and they invariably lead to a lower strength of fly ash concrete [6]. When fly ash is also used to replace part of the sand in a mix without changing the water and cement contents, the total cementitious material actually increases and the water / binder (w / b) ratio decreases accordingly. Theoretically, the strength of concrete increases with decreasing w / b ratio. Therefore, proper use of fly ash to partially replace sand will be advantageous in strength development. Since the fly ash particle is smaller than the

sand, the more the sand is replaced, the more the specific surface area is increased. However, if an excessive portion of sand is replaced by fly ash, the w / b ratio is also excessively reduced, and thus may, in turn, create workability problems.

When fly ash is used to replace part of the cement and sand simultaneously, the advantage gained from reducing the w / b ratio may be able to compensate the loss in early strength due to the presence of fly ash. In other words, using fly ash to replace both cement and sand partially appears to have a synergistic effect combining the benefits of both separate replacements.

The results in Table 4-1 also show that the difference in compressive strength between 350 kg/m³ mixes and 450 kg/m³ mixes is small. Both mixes give 12 to 20 MPa at 3 days, 20 to 30 MPa at 7 days, and 30 to 40 MPa at 28 days. At one year, the compressive strength ranged from 55 to 60 MPa, and in excess of 60 MPa at 18 months.

Table 4-2 and Fig 4-2 show the rate of gain of compressive strength as a percentage of the 28 day strength. The results confirm the role of pozzolanic reaction. At 7 days, compressive strength values ranged from 60 % to 75 % for the 350 kg/m³ concretes, and from 76 % to 81 % for the 450 kg/m³ concretes of their 28 day strength. This was followed by a larger increment after long term water curing. This increment at 18 months ranged from 157 % to 187 % for the 350 kg/m³ mixes and from 163 % to 201 % for the 450 kg/m³ concretes compared to the 28 day strength. These data show that, as expected, the strength development, in general, increases with age for all the concrete mixtures. The data show that for moist cured specimens, the higher the compressive strength, the greater was the increase in strength up to 28 days. The percentage gain in strength of the higher strength concrete was greater than that of the low strength concrete. However, this is reversed after about six months ; the stronger the concrete the lower is its subsequent proportionate gain in moist cured concrete. These results show that when curing conditions are favourable, the pozzolanic reaction of fly ash continues over a long period, with the contribution of pozzolanic reaction being especially more prominent for flexural and tensile strength than for compressive strength [19].

**Table 4-1 Compressive strength of HVFA concrete under water curing
(Unit : MPa)**

Age (days)	350F	350SF	350S	450F	450SF	450S
1	6.2	6.5	7.2	6.4	6.7	7.1
3	12.3	15.0	19.3	14.5	16.3	19.1
7	20.0	27.8	31.1	24.1	29.7	32.1
28	33.2	37.1	41.4	31.0	39.1	39.5
90	42.7	47.9	61.6	43.9	55.5	60.0
180	49.3	61.4	59.4	53.5	61.7	65.2
360	55.0	58.4	61.9	57.5	59.3	63.0
540	62.2	60.1	64.8	62.4	63.8	67.5

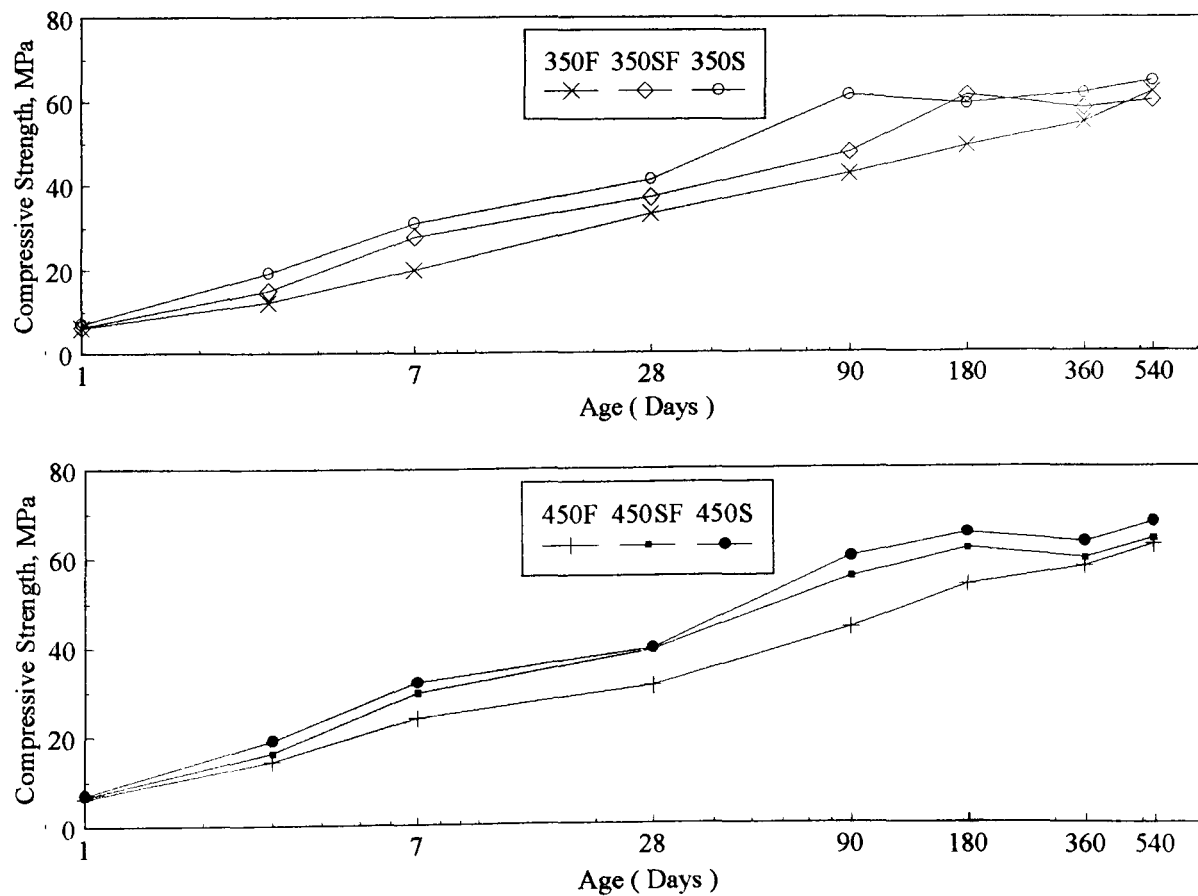


Figure 4-1 Compressive strength of HVFA concrete-Water curing

**Table 4-2 Rate of gain of compressive strength as a % of 28 days strength
(Water curing)
(Unit : %)**

Age (days)	350F	350SF	350S	450F	450SF	450S
1	19	18	17	20	17	18
3	37	40	47	47	42	48
7	60	75	75	78	76	81
28	100	100	100	100	100	100
90	129	129	149	142	142	152
180	148	165	143	173	158	165
360	166	157	150	185	152	159
540	187	162	157	201	163	171

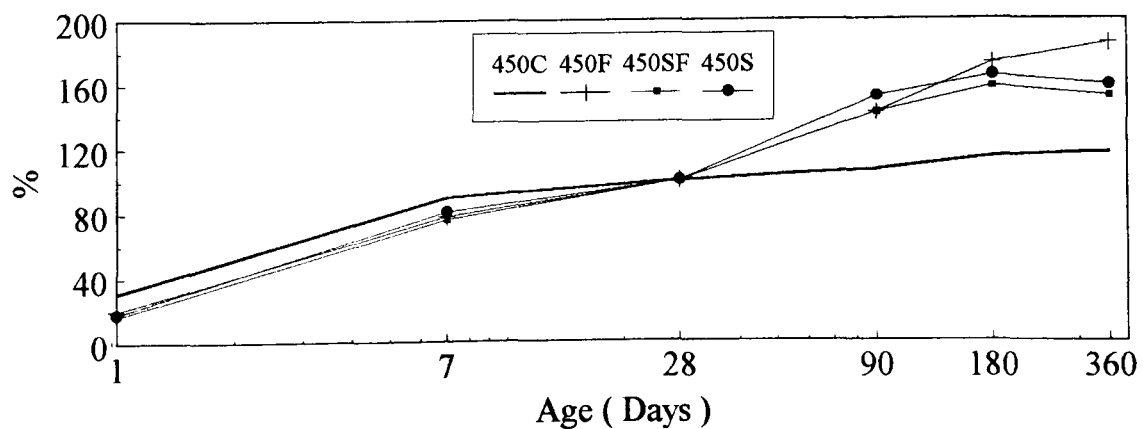
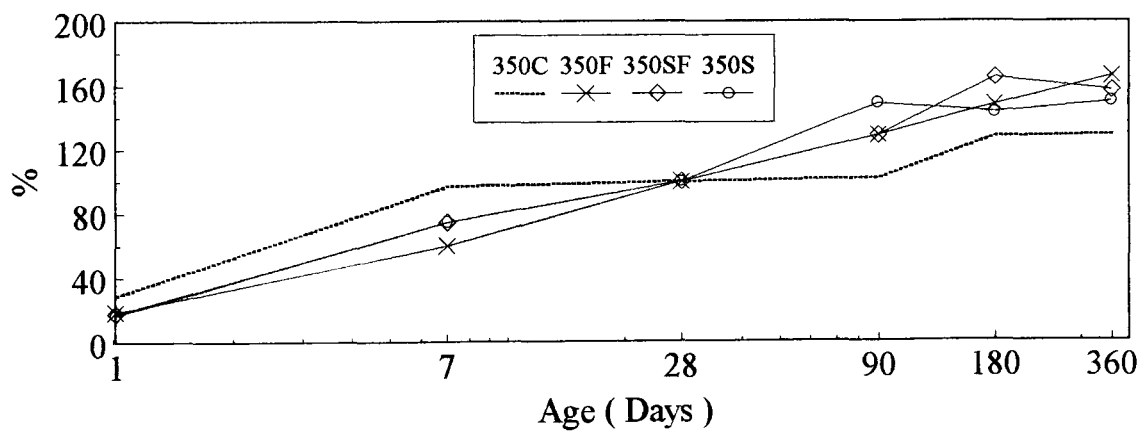


Figure 4-2 Rate of compressive strength as % of 28 days strength-Water curing

Fig 4-2 also shows that the 28 day strength appears to be some sort of a threshold stage. Before that mixes with pozzolanic materials appear to give lower strength than the control concrete, whereas beyond 28 days, the control concrete gives lower strength than the concrete with the pozzolanic materials.

Air curing on compressive strength development

Theoretically, curing is not generally considered as part of concrete mix design, but with mineral admixtures that depend on their reactivity to contribute to strength and durability, curing should be regarded as an essential ingredient of the mix design [6]. The strength development with age for concretes moist cured 7 days followed by air curing are shown in Table 4-3 and Fig 4-3.

Under air curing, the compressive strength development of all the concretes show a similar pattern to that previously observed with water curing, the strength increasing with increasing age for all the concrete mixtures. However, strength development is generally lower than that under water curing. All concrete mixtures had 28 to 40 MPa at 28 days compared to 33 to 41 MPa under water curing. Further, the data show that for all air cured specimens there is a gradual retrogression of compressive strength with continued air drying. At one year, the compressive strength of all air cured concretes was 47 to 62 MPa compared to 55 to 63 MPa for water curing. All the mixes except Mix-350S and Mix-450S generally showed lower strength than that water cured specimens. Surprisingly, Mix-350S, Mix-450S showed least loss of strength due to air drying. Both mixes gave about 57 ~ 58 MPa at 18 months compared to 65 ~ 68 MPa under water curing.

The rate of compressive strength development as a percentage of 28 days strength under air curing is shown in Table 4-4 and illustrated in Fig 4-4. The results show that the 7 day compressive strength values ranged from 70 % to 90 % for the 350 kg/m³ concretes and from 78 % to 84 % for the 450 kg/m³ concretes of their 28 days strength. These percentage values are higher than that the rate of compressive strength development under water curing.

**Table 4-3 Compressive strength of HVFA concrete under air curing
(Unit : MPa)**

Age (days)	350F	350SF	350S	450F	450SF	450S
1	6.2	6.5	7.2	6.4	6.7	7.1
3	12.3	15.0	19.3	14.5	16.3	19.1
7	20.0	27.8	31.1	24.1	29.7	32.1
28	28.4	29.9	38.9	28.6	38.1	39.3
90	41.0	46.0	56.3	42.7	56.0	58.5
180	42.0	56.5	61.9	51.7	54.6	63.0
360	46.8	54.8	60.9	47.0	55.7	62.0
540	47.1	52.6	58.2	45.9	56.4	57.2

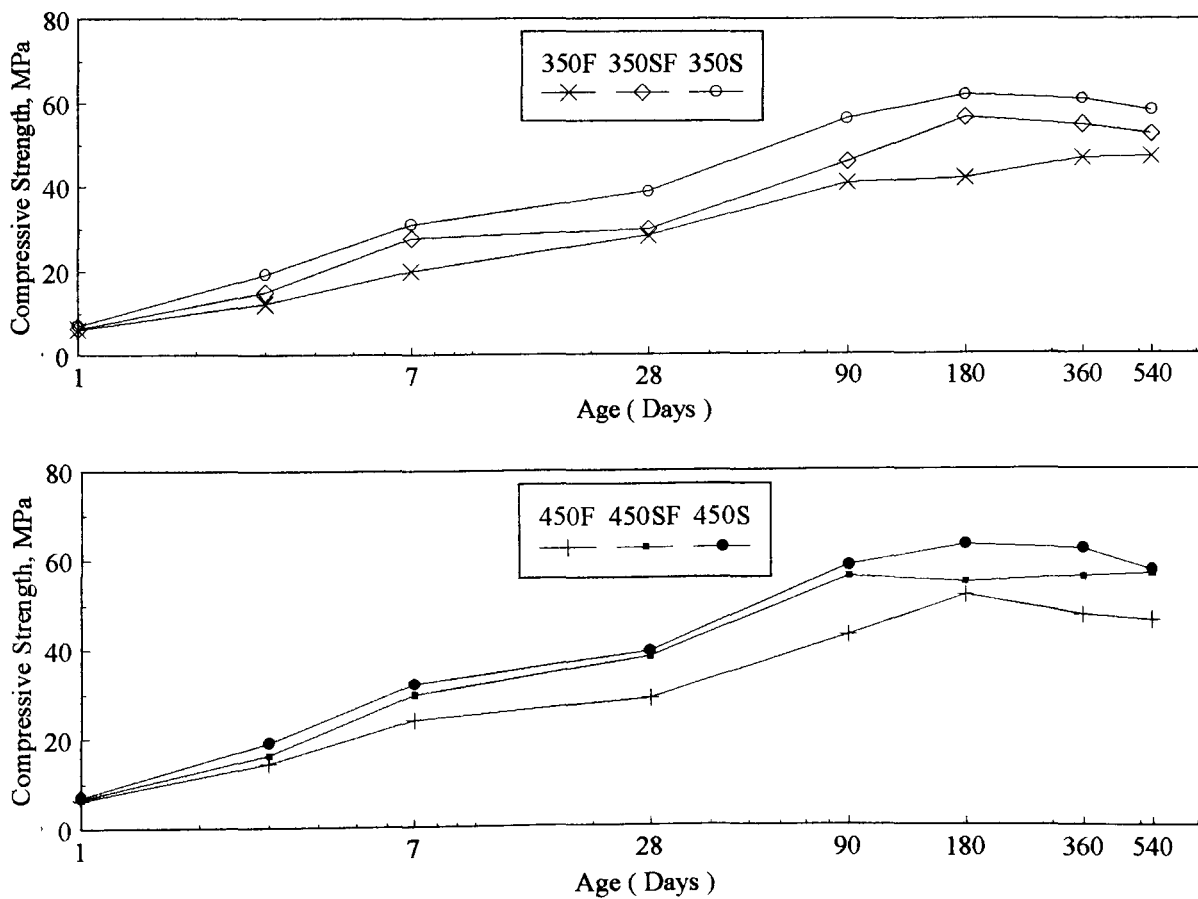


Figure 4-3 Compressive strength of HVFA concrete-Air curing

Table 4-4 Rate of gain of compressive strength as a % of 28 days strength (Air curing) (Unit : %)

Age (days)	350F	350SF	350S	450F	450SF	450S
1	22	22	18	22	18	18
3	43	50	50	51	43	49
7	70	93	80	84	78	82
28	100	100	100	100	100	100
90	144	154	145	149	147	149
180	148	189	159	181	143	160
360	165	183	157	164	146	158
540	166	176	150	160	148	146

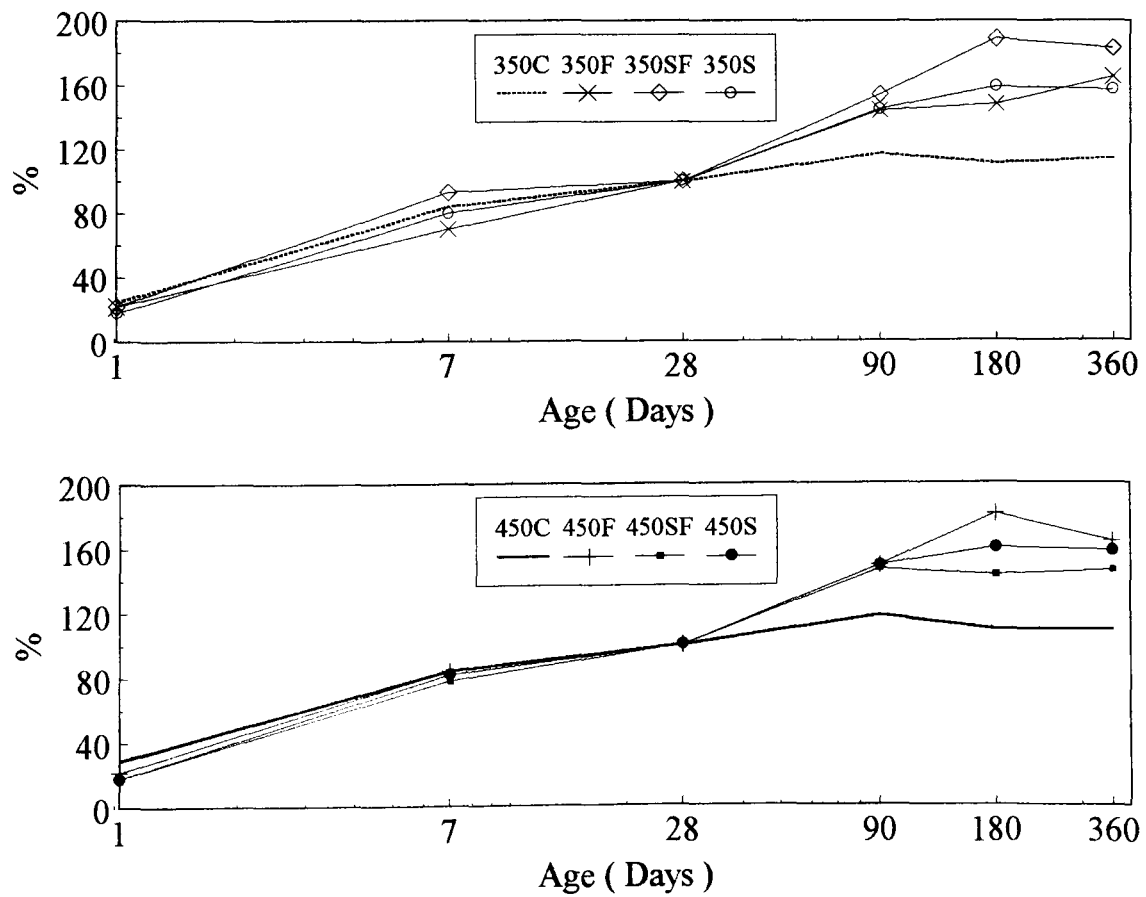


Figure 4-4 Rate of compressive strength as % of 28 days strength-Air curing

At one year and 18 months the rate of gain of strength under air curing was less than that under water curing

The relative rates of development of strength of HVFA concretes cured in water and in air are illustrated in Tables 4-5 and 4-6.

**Table 4-5 Influence of air curing on compressive strength-350 kg/m³ binder content
(Unit : %)**

Mix	350F		350SF		350S	
	Water curing	Air curing	Water curing	Air curing	Water curing	Air curing
28	100	85.5	100	80.6	100	94.0
90	100	96.0	100	96.0	100	91.4
180	100	85.2	100	91.7	100	104.2
360	100	85.1	100	93.8	100	98.4
540	100	75.7	100	87.5	100	89.8

**Table 4-6 Influence of air curing on compressive strength-450 kg/m³ binder content
(Unit : %)**

Mix	450F		450SF		450S	
	Water curing	Air curing	Water curing	Air curing	Water curing	Air curing
28	100	92.3	100	97.4	100	99.5
90	100	97.3	100	100.9	100	97.5
180	100	96.6	100	88.5	100	96.6
360	100	81.6	100	93.9	100	98.4
540	100	73.6	100	88.4	100	84.7

These results emphasize the effect of air curing in the long term. Air curing of all concrete mixtures exhibits a slight retrogression of strength with continued air drying. The average compressive strength of air cured concrete at 18 months varied from 76 % to 90 % for the 350 kg/m³ mixes, and from 74 % to 88 % for the 450 kg/m³ mixes of the water cured strength. It is recognized that high volume fly ash concretes are sensitive to moisture conditions.

The results indicate that the best development of strength gain occurs in moist curing rather than in air curing. The results also indicate that for a steady increase in strength for concrete incorporating high volume fly ash content a continuous moist environment is indispensable. In concretes with low water / cement ratios, once enough moisture is lost from the concrete, so that the internal relative humidity drops below about 80 % either by evaporation or self-desiccation, hydration will stop and strength development will be reduced below its potential, and this reduction will be greater in the case of high-strength concrete (low water / cement ratio) than it is in the case of low-strength concrete (high water / cement ratio) [13]. The loss of potential strength in the long term is a more widespread and insidious problem, but it is avoidable. Therefore, it is desirable to provide additional moisture during curing to ensure maximum hydration.

Concrete can be damaged by lack of proper curing. It is essential for the development of high strengths that the concrete should be kept moist for as a long period possible, and not allowed to dry out , until the concrete strength has attained its specific strength. Obviously, this is seldom a practical proposition, and some loss in strength is inevitable to allow acceptable construction schedules and to minimise cost.

The ACI Recommended Practice for moist curing for most structural concrete, is the time necessary to attain 70 % of the specified compressive or flexural strength, whichever is less. Various investigators have concluded that the percentage of strength of dry cured concrete to that of water cured concrete is between 60 % to 90 %, or sometime this varies even more widely.

The results from the present investigation of all concrete mixtures under air curing gave strength values from 70 % to 90 % to that under water curing at 18 months. These data emphasize dramatically the need for early incorporation and a minimum period of water curing as an integral part of mix proportioning fly ash concrete.

4-2-2. Effect of curing condition on flexural strength

The data on flexural strength development are presented in Tables 4-7, 4-9, and illustrated in Figs 4-5 and 4-7. The flexural strength expressed as a percentage of 28 day values are given in Table 4-8 and 4-10 and in Figs 4-6 and 4-8.

These results show that the development of flexural strength occurs in a similar way to that of the compressive strength for moist and dry cured specimens. As for compressive strength, air cured concrete showed lower flexural strengths compared to concrete subjected to continuous moist curing. At 18 months, flexural strength under moist curing varied from 5.7 to 6.4 MPa for the 350 kg/m³ mixes compared to 5.5 to 6.5 MPa for air cured specimens. Similarly, the flexural strength of 450 kg/m³ mixes under water curing varied from 5.8 to 6.6 MPa compared to 5.8 MPa for air cured concrete.

The rates of strength development in Tables 4-8 and 4-10 show similar patterns to compressive strength. Although the higher strength concrete had lower percentage gain, the flexural strength value in the stronger concrete was higher than that in the low strength concrete.

The relative rates of development of strength of high volume fly ash concrete cured in water and in air are illustrated in Tables 4-11 and 4-12. At the end of 18 months, all concrete mixtures exhibited a very minimal reduction in flexural strength with continued air drying, i.e. about 97 % of the average strength for water cured concrete. Except Mix-450S which showed a higher loss.

**Table 4-7 Flexural strength of HVFA concrete under water curing
(Unit : MPa)**

Age (days)	350F	350SF	350S	450F	450SF	450S
1	1.30	1.79	1.85	1.33	1.81	1.87
3	2.25	3.04	3.27	2.23	3.07	3.25
7	2.78	3.07	3.70	2.87	3.15	3.87
28	3.48	4.52	4.78	3.56	4.61	4.89
90	5.07	5.51	5.83	5.19	5.65	6.54
180	5.25	5.69	6.65	5.46	6.51	6.23
360	5.55	5.71	5.85	5.67	5.75	6.63
540	5.70	5.74	6.36	5.76	5.88	6.60

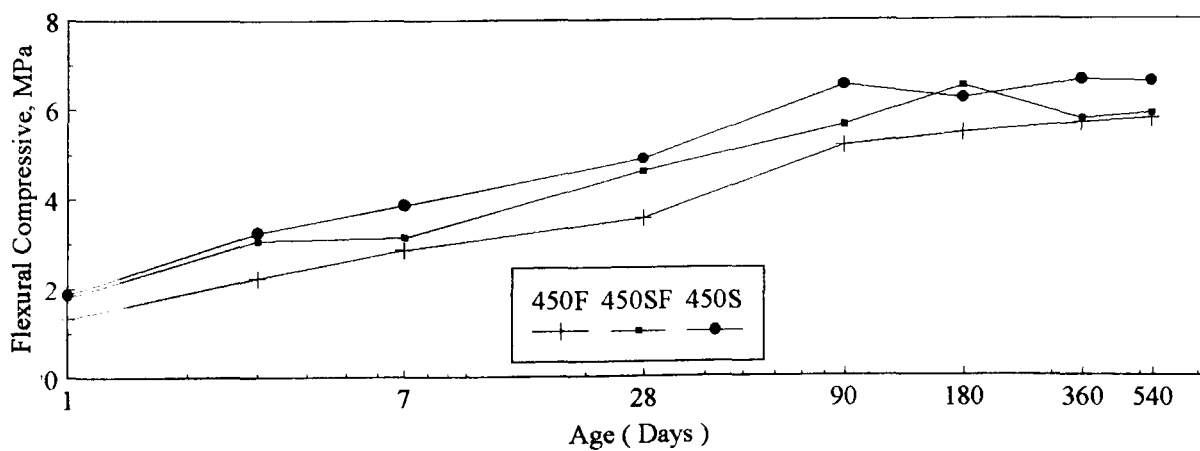
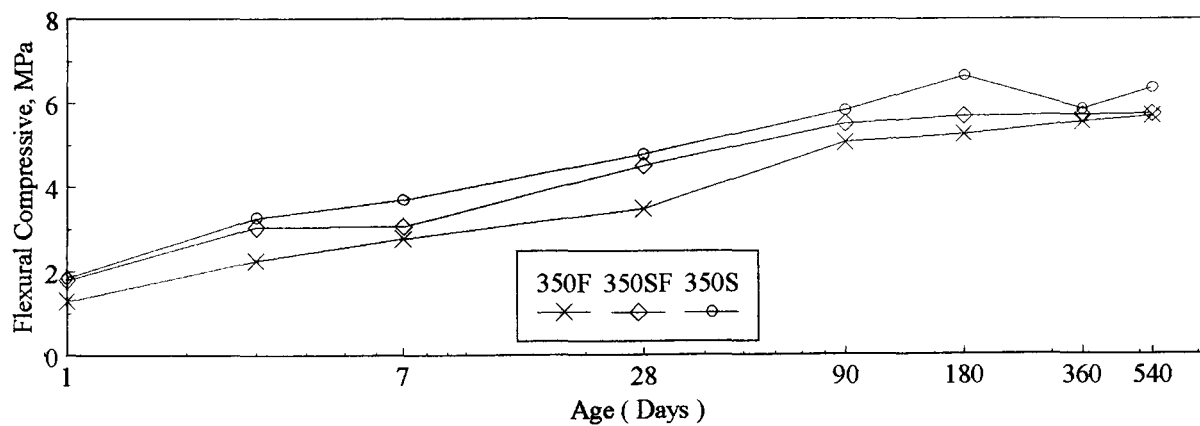


Figure 4-5 Flexural strength of HVFA concrete-Water curing

**Table 4-8 Rate of gain of flexural strength as a % of 28 day strength
(Water curing)
(Unit : %)**

Age (days)	350F	350SF	350S	450F	450SF	450S
1	37	40	39	37	39	38
3	65	67	68	63	67	66
7	80	68	77	81	68	79
28	100	100	100	100	100	100
90	146	122	122	146	123	134
180	151	126	139	153	141	127
360	159	126	122	159	125	136
540	163	127	133	162	128	135

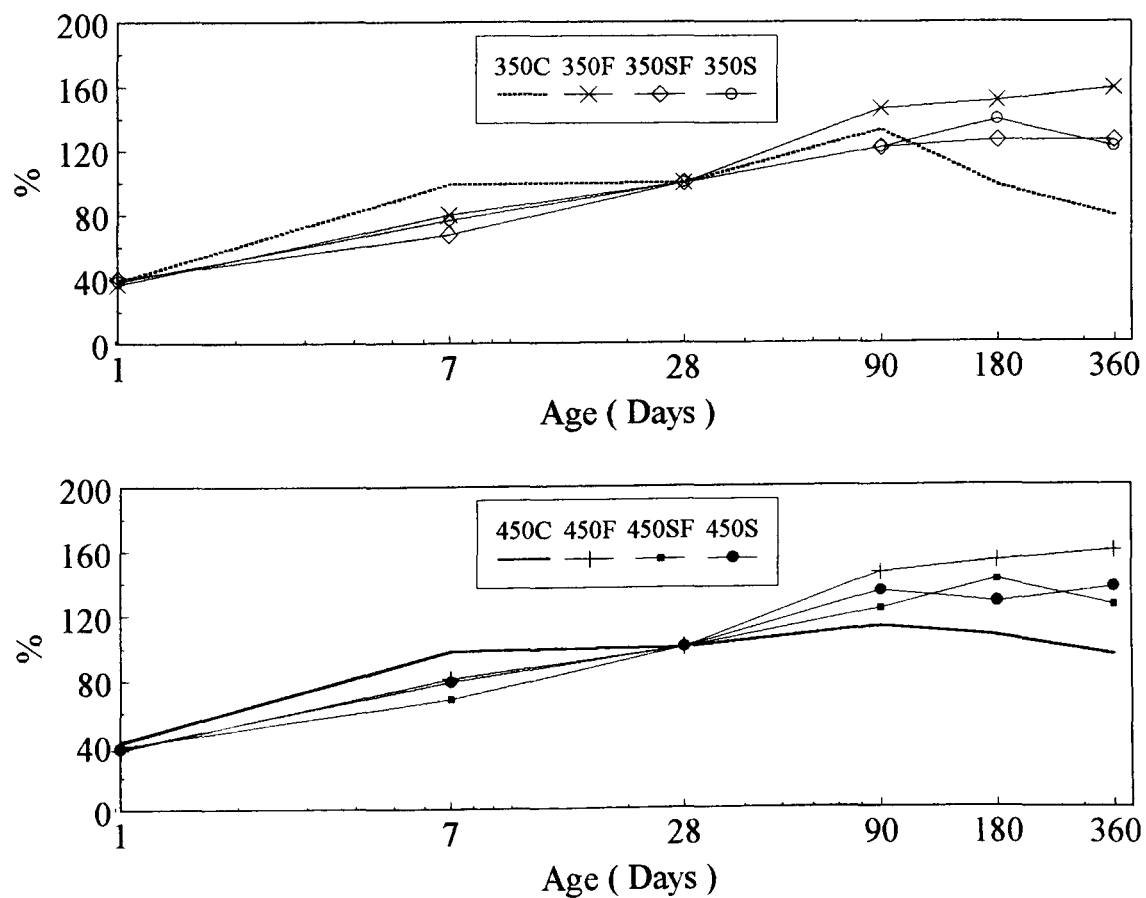


Figure 4-6 Rate of flexural strength as % of 28 days strength-Water curing

**Table 4-9 Flexural strength of HVFA concrete under air curing
(Unit : MPa)**

Age (days)	350F	350SF	350S	450F	450SF	450S
1	1.30	1.79	1.85	1.33	1.81	1.87
3	2.25	3.04	3.27	2.23	3.07	3.25
7	2.78	3.07	3.70	2.87	3.15	3.87
28	3.17	3.18	3.89	3.23	3.29	3.95
90	5.03	5.15	6.18	5.13	5.22	6.36
180	4.48	5.22	5.91	4.58	5.67	6.09
360	4.89	4.89	5.70	4.91	5.19	6.14
540	5.49	5.52	6.54	5.85	5.76	5.79

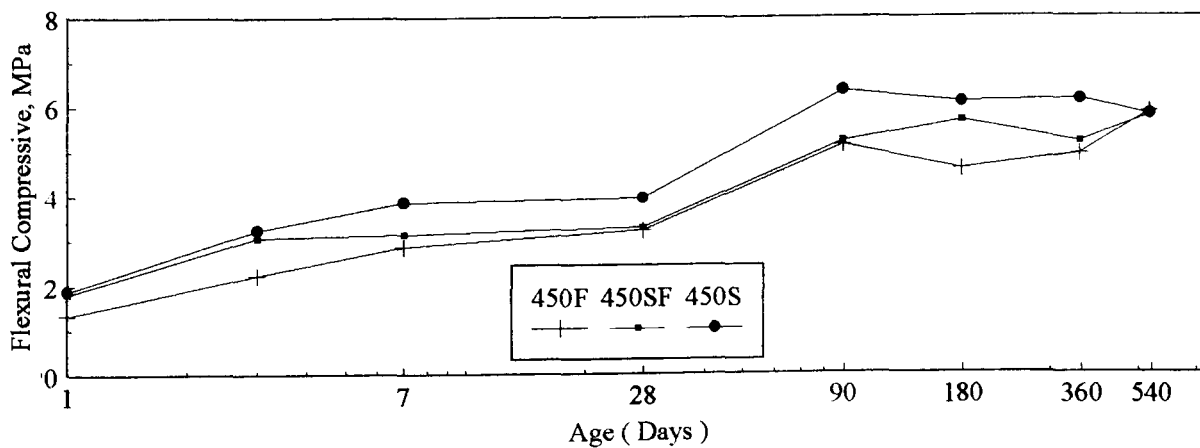
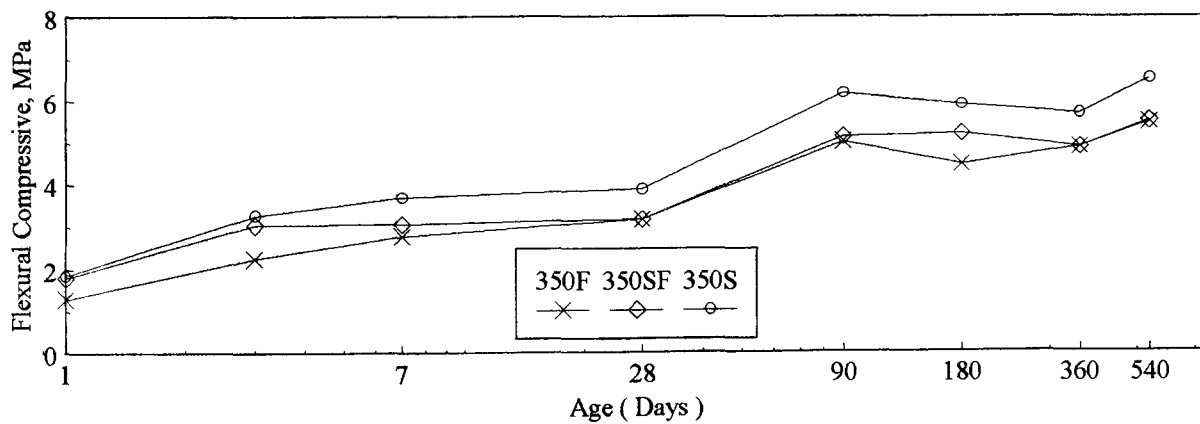


Figure 4-7 Flexural strength of HVFA concrete-Air curing

**Table 4-10 Rate of gain of flexural strength as a % of 28 days strength
(Air curing)
(Unit : %)**

Age (days)	350F	350SF	350S	450F	450SF	450S
1	32	56	48	41	55	47
3	71	96	84	69	93	82
7	88	97	95	89	96	98
28	100	100	100	100	100	100
90	159	162	159	159	159	161
180	141	164	152	142	172	154
360	154	154	147	152	158	155
540	173	174	168	181	180	147

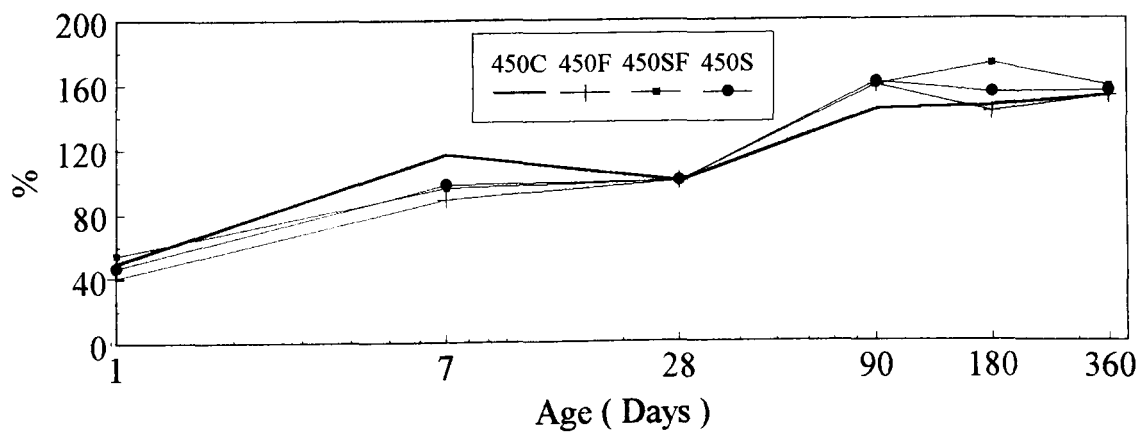
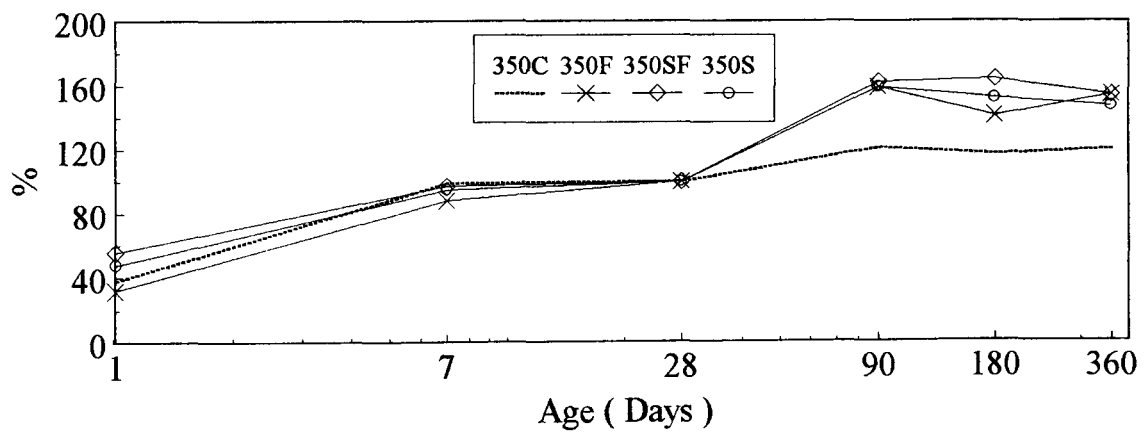


Figure 4-8 Rate of flexural strength as % of 28 days strength-Air curing

**Table 4-11 Influence of air curing on flexural strength-350 kg/m³ binder content
(Unit : %)**

Mix	350F		350SF		350S	
	Water curing	Air curing	Water curing	Air curing	Water curing	Air curing
28	100	91.1	100	70.4	100	81.4
90	100	99.2	100	93.5	100	106
180	100	85.3	100	91.7	100	88.9
360	100	88.1	100	85.6	100	97.4
540	100	96.3	100	96.2	100	102

**Table 4-12 Influence of air curing on flexural strength-450 kg/m³ binder content
(Unit : %)**

Mix	450F		450SF		450S	
	Water curing	Air curing	Water curing	Air curing	Water curing	Air curing
28	100	90.7	100	71.4	100	81.8
90	100	98.8	100	92.4	100	97.2
180	100	83.9	100	87.1	100	97.8
360	100	86.6	100	90.3	100	92.6
540	100	101.6	100	98.0	100	87.7

These results thus show that the decrease in flexural strength of air cured concretes is relatively small, and almost negligible. The results indicate that air curing preceded by moist curing, even for a short period, seems to have beneficial effects on strength development. These results are in accordance with those reported by Swamy who studied the effect of initial 7 day water curing on fly ash concrete, and indicated that early water curing for a minimum period of seven days is an essential ingredient

for the successful use and full realisation of the strength potential of fly ash concrete [6].

4-2-3. Relationship between flexural strength and compressive strength

The relationship between flexural and the compressive strength is generally of the form : [13]

$$f = a f_c^b \text{ ----- (4-1)}$$

where f is the flexural strength in MPa, f_c is the compressive strength in MPa, and a and b are constants.

The variation of flexural strength with compressive strength, for HVFA concrete is shown in Figs 4-9 and 4-10 for water and air curing respectively. The relationship shown is based on results tested at 1 day to 18 months for moist cured and dry cured HVFA concrete.

Regression analysis defining the relationship between the two strength properties gave as follows :

$$f = 0.52 f_c^{0.59} \text{ (moist) (} r = 0.98 \text{) ----- (4-2)}$$

$$f = 0.53 f_c^{0.58} \text{ (dry) (} r = 0.96 \text{) ----- (4-3)}$$

where r is the correlation factor.

The correlation factor for the two sets of equations is high, and hence, in practice, a single equation describing the two strength parameters can be used as given below and shown in Fig 4-11.

$$f = 0.52 f_c^{0.59} \text{ (moist + dry) (} r = 0.97 \text{) ----- (4-4)}$$

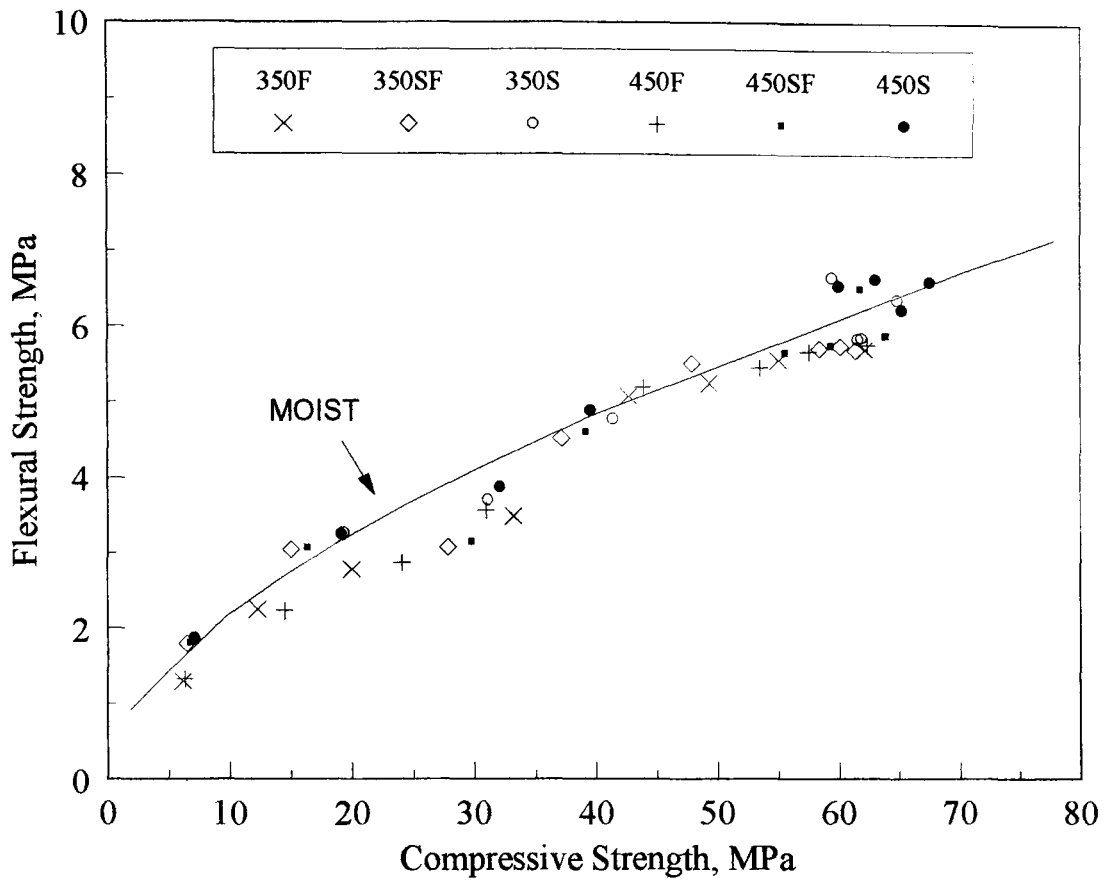


Figure 4-9 Relationship between flexural strength and compressive strength of HVFA concrete-Water curing

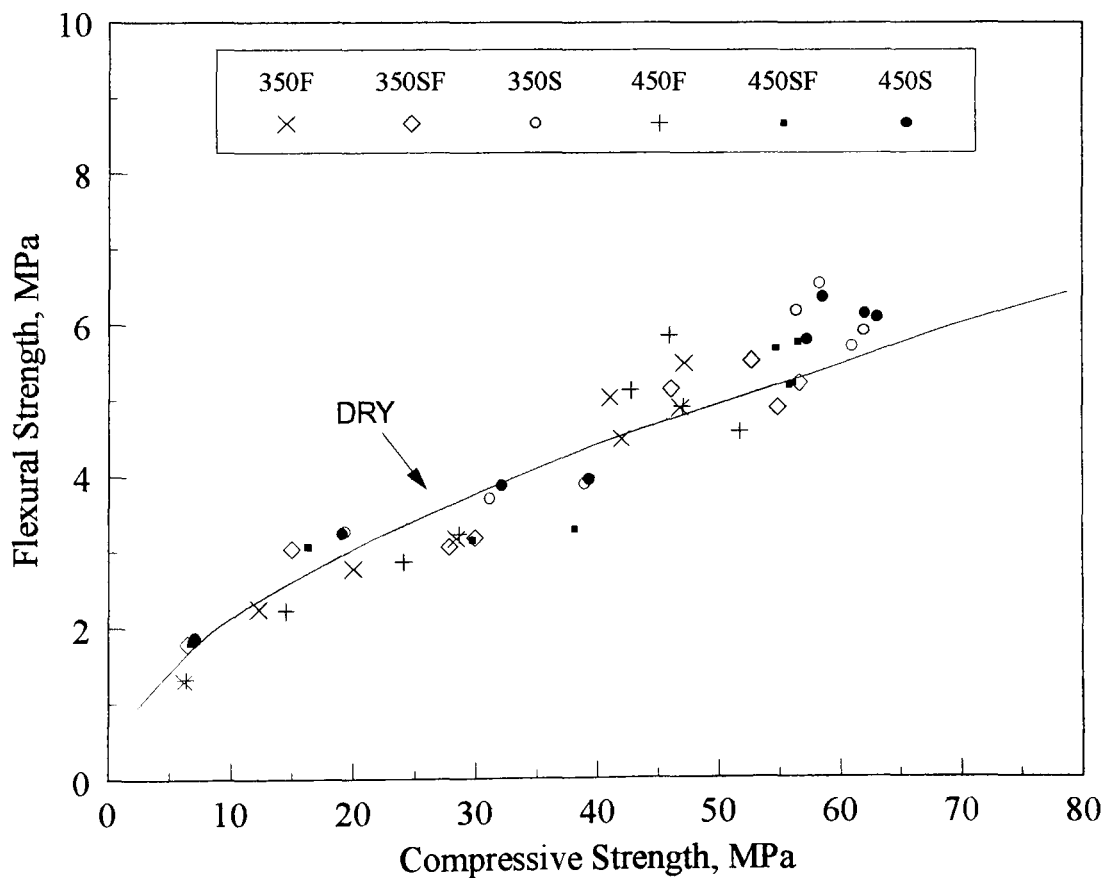


Figure 4-10 Relationship between flexural strength and compressive strength of HVFA concrete-Air curing

These data indicate a significant correlation between flexural strength and compressive strength of HVFA concretes at the 99 % confidence level. In other words, as the compressive strength, f_c , increases, the flexural strength, f , also increases.

Fig 4-11 is also compared to the data suggested by Swamy & Mahmud and the relationship obtained from several other authors [9,27,59,60]. Regression analysis of the data shown in the Fig 4-11 produced the following relationship :

$$f = 0.31 f_c^{0.71} \text{ (moist + dry) } (r = 0.97) \text{ ---- (4-5) Swamy \& Mahmud [59]}$$

$$f = 1.71 f_c^{0.33} \text{ (moist) } (r = 0.64) \text{ ---- (4-6) EPRI [9]}$$

$$f = 1.18 f_c^{0.46} \text{ (moist) } (r = 0.80) \text{ ---- (4-7) Langley et al [60]}$$

$$f = 1.17 f_c^{0.44} \text{ (moist) } (r = 0.95) \text{ ---- (4-8) Malhotra et al [27]}$$

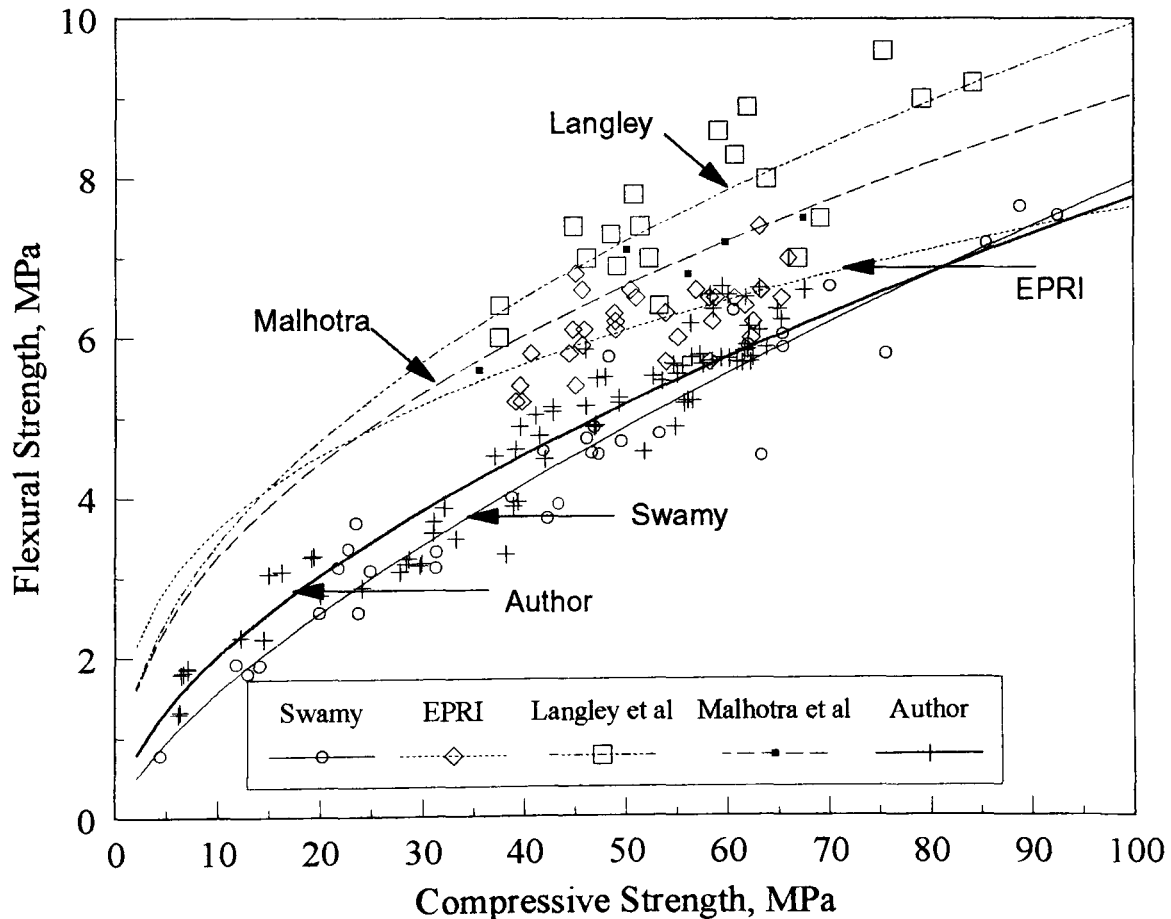


Figure 4-11 Relationship between flexural strength and compressive strength of HVFA concrete

The results in Fig 4-11 show a wide variation in strength development ; this is mainly due to the way the HVFA concretes are proportioned, differences in initial and type of curing, water / binder ratio, and age of testing. It can be observed from the figure that the author's results do not diverge greatly from a single relationship. Also, it is very comforting to see, a close similarity to the HVFA concrete data obtained from Swamy & Mahmud.

Regression analysis showed that the coefficient, "r", using strength development data in this relationship, was high for Swamy's and author's equations; they are higher than those given by the EPRI and Langley et al. Due to different test variables, it is difficult to interpret these results, and give definitive conclusions. However, it is obvious from the data that concrete having a high cementitious content, low water content and adequate curing, are most likely to possess a well-developed strength.

4-2-4. Comparison with normal OPC concrete

The strength characteristics of HVFA concretes can be clearly inferred from Tables 4-1, 4-3, 4-7, and 4-9. The results also indicate the need for a well-defined period of water curing for the strength development of such concrete. It would then be interesting to compare the strength development of HVFA concretes with that of normal portland concrete at different ages, and under different curing conditions.

Table 4-13 represents the strength data for both OPC concretes under both types of curing conditions. The rate of OPC concrete strength development as a percentage of 28 day strength development compared to all HVFA concretes is also shown in Figs 4-2, 4-4, 4-6, and 4-8.

Irrespective of the curing conditions, the rate of strength development in both compression and flexure for both OPC concretes is higher than that for HVFA

concretes at an early age, but after 28 days, it is lower than that for HVFA concretes under the same conditions.

Table 4-13 Strength development of normal OPC concrete

A. 350 kg/m³ mixes

Strength	Compressive strength		% of 28 day strength		Flexural strength		% of 28 day strength	
	Age (days)	Water curing	Air curing	Water curing	Air curing	Water curing	Air curing	Water curing
1	18.0	18.0	29	25	2.56	2.56	39	38
7	60.0	60.0	97	84	6.59	6.59	99	99
28	61.9	71.0	100	100	6.63	6.66	100	100
90	62.9	83.0	102	117	8.80	8.09	133	121
180	79.4	78.8	128	111	6.48	7.77	98	117
360	80.0	80.6	129	114	5.25	7.98	79	120

B. 450 kg/m³ mixes

Strength	Compressive strength		% of 28 day strength		Flexural strength		% of 28 day strength	
	Age (days)	Water curing	Air curing	Water curing	Air curing	Water curing	Air curing	Water curing
1	20.2	20.2	31	29	2.69	2.69	42	50
7	59.5	59.5	90	84	6.32	6.32	98	117
28	66.2	70.5	100	100	6.42	5.40	100	100
90	70.0	83.2	106	118	7.19	7.80	112	144
180	75.2	76.5	114	109	6.83	7.88	106	146
360	77.7	77.1	117	109	6.03	8.19	94	152

Remark : Compressive and flexural strength values are given in MPa

From the results, it can be seen that under continued moist curing condition, the percentage increase in compressive strength from 28 days to one year is 17 % ~

29 % for all normal OPC concretes. The corresponding increase in compressive strength for the HVFA concretes was 50 % ~ 85 % (Table 4-2). At the end of one year, the percentage gain of flexural strength of OPC concrete was only 79 % ~ 94 % of the 28 day flexural strength. The corresponding percentage gain in flexural strength for the HVFA concretes was 122 % ~ 159 % of the 28 day flexural strength (Table 4-8). The normal OPC concrete exhibited a slight degradation in flexural strength even under continuous moist curing. For the concrete Mix-450F, the percentage of compressive strength increase was more rapid after 90 days. Under water curing, the difference between 450F and 450C on compressive or flexural strength at one year was about 65 % respectively. These observations indicate the potential for strength growth at later ages for fly ash concretes in constant contact with moisture.

The results also indicate that under air curing, some loss of strength occurs with OPC concretes with age, whereas HVFA concretes are more likely to maintain hydration process with a gradual rate of increase. At the end of one year, a slight retrogression of strength on HVFA concretes with air curing was similar to that of normal OPC concrete, but the percentage gain on HVFA concrete was still higher. For example, the difference between 350SF and 350C, 450SF and 450C at one year with air curing was 69 % and 37 % on compressive strength, and 34 % and 6 % on flexural strength, respectively.

These results indicate that even under continuous air drying, the HVFA concretes are able to continue hydration process, although at a slower rate.

The superiority in the rate of later age strength development of the HVFA concretes is clearly seen, even though had lower strength than that of OPC concretes. This increase in the rate of strength development of the HVFA concretes over that of OPC concretes was about 40 % of the average values on compressive strength, and 30 % on the flexural strength. The incorporation of fly ash, silica fume and a superplasticizer in HVFA concrete is thus clearly beneficial to its long term strength development.

4-2-5. Comparison with total binder content

The effect of total binder content on concrete strength development under both types of curing conditions is shown in Figs 4-12, 4-13, 4-14, and 4-15. The results suggest several aspects related to the role played by the superplasticizer and the binder content. For purposes of comparison, the results for the normal portland cement concrete are also included in the above figures.

The results show that the total cementitious binder content does not have much effect on the value of strength. In general, concrete with 450 kg/m^3 is only marginally better than 350 kg/m^3 mixes under both types of curing conditions.

In the current study, the compressive strength of 450C under both curing conditions was somewhat lower than that of the concrete made of 350C. Previous discussion has shown that the concretes of 450C had superplasticizer demand of 2.5 %, higher than that for the concrete of 350C. The lower strength of concrete with increasing dosage of superplasticizer is due, at least in part, to the greater fluidity and the accompanying segregation and bleeding that occur in these concretes. These results conform to the explanation of Goldman and Bentur [66] who used progressively more superplasticizer as the silica fume content of their concrete was increased. It appears that, although the workability of their concrete was enhanced, the concretes became too fluid at the higher superplasticizer contents, resulting in a reduction in strength similar to that observed in this study.

The results stress two points : that for the HVFA concrete to have a certain specified strength, it is important to choose a suitable cementitious binder content with the object of producing, as economically as possible, concrete of the required strength. In addition, the selection of mix proportions has to take into account the method of transporting the HVFA concrete, especially if pumping is envisaged.

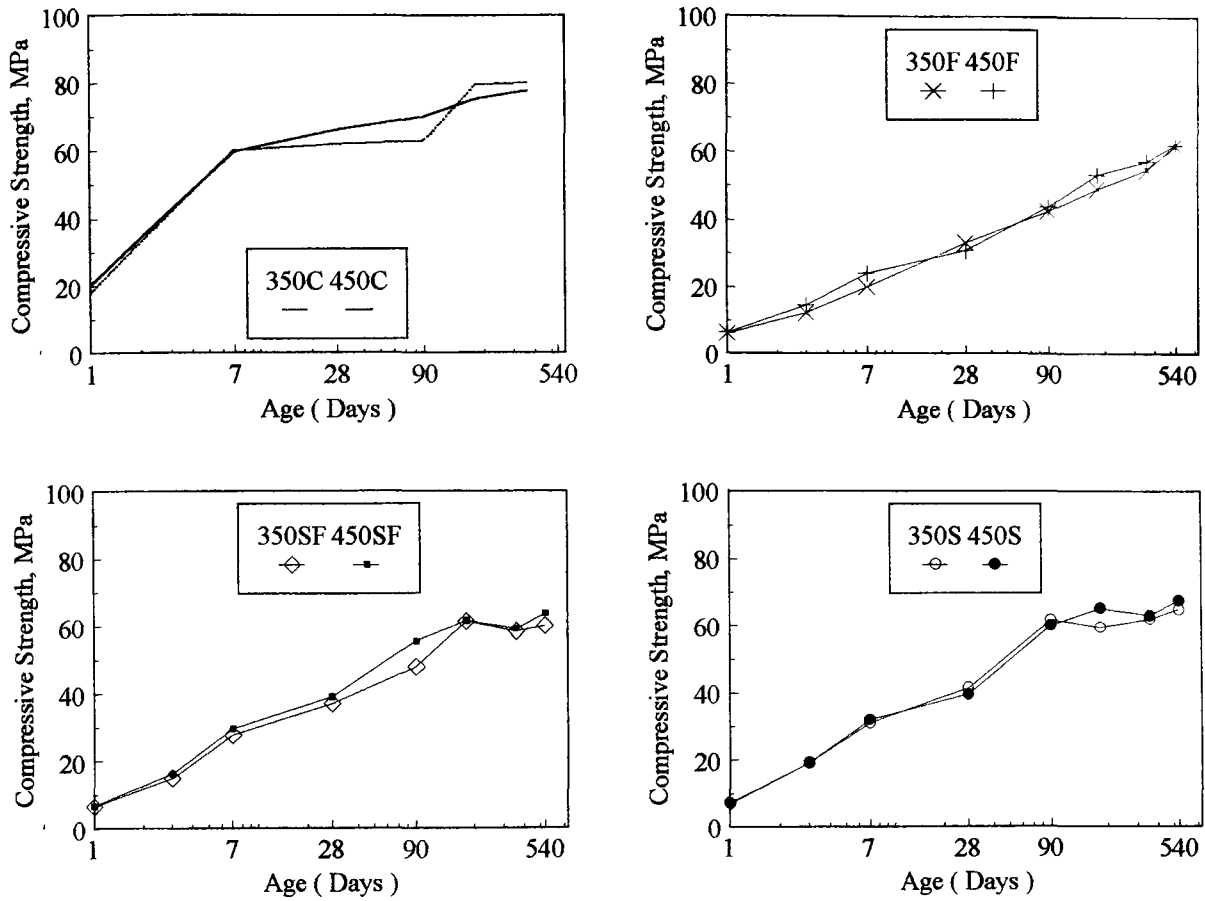


Figure 4-12 Effect of total binder content on compressive strength (Water Curing)

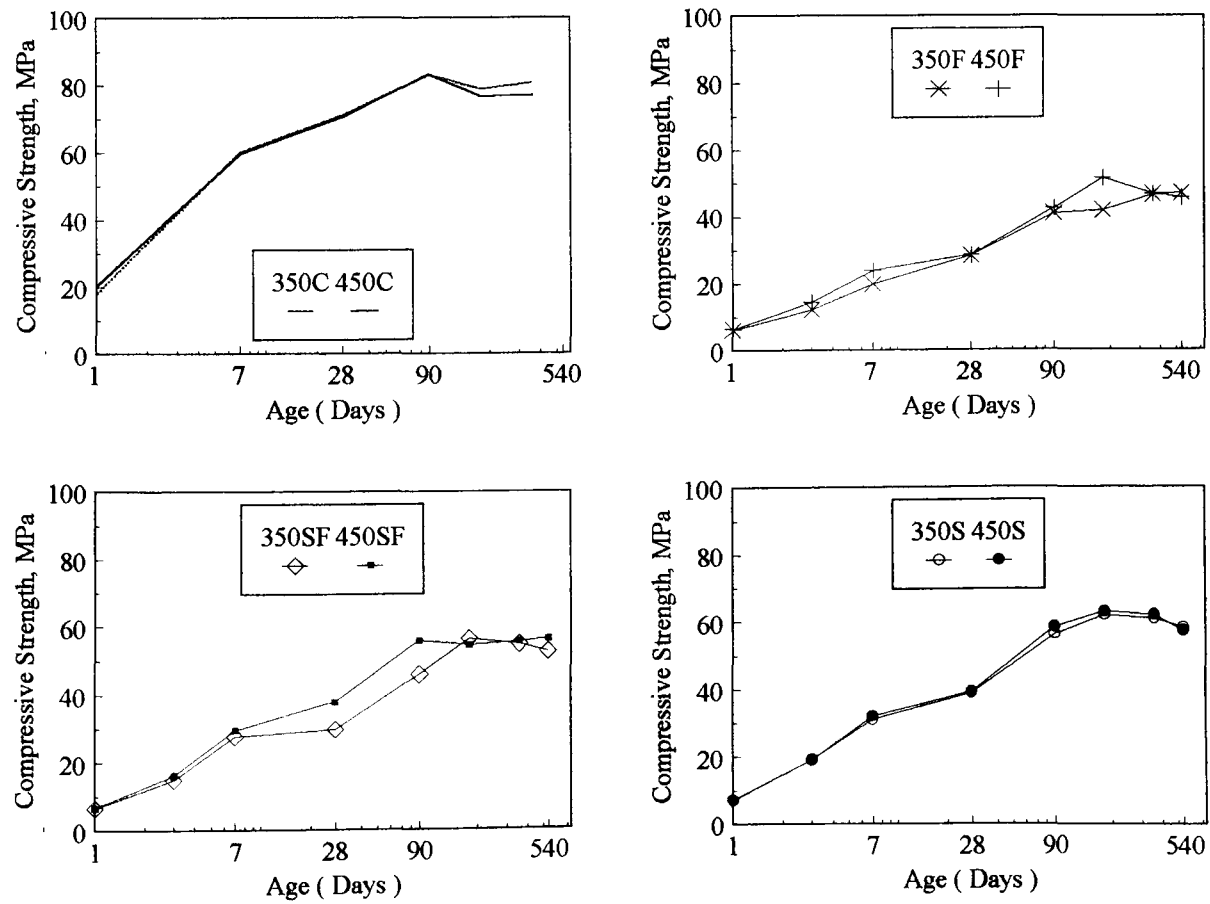


Figure 4-13 Effect of total binder content on compressive strength (Air curing)

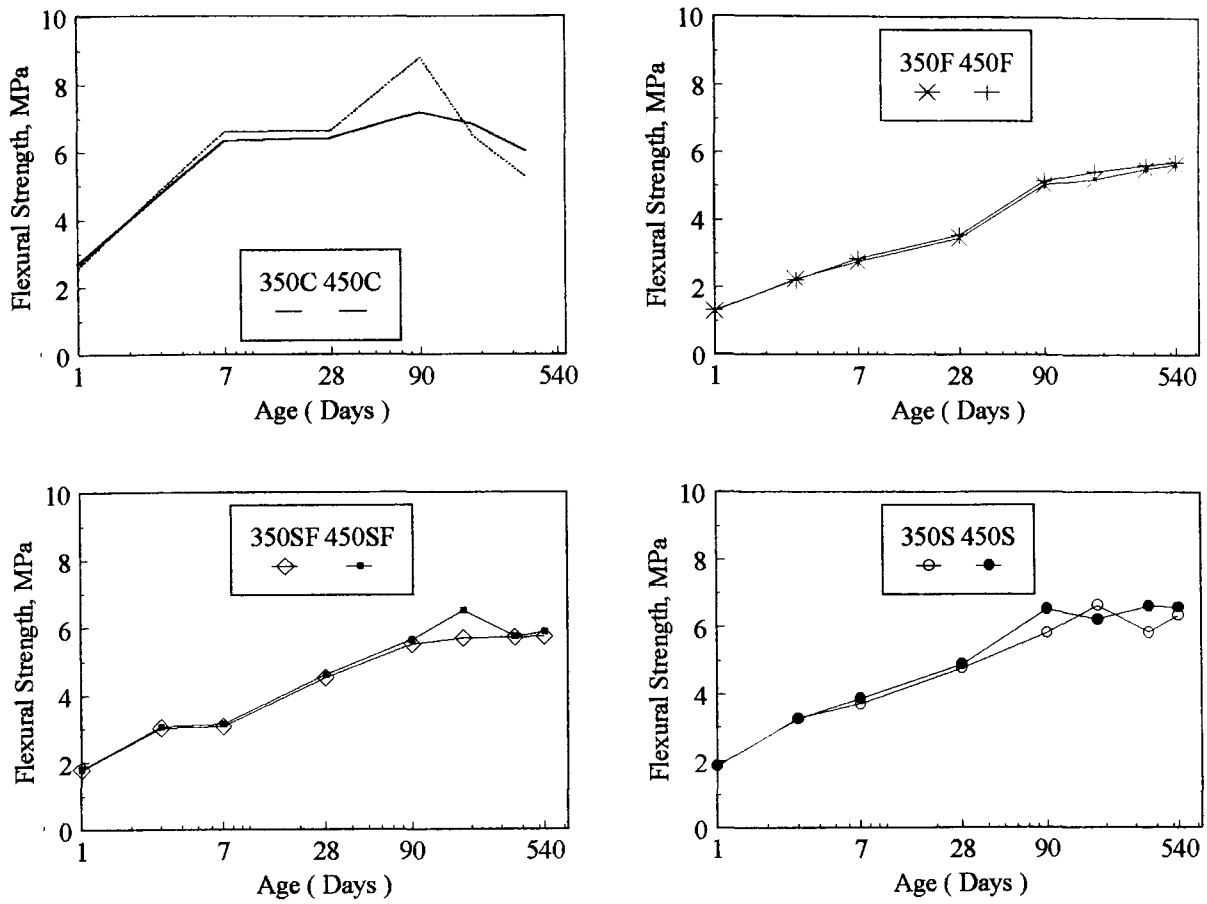


Figure 4-14 Effect of total binder content on flexural strength (Water curing)

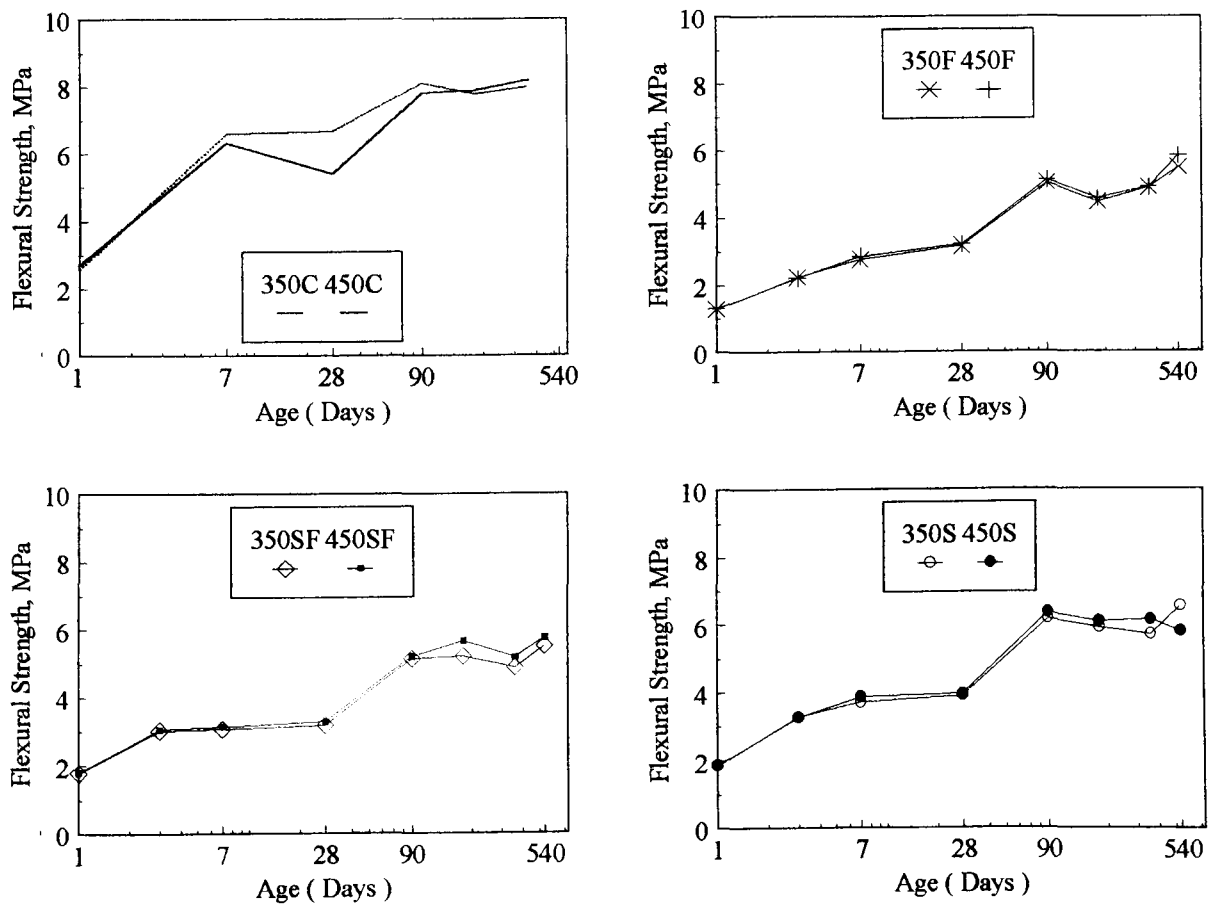


Figure 4-15 Effect of total binder content on flexural strength (Air Curing)

4-3. COMPARISON OF STRENGTH DEVELOPMENT WITH PUBLISHED DATA

The results of the present study emphasize the importance of the characteristics of concrete incorporating high volume fly ash. Compressive strength is in the range 30 to 40 MPa at 28 days, and 40 to 60 MPa was achieved for all the HVFA concretes at the age of 90 days. In published research, a higher amount of cementitious binder content, and lower water / binder ratios have been used to produce HVFA concrete systems. Swamy and Mahmud [59], for example, produced HVFA concrete with cube compressive strength of 23.7 to 63.3 MPa and prism flexural strength of 2.6 to 4.5 MPa at 28 days, using a total cementitious binder content of 266 ~ 466 kg/m³ and water / binder of 0.32 ~ 0.62. Malhotra and Giaccio used [61] cementitious content of 375 kg/m³ with water / binder 0.31, and the cylinder compressive strength of HVFA concrete was 32.5 MPa at 28 days, and 41 MPa at 91 days. Langley et al [60] developed HVFA concrete cylinder compressive strength of 23 to 57 MPa, and 38 to 75 MPa, and 6 to 6.9 MPa, and 8.9 to 9.6 MPa flexural strength at 28 days and 90 days respectively. The HVFA concrete was produced using a total binder content of 225 ~ 400 kg/m³ with water / binder 0.28 ~ 0.49. In Electric Power Research Institute (EPRI) research [9], a cementitious content of 365 kg/m³ with a water / binder 0.33 was used, and the cylinder compressive strength of HVFA concrete varied from 27.8 to 42.2 MPa at 28 days, with 50 MPa at 91 days. The prism flexural strength reached 5.2 ~ 6.5 MPa at 91 days. Table 2-5 in Chapter 2 also shows a comparison of strength development obtained from other investigators.

4-4. SWELLING OF HIGH VOLUME FLY ASH CONCRETE

Cement paste or concrete cured continuously in water from the time of placing exhibits a net increase in volume and an increase in mass. This swelling is due to the absorption of water by the cement gel ; the water molecules act against the cohesive forces and tend to force the gel particles further apart, with a resultant swelling

pressure. In addition, the ingress of water decreases the surface tension of the gel, and a further small swelling takes place.

Even though swelling associated with ettringite formation is known to be responsible for both deleterious and beneficial phenomena in portland cement concretes, this swelling, however, can make the concrete porous and permeable.

In this section a detailed analysis of the swelling of HVFA concretes is presented, and the results discussed in terms of the different replacement materials and the total cementitious content. Under water curing condition, the swelling each specimen was measured on all four sides, and the results are thus the average of twelve readings.

Typical swelling test data for all HVFA concretes are shown in Table 4-14 and illustrated in Figs 4-16 and 4-17.

The results show that the final swelling varied over a narrow range, between 100 and 125 micro-strain depending on the total cementitious content. The swelling initially increased rapidly, after which there was a steady increase with continued water curing. Between 9 months and one year, there was some sharp increase in swelling of all the HVFA concretes, beyond which the rate of swelling became more stabilized till the end of test period. In general, the concrete mix with 450 kg/m³, showed lower swelling. At the end of 504 days, the swelling value varied from 105×10^{-6} to 125×10^{-6} for the 350 kg/m³ mixes and 100×10^{-6} to 120×10^{-6} for the 450 kg/m³ concretes.

**Table 4-14 Swelling strain of HVFA concrete (Water curing)
(Unit : 10^{-6} m/m)**

Age (days)	350F	350SF	350S	450F	450SF	450S
1	0.00	0.00	0.00	0.00	0.00	0.00
7	49.25	38.33	46.25	45.13	36.12	45.23
28	58.33	48.67	56.25	46.45	41.79	52.21
91	68.16	51.75	65.12	53.78	38.52	46.67
189	84.33	56.01	82.33	86.12	44.83	61.25
364	115.21	94.33	113.67	113.21	85.45	97.45
504	124.67	104.67	116.01	118.67	97.33	109.21

The results also show that the HVFA concretes incorporating small amount of silica fume benefited marginally to suppress swelling. This finding implies that silica fume acted on the one hand as an intensifier of pozzolanic reaction, and on other, as an activator of fly ash, while the combined influence of silica fume and fly ash control led swelling to an even greater extent.

In view of the swelling of this type at an early age, it can be related to the hydration process in concrete. According to the swelling theory [67] swelling occurs because of wetting of the ettringite particles that are of colloidal size ($< 1 \mu\text{m}$ in length), from a topochemical growth of ettringite pushing against solid material in the concrete. The early hydration reaction is located at the acceleration stage of the calorimetric curve which is due to the formation of ettringite as the hydration of C_3A and sulphate ion occurs, and the extra pressure of the inner part in C_3S grains accelerates the concentration of calcium, in which a large amount of CH crystal as well as C-S-H gel will form.

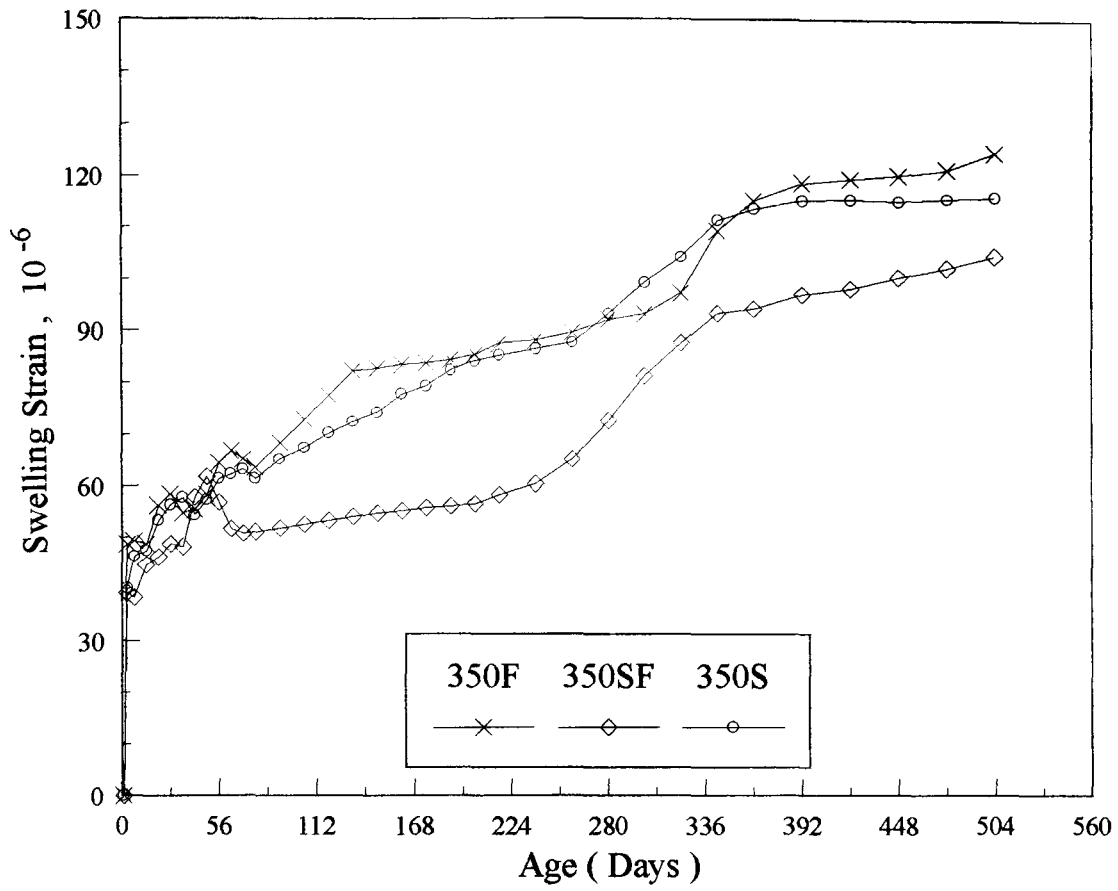


Figure 4-16 Variation of swelling of HVFA concrete-350 kg/m³ mixes

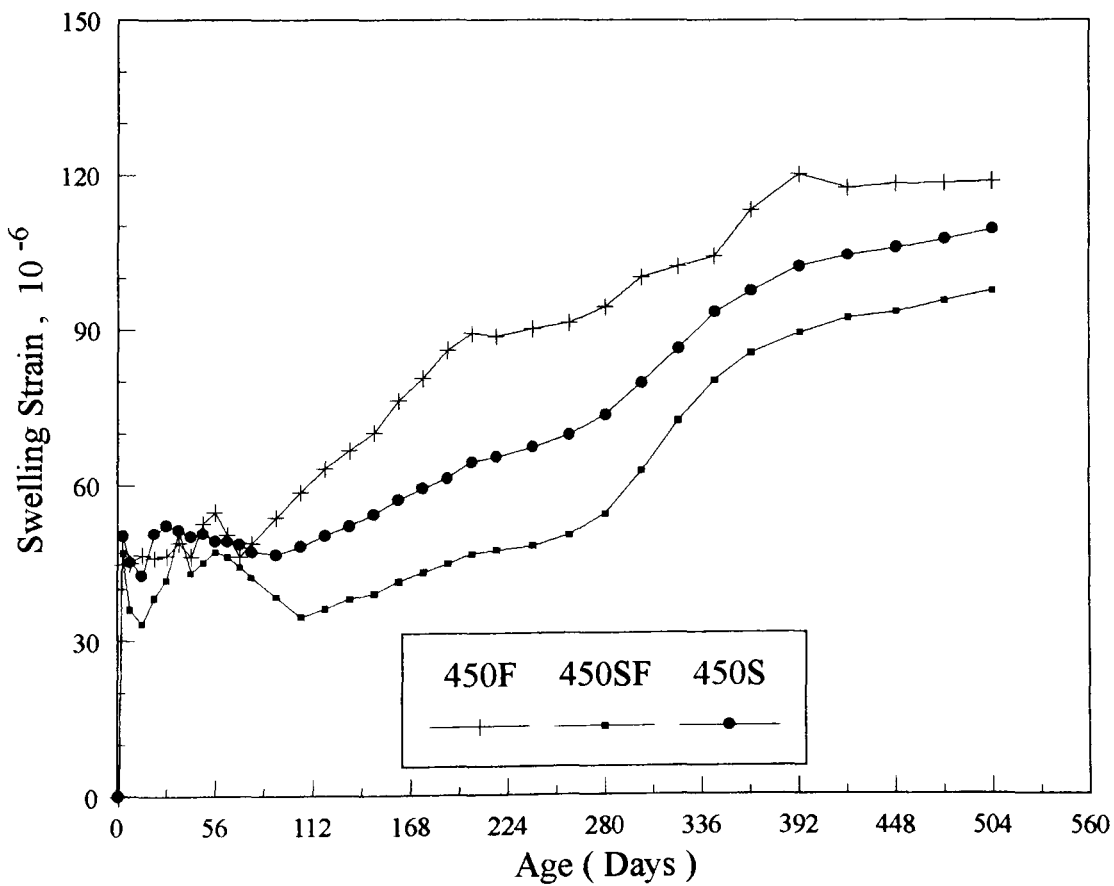


Figure 4-17 Variation of swelling of HVFA concrete-450 kg/m³ mixes

A comparison of the influence of the total cementitious content on the swelling of HVFA concretes under water curing is shown in Figs 4-18, 4-19, and 4-20. These results show that the binder content has some remarkable effect on the development of swelling. In general, 450 kg/m³ mixes had a lower swelling than those made with 350 kg/m³ mix. The difference in swelling between the two types of concretes is probably due to the higher superplasticizer content used in the 450 kg/m³ mixes. In the present study, the 450 kg/m³ concrete mixes were too glutinous to mix and cast. Hence, a relatively high superplasticizer dosage was needed for these mixes. With a higher superplasticizer dosage, the ettringite may have grown into the water-filled space, and resulted in reduced swelling strains [67].

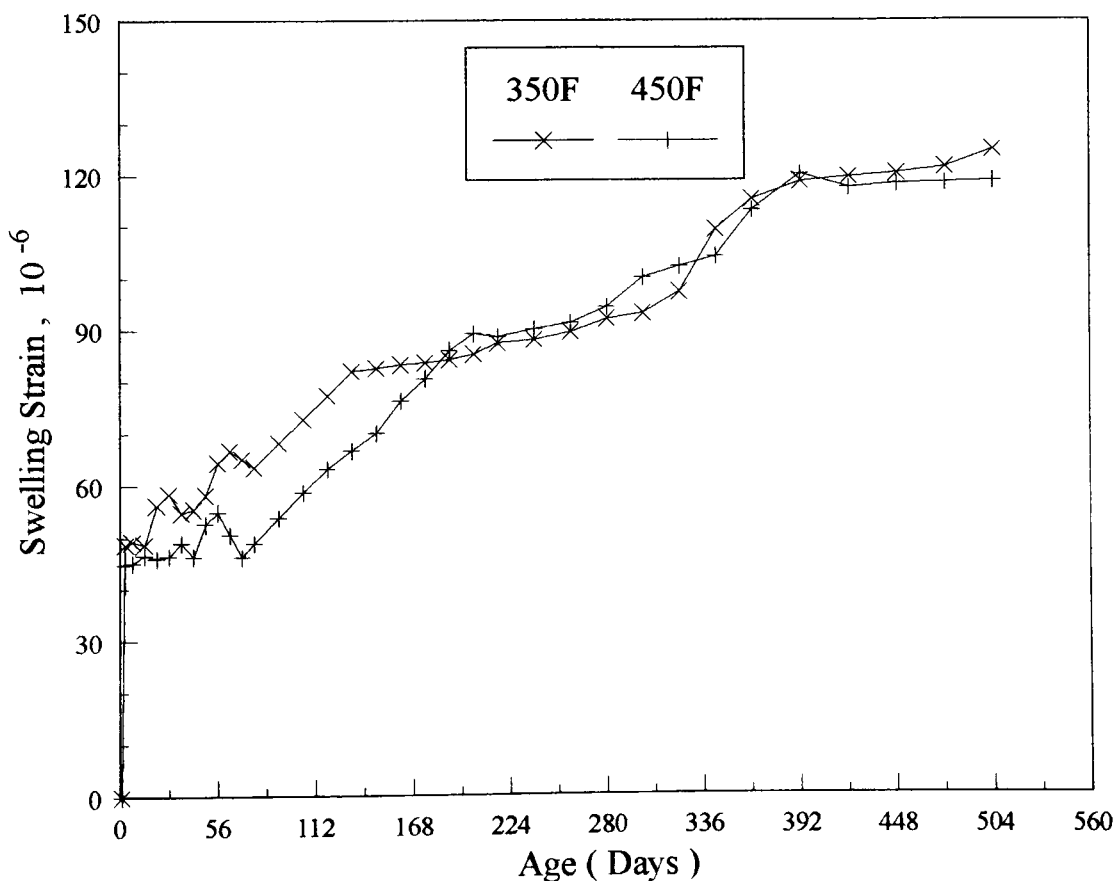


Figure 4-18 Effect of total binder content on swelling-350F/450F

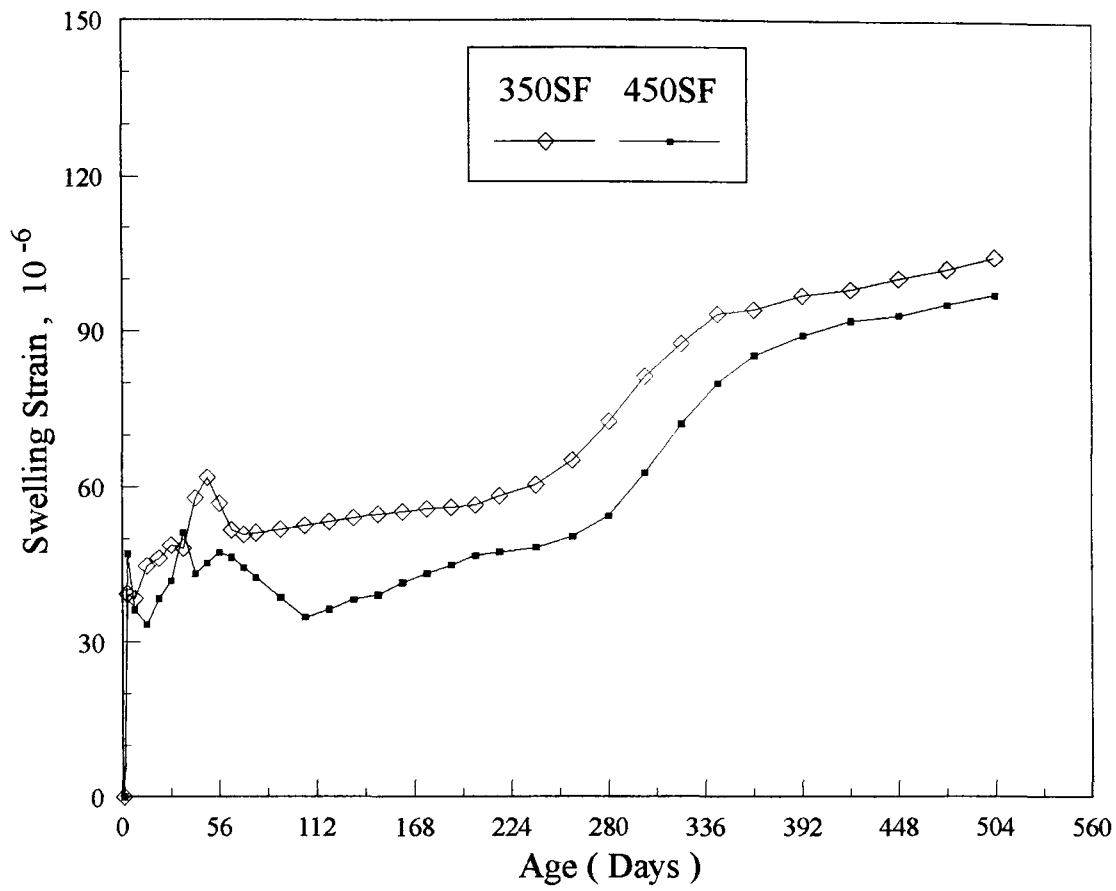


Figure 4-19 Effect of total binder content on swelling-350SF/450SF

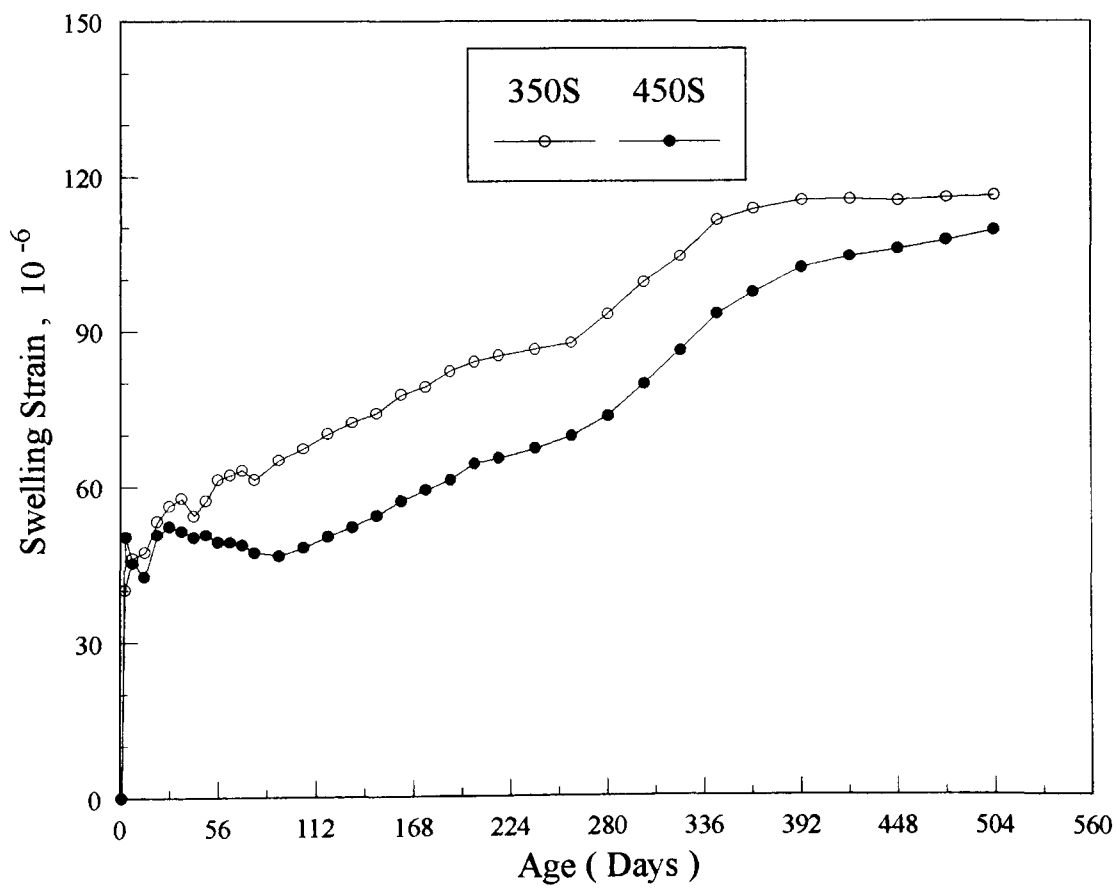


Figure 4-20 Effect of total binder content on swelling-350S/450S

4-5. DRYING SHRINKAGE OF HIGH VOLUME FLY ASH CONCRETE

Drying shrinkage of concrete is caused by the contraction of the calcium silicate gel in the hardened paste as the moisture content is reduced. As concrete dries, the water lost first comes from the capillaries and causes little shrinkage. After the capillary water has been lost, the water is removed from the cement gel pores and noticeable drying shrinkage occurs. While many factors determine the magnitude of drying shrinkage, the materials that mostly affect drying shrinkage are water, the cementitious paste, admixtures and aggregates [68].

In this section, the results of the tests on drying shrinkage of HVFA concretes are presented. The drying shrinkage specimens were initially moist cured for 7 days, after which they were transferred to the ambient environment in the laboratory and monitored over a period of 504 days at regular intervals of 7 days. The effect of variations in different replacement methods and total cementitious content was also investigated. The experimental drying shrinkage data are evaluated with the aid of Ross' formula [13]. The relationship between the drying shrinkage and the swelling is also reported.

4-5-1. Effect of different mixes on drying shrinkage

Drying shrinkage values are expressed as linear strain as a function of age and shown in Table 4-15 and illustrated in Figs 4-21 and 4-22.

At early ages, the HVFA concretes have not fully matured, and the high early drying shrinkage strain obtained at this stage were expected. A high proportion of the drying shrinkage strain for all the air dried HVFA concretes occurred during the initial 28 days, after which the shrinkage gradually increased with increase in age and then became somewhat stabilized with time until the end of the test period.

Compared with all HVFA concretes, it can be seen that the drying shrinkage strain results obtained in this study are relatively high. At the end of the test period, the drying shrinkage strain of all the HFVA mixtures varied between 550 and 640 microstrains. According to the data obtained in this investigation, mixtures with cement replaced partially by fly ash alone, i. e. mixes, 350F, 450F showed greater resistance to drying shrinkage. Mixes 350S and 450S with large amounts of fly ash in the concretes showed slightly higher drying shrinkage strain, whereas mixes 350SF and 450SF showed the highest drying shrinkage strain values at the age of 504 days. The addition of silica fume did not thus seem to restrain significantly the drying shrinkage of air dried HVFA concretes. In contrast, the swelling of HVFA concretes stored in water indicated that concretes incorporating of small amount silica fume, 350SF and 450SF, showed a significant reduction in swelling, and had good ability to suppress swelling.

The reduction in swelling could also be attributed to the lower water / binder ratio of the HFVA concrete, and the changed pore size distribution of the matrix, thereby slowing the rate of swelling. Normally, swelling and drying shrinkage are related - the higher the swelling reduction, the greater its the drying shrinkage [69].

Table 4-15 drying shrinkage strain of HVFA concrete (air curing)
(Unit : 10^{-6} m/m)

Age (days)	350F	350SF	350S	450F	450SF	450S
1	0.00	0.00	0.00	0.00	0.00	0.00
7	50.67	41.12	47.12	29.67	38.33	46.33
28	-176.70	-366.15	-340.15	-303.12	-362.45	-394.33
91	-387.33	-511.33	-450.67	-481.15	-533.67	-549.67
189	-475.33	-596.12	-557.15	-554.12	-616.12	-587.33
364	-530.21	-605.21	-565.12	-580.33	-615.67	-600.33
504	-550.21	-636.33	-590.12	-575.33	-642.33	-612.67

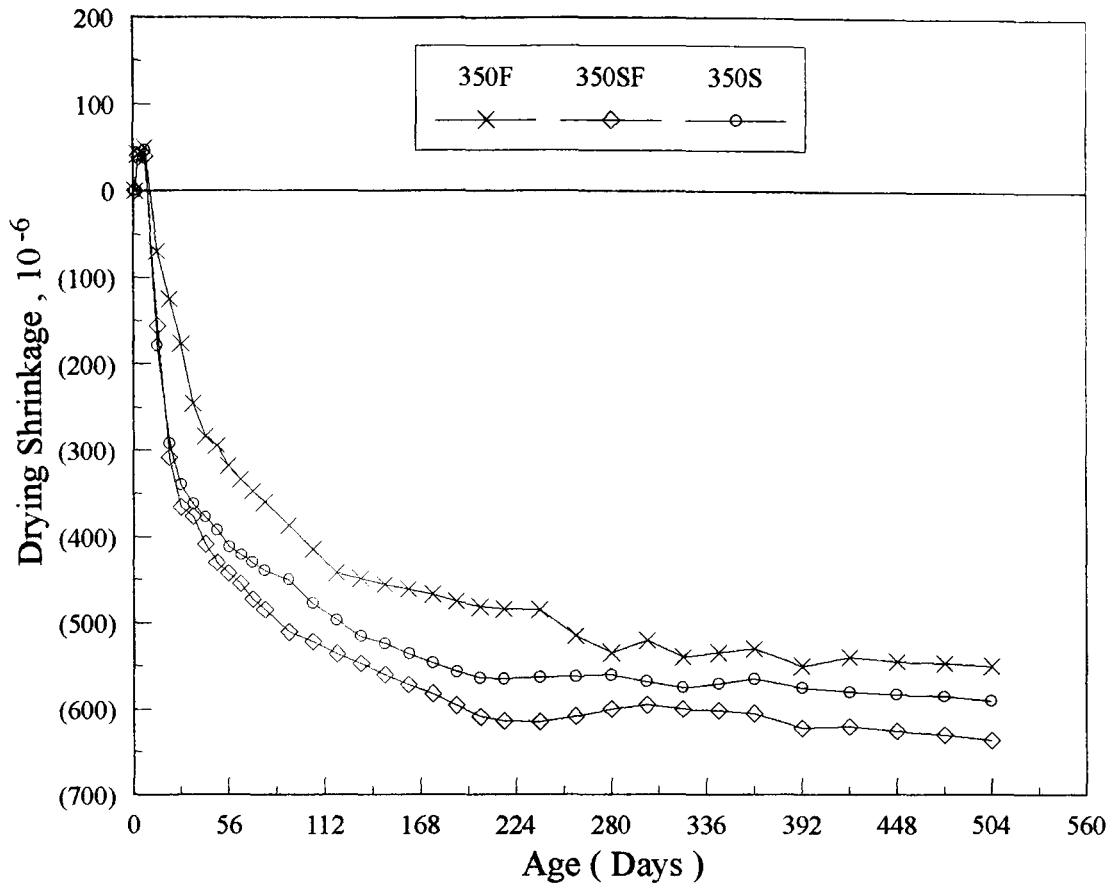


Figure 4-21 Variation of drying shrinkage of HVFA concrete-350 kg/m³ mixes

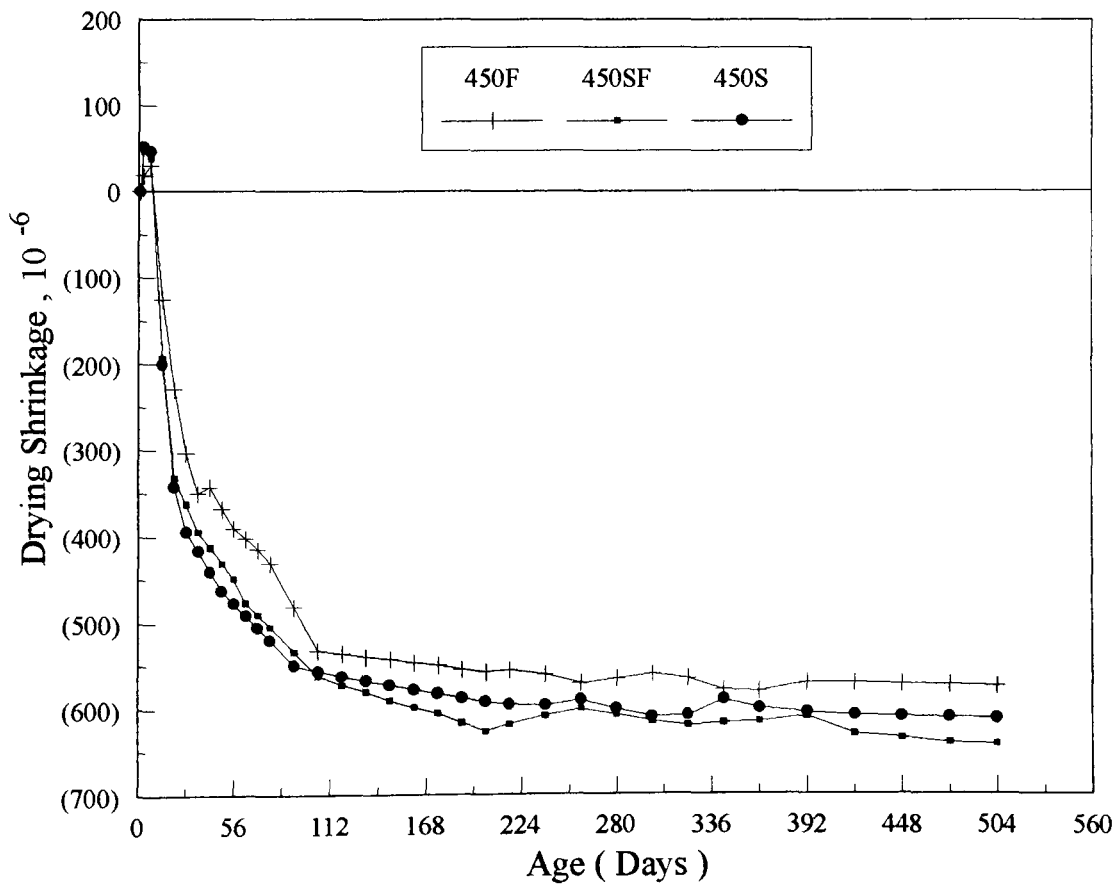


Figure 4-22 Variation of drying shrinkage of HVFA concrete-450 kg/m³ mixes

Figs 4-23 and 4-24 represent the swelling / shrinkage characteristics for HVFA concrete from the present study. It can be seen from the figures, that the higher the swelling of 350F and 450F, the lower is its drying shrinkage strain. To investigate the relationship between drying shrinkage and swelling of HVFA concretes, a plot of drying shrinkage data versus swelling at approximately the age of 504 days is presented in Fig 4-25. Regression analysis of the data shown in the figure produced the following relationship :

$$y = 879.69 - 2.59 x \quad (r = - 0.98) \text{ ----- (4-9)}$$

where y is the drying shrinkage of HVFA concretes in microstrain, x is the swelling of HVFA concretes in microstrain, and r is the correlation factor.

The figure indicates that the good inverse correlation between drying shrinkage and swelling is linear.

As was mentioned in the preceding review on drying shrinkage, a careful study of the pore size distribution may be useful in explaining some aspects of drying shrinkage which are not always well understood. There is reason to believe that drying shrinkage is the result of processes taking place with the finer pores of the system, i.e. drying of water from the mesopores causing capillary effects and from the micropores inducing drying shrinkage strains which may be the result of mechanisms such as changes in disjoining pressure or interlayer space [70].

Table 4-16 shows typical data from the present study of M. I. P. test on all HVFA concrete air dried specimens. It can be seen from the table, that at the age of 18 months, the percentage gain in coarse pore size of concretes with cement replaced partially by fly ash alone, 350F and 450F, is higher in comparison with those incorporating both fly ash and silica fume concretes. The drying shrinkage behaviour of HVFA concretes in the present study is explained in terms of coarse and fine pore size with increase in coarse pore size resulting in a decrease in drying shrinkage and increase in fine pores producing increased drying shrinkage. The results on drying shrinkage thus confirm those observed in published literature [71].

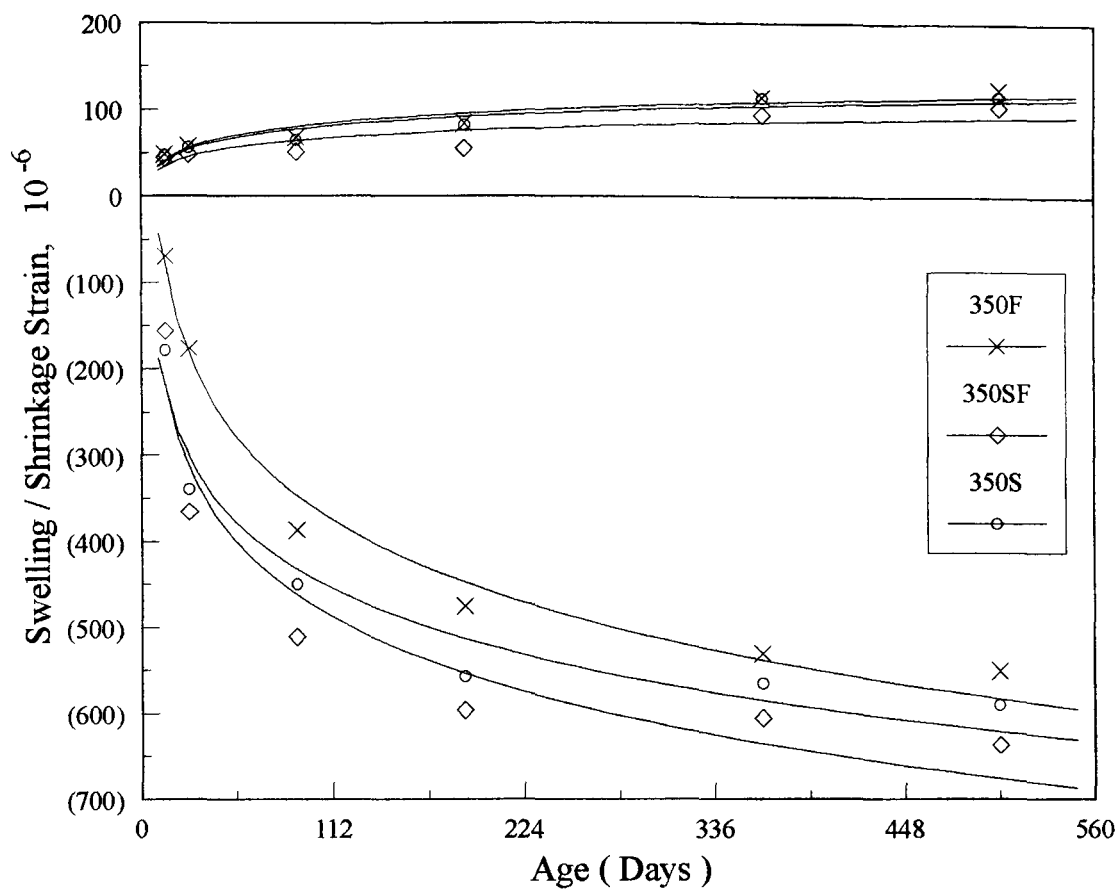


Figure 4-23 Swelling / drying shrinkage characteristics-350 kg/m³ mixes

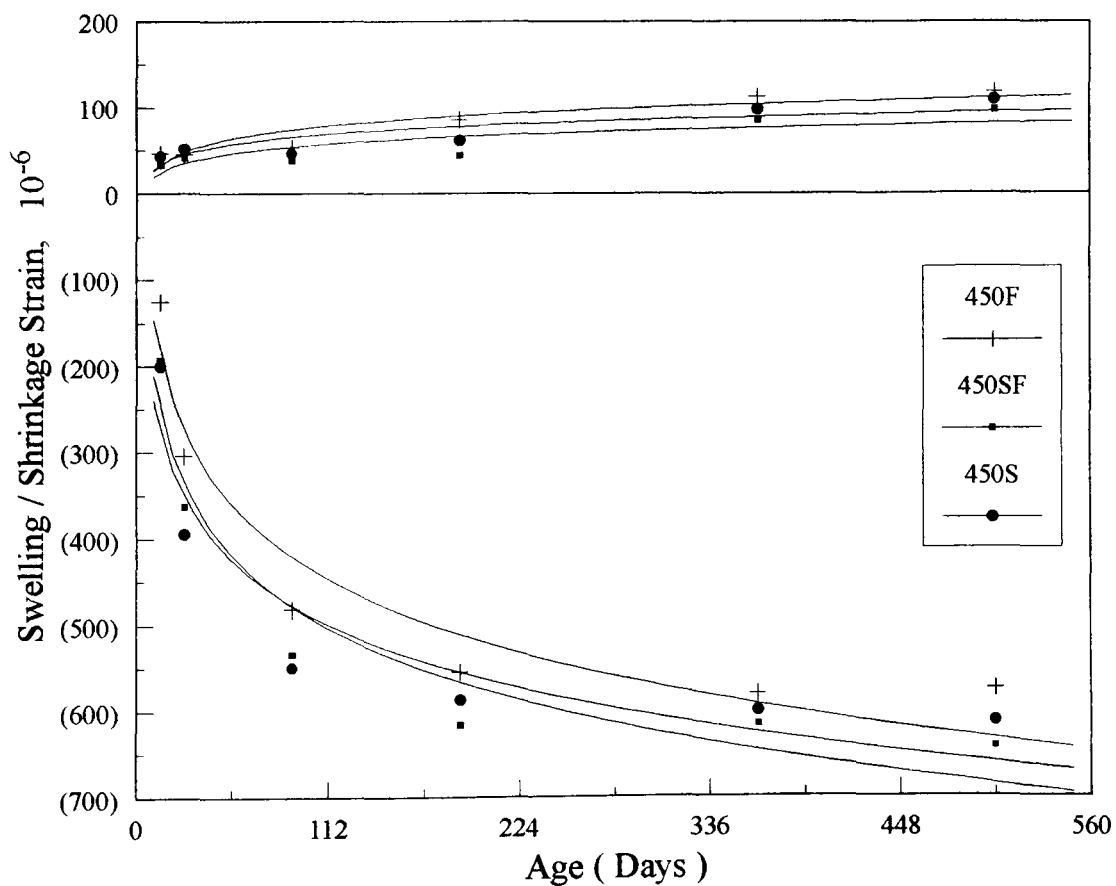


Figure 4-24 Swelling / drying shrinkage characteristics-450 kg/m³ mixes

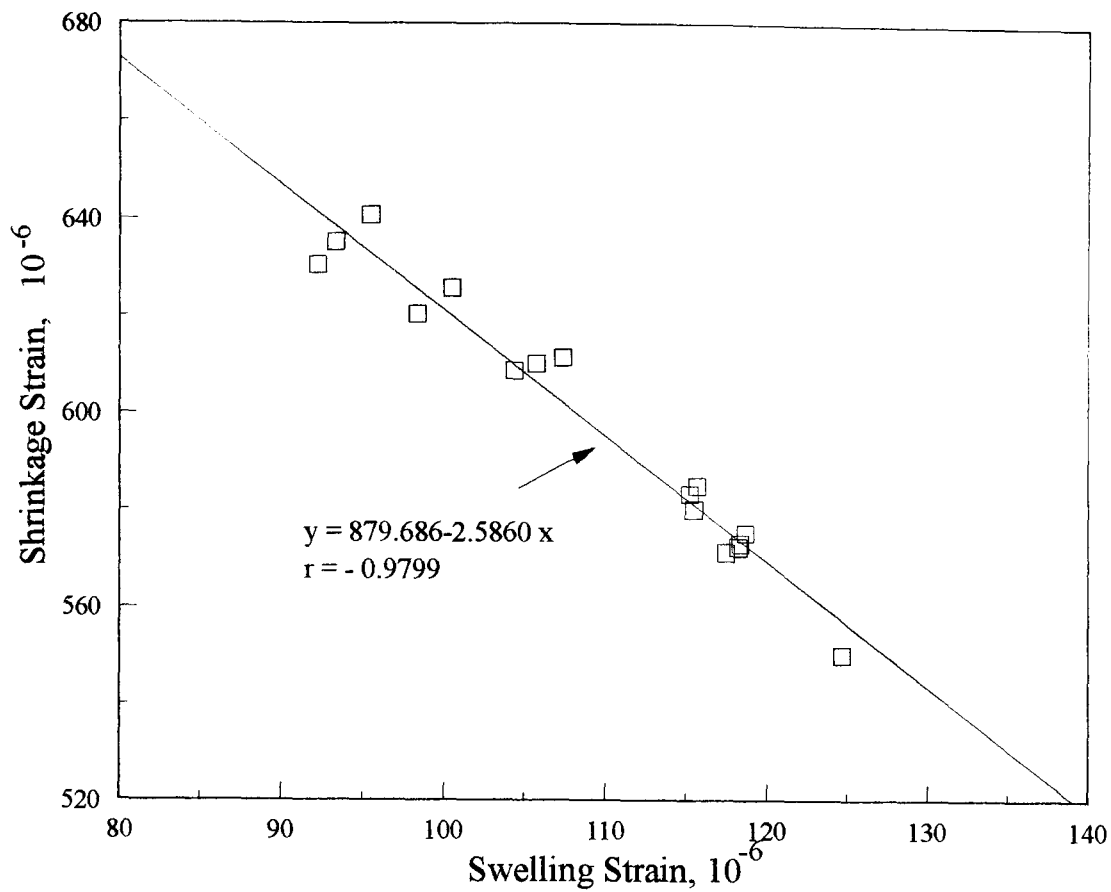


Figure 4-25 Relationship between drying shrinkage and swelling

**Table 4-16 Typical % of mesopore of high volume fly ash concrete under air curing
(Unit : %)**

Pore size	> 0.05 μm			0.05 μm ~ 0.0025 μm		
	28days	90days	18months	28days	90days	18months
350F	61.16	65.40	78.03	38.84	34.62	21.97
350SF	62.11	43.78	67.85	37.89	56.22	32.15
350S	37.93	31.26	61.21	62.07	68.74	38.79
450F	51.45	42.38	71.87	48.55	57.62	28.13
450SF	62.05	60.36	67.69	37.95	39.64	32.31
450S	47.60	36.41	61.03	52.40	63.59	38.97

Although the HVFA concrete exhibited high drying shrinkage strain values early in its life, these drying shrinkage strain levels are either comparable to or in a manner similar to those observed by Malhotra and his co-worker [9,43]. They obtained a range of drying shrinkage from 400 ~ 600 microstrains at the end of 448 days with similar concretes under essentially the same test conditions.

The effect of total binder content of all HVFA concretes on drying shrinkage is compared in Figs 4-26, 4-27, and 4-28. The figures show that the total cementitious content has only a marginal influence on the values of drying shrinkage. As expected, the 450 kg/m³ mixes had a slightly higher drying shrinkage strain than with 350 kg/m³. The higher drying shrinkage of 450 kg/m³ mixes is probably due to a combination of two factors - a higher binder content and superplasticizer dosage [42]. In addition, at a constant water / binder ratio, drying shrinkage increases with an increase in the cementitious content because this results in a large volume of hydrated cementitious paste which is liable to drying shrinkage [69].

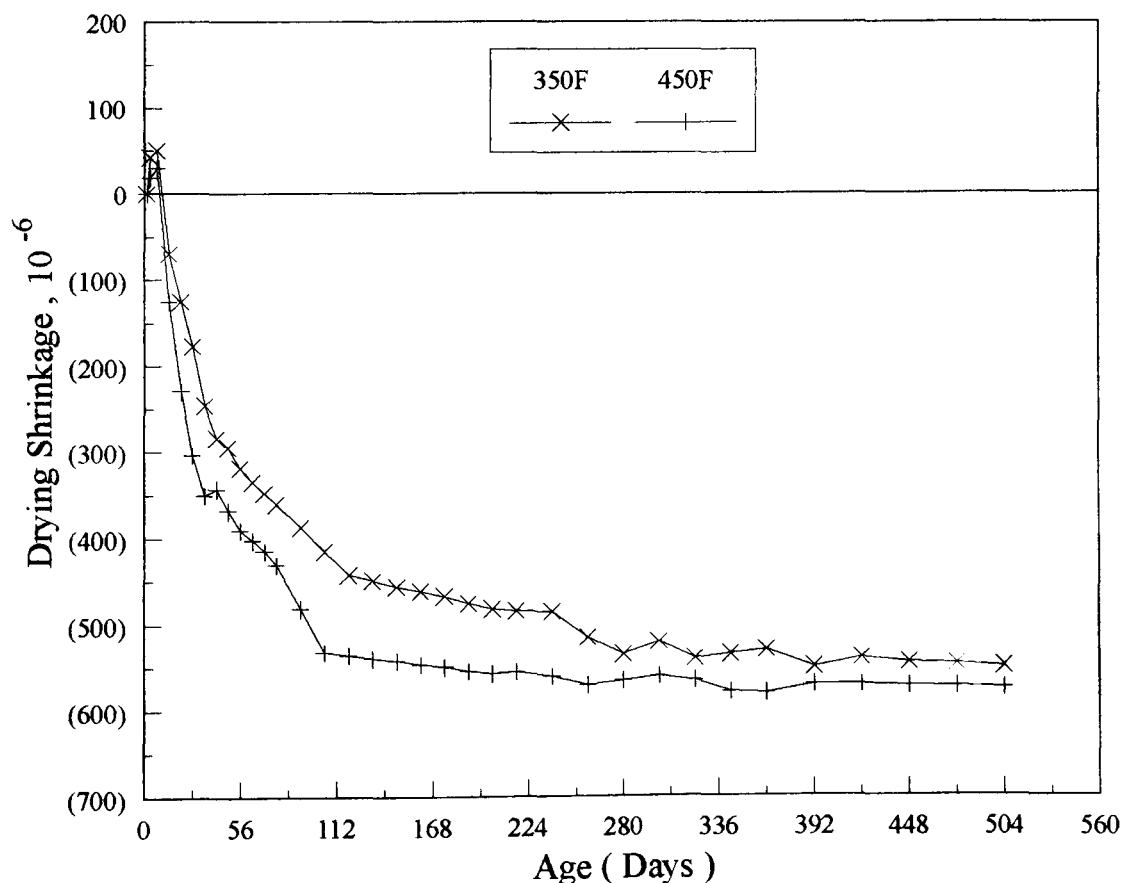


Figure 4-26 Effect of total binder content on drying shrinkage-350F/450F

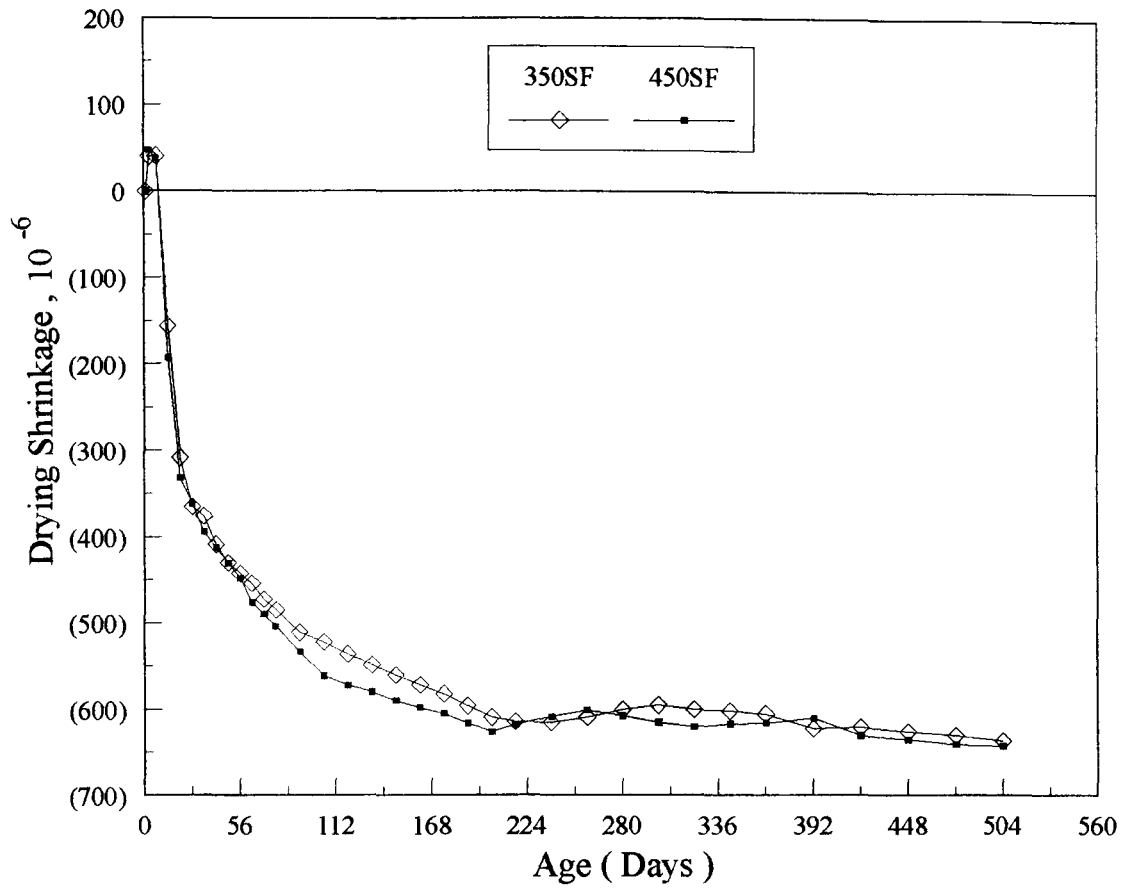


Figure 4-27 Effect of total binder content on drying shrinkage-350SF/450SF

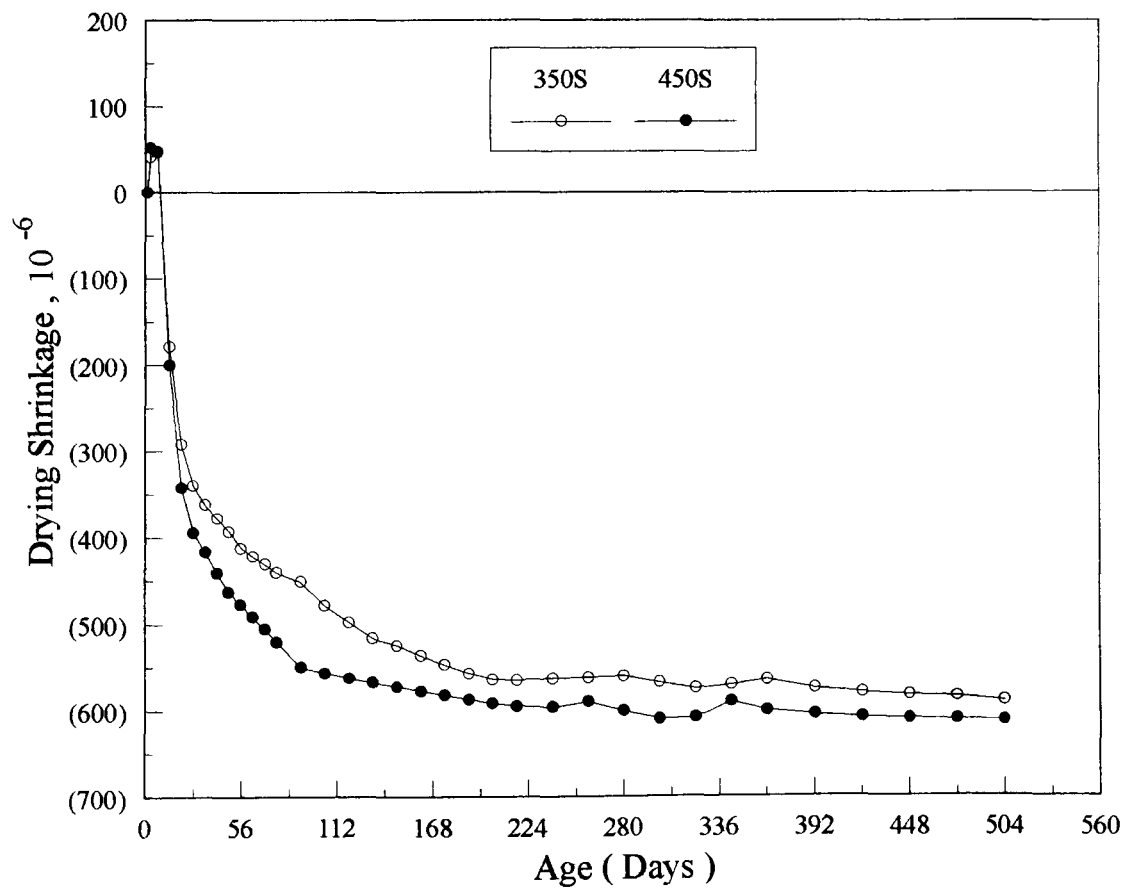


Figure 4-28 Effect of total binder content on drying shrinkage-350S/450S

4-5-2. Prediction of drying shrinkage on HVFA concrete

Many kinds of equations including ACI, CEB formulae, Meyer, and Bazant have been developed to predict the drying shrinkage of conventional concrete. In the analysis of the drying shrinkage of the HVFA concrete under investigation, a hyperbolic expression suggested by Ross has been used [69].

Ross's equation can be expressed as :

$$c = \frac{t}{a + bt} \text{ ----- (4-10)}$$

where c is the drying shrinkage of HVFA concrete in microstrain, t is the time after initial readings for drying shrinkage in days, and a and b are constants.

when $t = \infty$, then $c = 1 / b$, i. e. $1 / b$ is the limiting value of drying shrinkage. The symbols a and b represent constants determined from experimental results. A plot of test results of t / c against " t " gives a straight line relation of slope " b " and an intercept " a ".

Figs 4-29 and 4-30 show the curves for determining the constants " a " and " b " for all HVFA concretes undergoing drying shrinkage. Table 4-17 shows the constants derived from these results. In the same table, typical results of the measured and predicted values of drying shrinkage at various ages for all HVFA concretes are also shown.

From the results, during the first 3 months, the drying shrinkage strains obtained through Ross's formula are substantially higher compared to experimental results. However, as can be seen from the table, there is good agreement between the measured and predicted values, especially for ages greater than 6 months. The drying shrinkage strains measured on all HVFA concretes are comparable to predicted values, i. e., about 95 % of the average percentage of the latter.

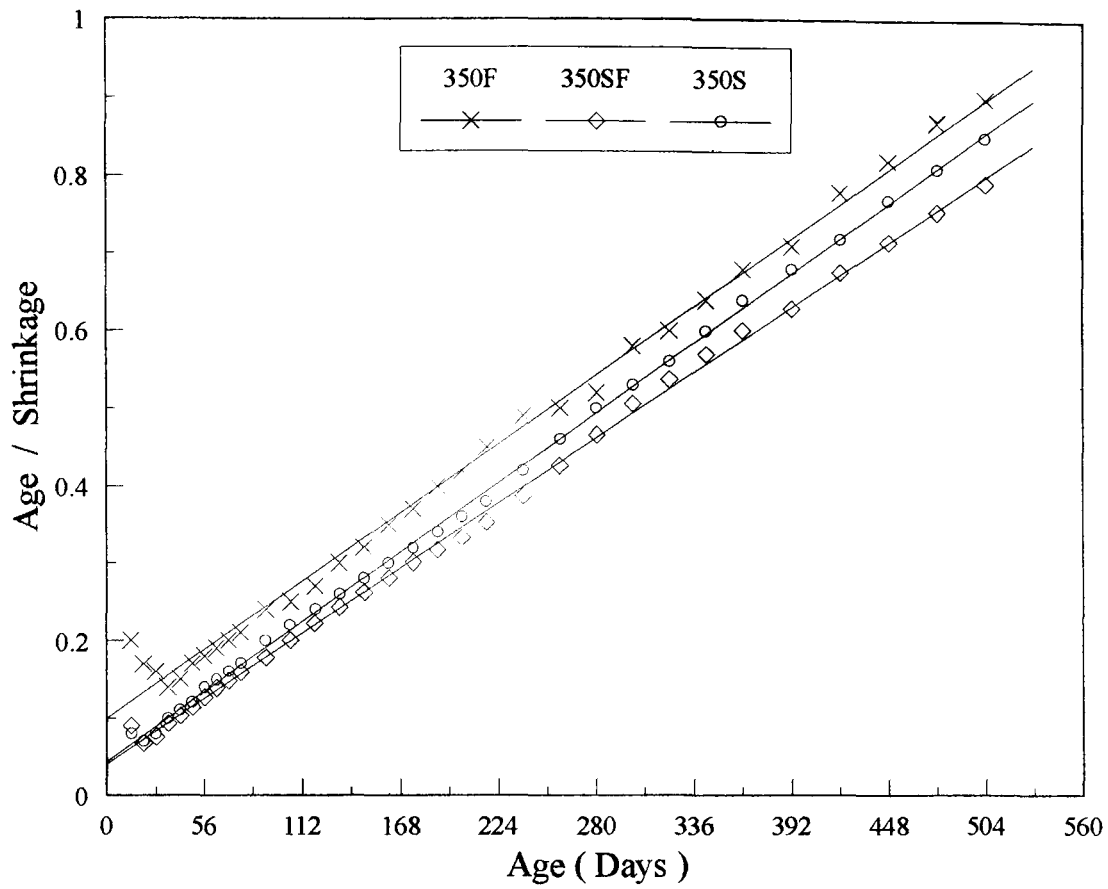


**Figure 4-29 The curve for determining the constants a and b
(350 kg/m³ mixes)**

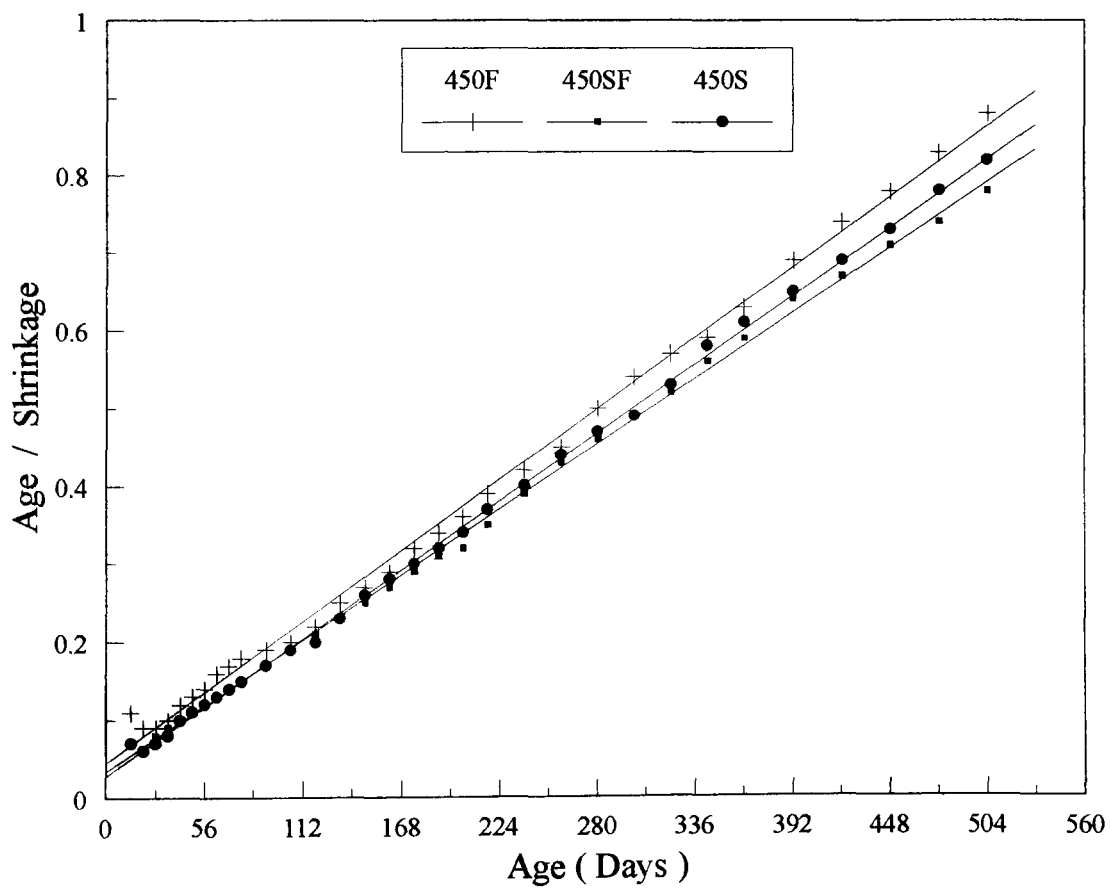


**Figure 4-30 The curve for determining the constants a and b
(450 kg/m³ mixes)**

**Table 4-17 Comparison between measured and predicted drying shrinkage
(Unit : 10^{-6} m/m)**

A. 350 kg/m³ mixes

Mix	350F $a = 99.73 \times 10^{-3}$ $b = 1.58 \times 10^{-3}$		350SF $a = 41.51 \times 10^{-3}$ $b = 1.50 \times 10^{-3}$		350S $a = 44.20 \times 10^{-3}$ $b = 1.60 \times 10^{-3}$	
	Measured	Predicted	Measured	Predicted	Measured	Predicted
Age (days)						
14	69.67	114.90	156.12	223.96	178.67	210.20
28	176.70	194.48	366.15	335.29	340.15	314.61
91	387.33	373.70	511.33	511.21	450.67	479.95
189	475.33	474.46	596.12	581.52	557.15	545.30
364	530.21	539.38	605.12	619.56	565.12	580.92
504	550.21	562.47	636.33	631.97	590.12	592.52

B. 450 kg/m³ mixes

Mix	450F $a = 44.82 \times 10^{-3}$ $b = 1.62 \times 10^{-3}$		450SF $a = 33.99 \times 10^{-3}$ $b = 1.50 \times 10^{-3}$		450S $a = 28.29 \times 10^{-3}$ $b = 1.57 \times 10^{-3}$	
	Measured	Predicted	Measured	Predicted	Measured	Predicted
Age (days)						
14	125.25	207.41	193.33	254.59	200.12	278.50
28	303.12	310.49	362.45	368.47	394.33	387.54
91	481.15	473.37	533.67	533.76	549.67	531.67
189	554.12	538.46	616.12	595.29	587.33	581.50
364	580.33	573.68	615.67	627.60	600.33	606.90
504	575.33	585.16	642.33	637.98	612.67	614.96

Remarks:

$$\text{Predicted drying shrinkage} = \frac{\text{age}}{a + b \times \text{age}}$$

4-5-3. Comparison of drying shrinkage with published data

Table 4-18 shows a comparison of drying shrinkage from the present investigation with the results of other researchers [9,29,44,59,72]. Data from the table show that

there is a wide range of data on drying shrinkage reported on fly ash concrete mainly due to the different concretes tested, differences in type of curing, and age of testing. When all the fly ash concretes under various curing regimes are considered, the drying shrinkage varies from 385 to 642 microstrain. From these data, it is obvious that it is impossible to make in any general conclusions covering all types of fly ash concretes. It is worth to point out, however, that the results of drying shrinkage obtained in the present study are similar to those reported by EPRI and Malhotra ; they are, however, much higher than the results reported by Swamy. The reason for this difference is probably due to the mix proportions and the water / binder ratio.

Table 4-18 Comparison of drying shrinkage with published data

Researchers	Fly ash content (%)	W / C	Cube St. (28d) MPa	Curing conditions	Age at last reading (days)	Drying shrinkage (microstrain)
Cripwell [29]	35	0.46	44.5	20 °C + 70 % R. H	300	485
	"	0.35	53.0	"	"	400
Ward [72]	40	0.43	26.8*	23 °C + 70 % R. H	91	500
	50	0.41	26.0*	"	"	580
Malhotra [44]	58	0.32	35.0*	7 wet + air curing	448	500
Swamy [59]	50	0.32~0.62	24~63	Outside	550	385 ~ 422
	"	"	"	Laboratory	730	460 ~ 485
EPRI [9]	58	0.33	27.8*	7 wet + air curing	448	454
	"	"	32.5*	"	"	606
	"	"	38.5*	"	"	457
	"	"	28.8*	"	"	433
	"	"	38.1*	"	"	504
	"	"	41.4*	"	"	535
Author	350F(57%)	0.40	28.4	7 wet + air curing	504	550
	350SF(51%)	"	29.9	"	"	636
	350S(97%)	"	38.9	"	"	590
	450F(56%)	"	28.6	"	"	575
	450SF(51%)	"	38.1	"	"	642
	450S(97%)	"	39.3	"	"	613

Remarks : * - Cylinder strength

4-6. DYNAMIC MODULUS OF ELASTICITY OF HVFA CONCRETE

Modulus of elasticity is important in structural design of reinforced concrete, and is used primarily to evaluate soundness of concrete as a measure of durability. It is often used as a non-destructive test to determine the progression of internal changes in the material, as for example, a consequence of repeated freeze-thaw cycles, and ageing, or of chemical attack.

For this purpose, modulus of elasticity measurements are very convenient, since they are non-destructive, and since there is also a general (if empirical) relationship between the modulus of elasticity and compressive strength. Like many other structural materials, concrete is, to a certain degree, elastic. The modulus of concrete represents its response to elastic deformation, and it also exhibits a very high sensitivity in reflecting the internal changes in the structure of concrete.

There is now absolutely no doubt that the use of high strength and high performance concrete in construction will continue to grow. The elastic deformation of high strength / high performance concrete is of particular importance. Because the modulus of elasticity of the strong hardened cement paste and of the aggregate differ less from one another than in medium strength concrete, the behaviour of high strength / high performance concrete is more monolithic, and the strength of the aggregate-matrix interface is higher.

In this section the main results deal with the characteristics of dynamic modulus of elasticity in different mixes and different binder contents concrete under both types of curing conditions. For purpose of comparison the results of the normal OPC concretes are also discussed. A comparison of the correlation between the dynamic modulus of elasticity and compressive strength of HVFA concrete is also reported.

4-6-1. Effect of curing condition and different mixes on dynamic modulus of elasticity

Under both curing conditions at various ages, the dynamic modulus of elasticity of HVFA concretes with both cementitious contents is illustrated in Figs 4-31, 4-32, 4-33, and 4-34. Tables 4-19 and 4-20 summarize typical data of all HVFA concretes under water and air curing, respectively.

**Table 4-19 Dynamic modulus elasticity of HVFA concrete (Water curing)
(Unit : GPa)**

Age (days)	350F	350SF	350S	450F	450SF	450S
1	23.01	23.11	24.25	38.11	32.00	31.01
7	35.25	35.01	34.21	45.07	46.01	45.78
28	36.03	38.85	39.69	46.07	50.25	51.21
91	39.50	42.29	41.96	50.78	54.83	54.52
189	44.49	43.85	43.16	55.04	56.96	55.97
364	45.70	45.40	44.59	58.85	59.24	58.01
504	46.45	46.22	45.18	59.51	60.14	58.75

**Table 4-20 Dynamic modulus elasticity of HVFA concrete (Air curing)
(Unit : GPa)**

Age (days)	350F	350SF	350S	450F	450SF	450S
1	22.69	22.43	23.99	37.92	31.15	30.85
7	35.04	34.03	34.99	44.85	45.57	45.56
28	35.50	36.58	37.86	45.37	47.96	47.42
91	34.30	35.60	36.44	43.24	46.37	45.45
189	33.60	34.65	35.76	42.09	45.61	44.68
364	33.55	34.72	36.08	42.35	45.62	44.95
504	34.20	35.16	36.30	43.53	45.91	45.68

The results indicate that the modulus increased rapidly during the first few days, it then increased slightly with further curing, and finally reached a stable value with continuing hydration reaction. Data from the tables show that the modulus of elasticity of moist cured specimens is consistently higher than that of the dry cured specimens. The results also show that the total binder content is a predominant factor in determining, the value of dynamic modulus. Concrete with 450 kg/m^3 was superior to those with 350 kg/m^3 under both types of curing. Irrespective of the cement replacement methods, the difference between 350 kg/m^3 and 450 kg/m^3 mixes under both curing conditions is seen to be identical. At the age of 504 days, the difference in modulus of elasticity values between 350 kg/m^3 and 450 kg/m^3 mixes is about 20 - 25 % for both curing conditions. The total binder content generally controls the concrete making properties of the aggregate, because it determines the amount of binder paste needed to cover the aggregate surface. A high binder content of concrete means that it can be significantly enhanced via the physical mechanisms of improved packing of hydration products, so that the strength of the matrix is high. Because hydration starts at the surface of the binder particles, it is the total surface area of binder that represents the material available for hydration. Therefore, the strength between the coarse aggregate and the matrix, and the elastic properties of aggregate have considerable influence on the dynamic modulus of elasticity of concrete.

The densifying effect of fly ash and silica fume are demonstrated in the data presented here. However, Mix-450SF concrete with silica fume had a higher dynamic modulus of elasticity, whereas Mix-450S with a large amount of fly ash had a slightly lower modulus than the concrete made of 450F.

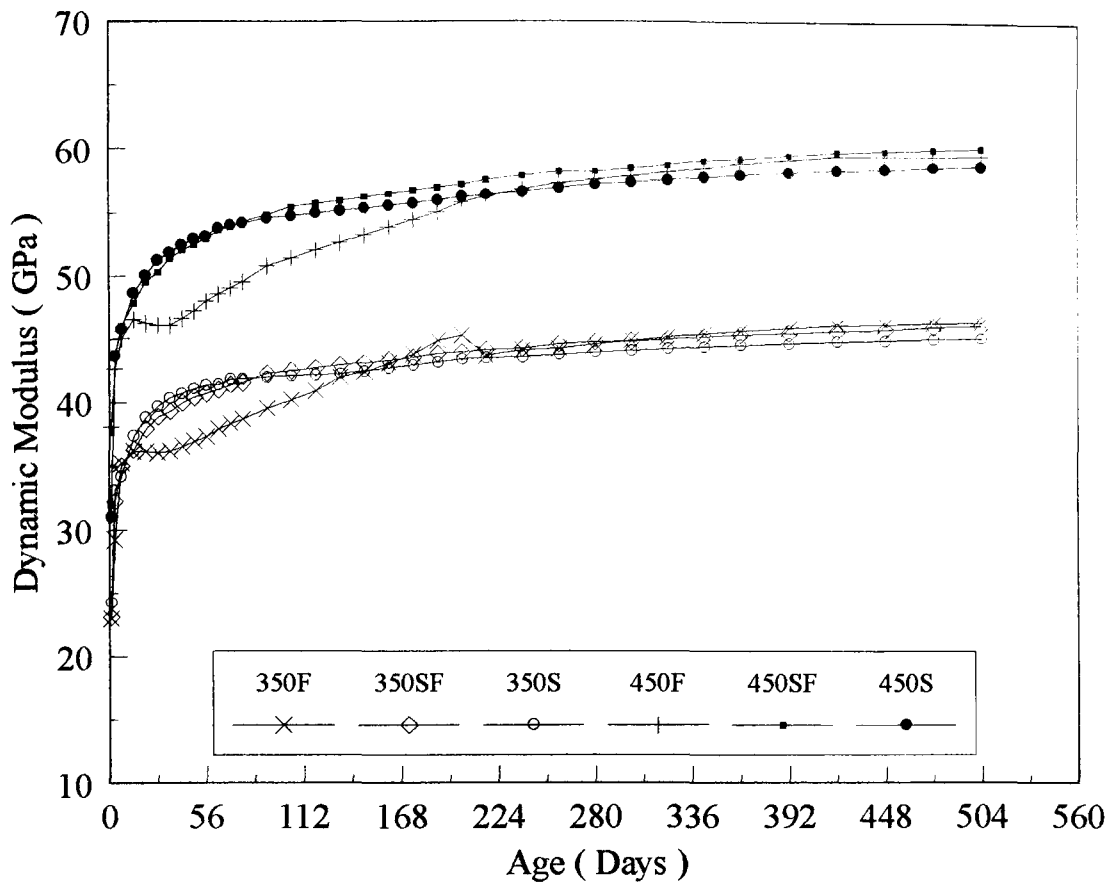


Figure 4-31 Variation of dynamic modulus of HVFA concrete (Water curing)

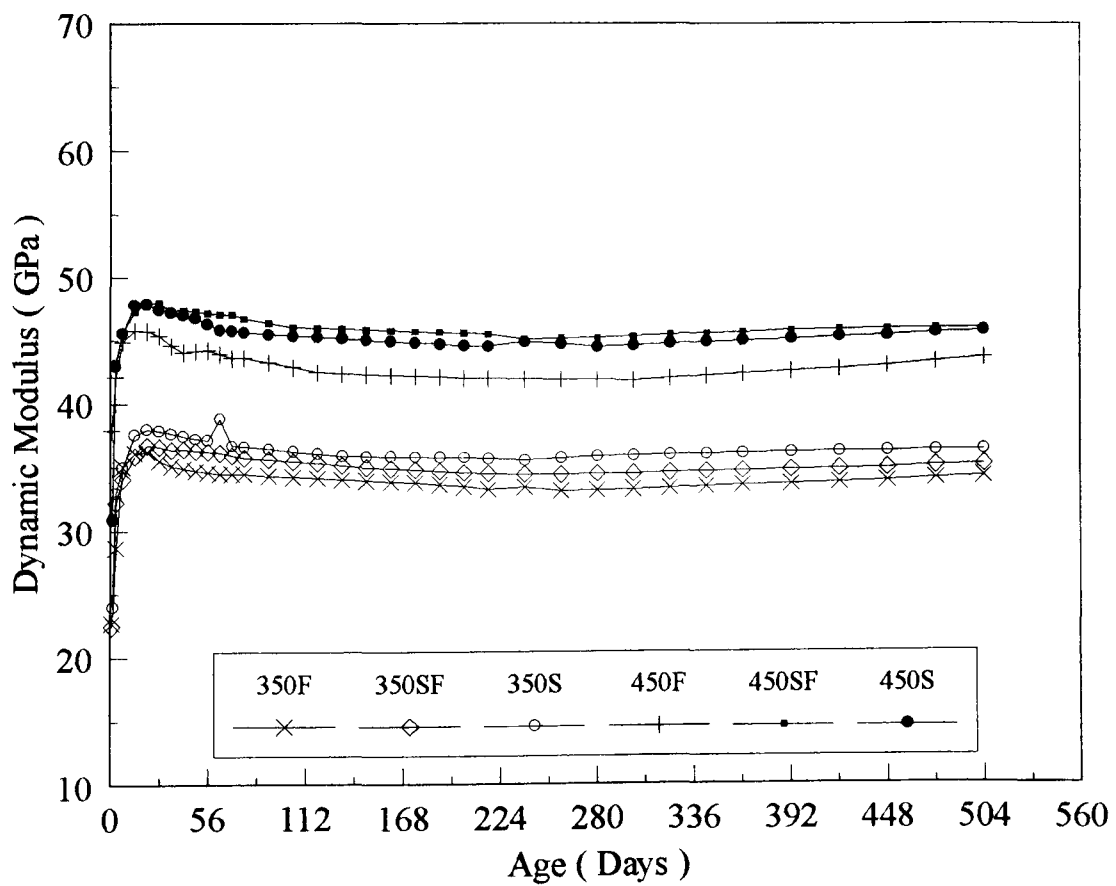


Figure 4-32 Variation of dynamic modulus of HVFA concrete (Air curing)

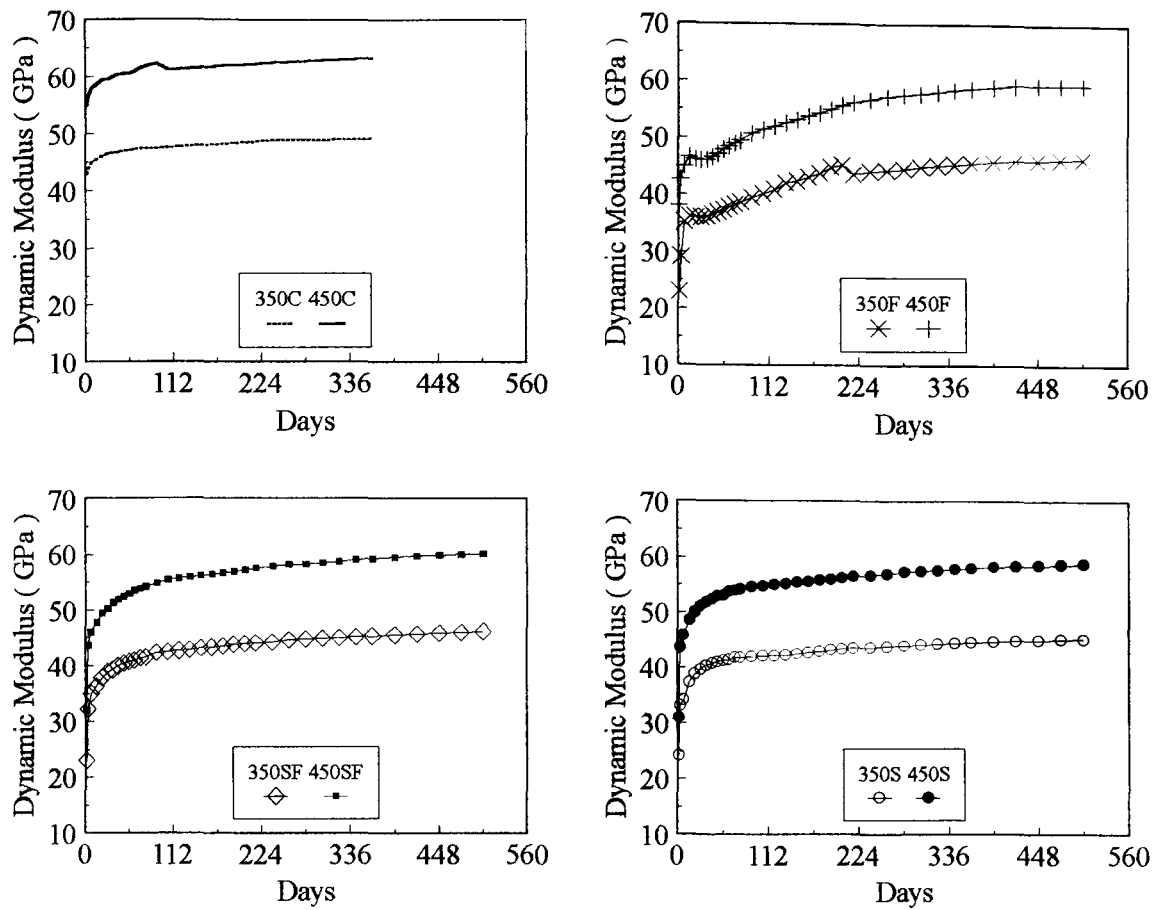


Figure 4-33 Effect of total binder content on dynamic modulus (Water curing)

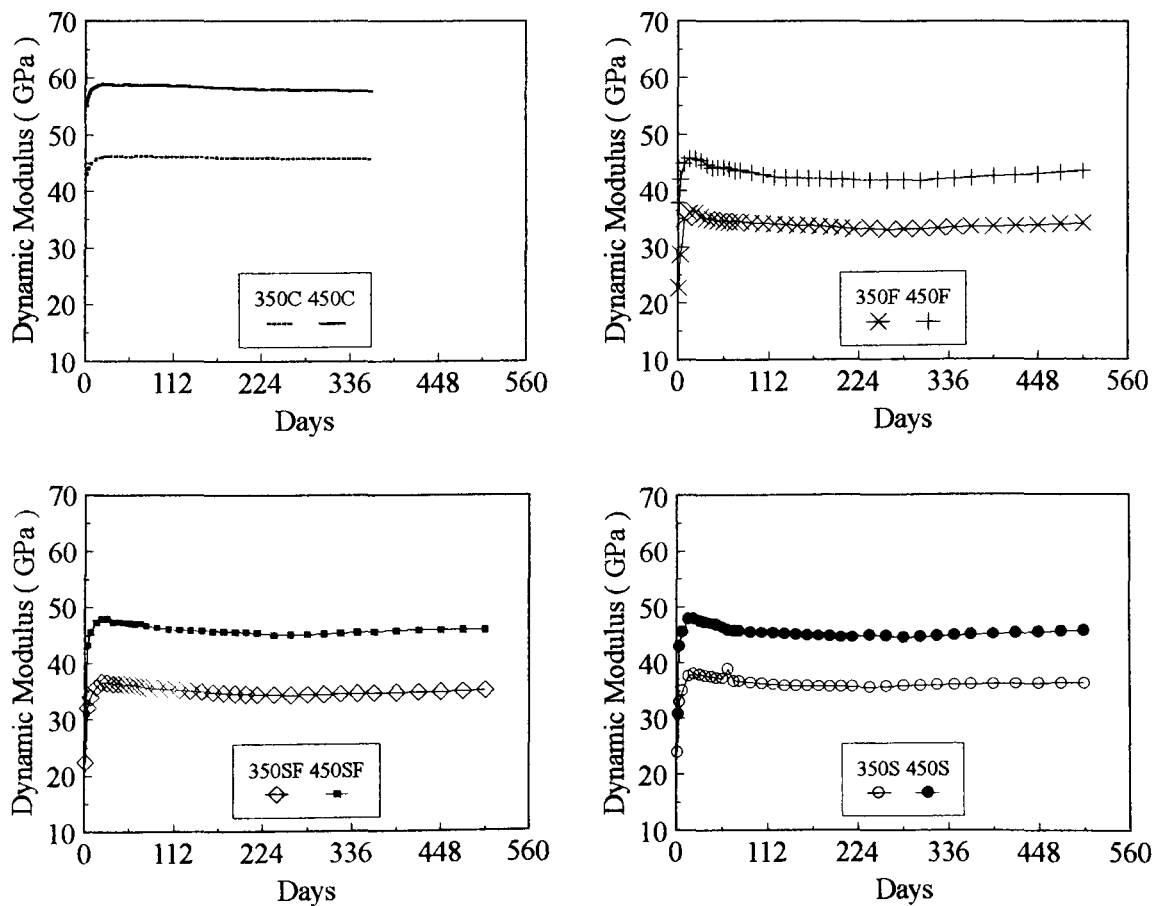


Figure 4-34 Effect of total binder content on dynamic modulus (Air curing)

From the Table 4-19, the dynamic modulus of elasticity of HVFA concretes ranged from 36 to 51 GPa at 28 days, from 39 to 55 GPa at 91 days, and from 45 to 60 GPa at 18 months for both cementitious contents. Considering the levels of compressive strength of HVFA concrete at these three ages, the dynamic modulus of elasticity values are rather high. As mentioned in the previous section, the generally high dynamic modulus of elasticity values are due to the unhydrated fly ash particles acting as fine aggregate. As for the chemical reaction of silica fume, because of high surface area and high content of amorphous silica in silica fume, this highly active pozzolan reacts more quickly than ordinary pozzolans [73].

From the Fig 4-32, air dried specimens showed slight retrogression of dynamic modulus of elasticity and show similar trends to changes in strength when concretes are exposed to a drying environment. As in the strength development studies, the effect of curing conditions on dynamic modulus of elasticity is significant. At the end of 504 days, the dynamic modulus of elasticity of HVFA concretes under air drying ranged from 34 to 46 GPa compared to 45 to 60 GPa for water cured specimens. Concretes made with both fly ash and silica fume exhibited slightly higher values than concrete made of 350F and 450F.

The relative rates of development of dynamic modulus of HVFA concrete cured in water and air are illustrated in Table 4-21.

**Table 4-21 Influence of air curing on dynamic modulus of elasticity
(Unit : %)**

Age (days)	350F	350SF	350S	450F	450SF	450S
14	100	99	100	98	99	98
28	98	94	95	98	95	93
91	87	84	87	85	85	83
189	75	79	83	76	80	80
364	73	76	81	72	77	77
504	74	76	80	73	76	78

Remarks : Water cured specimen is 100 %

The percentage reduction in dynamic modulus is about 5 % of average values for all HVFA concretes when compared to the moist cured concrete at the age of 28 days. Even though air curing showed a little retrogression of dynamic modulus, a modest increase of modulus with continued air drying was also observed. At the end of air curing, the average percentage of the dynamic modulus of elasticity of all HVFA concretes is about 76 % of that under water curing.

4-6-2. Comparison with normal OPC concrete

It would then be interesting to compare the dynamic modulus of elasticity development of this HVFA concrete with that of normal OPC concrete with age and under both curing conditions. Table 4-22 represents some typical data of dynamic modulus of elasticity for two normal OPC concretes under both types of curing conditions. The rate of gain of modulus as a % of 28 day modulus for HVFA concretes under both curing conditions is shown in Tables 4-23 and 4-24.

Table 4-22 Dynamic modulus elasticity of normal OPC concrete

Mix	350 kg/m ³ mixes				450 kg/m ³ mixes			
	Dynamic modulus (GPa)		% of 28 day development (%)		Dynamic modulus (GPa)		% of 28 day development (%)	
Age (days)	Water curing	Air curing						
1	42.77	42.82	92	93	54.77	55.01	92	94
7	44.84	44.95	96	97	57.94	58.04	97	99
28	46.52	46.23	100	100	59.54	58.82	100	100
91	47.48	46.13	102	99	62.30	58.68	105	99
189	48.35	45.98	104	99	62.11	58.26	104	99
364	49.02	45.78	105	99	63.34	57.71	106	98

**Table 4-23 Rate of gain of modulus as a % of 28 day modulus (Water curing)
(Unit : %)**

Age (days)	350F	350SF	350S	450F	450SF	450S
1	64	59	61	82	64	61
7	98	90	86	98	92	89
28	100	100	100	100	100	100
91	110	109	106	110	109	106
189	125	113	109	119	113	109
364	127	117	122	128	118	113
504	129	119	114	129	120	115

**Table 4-24 Rate of gain of modulus as a % of 28 day modulus (Air curing)
(Unit : %)**

Age (days)	350F	350SF	350S	450F	450SF	450S
1	64	61	63	84	65	65
7	99	93	92	99	95	96
28	100	100	100	100	100	100
91	97	97	96	95	97	96
189	95	95	94	93	95	94
364	95	95	95	93	95	95
504	96	96	96	96	96	96

From the results, it can be seen that, under continuous moist curing conditions, the percentage increase of dynamic modulus of elasticity of normal OPC concrete from 28 day to one year is 5 % to 6 %. The corresponding average increase for the HVFA concrete was 13 % to 28 %. The percentage increment of dynamic modulus of elasticity of HVFA is thus about 3 ~ 4 times that of the normal OPC concrete. As water curing continued, the HVFA concrete appeared to undergo some

more hydration reaction than the OPC concrete although equivalent mechanical properties were never reached.

At the end of 504 days, the average percentage loss on dynamic modulus for dry cured specimens of HVFA concrete is quite low, about 4 %, after the 28 day value. The decrease in modulus of HVFA concrete is thus very small and almost negligible. It is worth recalling the effect of prolonged air drying on strength development. With a short period of seven days moist curing, it is possible not only make the full achievement of the strength potential of HVFA concrete, but in effect also preserve the complete development of its modulus of elasticity [6].

4-6-3. Relationship between the dynamic modulus and compressive strength

The modulus elasticity is greatly influenced by the strength of concrete, stiffness of the aggregate, and by the volumetric proportion of aggregate in the concrete. It is also influenced by curing conditions, the age of the concrete, and mix proportions of the concrete. Although individual studies have shown that the modulus elasticity increases with an increase in the compressive strength of concrete, there is no agreement on the precise form of the relationship [74,75,76].

When high volume fly ash / high strength concrete began to be developed, efforts were made to see whether the existing relationships could be used to predict high volume fly ash concrete modulus of elasticity or new formulae had to be developed.

The relationship between the dynamic modulus of elasticity, E_D , and compressive strength, f_c , is generally by the following equation :

$$E_D = a f_c^b \text{ ----- (4-11)}$$

where E_D is the dynamic modulus of elasticity of concrete in GPa, f_c is the compressive strength, in MPa, and a and b are constants.

The relationship between dynamic modulus of elasticity and compressive strength for moist and dry cured specimens, at ages of 1 day to 18 months, is shown in Figs 4-35 and 4-36. Due to the influence of the total cementitious content on concrete and the wet specimens having higher dynamic modulus of elasticity than the dried specimens, it is recommended that separate equations be used for the two conditions.

Regression analysis of the data shown in these figures produced the following relationships :

Under water curing

$$E_D = 14.07 f_C^{0.30} \text{ (350 kg/m}^3 \text{ mixes) } (r = 0.98) \text{ ----- (4-12)}$$

$$E_D = 21.50 f_C^{0.30} \text{ (450 kg/m}^3 \text{ mixes) } (r = 0.96) \text{ ----- (4-13)}$$

Under air curing

$$E_D = 17.94 f_C^{0.18} \text{ (350 kg/m}^3 \text{ mixes) } (r = 0.88) \text{ ----- (4-14)}$$

$$E_D = 28.32 f_C^{0.13} \text{ (450 kg/m}^3 \text{ mixes) } (r = 0.79) \text{ ----- (4-15)}$$

Irrespective of the total cementitious content, for the wet cured concrete, the dynamic modulus of elasticity, E_D , increases approximately with the cube root of its curing compressive strength, f_C . It is clear that dynamic modulus of elasticity can be accurately predicted from compressive strength, for moist cured specimens. Each individual equation produces a high correlation factor between the two parameters under water curing and there is a significant correlation at the 99 % confidence level between dynamic modulus of elasticity and compressive strength of HVFA concrete.

In Fig 4-36, the relationship is observed to be markedly influenced by both the total cementitious content and the air drying. Although these correlation coefficients are somewhat low, there is a significant correlation at the 96 % confidence level between dynamic modulus of elasticity and compressive strength of HVFA concretes under air curing.

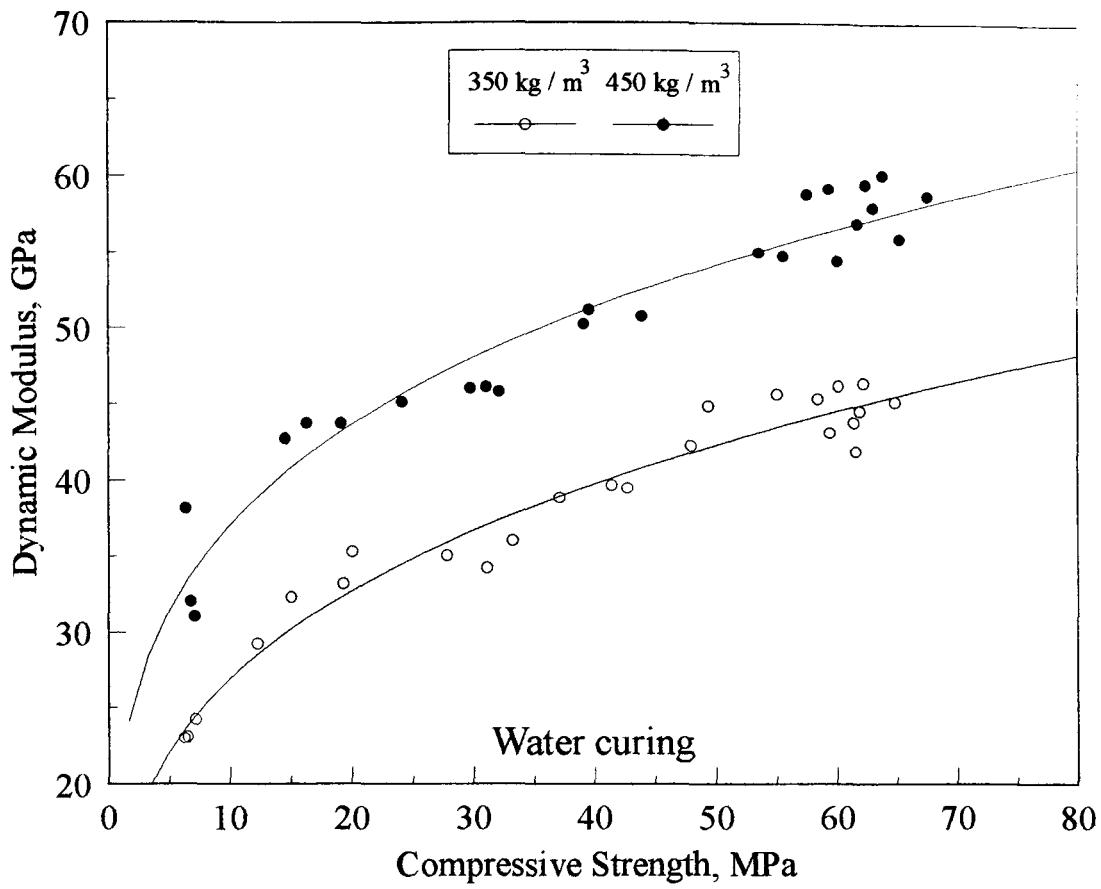


Figure 4-35 Relationship between dynamic modulus elasticity and compressive strength (Water curing)

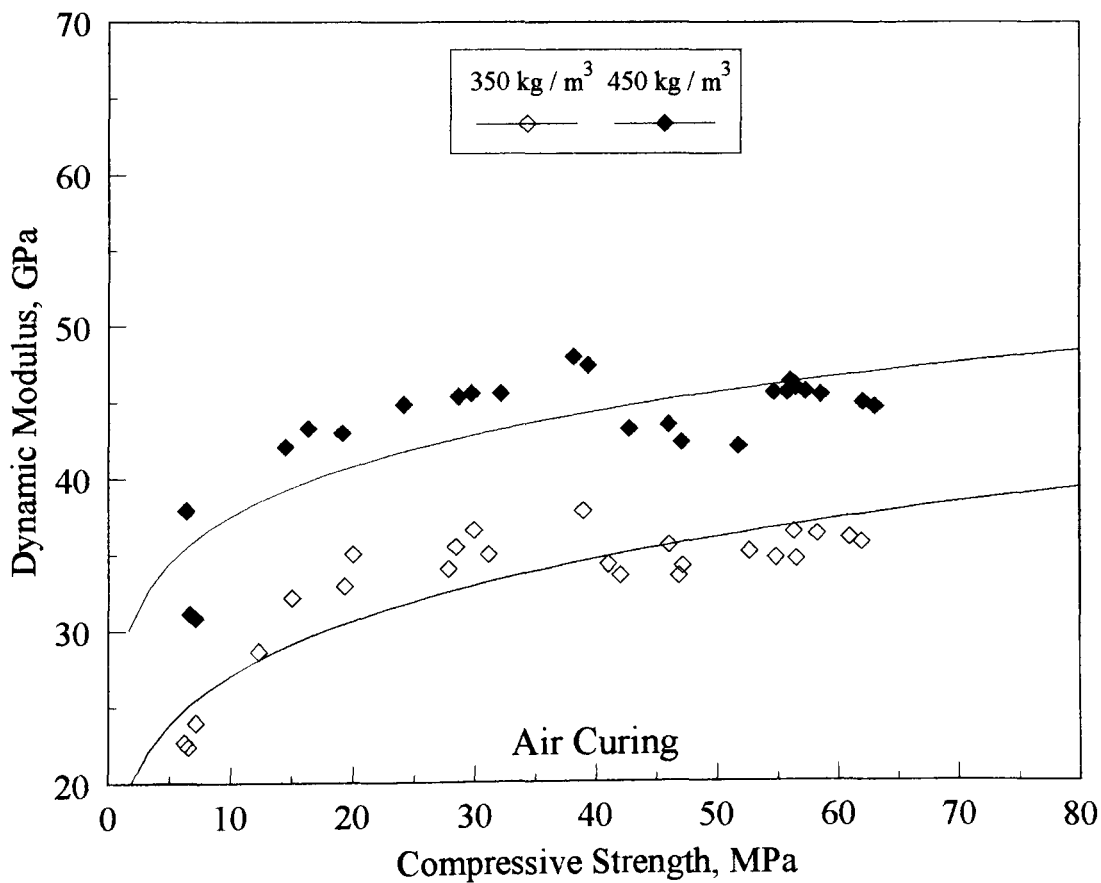


Figure 4-36 Relationship between dynamic modulus elasticity and compressive strength (Air curing)

On the basis of the above results, the relationships between dynamic modulus of elasticity and compressive strength are curvilinear since the dynamic modulus of elasticity is more dependent on the moisture gradient.

4-6-4. Comparison of modulus elasticity prediction

While many results of tests for modulus of elasticity of concrete have been published, there are only a few where the dynamic modulus of elasticity on HVFA concrete have been tested and its relationship reported. Most of the researchers [9,27,43,59] have presented the results of static modulus of elasticity. For this reason, Eqn. 4-16, as suggested by the British Code for design of concrete structures, CP 110 : 1972 is also used in the present investigation. The equation may be more convenient to estimate the static modulus of elasticity, E_C , from the measured dynamic modulus of elasticity, E_D .

$$E_C = 1.25 E_D - 19 \text{ (Both moduli being expressed in GPa) ----- (4-16)}$$

A summary of the functions proposed by various researchers including those obtained from the results for all the HVFA concretes are shown in Tables 4-25 and 4-26, and compared in Fig 4-37. Comparison is also made with the relationship predicted by ACI 318-89 and CP 110, as follows :

$$E_C = 4.73 f_c^{0.50} \quad \text{(ACI 318-89) ----- (4-17)}$$

$$E_C = 9.10 f_c^{0.33} \quad \text{(CP 110) ----- (4-18)}$$

Form the figure, good agreement was found between the predicted and measured values for the modulus of elasticity of HVFA concrete made of 350 kg/m³ mixes, but, it was lower than the reported by EPRI [9] and Swamy [59]. However, the levels of compressive strength of the HVFA concrete at 28 and 504 days, and the modulus of elasticity of 450 kg/m³ mixes are rather high. At the end of 18 months, the test results are higher than the ACI Building Code 318-89 calculated values by about 43 ~ 49 % for the 450 kg/m³ mixes.

Table 4-25 Comparison of predicting modulus elasticity and published data under water curing (28 days)

Measured values of compressive strength and modulus by Author						
Mix	350F	350SF	350S	450F	450SF	450S
f_c (MPa)	33.2	37.1	41.4	31.0	39.1	39.5
$*E_c = 1.25 E_D - 19$ (GPa)	26.3	29.6	30.6	38.6	43.8	45.0
Calculated value (GPa)						
$E_c = 4.73 f_c^{0.5}$ (ACI 318-89)	27.3	28.8	30.4	26.3	29.6	29.7
$E_c = 9.10 f_c^{0.33}$ (CP 110)	29.2	30.4	31.5	28.6	30.9	31.0
$E_c = 10.95 f_c^{0.3}$ (Swamy)	31.4	32.4	33.5	30.7	32.9	33.0
$E_c = 8.79 f_c^{0.39}$ (EPRI)	34.5	36.0	37.6	33.5	36.7	36.9
(* $E_c - E_c$) / E_c (%)						
ACI 318-89	-4	+3	+1	+47	+48	+52
CP 110	-10	-3	-3	+35	+42	+45
Swamy [59]	-16	-9	-9	+26	+33	+36
EPRI [9]	-24	-18	-19	+15	+19	+22

Table 4-26 Comparison of predicting modulus elasticity and published data under water curing (504 days)

Measured values of compressive strength and modulus by Author						
Mix	350F	350SF	350S	450F	450SF	450S
f_c (MPa)	62.2	60.1	64.8	62.4	63.8	67.4
$*E_c = 1.25 E_D - 19$ (GPa)	39.1	38.8	37.5	55.4	56.2	55.4
Calculated value (GPa)						
$E_c = 4.73 f_c^{0.5}$ (ACI 318-89)	37.3	36.7	38.1	37.4	37.8	38.8
$E_c = 9.10 f_c^{0.33}$ (CP 110)	36.1	35.6	36.6	36.1	36.4	37.0
$E_c = 10.95 f_c^{0.3}$ (Swamy)	37.9	37.5	38.3	37.9	38.1	38.8
$E_c = 8.79 f_c^{0.39}$ (EPRI)	44.0	43.4	44.7	44.1	44.5	45.4
(* $E_c - E_c$) / E_c (%)						
ACI 318-89	+5	+6	-2	+48	+49	+43
CP 110	+8	+9	+3	+53	+54	+50
Swamy [59]	+3	+4	-2	+46	+48	+43
EPRI [9]	-11	-11	-16	+26	+26	+22

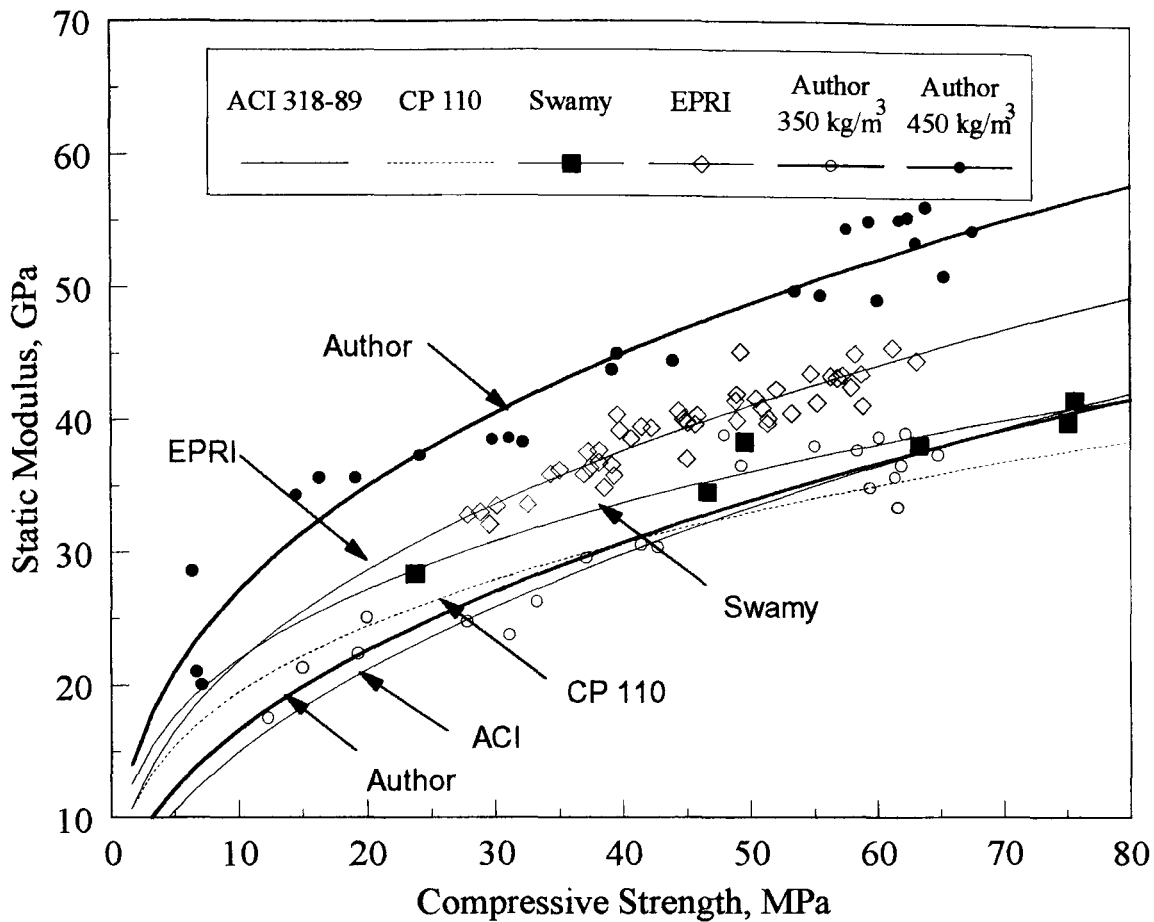


Figure 4-37 Comparison of predicting modulus elasticity and published data

4-7. ULTRASONIC PULSE VELOCITY OF HVFA CONCRETE

The ultrasonic pulse velocity through concrete is the outcome of the time taken by the pulse to travel through the hardened cement paste and through the aggregate. The pulse velocity change is useful information for understanding the development of the inner structure of the hardened concrete. The test is, therefore, useful to detect cracking, voids, deterioration due to frost or fire, and the uniformity of concrete in similar elements.

The process of hydration can provide strength because of microstructure growth. The ultrasonic travel time then gradually decreases since cement paste gradually transfers from a plastic to a solid, and that accelerates the ultrasonic pulse velocity.

In this section a detailed analysis of the ultrasonic pulse velocity on HVFA concretes will be discussed, and the effect of curing conditions and different mixes on

their values will be described. The experimental ultrasonic pulse velocity data on HVFA concretes and normal OPC concrete are also compared. A relationship between the ultrasonic pulse velocity and the dynamic modulus of elasticity is also described.

4-7-1. Effect of curing condition and different mixes on HVFA concrete

The variation of ultrasonic pulse velocity of HVFA concretes with both binder contents under the two curing regimes is illustrated in Figs 4-38 and 4-39. Some typical data of pulse velocity of HVFA concrete under water and air curing are shown in Tables 4-27 and 4-28, respectively.

These results show that the ultrasonic pulse velocity curves can be divided into three stages for all the HVFA concretes. In the first stage, the pulse velocity increased rapidly for about one week, after which the reading showed an obvious change under the two curing regimes. The second stage was a transition stage, and the pulse velocity in this section exhibited a gradual increase or decrease about for 3 months. This changeable stage appears over the period between the end of the early hydration and the pozzolanic activity period. There was seen during this period from the preceding sections, a large variation of the swelling due to the formation of ettringite ; growth of ettringite at early ages becomes more efficient in producing swelling in the HVFA concretes and therefore, a little unstable stage of pulse velocity development between the early hydration and the pozzolanic activity period is understandable [77].

The third stage is a steady and stable phase with a gradual increase in pulse velocity. The readings remained relatively constant with age at this stage as the curing continued. From the data it can be inferred that the steady state implies that the hydration products fill pore spaces and that the hydration reaction continues. During the pozzolanic activity, the growth of hydration products continues to progress gradually, and so, the pulse velocity reaches a stable progressive state.

**Table 4-27 Ultrasonic pulse velocity on HVFA concrete (Water curing)
(Unit : km/sec)**

Age (days)	350F	350SF	350S	450F	450SF	450S
1	3.57	3.47	3.62	3.51	3.65	3.65
7	4.25	4.16	4.22	4.23	4.24	4.28
28	4.23	4.47	4.53	4.31	4.5	4.53
91	4.55	4.61	4.66	4.55	4.65	4.66
189	4.68	4.71	4.71	4.69	4.72	4.69
364	4.78	4.73	4.75	4.77	4.78	4.75
504	4.78	4.77	4.74	4.79	4.77	4.75

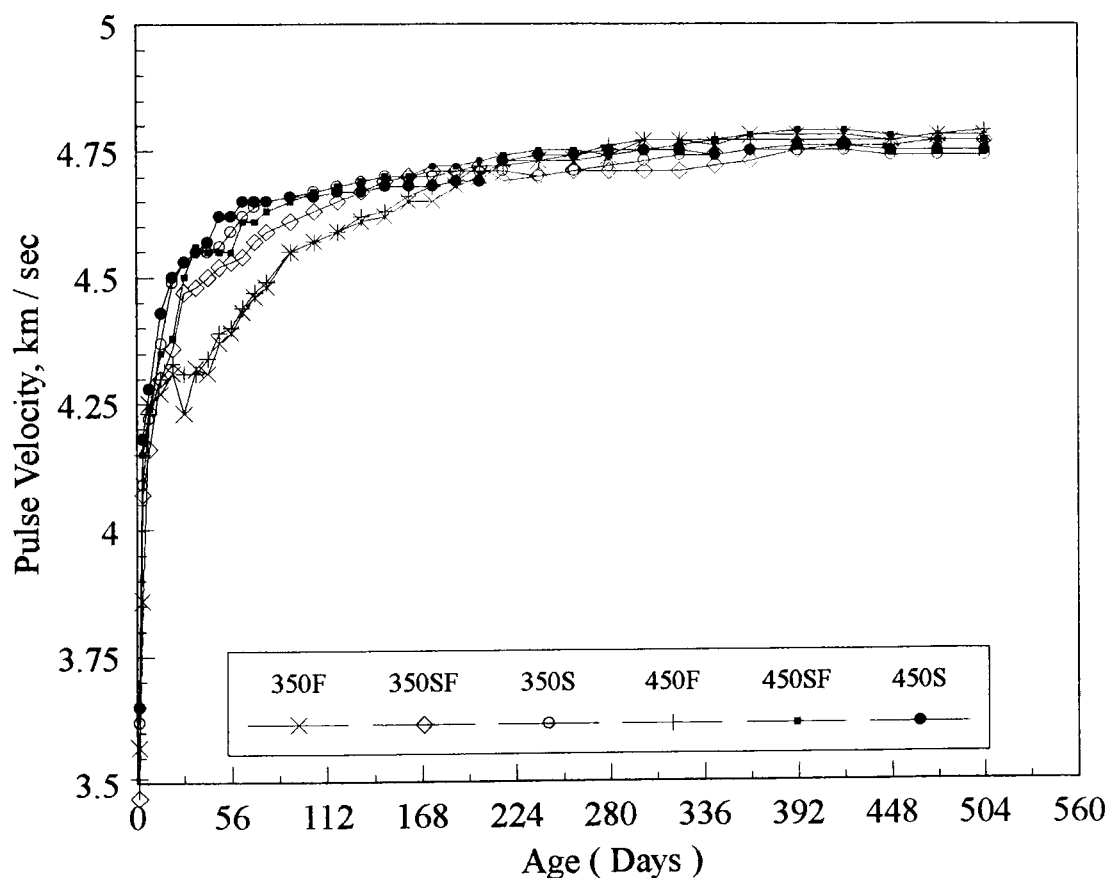


Figure 4-38 Variation of pulse velocity on HVFA concrete under water curing

Data from the results indicated that the ultrasonic pulse velocity was the highest in water cured concretes. From Fig 4-38 it is seen that the presence of silica fume in Mix-350SF and 450SF helped these concretes to develop a denser internal structure from an early age. Mixes 350S and 450S with large amounts of fly ash also

developed a dense structure and their pulse velocity increased very rapidly from early ages, also all they showed marginally better performance than the silica fume mixes, but by about six months, all the mixes appeared to have more or less the same value of ultrasonic pulse velocity. Beyond the age of six months, the pozzolanic reaction activated by the fly ash and silica fume with the hydration of cement reduced the gap between the different mixes. The long term pulse velocity developed for all the HVFA concretes ranged from 4.74 km / sec to 4.79 km / sec at the age of 504 days.

Under prolonged air curing all the HVFA concretes behaved somewhat similarly, and showed a pattern of behaviour similar to that of dynamic modulus of elasticity - a significant fall with age soon after the cessation of water curing, even though the concretes had high strength. The results show that mixes 350S and 450S performed best followed by those incorporating both fly ash and silica fume. At the end of 504 days, the pulse velocity development of HVFA concretes ranged from 3.98 km / sec to 4.13 km / sec.

**Table 4-28 Ultrasonic pulse velocity on HVFA concrete (Air curing)
(Unit : km/sec)**

Age (days)	350F	350SF	350S	450F	450SF	450S
1	3.64	3.49	3.63	3.47	3.67	3.65
7	4.28	4.16	4.22	4.24	4.24	4.28
28	4.15	4.23	4.30	4.08	4.23	4.29
91	4.06	4.17	4.23	4.01	4.19	4.17
189	3.99	4.11	4.14	3.97	4.11	4.13
364	3.98	4.04	4.15	3.94	4.11	4.14
504	4.02	4.07	4.13	3.98	4.09	4.10

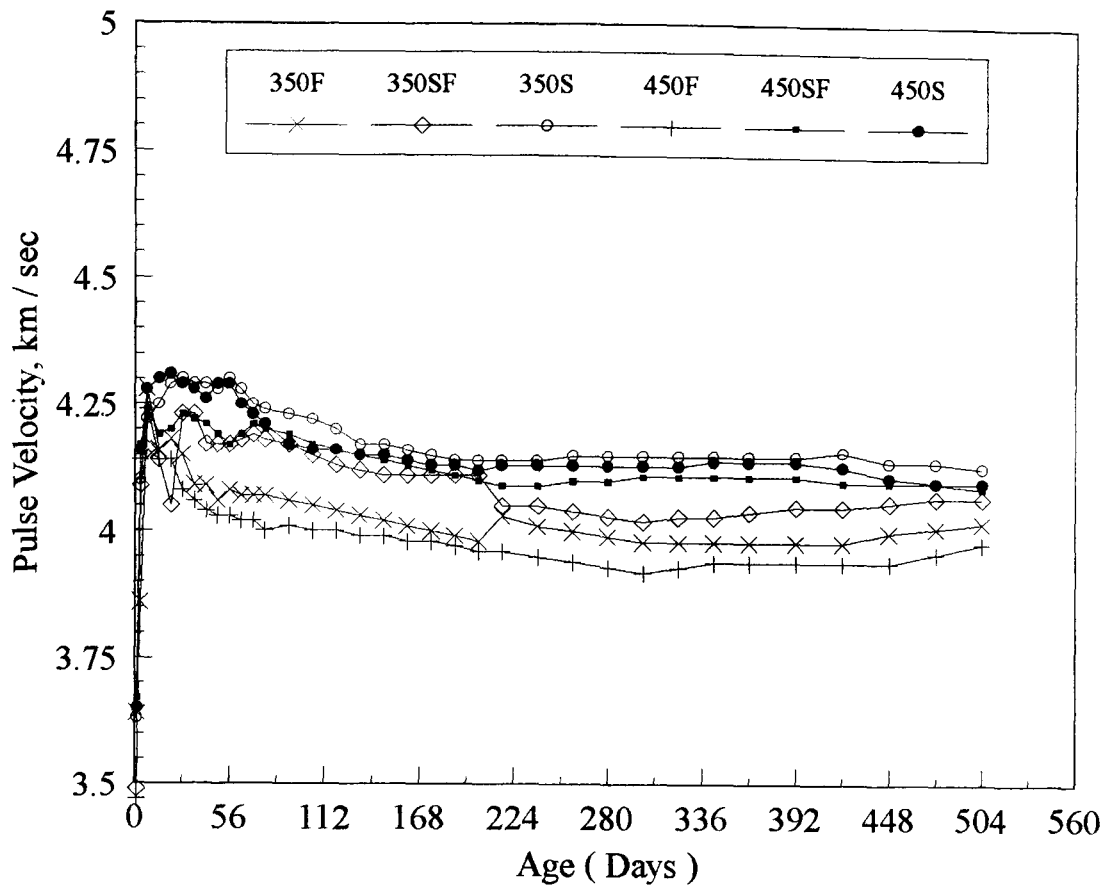


Figure 4-39 Variation of pulse velocity on HVFA concrete under air curing

The relative rates of development of pulse velocity of HVFA concretes cured in water and air are illustrated in Table 4-29.

Table 4-29 Influence of air curing on pulse velocity
(Unit : %)

Age (days)	350F	350SF	350S	450F	450SF	450S
14	97	96	97	96	96	97
28	98	95	95	95	94	95
91	89	90	91	88	90	90
189	85	87	88	85	87	88
364	83	86	87	83	86	87
504	84	85	87	83	86	86

Remarks : Water cured specimen is assumed 100%

The results indicate that exposure to ambient air of all HVFA concretes caused a slight retrogression of ultrasonic pulse velocity with continued air drying. The pulse velocity of air cured concrete is about 85 % of the average velocity of water cured concrete at 504 days. The percentage gain of pulse velocity with continued air drying is almost the same as the compressive strength development under similar conditions. In general, the more dense and strong the HVFA concrete, the lower is the value of the reduction. At the end of 504 days, the values of the pulse velocity were in a manner similar to those of dynamic modulus of elasticity. The average percentage loss on pulse velocity for all HVFA concretes is somewhat lower, about 3 %, compared to the same concretes at the age of 28 days. The reduction in pulse velocity is almost the same as the loss in dynamic modulus of elasticity, as was also found by others [41].

A comparison of the influence of the total binder content on pulse velocity under both types of curing conditions is shown in Figs 4-40 and 4-41. The results show that the total binder content does not seem to have much effect on changes in the pulse velocity under both types curing conditions. The reason may be explained by the fact that, the pulse velocity is controlled primarily by the modulus of elasticity of the material and not by its strength alone, because the composition of a concrete does not affect its strength in the same way as it does its pulse velocity.

From the preceding data in Tables 4-23 and 4-24, similar rates of development of dynamic modulus of elasticity due to total binder content were observed. Therefore, for a given aggregate and a given richness of the mix, the pulse velocity of the concrete is affected more by the modulus of elasticity, and consequently, no unique relation between pulse velocity and compressive strength exists [78].

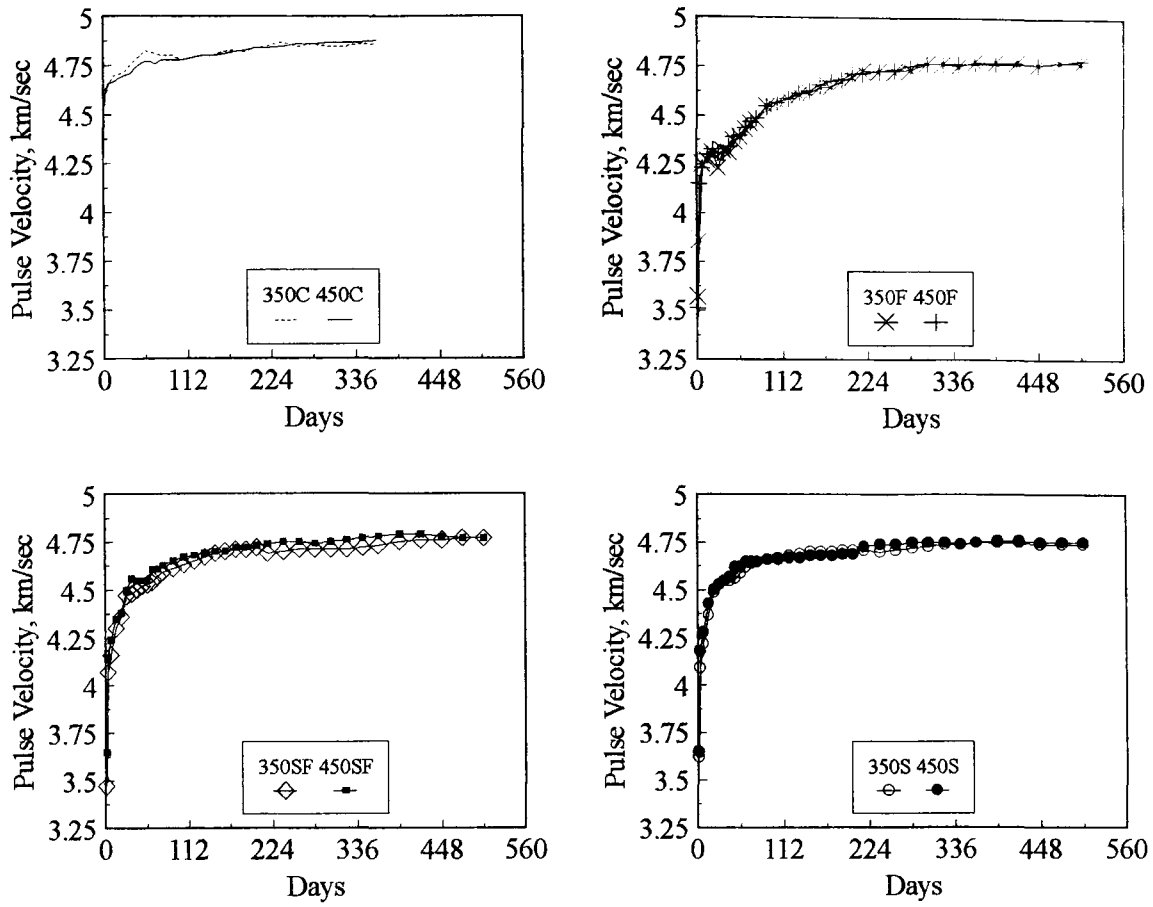


Figure 4-40 Effect of total binder content on pulse velocity (Water curing)

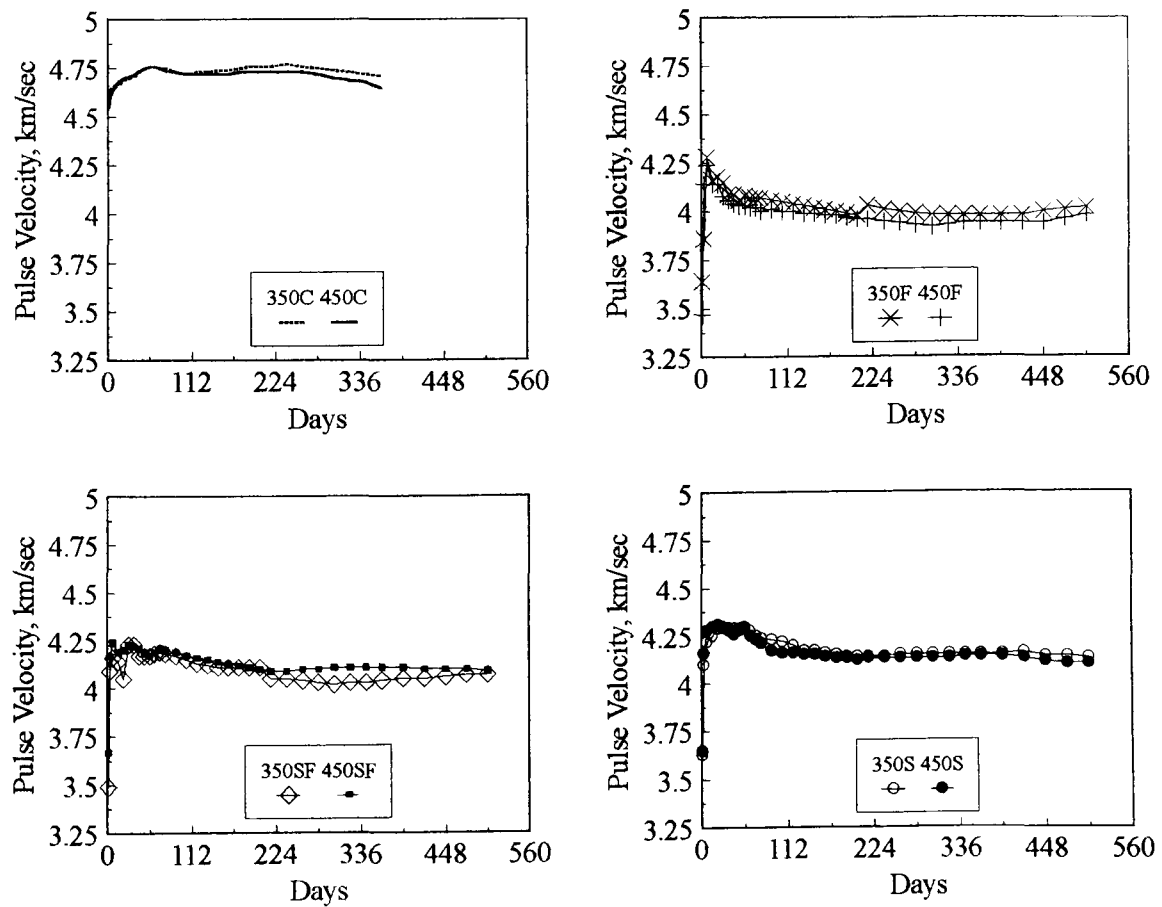


Figure 4-41 Effect of total binder content on pulse velocity (Air curing)

4-7-2. Comparison with normal OPC concrete

Table 4-30 represents some typical data of ultrasonic pulse velocity for the OPC concrete mixes under both types curing conditions. The rate of gain of pulse velocity as a % of 28 day velocity are is shown in Tables 4-31 and 4-32.

From the results, it can be seen that, under continued moist curing condition, the percentage increase in pulse velocity from 28 days to one year is 3 % to 4 % for all of normal OPC concretes. The corresponding average increase for the HVFA concretes was 5 % to 13 %. The differences of between 350F and 350C, 450F and 450C mixes in pulse velocity at one year under water curing were about 10 % and 7 %, respectively.

At the end of one year, very little reduction in pulse velocity of OPC concrete with air curing was observed. The differences between 350F and 350C, 450F and 450C mixes in pulse velocity at the end of on year under air curing were only 4 % and 2 % respectively. Undoubtedly, the potential for pulse velocity development at later ages for HVFA concretes exists, even if at a slow rate.

Table 4-30 Ultrasonic pulse velocity of normal OPC concrete

Mix	350 kg/m ³ mixes				450 kg/m ³ mixes			
	Pulse velocity (km/sec)		% of 28 day velocity (%)		Pulse velocity (km/sec)		% of 28 day velocity (%)	
Age (days)	Water curing	Air curing	Water curing	Air curing	Water curing	Air curing	Water curing	Air curing
1	4.60	4.58	97	97	4.55	4.55	97	97
7	4.66	4.66	99	99	4.66	4.65	99	99
28	4.72	4.70	100	100	4.70	4.71	100	100
91	4.80	4.73	102	101	4.78	4.73	102	100
189	4.82	4.76	102	101	4.83	4.73	103	100
364	4.86	4.71	103	100	4.88	4.65	104	99

**Table 4-31 Rate of gain velocity as a % of 28 day pulse velocity (Water curing)
(Unit : %)**

Age (days)	350F	350SF	350S	450F	450SF	450S
1	84	78	80	81	81	81
7	100	93	93	98	94	94
28	100	100	100	100	100	100
91	108	103	103	106	103	103
189	111	105	104	109	105	104
364	113	106	105	111	106	105
504	113	107	105	111	106	105

**Table 4-32 Rate of gain velocity as a % of 28 day pulse velocity (Air curing)
(Unit : %)**

Age (days)	350F	350SF	350S	450F	450SF	450S
1	88	83	84	85	87	85
7	103	98	98	104	100	100
28	100	100	100	100	100	100
91	99	99	98	98	99	97
189	96	97	96	97	97	96
364	96	96	97	97	97	96
504	97	96	96	98	97	96

4-7-3. Relationship between the pulse velocity and the dynamic modulus elasticity

The relationship between the pulse velocity, V , and the dynamic modulus of elasticity, E_D , can be represented by the following equation :

$$V = a + b E_D \text{ ----- (4-19)}$$

where V is in km / sec, E_D is in GPa, and a and b are constants.

The binder content had shown similar influence on pulse velocity under both curing conditions, the total binder content had a marked influence on the dynamic modulus of elasticity. Further, the wet concretes had generally higher values of pulse velocity and dynamic modulus of elasticity than those under dry curing. It is therefore suggested that separate equation be used for each curing condition and total binder content.

The variation of pulse velocity with dynamic modulus of elasticity for HVFA concretes under the water curing is shown in Fig 4-42.

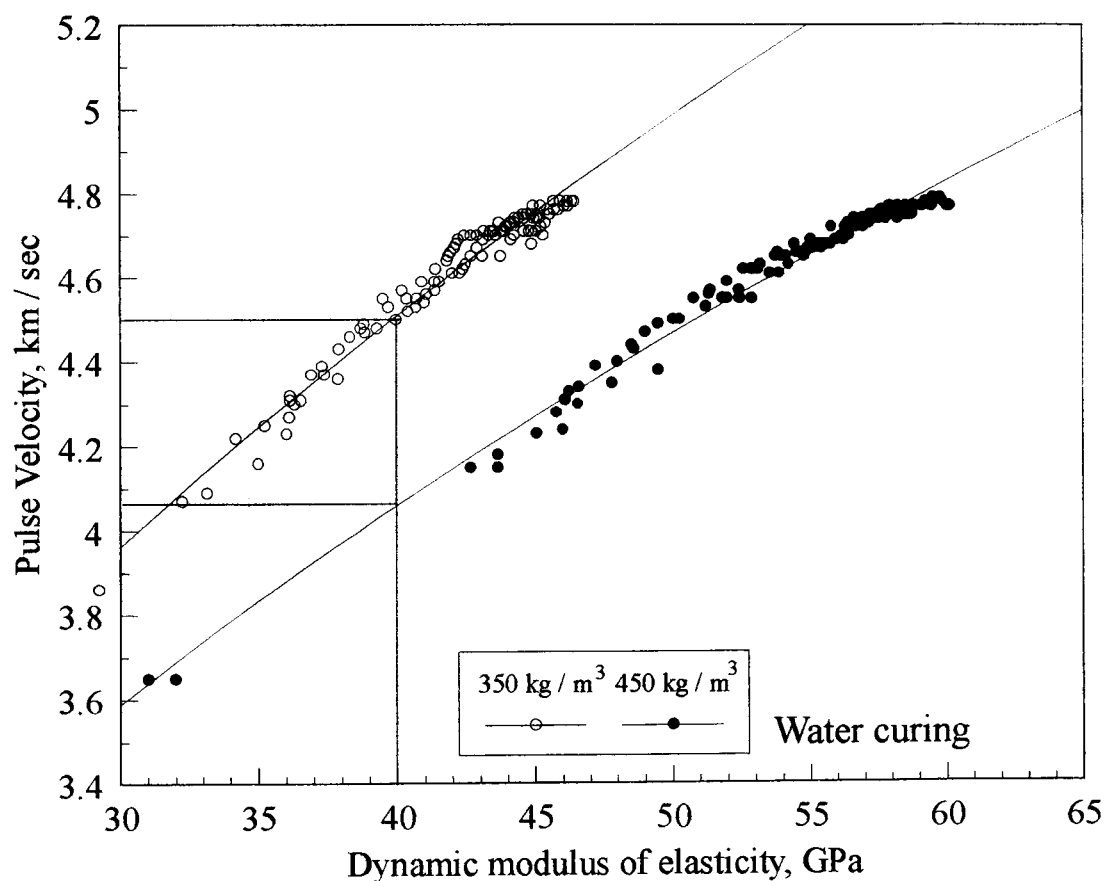


Figure 4-42 Relationship between pulse velocity and dynamic modulus of elasticity (Water curing)

The relationship is based on measurements from 1 day to 504 days for moist cured HVFA concretes. Regression analysis of the data shown in the figure produced the following relationships :

$$V = 0.86 + 0.45 E_D \quad (350 \text{ kg/m}^3 \text{ mixes}) \quad (r = 0.99) \quad \text{-----} \quad (4-20)$$

$$V = 0.84 + 0.44 E_D \quad (450 \text{ kg/m}^3 \text{ mixes}) \quad (r = 0.99) \quad \text{-----} \quad (4-21)$$

For the wet cured concrete, the two equations above are more or less identical the same for the two total binder content concretes. The linear regression shown in the figure has a correlation coefficient of 0.99. These data indicate a significant correlation between ultrasonic pulse velocity and dynamic modulus of elasticity for HVFA concretes at the 99 % confidence level.

In Fig 4-43, results of the one day to 504 days pulse velocity are plotted against the dynamic modulus of elasticity for the air cured HVFA concretes. Regression analysis of the test data shown in the figure produced the following equations :

$$V = 0.44 + 0.63 E_D \quad (350 \text{ kg/m}^3 \text{ mixes}) \quad (r = 0.98) \quad \text{-----} \quad (4-22)$$

$$V = 0.39 + 0.62 E_D \quad (450 \text{ kg/m}^3 \text{ mixes}) \quad (r = 0.93) \quad \text{-----} \quad (4-23)$$

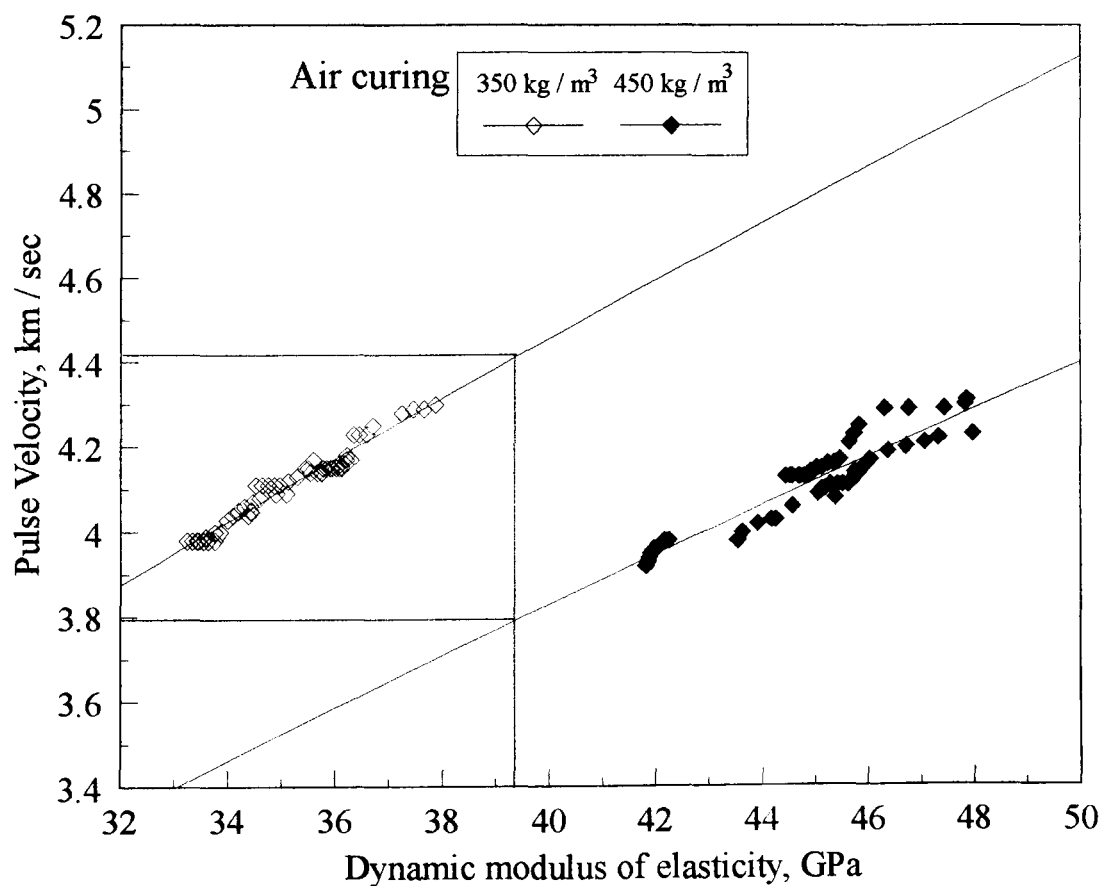


Figure 4-43 Relationship between pulse velocity and dynamic modulus of elasticity (Air curing)

Again, the correlation factor between the two sets of equations is still high, and the equation relating the two is approximately the same for the two total cementitious content concretes. Irrespective of the curing condition, the pulse velocity is controlled primarily by the dynamic modulus of elasticity of the concrete, and ultrasonic pulse velocity increases with an increase in dynamic modulus of elasticity.

It is worth pointing out, from the data for both types of curing conditions, that concretes with the lower binder content have a marginally higher pulse velocity than that with the higher binder content. This is in agreement with the concept, in general, that the pulse velocity varies inversely to the density of concrete- $V^2 = E_D / \rho$, where ρ is density.

4-8. CARBONATION OF HVFA CONCRETE

As mentioned in the literature review, one of the main causes of reinforcement corrosion is the inadequate concrete cover, which is to protect the steel and keep it in a passive state. This passivating film can be broken by the process of carbonation, which reduces the level of pH adjacent to the steel to values that can no longer maintain passivation. Once the steel has become depassivated, corrosion can occur if moisture, chloride ions, and oxygen are present.

Because blended cements are widely used nowadays, it is important to know the carbonation behaviour of concretes containing fly ash and silica fume. In HVFA concrete, the replacement level is also a factor that affects carbonation rate. The starting point in this section is the knowledge of the properties of the hardened concrete resulting from the use of the various binder materials in so far as the influence of these properties, physically or chemically, on carbonation is concerned.

The effect of the variables such as, mix proportions, and age of HVFA concretes on carbonation were studied in a programme over 18 months under both curing conditions. The relationship between carbonation depth and compressive strength was also investigated.

4-8-1. Effect of curing condition and different replacement methods

The results of this investigation on carbonation for all the concrete mixtures under both curing conditions are shown in Tables 4-33 and 4-34. For purposes of comparison, the results of the normal OPC concrete on carbonation depth are also included in the above table. Figs 4-44, 4-45, and 4-46 show the relationship between the exposure period and carbonation depth of various HVFA and OPC concretes stored in air. Figs 4-47 and 4-48 show typical examples of carbonation of HVFA and OPC concretes stored in air at various ages.

**Table 4-33 Carbonation depth - 350 kg/m³ mixes
(Unit : mm)**

Age (days)	Mix	350C		350F		350SF		350S	
		Curing	Water curing	Air curing	Water curing	Air curing	Water curing	Air curing	Water curing
28	Max.	0.0	0.0	0.0	1.4	0.0	1.4	0.0	1.3
	Min.	0.0	0.0	0.0	1.0	0.0	1.0	0.0	1.0
	Ave.	0.0	0.0	0.0	1.3	0.0	1.3	0.0	1.1
90	Max.	0.0	1.8	0.0	6.4	0.0	5.7	0.0	2.8
	Min.	0.0	0.0	0.0	3.2	0.0	2.0	0.0	2.0
	Ave.	0.0	1.8	0.0	6.1	0.0	4.8	0.0	2.6
180	Max.	0.0	2.1	0.0	8.2	0.0	7.2	0.0	5.3
	Min.	0.0	1.0	0.0	6.0	0.0	4.0	0.0	3.2
	Ave.	0.0	2.0	0.0	6.5	0.0	5.1	0.0	3.5
360	Max.	0.0	2.3	0.0	10	0.0	8.6	0.0	6.5
	Min.	0.0	1.5	0.0	9.0	0.0	6.0	0.0	5.0
	Ave.	0.0	2.1	0.0	9.4	0.0	8.3	0.0	6.4
540	Max.	---	---	0.0	13.5	0.0	13.4	0.0	11.3
	Min.	---	---	0.0	11.2	0.0	10.5	0.0	10.1
	Ave.	---	---	0.0	13.3	0.0	13.2	0.0	11.1

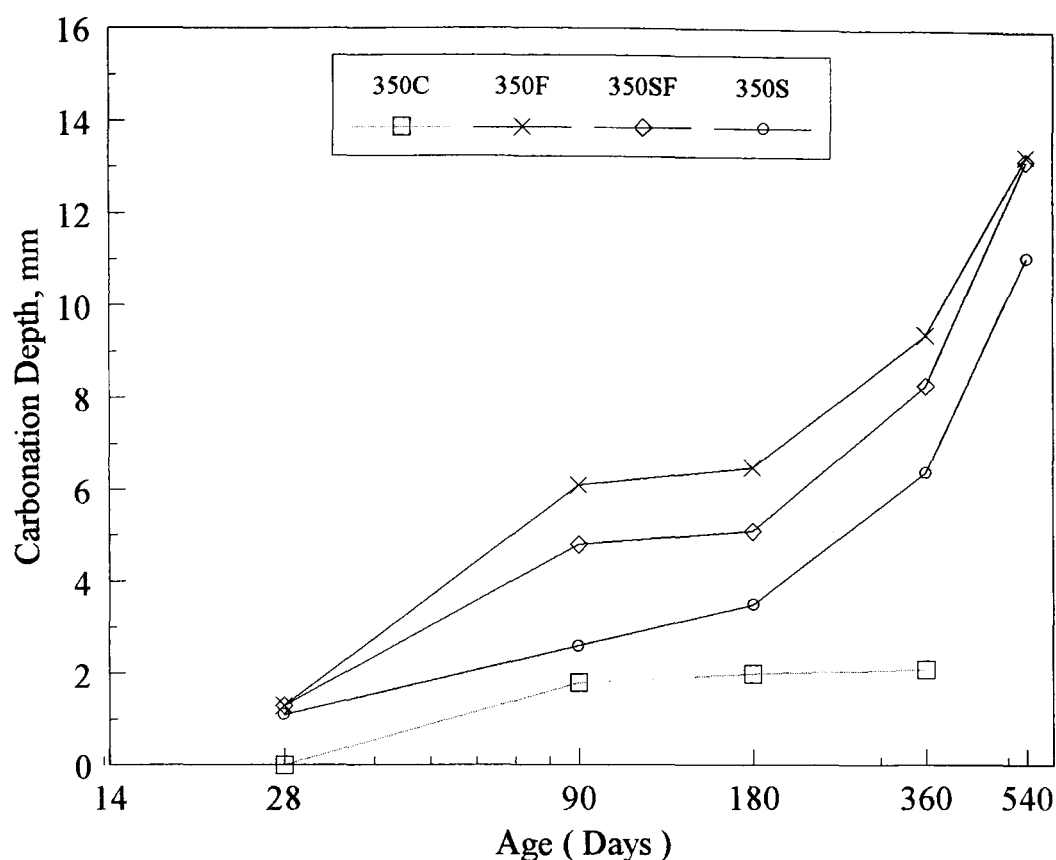


Figure 4-44 Carbonation depth of concrete - 350 kg/m³ mixes (Air curing)

It is clear from the tables that, as expected, no trace on carbonation was found in concretes stored continuously in water. The results for the air cured concretes are, however, very different from those for the concretes stored in water.

Irrespective of initial water curing, the results show that the carbonation rate increases as the environment becomes drier, and the values of carbonation depth increase with increase in the exposure period. For both types of binder content concretes, the normal OPC concrete showed higher carbonation resistance, and smallest carbonation depths compared to HVFA concrete. Further, with continued air drying up to 18 months, concretes made of 450 kg/m³ showed a similar rate of carbonation compared to the 350 kg/m³ mixes.

At one year, HVFA concretes that were water cured initially for 7 days showed a significantly higher depth of carbonation than the corresponding normal OPC concretes for both types of binder contents. The depth of carbonation in normal OPC concrete is, on average, only 25 % of that of the HVFA concrete. The higher carbonation of HVFA concrete is attributed to greater permeability of the surface concrete containing fly ash.

**Table 4-34 Carbonation depth - 450 kg/m³ mixes
(Unit : mm)**

Age (days)	Mix	450C		450F		450SF		450S		
		Curing	Water curing	Air curing	Water curing	Air curing	Water curing	Air curing	Water curing	Air curing
28	Max.		0.0	0.0	0.0	1.4	0.0	1.5	0.0	1.3
	Min.		0.0	0.0	0.0	1.0	0.0	1.0	0.0	1.0
	Ave.		0.0	0.0	0.0	1.3	0.0	1.2	0.0	1.1
90	Max.		0.0	1.3	0.0	5.7	0.0	3.9	0.0	2.1
	Min.		0.0	1.0	0.0	3.3	0.0	2.0	0.0	1.0
	Ave.		0.0	1.3	0.0	5.3	0.0	3.7	0.0	1.5
180	Max.		0.0	1.9	0.0	7.3	0.0	6.1	0.0	5.2
	Min.		0.0	1.7	0.0	4.0	0.0	3.5	0.0	2.8
	Ave.		0.0	1.8	0.0	5.5	0.0	4.5	0.0	2.7
360	Max.		0.0	2.1	0.0	9.3	0.0	7.4	0.0	6.3
	Min.		0.0	2.0	0.0	4.0	0.0	3.5	0.0	5.0
	Ave.		0.0	2.0	0.0	9.2	0.0	7.2	0.0	5.1
540	Max.		---	---	0.0	13.5	0.0	12.5	0.0	11.0
	Min.		---	---	0.0	11.0	0.0	11.1	0.0	11.0
	Ave.		---	---	0.0	13.3	0.0	12.2	0.0	11.0

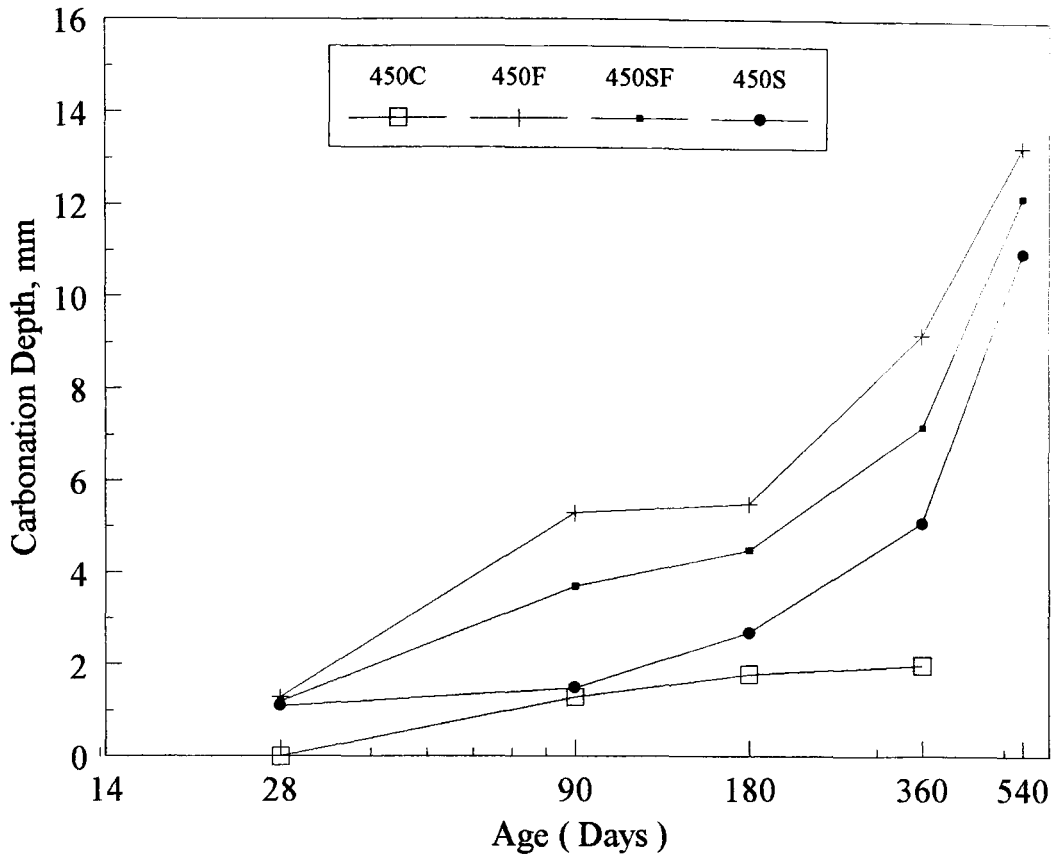


Figure 4-45 Carbonation depth of concrete-450 kg/m³ mixes (Air curing)

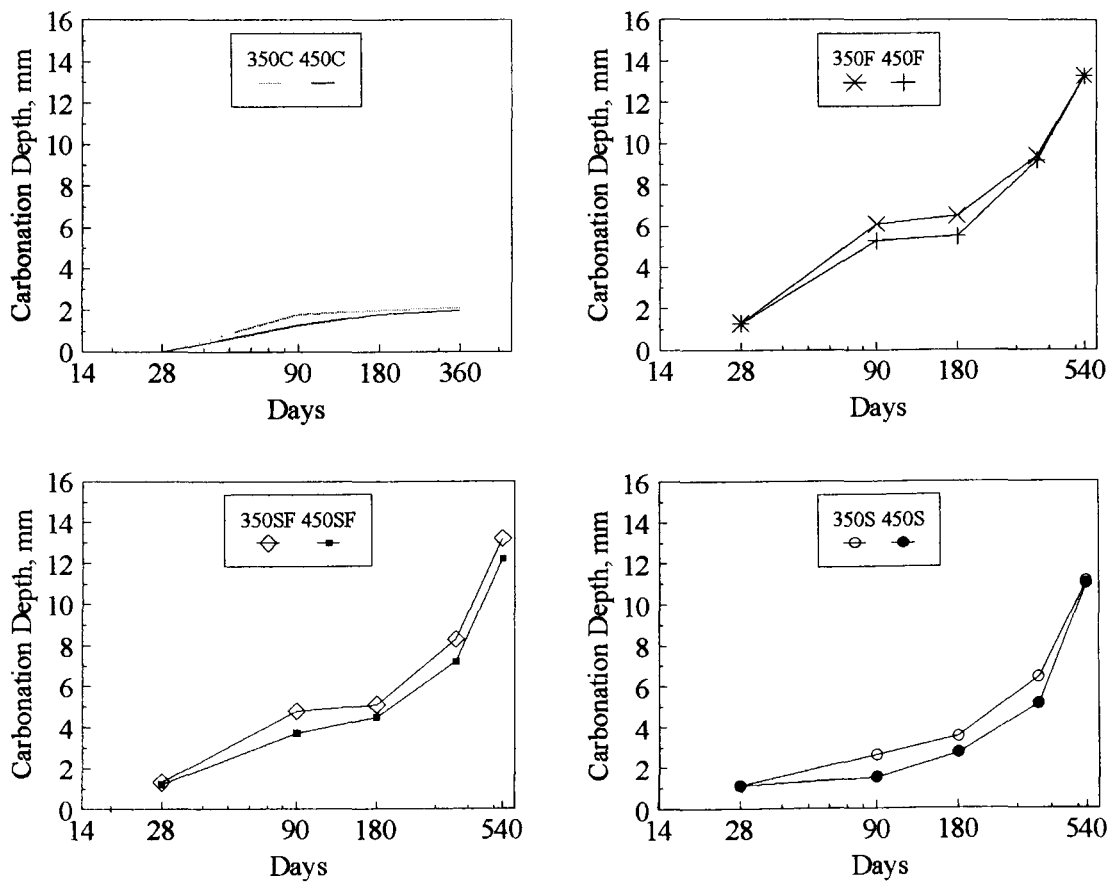


Figure 4-46 Effect of total binder content on carbonation depth (Air curing)



Figure 4-47 Carbonation of specimens stored in the laboratory-180 days



Figure 4-48 Carbonation of specimens stored in the laboratory-540 days

Further, under air curing, it is also clear from the above data that concrete, Mix-350F and Mix-450F, exhibited higher carbonation depths than those obtained in the concretes incorporating both fly ash and silica fume.

At the end of 18 months, for all HVFA concretes under air drying, the depth of carbonation was a great deal higher than the values received at one year. For specimens stored in air, differences in carbonation depth were found for concrete mixes 350F and 450F, and the mixes containing fly ash as a partial replacement for both sand and cement.

The influence of fly ash and silica fume on carbonation of concretes found in this study is in agreement with the results of other investigators [27,44,79]. The increase in the carbonation depth of HVFA concrete compared to OPC concrete may be due to the individual or combined effect of their greater surface porosity, and its smaller concentration of carbonatable constituents [5]. This indicates that the addition of such mineral admixtures to concrete which does not form proper matrix films upon coalescence, may rather increase the risk of carbonation. Kokubu & Nagataki also observed that the carbonation was distinctly increased due to raising the fly ash replacement ratio, among other things [80].

The important influence of curing condition on carbonation is clearly seen in those results. As for depth of carbonation, the depth increases the longer the period of exposure in air, which is considerably higher than that of the concrete exposed to moist curing. The results are also relevant for the strength development as well as dynamic modulus of elasticity, ultrasonic pulse velocity for high strength concretes. If the concrete matrix is porous due to carbonation, strength reduction generally occurs. As discussed in preceding sections, strength development of HVFA concrete in case of curing in water increases with age. When cured in air, although there is an increase in strength seen from the age of four weeks to one year, a trend of decline is recognised. Similar trends were observed for the dynamic modulus of elasticity and pulse velocity. These results indicate that high strength alone is not sufficient to prevent carbonation, moisture is also needed to slow down the carbonation process. These findings are in accordance with the results of other investigators [48,81,82,83]. Many of them suggest that an increase in curing time of the concretes with admixture

reduces the difference with OPC concrete regarding the rate of carbonation, as well as other physical and mechanical properties of concrete.

4-8-2 Carbonation rate coefficient

In literature [83,84] the rate of carbonation is found to be calculated as a function of exposure time, water / binder ratio, strength development, etc.

It is thus possible to express the depth of carbonation as :

$$C = a + K \sqrt{t} \text{ ----- (4-24)}$$

where C is the carbonation depth in mm, K is the carbonation rate coefficient, t is the time of exposure in sec, and a is constant.

Regression analysis to define the relationship between exposure period (\sqrt{t}) and the depth of carbonation is shown in Figs 4-49 and 4-50. The parameters, a, and, K, and the coefficients of determination, (r), are given in Table 4-35.

Table 4-35 Estimated parameters of equation $C = a + K\sqrt{t}$ ($t = \text{sec}$)

Mix	a	K	r
350C	-0.16806	0.00047	0.81882
350F	-0.61110	0.00185	0.94733
350SF	-0.72942	0.00161	0.96740
350S	-1.06045	0.00128	0.98733
450C	-0.38068	0.00047	0.90919
450F	-0.96996	0.00181	0.96348
450SF	-0.79531	0.00142	0.98826
450S	-0.92199	0.00101	0.96652

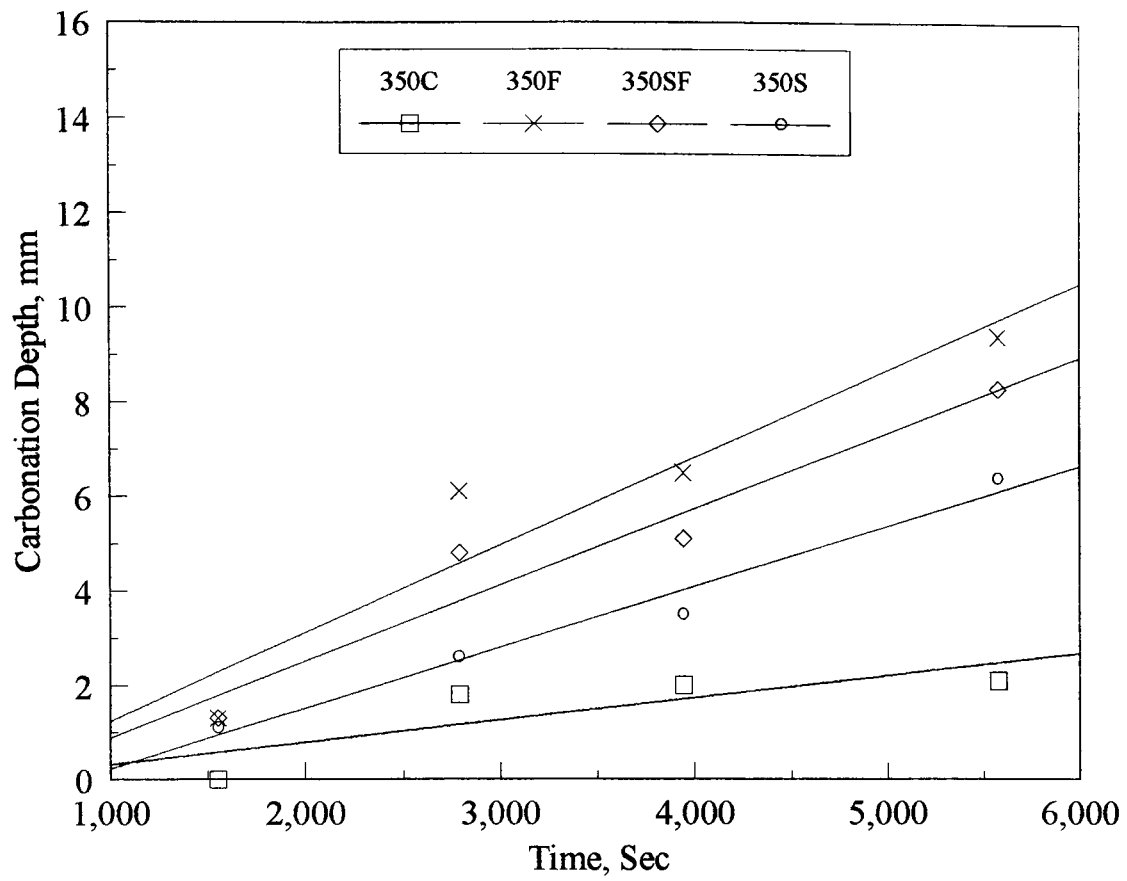


Figure 4-49 Exposure period versus carbonation depth of concrete-350 kg/m³ mixes

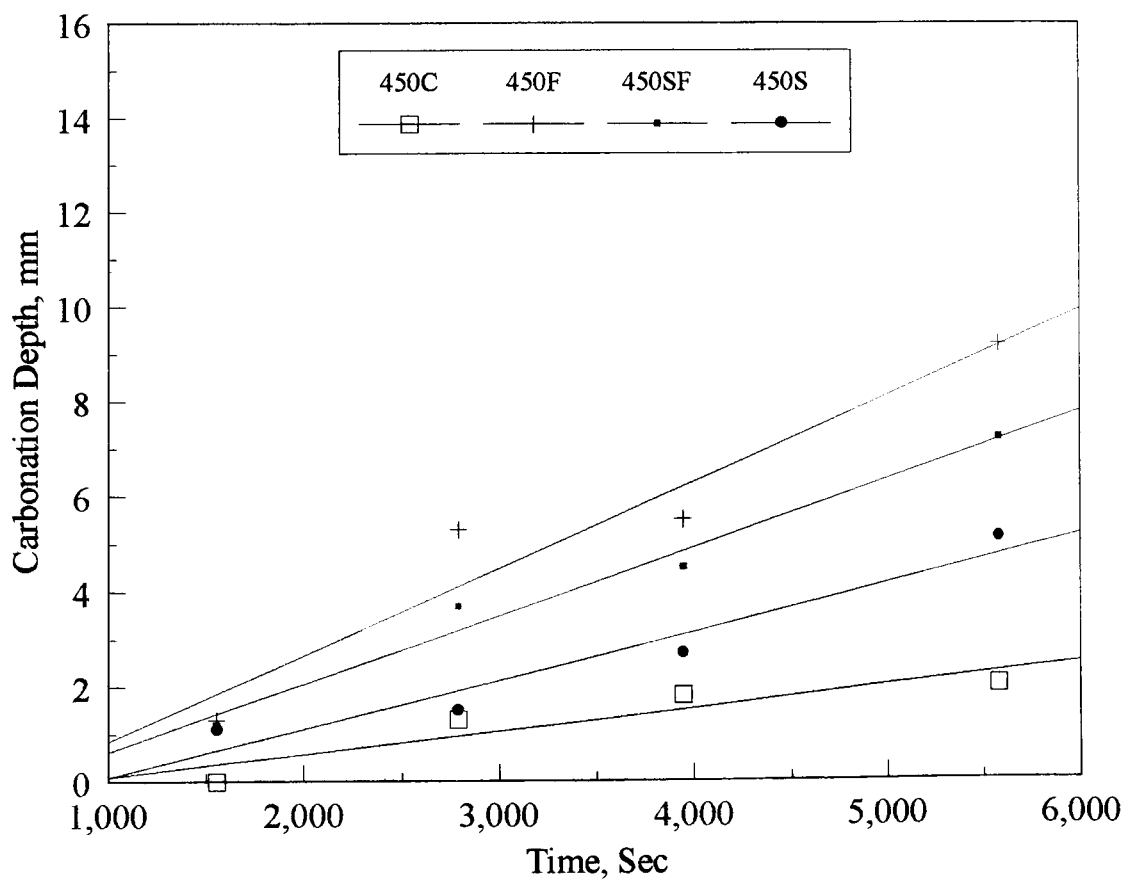


Figure 4-50 Exposure period versus carbonation depth of concrete-450 kg/m³ mixes

These parameters are valid for exposure times up to one year. All the HVFA concretes show higher carbonation rate coefficient, K , in comparison to normal OPC concretes because of the reasons mentioned earlier. Further, concrete with the 350 kg/m^3 binder content had a higher carbonation rate coefficient than that of the 450 kg/m^3 mixes. Again, the concretes made of 350F and 450F exhibited the poorest results.

4-8-3. Relationship between the carbonation depth and compressive strength

In general, the behaviour of concrete is always based on the assumption that the ambient medium, i. e., air does not react with the hydrated cement. In fact, structural concrete is always exposed to the atmosphere which contains high levels of carbon dioxide. In the presence of moisture, the carbon dioxide reacts with the hydrated cement, and this results in carbonation taking place through the pore system in the hardened cement concrete, which may result in a decrease in strength. The rate of carbonation depends on the atmospheric carbon dioxide, cement content, relative humidity, temperature, and the porosity of the concrete, the latter depending upon the type of cement, the water / binder ratio, and the degree of hydration.

The relationship between the depth of carbonation and compressive strength for dry cured HVFA concretes, at ages of 180 days, 360 days, and 540 days is shown in Fig 4-51.

Regression analysis of the data shown in the figure produced the following relationships :

$$f_c = 87.39 - 6.80 C \quad (180 \text{ days }) \quad (r = - 0.95) \text{ ----- } (4-25)$$

$$f_c = 87.40 - 4.37 C \quad (360 \text{ days }) \quad (r = - 0.98) \text{ ----- } (4-26)$$

$$f_c = 102.9 - 3.99 C \quad (540 \text{ days }) \quad (r = - 0.85) \text{ ----- } (4-27)$$

where f_c is the compressive strength in MPa, and C is the carbonation depth in mm.

It is often said that the rate of carbonation is simply a function of the strength of concrete. As shown in the figure, there is a reasonable inverse correlation between the depth of carbonation, C , and compressive strength, f_c , of HVFA concrete : in other words, the depth of carbonation of concrete increases with decrease in strength.

As for depth of carbonation, the depth increases the longer period the of time left in air. At the end of 540 days, although the carbonation and strength relationship shows a lower correlation coefficient, the data indicate still significant correlation at the 99 % confidence level between the depth of carbonation and compressive strength. On the basis of the present studies, of the factors affecting carbonation, strength appears to be an important factor.

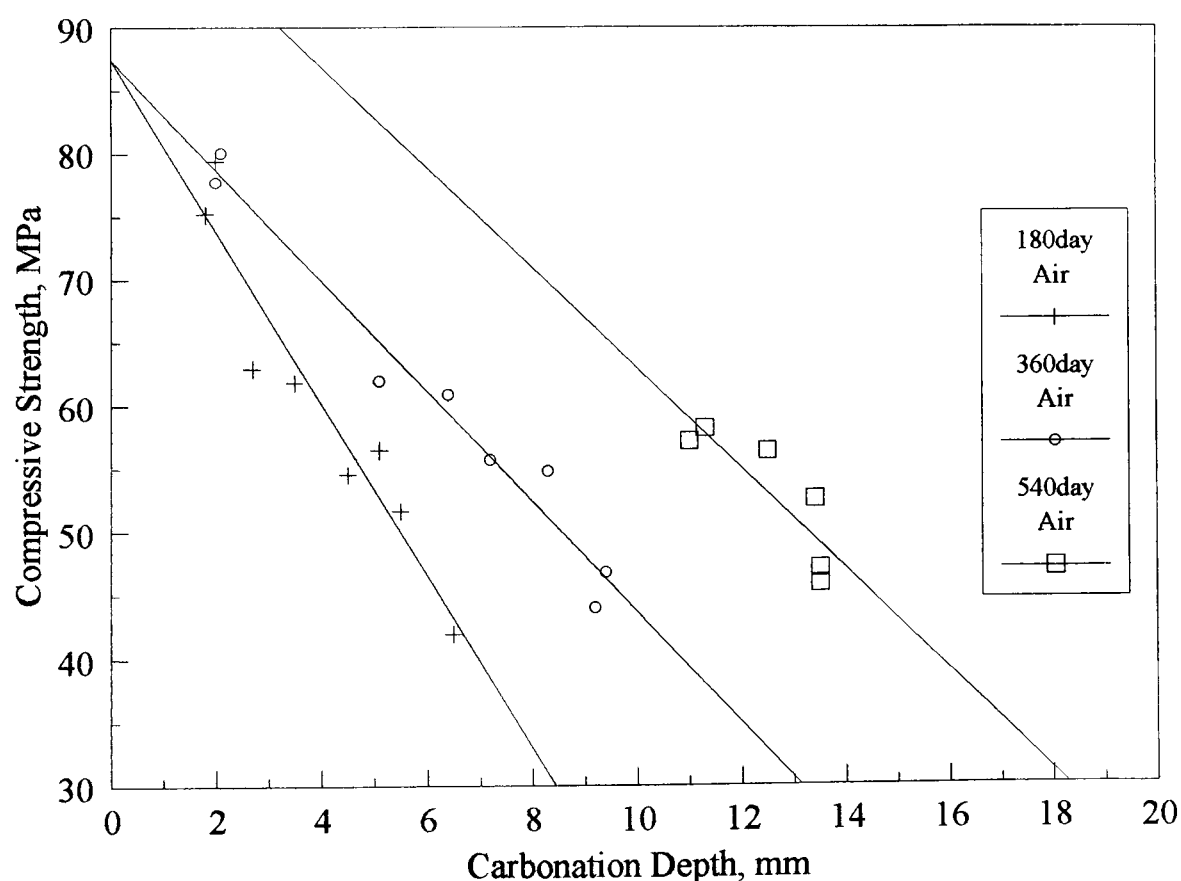


Figure 4-51 Relationship between carbonation depth and compressive strength

4-8-4. Comparison with published data

Comparison of carbonation depth with those of other investigators [27,44,48,59] is shown in Table 4-36. Data in table clearly shows that there is a wide difference in carbonation depths. Due to the different test parameters, it is difficult to analyse the test results from the data and give a definite conclusions. However, it is obvious from the results that fly ash concretes having higher cementitious content, low water / binder ratio and moisture, are most likely to well resist from carbonation. Meanwhile, the importance of early strength is also clearly indicated by the data.

Table 4-36 Comparison of carbonation depths with published data

Researchers	Binder content (kg/m ³)	Fly ash content (%)	W / B	28 day strength (MPa)	Carbonation depth (mm)	Test age (Months)
Malhotra & Bilodeau [44]	370	58	0.32	35.0	4.0	31
	"	"	"	"	7.0	50
	"	"	"	"	8.0	90
Swamy & Mahmud [59]	266	50	0.62	23.7	23.6 ~ 27.2	33
	348	"	0.42	46.6	13.2 ~ 17.9	"
	466	"	0.32	63.3	6.3 ~ 11.1	"
Langley et al [27]	400	55	0.27	44.0	3.0	24
	225	56	0.49	22.1	10.0	"
Kawamura & Haque [48]	250	30	0.55	35.0	7.5	48
	350	"	0.49	45.0	5.0	"
Author	350F	57	0.40	28.4	13.3	18
	350SF	51	"	29.9	13.2	"
	350S	97	"	38.9	11.1	"
	450F	56	"	28.6	13.3	"
	450SF	51	"	38.1	12.2	"
	450S	97	"	39.3	11.0	"

4-9. CONCLUSIONS

This chapter has examined the effect of curing condition on the engineering properties of HVFA concrete with and without silica fume. The following conclusions are based on the results and analyses presented in this chapter.

1. For the HVFA concrete investigated, continuous moist curing gave higher strength, dynamic modulus of elasticity, and ultrasonic pulse velocity than prolonged exposure to air drying.
2. Under moist curing, there was a continuous increase in compressive strength with age. The strength at 18 months expressed as a percentage of the 28 day strength varied between 157 % and 201 %.
3. Air curing preceded by 7 days moist curing is beneficial to the flexural strength development of HVFA concretes. At 90 days, concrete under this condition exhibited the highest flexural strength.
4. A significant correlation between flexural strength and compressive strength exists for HVFA concrete at the 99 % confidence level.
5. In general, increasing the binder content of the concrete from 350 kg/m³ to 450 kg/m³ of binder content had little effect on strength, but did yield a large benefit in terms of dynamic modulus of elasticity, and pulse velocity in most of the HVFA concretes.
6. Under the same conditions, concretes made with both fly ash and silica fume had engineering properties in most respects which were as good as, or superior to, those made by fly ash alone as cement replacement. The use of fly ash to replace both cement and sand was able to combine the benefits of both separate replacements.
7. Air curing causes a substantial reduction in the engineering properties of HVFA concretes. For example, the compressive strength of dry cured HVFA concrete is about 83 % of the strength of wet cured concrete. The average percentage loss

- of dynamic modulus of elasticity, or pulse velocity for all HVFA concretes was, on the other hand, very low, only about 3 %, when compared to the same concretes air cured for 28 days.
8. The deterioration of concrete also influences the cement paste in the interior of HVFA concrete, and has a close relationship with carbonation. The phenomenon of a decline in engineering properties accompanying increase in depth of carbonation is also seen in normal portland cement concrete.
 9. Although the early strength of concrete made with HVFA was found to be low, those at ages beyond 28 days showed a continued rate of development of hydration, superior to that of the normal concrete. The HVFA concrete in this study has good potential for use in structural and mass concrete applications.
 10. The swelling in the HVFA concretes was associated with formation of ettringite. The ettringite formed in the early ages of hydration was more efficient in producing swelling. This suggests that swelling began at a lower critical degree of hydration ; the slower rate hydration of the HVFA concrete probably resulted in slightly more swelling due to adsorption of water.
 11. Drying shrinkage did not correlate with total porosity but correlated reasonably well with the volume of micropores plus mesopores.
 12. The drying shrinkage strain measured on all HVFA concretes was comparable to Ross's formula, and was about 95 % of the average percentage of the latter.
 13. The values of static modulus of elasticity, E_c , of 450 kg/m³ mixes under water curing are higher than the calculated values according to ACI building Code 318-89.
 14. The dynamic modulus of elasticity varies with changes in the total binder content similarly to normal portland concrete mixes, and is curvilinear in its relation to compressive strength.

15. There is no physical relation between the ultrasonic pulse velocity and strength. The pulse velocity was found to be very sensitive and related to the density of concrete, and linearly related to the dynamic modulus of elasticity. The total binder content does not seem to have much effect on pulse velocity under both types curing conditions. Under moist curing, all of HVFA mixtures appeared to have more or less the same value of pulse velocity beyond about six months.
16. Overall, the depth of carbonation was found to be related to the compressive strength of concrete, with and without fly ash. Generally, the HVFA concrete carbonated to somewhat higher depth compared to the normal portland concrete exposed to air curing.
17. High strength alone is not sufficient to prevent carbonation, moisture is also needed to slow down the carbonation.

CHAPTER FIVE

MICROSTRUCTURE OF HYDRATED CEMENT PASTES

5-1. INTRODUCTION

The engineering properties of normal OPC concrete, and, of HVFA concrete, containing silica fume were presented in Chapter 4, together with a discussion of the influence of fly ash and silica fume on the properties of HVFA concrete. In practice, however, most of the important properties of hardened concrete are related to the quantity, and the characteristics, of the various types of pores and hydration products in the concrete. Indeed, the engineering properties, such as strength development, drying shrinkage, swelling, and permeability are directly influenced and controlled by the relative amounts of the pores and the hydration products.

There is, thus, a great impetus to study the microstructure of such a concrete in order to examine the changes of hydration of HVFA concrete progressing with time. To a lesser extent, the influence of the characteristics of microstructure are also discussed but, it is useful to review the pore structure and mineralogical compositions of concrete.

5-2. CLASSIFICATION OF PORE SIZE IN HYDRATED CEMENT PASTES

The pores formed in fresh concrete are either water-filled or gas-filled. At the initial mixing period, the cement grains, and the conglomerates in the fresh pastes, are separated individually by the mixing water, which forms the water-filled space. The

water-filled space in the freshly mixed cement paste represents space that is available for the formation of cement hydration products.

As hydration proceeds, the volume of this space, which has a bulk volume larger than that of the original unhydrated cement, is continually reduced by the formation of the hydrate products that form a continuous matrix and bind the residual cement grains together over a period of time. At any time, that part of the original water-filled space not occupied by hydration products constitutes part of the pore system of the paste, and generally speaking, that part with the largest pores sizes. Hydration reduces the size and volume of this capillary space. If the original capillary space is small, the bulk volume of the gel eventually will be sufficient to fill this space and produce a paste free from capillary space.

In general, the volume of the water filled spaces in fresh paste must exceed the absolute volume of the cement, or some of the original cement must remain unhydrated. For this reason, the hydration products are not sufficient to fill the original water space in the paste, even after complete cement hydration, and pastes having a relatively large volume of capillaries will be produced.

Studies on the hardened cement pastes have shown that the size of its largest pores depends principally on the degree of hydration, varying from about $1\mu\text{m}$ for young pastes in which the cement hydration has progressed only a little, to about $0.1\mu\text{m}$ in mature pastes that are more completely hydrated.

As the spaces become filled with hydration products on continued curing, a time may come, if the original water / cementitious ratio was small enough, that most of the capillary spaces become isolated cavities, separated from each other by the gel that is the hydration product. This gel is itself a porous solid, most of which is the calcium silicate hydrate (C-H-S gel), and the non-solid part.

As mentioned in section 2-4, the C-S-H gel is a rigid substance, made up of colloid-size particles, and has a characteristic porosity of 28 %. The average width of the pores involved is about 15 \AA and they are known as “gel pores” [13]. The gel pore sizes are too small to allow the nucleation of new hydration products. If a paste

has such a low water / cementitious ratio that not all the cement can even become hydrated, the gel will fill completely all the space not occupied by unhydrated cement, and will contain porosity.

Measurement and classification of pore size is surrounded by experimental difficulties and by controversy. There are two main problems. First, the paste must be dried in order to make measurements, and drying almost certainly changes the pore structure. Second, a definite geometrical shape of pore must be assumed while S.E.M. micro-graphs show that the pores form a network of very irregularly shaped pores.

Pore sizes have been classified in different ways by Powers, Feldman and Sereda, Diamond et al , IUAPC, and Bentur et al [85,86,87,88]. A comparison of pore classification is shown in Fig 5-1. Table 5-1 shows a classification of porosity in cement paste by Powers model, it can be seen that there is an enormous range of pore sizes, from 10 μm to less than 0.005 μm (0.5 nm) in diameter.

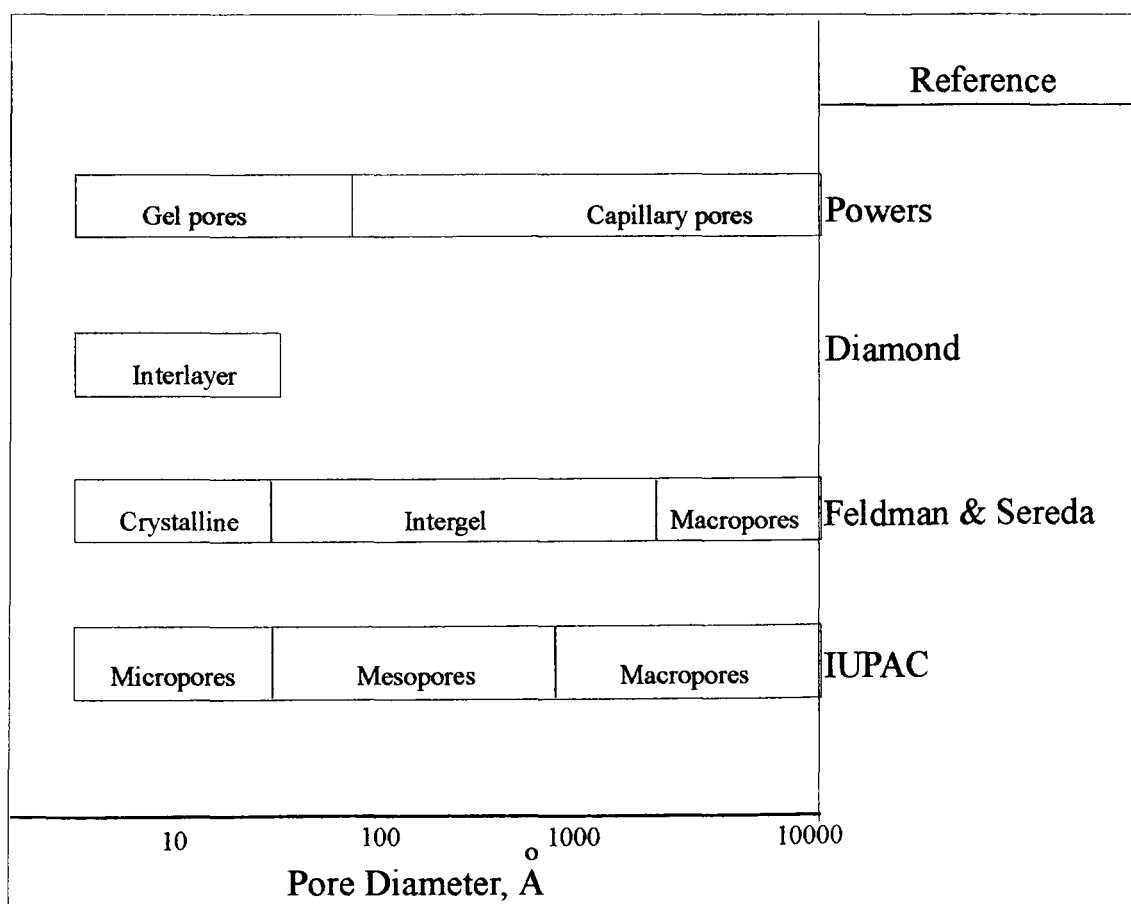


Figure 5-1 Comparison of pore classifications [85,86,87,88]

Table 5-1 Classification of pore sizes in hydrated cement pastes [13]

Designation	Diameter	Description	Role of water	Paste properties affected
Capillary pores	10 ~ 0.05 μm	Large capillaries	Behaves as bulk water	Strength permeability
	50 ~ 10 nm	Medium capillaries	Moderate surface tension forces generated	Strength permeability shrinkage at high humidities
Gel pores	10 ~ 2.5 nm	Small (gel) capillaries	Strong surface tension forces generated	Shrinkage to 50 % RH
	2.5 ~ 0.5 nm	Micropores	Strongly adsorbed water	Shrinkage creep
	< ~ 0.5 nm	Micropores	Structural water involved in bonding	Shrinkage creep

5-3. INFLUENCE OF POROSITY ON STRENGTH

All porous materials have this same inverse dependency between strength and porosity. Both theory and experiment lead to relationships that are either parabolic or exponential between the two. The effect of porosity on the strength of hydrated cement paste has been studied widely. Many investigators [89] have recognised that porosity is an important parameter in determining strength of hardened cement pastes, and its effect is expressed by a power function of the type :

$$f_c = f_0 X^n \text{ ----- (5-1)}$$

where f_c is strength of the paste, f_0 is a constant representing the intrinsic strength of the cement gel (i. e., the strength at a gel / space ratio of 1.0), and n is a constant, which has values in the range 2.6 to 3.0, depending on the characteristics the cement.

X is the gel / space ratio, which is defined as :

$$X = \frac{0.68\alpha}{0.32\alpha + w/c} \text{----- (5-2)}$$

where α is the degree of hydration, and w / c is the water / binder ratio.

This knowledge has been used in preparing cement paste; cement is mixed with only enough water to make it workable, thereby minimising the water remaining in pores after the paste hardens.

Relationship between the strength and gel / space ratio is shown in Fig 5-2. The relationship is based on results tested from 2 in. mortar cubes [69]. A linear relation between strength and porosity, within the range of the latter between 5 and 28 %, was established by Rössler and Odler [90].

Watson [91] has pointed out the importance of porosity and derived a formula which expresses the relationship between strength and V_s / V_p , the solid / pore volume ratio, where V_s and V_p are the volume fractions of the solid material and pores respectively as determined by helium pycnometry. Meanwhile, Feldman and Beaudoin [92] have emphasized that the porosity is a major factor in controlling strength, and modulus of elasticity of normal OPC concrete systems. The relation between the strength of mortar based on volume of pores larger than 20 nm in diameter is shown in Fig 5-3 [93].

Consequently, in addition to total porosity, the effect of pore size distribution on strength must be considered. Generally, at a given porosity, small pores lead to higher strength of the cement paste. Goto and Roy [94] also report results for cement pastes which agree well with experimental data from Bentur [71].

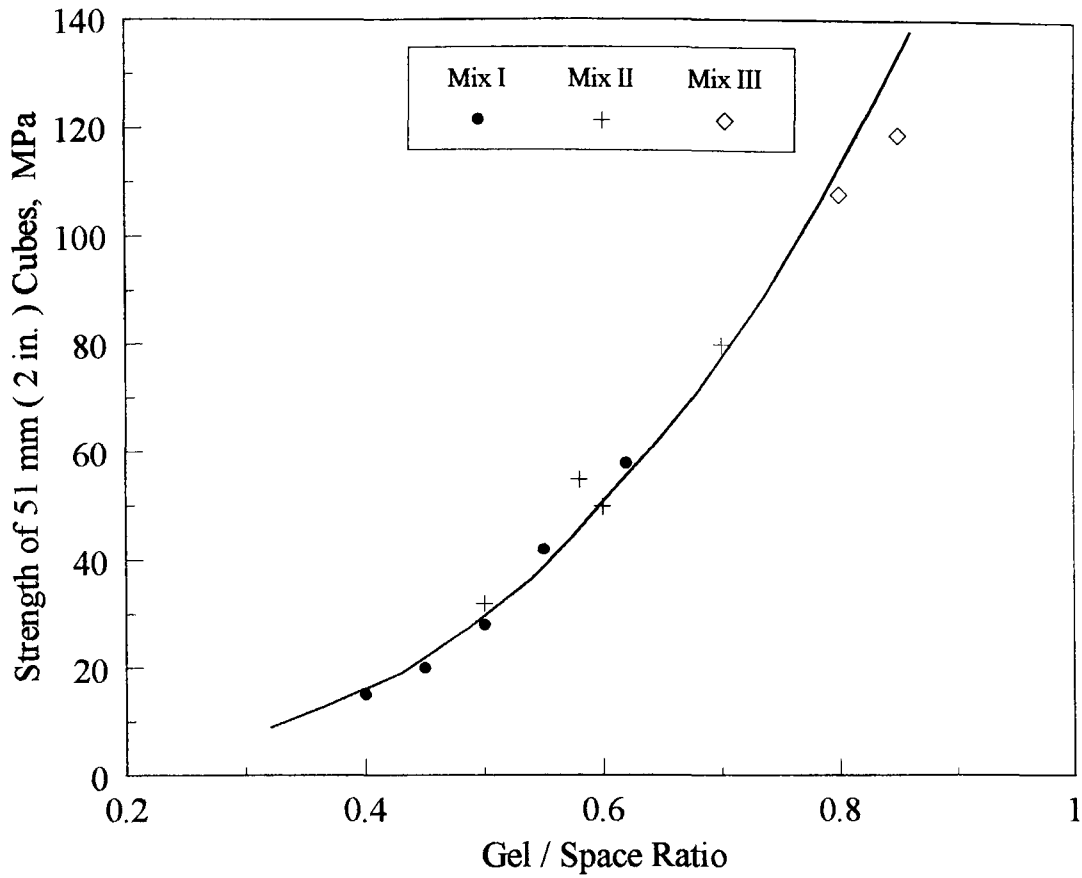


Figure 5-2 Relation between the compressive strength of mortar and gel / space ratio [69]

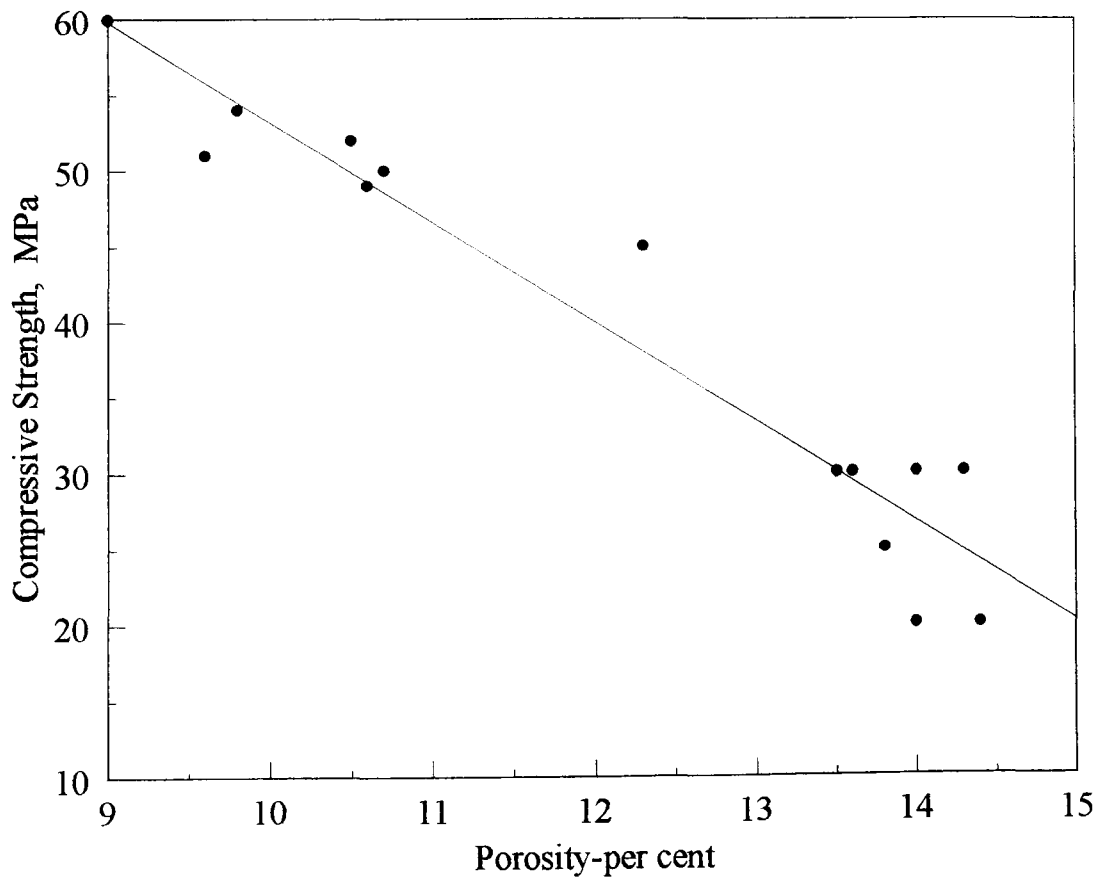


Figure 5-3 Relation between compressive strength of mortar and calculated from the volume of pores larger than 20 nm in diameter [93]

5-4. INFLUENCE OF POROSITY ON DRYING SHRINKAGE

The pore size distribution of a paste is considered important in determining drying shrinkage behaviour. For example, the addition of calcium chloride, increases irreversible shrinkage on first drying, and a higher contribution to shrinkage attributable to the capillary component [70,71].

Young and co-workers [95] have attempted to correlate microstructure with shrinkage. Various microstructural parameters were measured and the shrinkage behaviour studied ; however, it was found that no one parameter could correlate with shrinkage and porosity. Another approach using composite structure factor showed good correlation, and it was also found that this relationship can be applied to portland cement pastes, with reasonable success. The polysilicate content was also used as a microstructural parameter in a study linking shrinkage with microstructural properties [70,71].

From above analysis and further studies, Young and co-workers [96] conclude that shrinkage is the result of two components which are superimposed upon one another :

1. Capillary drying shrinkage - loss of moisture from the “pore component”, mesopores : $25 \text{ \AA} \sim 300 \text{ \AA}$, which is assumed to be due to capillary effects ; and
2. Gel drying shrinkage - loss of moisture from the “C-S-H component” which includes the C-S-H particles and the pores smaller than 25 \AA (micropores).

5-5. INFLUENCE OF POROSITY ON PERMEABILITY

Establishing the pathways and mechanisms for fluid flow through cementitious materials is an important part of the development of the understanding of mechanisms of ionic transport. The permeability is affected by many factors such as hydrostatic pressure, osmotic effects, pore differentials, and temperature differentials. The

permeability of concrete can be measured by determining the rate of flow of water or air through a concrete.

Flow in concrete paste and concrete obeys Darcy's law :

$$\frac{dv}{dt} = K \frac{h}{x} \text{----- (5-3)}$$

where v is the velocity of flow, K is the coefficient of permeability, h is the pressure head, and x is the thickness of the specimen.

In a fresh paste, the flow of water is controlled by the size, shape, and concentration of the original cement particles. With the progress of hydration, the permeability decreases rapidly because the gross volume of gel (including the gel pores) is approximately 2.1 times the volume of the unhydrated cement, so that the gel gradually fills some of the original water-filled space. As hydration proceeds, the capillary network is cut off by C-S-H gel, and then the capillary pore system becomes discontinuous. Flow is now controlled by micropores and this is very slow. This is accompanied by a continuous decrease in coefficient of permeability, " K ".

In general, water can flow more easily through the capillary pores than through the much smaller gel pores. The cement paste as a whole is 20 to 100 times more permeable than the gel itself [69]. In a mature paste, the permeability depends on size, shape, and concentration of the gel particles, and on whether or not the capillaries have become discontinuous. It is worth to note that low-pressure steam curing shows a slight increase in permeability [97].

If the specimen is not cured well, drying shrinkage may rupture some of the gel between the capillaries, and thus result in larger permeability coefficient values. On the contrary, the specimen cured sufficiently in water has more moisture, and it has denser structure because of more hydration than in specimen with drying.

Goto and Roy [94] presented some experimental results showing the existence of a relationship between permeability, and pore size distribution. The relationship between porosity and permeability was also demonstrated by Powers

who confirmed that the coefficient of permeability decreases with a decrease in the percentage of capillary porosity.

Mehta [12] showed that additions of pozzolanic and cementitious admixtures, such as fly ash, to normal OPC cement were instrumental in causing pore refinement or transformation of large pores into fine pores - a process which had a far reaching influence on the permeability of the hardened cement pastes.

5-6. INFLUENCE OF POROSITY ON ABSORPTION

The term “absorption” is usually applied to concrete in regard to the weight gain of partially dried specimens upon contact with or immersion in water. However, water can enter the pores, the amount of the absorbed water depending primarily on the abundance and continuity of the pores in the particle, whereas the rate of absorption depends on the size and continuity of these pores.

During absorption, it may be considered that the larger capillary spaces in the paste are the first to be wetted, with the finer gel pores perhaps next, their rate of absorption being slow because of their low water permeability. Thus, these features of the pores are more important than merely their total volumes as reflected by the magnitude of water absorption.

Although there is no clear-out relation between the strength of concrete and the water absorption of aggregate used, the pores at the surface of the particle affect the bond between the aggregate and the cement paste, and may thus exert some influence on the strength of concrete. Because the materials of aggregates always contain more or less pores inside, practically all dry particles are capable of absorbing water. Meanwhile, the coarse pores in aggregate can become nearly filled with water, when a relatively high degree of saturation is established in the paste surrounding the aggregate.

It may be noted that gravel has generally a higher water absorption than crushed rock of the same petrological character, because weathering results in the outer layer of the gravel particles being more porous and absorbent [69].

From further studies, it is generally held that the water absorption of mature concrete is not a simple function of its porosity, but depends also on the pore size, distribution, water / cementitious ratio, aggregate characteristics, air content, cement type and fineness (particularly at early ages), specimen size and shape, method of surface preparation (cast, broken), degree of hydration, continuity of the pores, and so on.

5-7. MICROSTRUCTURE OF HARDENED CEMENT PASTE

Research into the hydration of cement has been directed, on the one hand, towards the phenomenon of engineering characteristics in term of microstructure and porosity, and, on the other, to the way in which the chemical composition of the cement and its hydration products can affect its properties or be modified to improve them.

A considerable amount of knowledge of the mechanism of hardened cement paste has been built up as a result of studies on the microstructure. In a recent review, Skalny, Jawed and Taylor have considered various mechanisms proposed for the hydration of cement, and compared them with new experimental approaches. The kinetics of reactions have been summarised by Kantro, Weise & Brunauer and by Kondo & Veda. The structure of the calcium silicate hydrates has been reviewed by Taylor and the structure of calcium aluminate hydrates by Turriziani and Schweite & Ludwig. Powers and Brownyard, who studied the microstructure of hardened cement in relation to its physical properties, hypothesised that gel particles 100 Å in diameter are separated by a water film 6 Å thick. Subsequent investigations, however, indicated a structure with a unit layer ≈ 10 Å thick [98,99,100].

According to Powers-Brunauer model, the cement gel itself contains gel pores $\approx 15 \text{ \AA}$ trapped between folded sheets of crystalline layers of Ca, Si, and Al atoms. These layered sheets some $20 \sim 30 \text{ \AA}$ thick may touch in places and be as much as $500 \text{ \AA} \times 1 \text{ \mu m}$ in extent. Water held between the layers is considered tightly bound water, part of the crystal lattice, but the water in the gel pores can be more readily lost, and it is this water that accounts for shrinkage and creep.

Chapter two briefly dealt with the hydration reaction of portland cement in general, and cements differing in chemical composition may exhibit different hydration products when hydrated.

Upon addition of water the cement begins a series of hydration reactions, the most important of which is the formation of a poorly crystallised hydration product called calcium silicate hydrate gel (C-S-H gel), and calcium hydroxide (CH) by the calcium silicates. Other hydration products involving iron, aluminium and sulphur constituents are also formed. Thus, this section deals with the hydration products of portland cement, and its crystal structure, and properties relevant to the present aim of the investigation.

5-7-1. Calcium silicate hydrate gel (C-S-H gel)

The C-S-H gel formed in cement paste has been thought to have a highly disordered structure with a small particle size (dimension small than 150 \AA), and a high surface area [101]. It is termed “gel” because its dimensions are in the colloid range (less than 1000 \AA) and is poorly crystalline, being essentially amorphous. Jennings and Pratt [85,102] have shown the thin sheets or foil-shaped C-S-H structures in the saturated state from T.E.M. (Transmission Electron Microscope) observations.

Based on the C / S and H / S ratio so far reported, the composition of the C-S-H gel may be represented by the ternary diagram of Fig 5-4 [103]. From the figure, there are three main varieties of well crystallised tobermorites. All three varieties are lamella, and have the basal spacing 9.3 \AA , 11.3 \AA , and 14 \AA . There are also semi-

crystalline tobermorites known as C-S-H (I) and C-S-H (II) where the C / S ratio varies over the range 0.5 ~ 3.0. C-S-H (I) is usually observed as crumpled foils and C-S-H (II) appears mostly as fiber.

The similarity between C-S-H gels and tobermorite has been demonstrated by thermal analysis, electron and X-ray diffraction, and infrared spectroscopy. Results of X-ray diffraction analysis, however, remain the main basis for this association between C-S-H gels and tobermorite. The C-S-H gels give three broad lines corresponding to 3.05 Å, 2.8 Å, and 1.82 Å reflections of crystalline tobermorites [103].

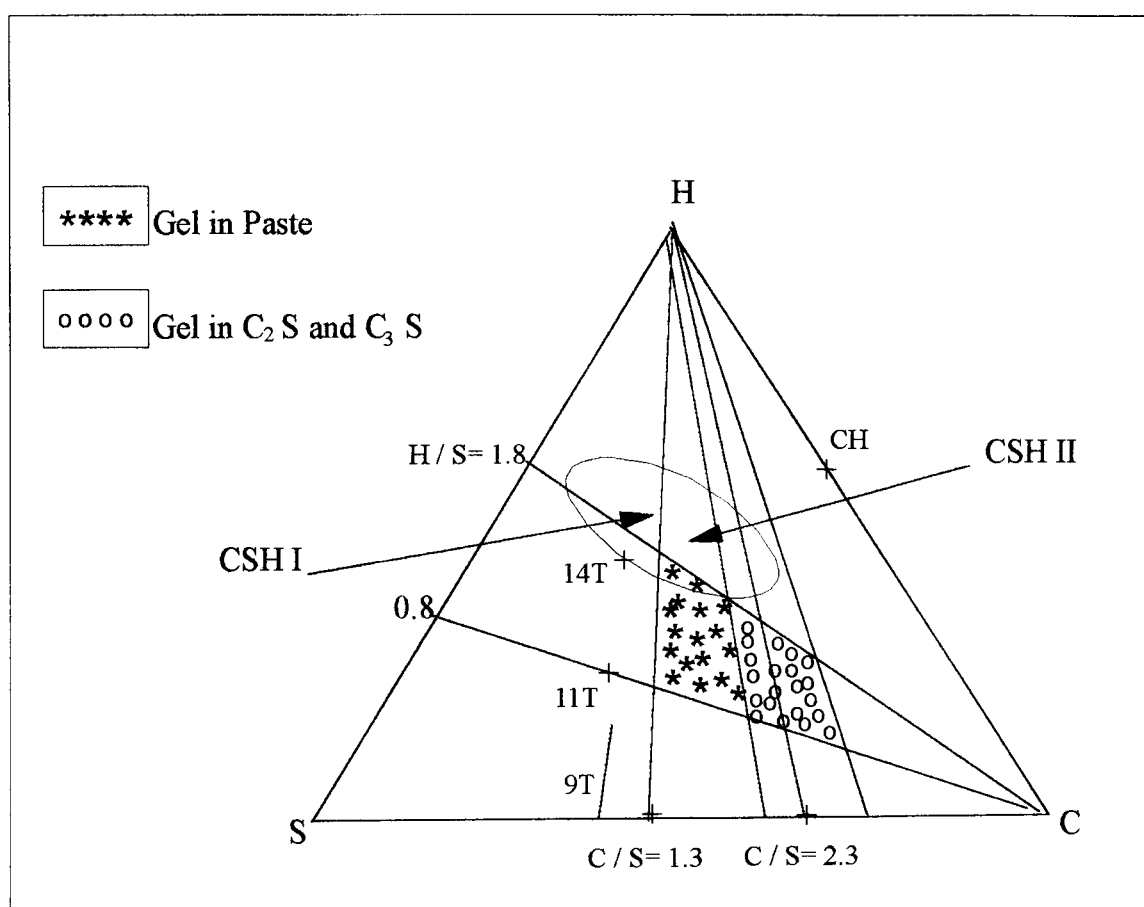


Figure 5-4 The composition of the calcium silicate hydrates [103]

The chemical compositions of C-S-H gel are quite diverse, especially when other chemical compounds are added, and it is believed that solid state substitutions will occur, which has been confirmed by electron beam micro-analysis [104].

Recently, the C-S-H chemical composition studies have concentrated on silicate structure analysis. C-S-H can be considered to be a polydisperse material with a relatively low degree of silicate polymerisation [86,105,106,107].

The physical characteristics of C-S-H are also diverse, and these characters dependent on the technique of measurement, the sample preparation procedure and the environmental condition. The mechanical properties of the hydrated gel are described by Powers and Brunauer, who presumed that the particles are to be held together by Van der Waals forces. Swelling on exposure to water is explained by the individual particles separating due to layers of water molecules existing between them, and this model also includes the existence of some chemical bonds between the particles to explain the limited swelling nature of the materials. Feldman and Sereda have postulated that the interlayer regions of C-S-H play an important role in shrinkage, particularly irreversible shrinkage.

The exact nature of the C-S-H microstructure is still uncertain, due mainly to the lack of direct structure determination techniques [108]. However, the C-S-H gel is still considered to be primarily responsible for the strength and cementing characteristics of the concrete. Also, it is now believed that the removal of water by any drying process will more or less change the C-S-H structure, and that the dried paste will be different from the saturated paste. The various morphologies and the various compositions of C-S-H also cause problems in understanding.

5-7-2. Calcium hydroxide (CH)

A major constituent of hydrated portland cement is generated by reaction of alite and belite with water. It is a well-crystallised solid containing hydroxyl ions, but no water molecules.

Calcium hydroxide dehydrates to calcium oxide at about 400 °C, in D.T.A, and this gives rise to a strong endothermic peak at about 550 °C. Calcium hydroxide in cement pastes may vary in morphology, being found as small equidimensional

crystals, thin plates, elongated crystals, flakes, or variation of these forms [87]. The phase of calcium hydroxide gives six strongest X-ray diffraction peaks corresponding to the 2.63 Å, 4.90 Å, 1.93 Å, 1.80 Å, 3.11 Å, and 1.69 Å. Its morphology is particularly affected by admixtures and by the temperature of hydration.

5-7-3. Calcium sulfoaluminate hydrates

The calcium sulfoaluminates are a relatively minor constituent of a cement paste, making up perhaps 10 to 20 % by volume. Thus, they are generally ignored due to their correspondingly minor role in the microstructure of the hydrated cement pastes. This hypothesis may not be entirely justified, however, since these compounds do contain relatively large amount of quite unstable ettringite, and the hexagonal hydrates.

The ettringite takes the form of needles, and because of its relatively low specific gravity (1.70) occupies a correspondingly large volume. Excessive formation of ettringite may lead to tensile stresses in the concrete, which may lead to cracking of the concrete.

The morphology of hexagonal hydrates, C_4AH_{13} , C_2AH_8 , can be clusters of small, plate crystals instead of well hexagonal crystal. The X-ray basal spacing of C_4AH_{13} is 7.9 Å . There is an unsettled dispute as to whether the composition of this phase is really C_4AH_{13} or C_4AH_{12} . The compound may be formed in hydrated portland cement high in alumina and low in sulphate. The water molecules are loosely held in the layer structure of the hexagonal hydrates. Drying can remove some of the water between the layers forming new hydrates. Thus, loss of water might possibly cause a bulk contraction of the crystal.

The hexagonal calcium aluminate hydrates in solution convert slowly to a more stable cubic hydrate C_3AH_6 . C_3AH_6 is the chemically stable final product at room temperature, and is a member of the hydro-garnet solid solution series. It

occurs sporadically, and to a limited extent in portland cement concrete, and is more commonly found in lime-pozzolan systems.

5-7-4. Carbonates

Deterioration of concrete service may be the result of a variety of physical and chemical processes, such as attack by acids, sulphates, or alkalis, alkali-aggregate reactions, freeze-thaw cycles, etc. These transport mechanisms include diffusion of such gases as O_2 , CO_2 or SO_2 in the gaseous phase of the pores, from the environment to interior regions. Of the hydrates in the cement paste, the one which reacts with CO_2 most readily is $Ca(OH)_2$, the product of the reaction being $CaCO_3$, but other hydrates are also decomposed, hydrated silica, alumina, and ferric oxide being produced.

$CaCO_3$ dehydrates to calcium oxide (CaO) at about $900^\circ C$, with strong endothermic peak on D.T.A. The phase of $CaCO_3$ (calcite) gives five strongest X-ray diffraction peaks corresponding to the 3.04 \AA , 2.29 \AA , 2.10 \AA , 1.91 \AA , and 2.50 \AA .

Carbonation shrinkage is probably caused by the dissolving of crystals of $Ca(OH)_2$ while under a compressive stress (imposed by the drying shrinkage) and depositing $CaCO_3$ in spaces from stress, the compressibility of the hydrated cement paste is thus temporarily increased. If carbonation proceeds to the stage of dehydration of C-S-H, this also produces carbonation shrinkage.

CHAPTER SIX

EXPERIMENTAL PROGRAMME OF PART II

6-1. INTRODUCTION

The study of the microstructure mechanism is a great benefit in understanding the properties of macrostructure in concrete science, and can predict the behaviour of concrete macrostructure. There are many analytical procedures which can be used to determine the microstructure mechanism of concrete such as X-ray diffraction, mercury intrusion porosimetry, and scanning electron microscopy.

The effects of physical properties, mineralogical compositions and pore size distribution due to pozzolanic activity in concrete containing high volume fly ash were described in Chapter 4. The present study concentrates on the microstructure development, and the mechanism of the fly ash reaction process occurring in different proportions of high volume fly ash concrete combinations.

During this study, mercury intrusion porosimetry (MIP) was introduced and used to perform pore size distribution analysis to characterize the particle size of the cementitious constituents of different mix proportions. X-ray diffraction (XRD) analysis technique is used to identify the mineralogical products, and monitor the progress of hydration. This study also examines the effects of HVFA concrete on permeability and water absorption, in order to investigate the density of HVFA concrete under pozzolanic activity, and the effect of short and long term hydration reaction. In this chapter, the experimental programme and the preparation of test samples used in Part II of the research project are described.

6-2. CONCRETE MIXTURES AND CHARACTERISTICS OF MATERIAL

The material used and mixing proportions of the mixes were the same as those used in Part I of the project, and have been discussed in Chapter 3, Section 3-3.

6-3. TEST PARAMETERS, PREPARATION OF TEST SPECIMENS

In the present investigation, a series of concrete samples of the same concrete mix proportions were tested at corresponding ages to correlate microstructure development with strength characteristics. Immediately following compressive strength testing of the specimens, experimental samples were taken from the centre of each specimen after cutting away all surfaces to be free of the mold-wall impression. The samples were then split into smaller pieces and immersed in high purity methanol in order to avoid further hydration of cement, and dissolution of hydration products. The samples were kept in methanol for at least 21 days before use. The microstructure mechanism tests were carried out for all the concretes after 28, 90 days and 18 months of moist and air curing.

6-4. TEST DETAILS AND PROCEDURE

6-4-1. Mercury intrusion porosimetry study

The technique used to measure the pore size distribution was mercury intrusion porosimetry. Mercury intrusion porosimetry is based on the capillary law governing liquid penetration into small pores. The pressure required intrude the pore is a function of the contact angle, the surface tension of the intruding liquid, and the shape of the pore to be intruded.

A general expression, in the case of a non-wetting liquid like mercury relating to these factors is given by the Washburn Equation

$$D = - \frac{\gamma \phi \cos \theta}{P} \text{----- (6-1)}$$

where :

P = the pressures required to intrude into the pore

D = the narrow dimension of the pore

γ = the surface tension of the liquid in dyne / cm

θ = the contact angle between the mercury and the pore wall

ϕ = the shape factor of the pore

The pore system of concrete is complex due to the morphology of the hydration products being of “needle-like”, “wall-like”, or “amorphous structure”. Therefore, the feature of pore shape could be cylindrical, elliptical or slit pores. From the surveyed literature for porosimetry on concrete materials, the shape factor (ϕ) for the cylindrical and the slit pore is 4 and 2 respectively, while the elliptical pores take the values between 2 and 4 [109].

Most researchers assume the pores to be of cylindrical cross section, so selection of a shape factor (ϕ) of 4 will yield results directly comparable to most of the published research. Such a selection may not be the best to represent pores in actual materials, but its use is generally accepted, as the practical means for treating what would be a most complex problem.

The contact angle (θ) between mercury and the solid containing the pores varies somewhat with the methods adopted for drying the concrete sample, maturity of the concrete and solid composition [110]. Winslow and Diamond [111] measured the contact angles (θ) for specimens oven dried at 105 °C in oven and dried over magnesium perchlorate hydrate. These measurements indicated contact angles (θ) of 117 degrees and 130 degrees for the oven dried samples and perchlorate dried respectively.

The volume (V) of mercury penetrating the pores is measured directly as a function of applied pressures (P). This P-V information provides a set of pressure and corresponding values of the cumulative pore volume. From the pore size distribution calculation, cumulative pore size distribution and differential pore distribution (dV / dD) or $dV/d (\log D)$ can also be determined.

The pore size distribution studies were carried out using a Micromeritics Poresizer (Model 9320). A photograph of the instrument is shown in Fig 6-1. Samples used for the porosity test were fragments of concrete by taking from the internal parts of specimens with all coarse aggregate removed. These fragments were then broken into pieces of approximately 3 mm, and immersed in methanol for at least 21 days. Prior to testing, the samples were oven-dried until they were of a constant weight.

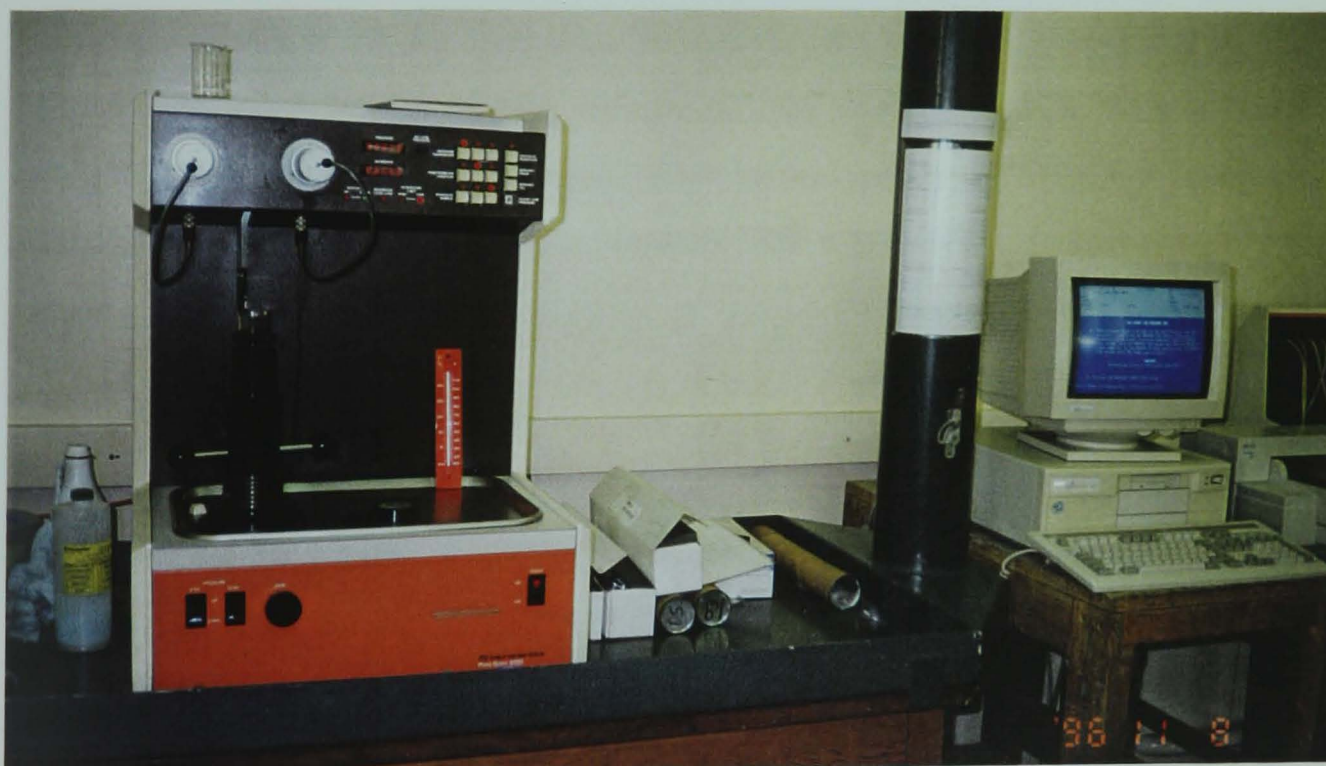


Figure 6-1 Photograph of the Micromeritics Poresizer (Model 9320)

About 1.5 ~ 2 grams of sample were then weighed, and inserted into a glass penetrometer tube of known weight and volume. This penetrometer tube was then fitted with a sealing cap, and a special grease (Apiezon H) applied to provide an air-tight seal. The sealed penetrometer tube was then inserted into the low-pressure port

of the Poresize 9320, and de-gassed by evacuating to a pressure below 50 μmHg , to remove any remaining moisture and methanol.

After de-gassing, the penetrometer tube was filled with mercury, at a filling pressure of 0.5 ~ 1.5 psia, and the combined weight of the penetrometer, sample and mercury was recorded. The penetrometer tube was then placed in the high pressure port of the poresizer, where pressure was increased slowly from atmospheric up to 30,000 psia, and the amount of mercury intrusion measured at various points during the pressure increase. A dedicated computer fitted with a maths co-processor was used to control the instrument to record data, and to calculate various parameters.

The penetrometer used had a bulb volume of 5.89 mL and a stem volume of 1.131 mL. The value used for the surface tension of the mercury (γ) was 485.00 dynes / cm. The shape factor (ϕ) used was equal to 4, assuming all the pores to be of cylindrical shape. For the pore diameter calculations a contact angle (θ) of 117 degrees was used for the present samples, (oven dried to 105 °C to a constant weight), based on the previous investigation carried out by Winslow and Diamond. Table 6-1 presents a typical output obtained with a pressure run from the present study.

Table 6-1 A typical output of micromeritics pore size analyses (Contd./)**POROSITY OF CONCRETE SAMPLES**

PORESIZER 9320 V2.04	PAGE 2
SAMPLE DIRECTORY/NUMBER : HUNG /022	
OPERATOR : HUNG	LP 11:28:43 06/29/96
SAMPLE ID : 350FW18M	HP 11:57:04 06/29/96
SUBMITTER :	REP 12:06:18 06/29/96

PRESSURE psia	PORE DIAMETER μm	LOG DIFF VOL dV/dlogD mL/g	CUMULATIVE VOLUME mL/g	INCREMENTAL VOLUME mL/g	DIFFEREN. VOL dV/dD mL/g- μm
0.49	260.3412	9.67E-05	0	0	1.58E-07
30.28	4.2183	5.78E-04	0.0002	0.0002	5.81E-05
50.78	2.5156	3.55E-03	0.0007	0.0005	5.99E-04
69.78	1.8307	3.19E-03	0.0012	0.0005	7.41E-04
101.44	1.2593	2.57E-03	0.0017	0.0004	8.67E-04
149.44	0.8548	2.42E-03	0.0021	0.0004	1.21E-03
199.93	0.6389	2.40E-03	0.0024	0.0003	1.59E-03
252.27	0.5064	2.94E-03	0.0026	0.0002	2.46E-03
305.43	0.4182	3.43E-03	0.0029	0.0003	3.48E-03
352.26	0.3626	3.39E-03	0.0031	0.0002	3.97E-03
402.43	0.3174	3.28E-03	0.0033	0.0002	4.36E-03
455.09	0.2807	2.62E-03	0.0035	0.0002	3.97E-03
522.76	0.2444	2.14E-03	0.0036	0.0001	3.72E-03
754.09	0.1694	2.57E-03	0.004	0.0004	6.44E-03
1007.26	0.1268	3.00E-03	0.0043	0.0003	1.00E-02
1256.42	0.1017	2.61E-03	0.0046	0.0003	1.09E-02
1507.09	0.0848	2.57E-03	0.0048	0.0002	1.29E-02
1754.25	0.0728	2.27E-03	0.005	0.0002	1.33E-02
2029.75	0.0629	2.72E-03	0.0051	0.0001	1.84E-02
2507.75	0.0509	1.96E-03	0.0055	0.0004	1.63E-02
3003.42	0.0425	6.33E-04	0.0055	0	6.32E-03
3505.25	0.0364	6.07E-04	0.0055	0.0001	7.09E-03
4000.42	0.0319	1.79E-04	0.0055	0	2.38E-03
4999.76	0.0255	1.15E-03	0.0056	0	1.92E-02
5998.92	0.0213	5.43E-03	0.0058	0.0002	1.08E-01
6988.26	0.0183	1.07E-02	0.0063	0.0005	2.49E-01
7986.25	0.016	2.03E-02	0.0068	0.0005	5.40E-01
8524.58	0.015	2.50E-02	0.0081	0.0013	7.09E-01
9008.25	0.0142	2.82E-02	0.0084	0.0003	8.43E-01
10006.07	0.0128	2.94E-02	0.0098	0.0014	9.79E-01
10959.9	0.0117	3.67E-02	0.0111	0.0012	1.34E+00
12181.39	0.0105	5.25E-02	0.0124	0.0014	2.13E+00
12502.05	0.0102	5.70E-02	0.0135	0.001	2.37E+00

Table 6-1 A typical output of micromeritics pore size analyses (Contd./)**POROSITY OF CONCRETE SAMPLES**

PORESIZER 9320 V2.04	PAGE 3
SAMPLE DIRECTORY/NUMBER : HUNG /022	
OPERATOR : HUNG	LP 11:28:43 06/29/96
SAMPLE ID : 350FW18M	HP 11:57:04 06/29/96
SUBMITTER :	REP 12:06:18 06/29/96

PRESSURE psia	PORE DIAMETER μm	LOG DIFF VOL dV/dlogD mL/g	CUMULATIVE VOLUME mL/g	INCREMENTAL VOLUME mL/g	DIFFEREN. VOL dV/dD mL/g- μm
10959.9	0.0117	3.67E-02	0.0111	0.0012	1.34E+00
12181.39	0.0105	5.25E-02	0.0124	0.0014	2.13E+00
12502.05	0.0102	5.70E-02	0.0135	0.001	2.37E+00
13352.54	0.0096	6.57E-02	0.0151	0.0017	2.92E+00
13986.54	0.0091	7.02E-02	0.0164	0.0013	3.26E+00
14208.53	0.009	7.13E-02	0.0176	0.0012	3.37E+00
14813.35	0.0086	7.28E-02	0.019	0.0014	3.59E+00
14998.69	0.0085	7.29E-02	0.0193	0.0003	3.64E+00
15786.51	0.0081	7.29E-02	0.0205	0.0012	3.83E+00
16380.17	0.0078	7.22E-02	0.0217	0.0012	3.94E+00
17122.67	0.0075	7.10E-02	0.0232	0.0015	4.04E+00
17493.83	0.0073	7.04E-02	0.024	0.0008	4.10E+00
18211.32	0.007	6.89E-02	0.0251	0.0012	4.17E+00
19004.98	0.0067	6.73E-02	0.0264	0.0013	4.26E+00
19915.14	0.0064	6.75E-02	0.028	0.0016	4.47E+00
20880.47	0.0061	6.61E-02	0.0292	0.0012	4.58E+00
22227.63	0.0057	5.80E-02	0.0303	0.0011	4.29E+00
22487.12	0.0057	5.58E-02	0.0311	0.0008	4.18E+00
23634.45	0.0054	4.53E-02	0.0323	0.0012	3.55E+00
24156.61	0.0053	4.08E-02	0.0339	0.0016	3.28E+00
24990.44	0.0051	3.50E-02	0.0341	0.0002	2.91E+00
27472.96	0.0046	1.86E-02	0.0341	0	1.70E+00
28318.45	0.0045	1.40E-02	0.0341	0	1.32E+00
29757.12	0.0043	1.16E-02	0.0348	0.0007	1.16E+00
29975.62	0.0043	1.16E-02	0.0348	0	1.16E+00

6-4-2. Air permeability

At the specific age of the air permeability test, a set of three specimens were drilled from the full thickness of the concrete to produce 50 mm diameter core samples. These cylindrical cores were then sliced at each end to produce samples of between 30 ~ 40 mm height for air permeability testing. The test apparatus was developed at the University of Leeds [112] and a general view of the cells in use is shown in Fig 6-2.



Figure 6-2 A general view of “The Leeds Permeability Cells”

The permeability cell consists of a sample holder, pressure gauge, gas supply and flow meter at the downstream side. The cell was designed to test concrete specimens of 50 mm diameter and 10 mm to 50 mm height. Due to the sensitivity of oxygen permeability measurements to the presence of moisture content in the concrete, after the prescribed period of curing, the specimens were oven dried at 105 °C to constant weight, until weight change was less than 0.1 percent over a 24 hour period (BS 1881 : part 5). The sample was placed in a rubber cylinder inside a steel ring cylinder. Gas was forced to flow in the vertical direction through the sample.

Flow rates were recorded by using a 1.7 mm diameter bubble flow meter at one bar pressure when a steady state of flow occurred.

6-4-3. Water absorption

The water absorption test in the present study was according to BS 1881 : Part 122 : 1983 “Method for determination of water absorption”. Similarly, a set of three specimens were core-drilled from the full thickness of the concrete to produce cylindrical samples of 75 mm diameter, with a height of 100 mm. These samples were then used for determining water absorption. The core samples were then oven dried at 105 °C for 72 ± 2 h, removed from the oven, and cooled for 24 ± 0.5 h in a dry airtight vessel. Each sample was weighed and immediately and completely immersed in a tank with its longitudinal axis horizontal and at a depth such that there was 25 ± 5 mm of water over the top of the sample. The samples were kept immersed in the water tank for 30 ± 0.5 min. Each sample was removed and shaken to remove the bulk of the water and dried with a cloth until all free water was removed from the surface. Each sample was then re-weighed.

The measured water absorption, W_{abs} , of the sample was calculated as the increase in mass resulting from immersion expressed as a percentage of the mass of the dry specimen :

$$W_{abs} = \frac{W_{SSD} - W_{OD}}{W_{OD}} \times 100\% \quad \text{----- (6-2)}$$

where W_{SSD} and W_{OD} represent the weight of the concrete sample in the SSD (Saturated-surface-dry) and OD (Oven-dry) states, respectively.

A correction factor according to the length of the specimen was obtained from the curve shown in Fig 6-3 [113]. The product of this correction factor and the measured absorption was the corrected absorption, this being the equivalent absorption of a core having a length of 75 mm.

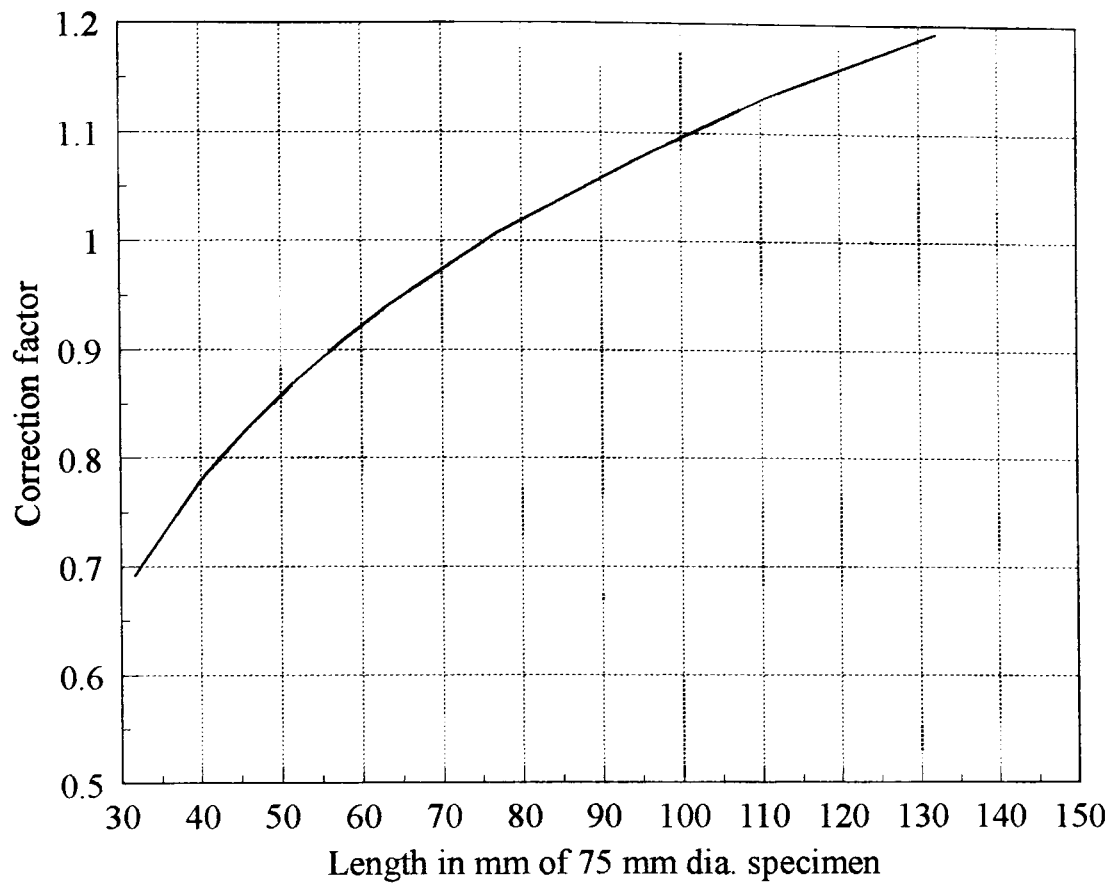


Figure 6-3 Correction factor related to the length of the specimen [113]

6-4-4. X-ray diffraction

Diffraction can be described as a coherent scattering phenomenon in which a large number of atoms cooperate. The phenomenon occurs when radiation interacts with a regular array of scattering points whose spacing is of the same magnitude as the incident radiation. A crystal contains a regular array of atoms in three dimensions with spacing in the range 1 ~ 5 Å.

X-ray radiation has wavelengths in the same range and is scattered by atoms through an interaction with the electrons. The diffraction phenomenon can be visualised as a reflection by a set of parallel planes of atoms lying in the plane. Diffraction occurs when the Bragg Equation [114] is satisfied :

$$\lambda = 2 d \sin\theta \text{ ----- (6-3)}$$

Were :

λ = wavelength of radiation

d = distance between the planes

θ = the angle of incidence

Diffraction will occur for the many different sets of atomic planes which can occur in the crystal. A monochromatic X-ray beam will be diffracted at different angles by the crystal structure of different minerals.

A diffraction pattern is derived by detecting diffracted X-ray beams with a radiation detector as a random array of crystals is rotated in an incident beam of X-rays. Thus, 2θ is measured experimentally, which can be converted into “ d ” spacing using the Bragg equation. A pattern consists of a series of diffraction peaks or reflections whose positions and intensities are unique for each chemical compound which forms crystals. It can thus be used for identification of that compound ; or for quantitative analysis, since the intensity of a reflection is proportional to the weight fraction of the compound in a mixture.

A well-crystallised material will have sharp diffraction peaks in considerable numbers. Poorly crystalline compounds, where long-range symmetry is disturbed, have fewer reflections which tend to be rather broad and diffuse.

In the present investigation, X-ray diffraction was only used to do qualitative analysis because the systems involved complicated phases which are difficult to analyse. The powder method of X-ray diffraction was used in the present study.

A sample, pre-treated with methanol for at least 21 days, was dried in laboratory and crushed to powder using a pestle and then the powder was sieved to pass the 150 micron sieves. Samples were examined using a Phillips Norelco X-ray diffractometer using Cu ($K\alpha$) radiation and a scan rate of $2^\circ / \text{min}$, scan step 0.02° , time / step 0.01° over the range $10^\circ \sim 70^\circ$. The Cu ($K\alpha$) radiation of wavelength 1.541838 \AA was used as the X-ray source. Any one power pattern is characterized by a set of line positions 2θ and a set of relative line intensities, “ I ”.

The powder pattern X-ray data manual on cement minerals are according with the Joint Committee on Powder Diffraction Standards (JCPDS) and the Powder Diffraction File (PDF), and these were used to identify compounds, by comparing known patterns from the manual with the test-result pattern until a suitable match was obtained.

CHAPTER SEVEN

TEST RESULTS AND DISCUSSION OF PART II

7-1. INTRODUCTION

In Chapter four the mechanical behaviour of HVFA concretes was investigated in order to attempt to find relations between these properties and the engineering characteristics of the HVFA concretes. To understand the chemical and physical processes governing mechanical behaviour, an extensive study was carried out in this research, in which changes in mechanical properties of various concretes were investigated in parallel with a study of their physical and chemical structure.

The goal of this chapter is to investigate the role of fly ash in HVFA concrete in microstructure mechanisms due to pozzolanic reaction. Control concrete specimens containing ASTM Type I cement with mineral admixture were also investigated for comparison purposes.

The pore structure of HVFA concretes with different replacement mixtures was studied, and the effect of other factors such as curing regime, age, and cementitious material content were examined. A similar study, investigating the effect on air permeability and water absorption of HVFA is reported. The relations of the pore structure with strength, permeability, absorption are then discussed. A detailed discussion dealing with the changes of morphological phase in different mixtures under different curing regimes is also presented.

In the present investigation, samples were taken from the same concrete test specimens, and were tested at corresponding ages to correlate microstructure development with strength increase. Details of concrete mix proportions and testing procedures have been described in Chapter three and Chapter six respectively.

7-2. PORE SIZE DISTRIBUTION ON NORMAL OPC AND HVFA CONCRETE

Pore size distribution is a very important parameter that will indicate the change in pore size under different conditions, since it will be affected by experimental parameters such as degree of hydration, curing temperature, ageing, water / cementitious ratios, and cement composition [70,71,115]. Pore size distribution in combination with strength may give a more clear idea what mechanism controls the strength when the experimental parameters are changed.

In this section a detailed analysis of the pore size distribution curves will be presented, and on its basis, some conclusions will be drawn about the relationship of both types of curing conditions on the pore structure of HVFA concretes. Some relations between pore structure and mechanical properties will also be presented.

In the present investigation, plots were made of various experimental parameters, primarily : (a), intruded volume as a function of pore diameter, and (b), $dv / d (\log d)$ as a function of pore diameter. The most useful parameter is provided by the $dv / d (\log d)$ against pore diameter plots, from which the “maximum continuous pore diameter” or the “threshold diameter” could be determined.

7-2-1. Effect of different mixes and curing conditions on pore size distribution

The results of Mercury Intrusion Porosimetry studies on HVFA concrete are summarized in the data presented in the following series of figures, Figs 7-1, 7-2, 7-3 and 7-4. For purpose of comparison the result of the normal OPC concretes are also included in the above figures.

Under both types curing conditions with different curing periods, the total accessible pore volume and porosity of OPC and HVFA concrete are also shown in Tables 7-1, 7-2, 7-3, and 7-4.

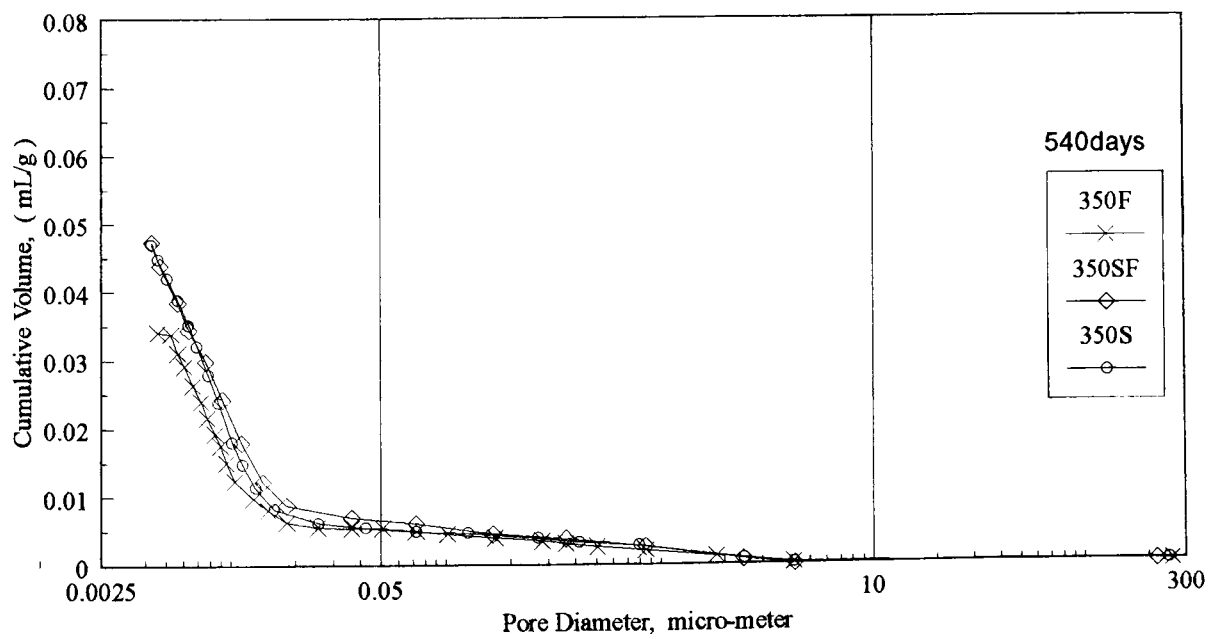
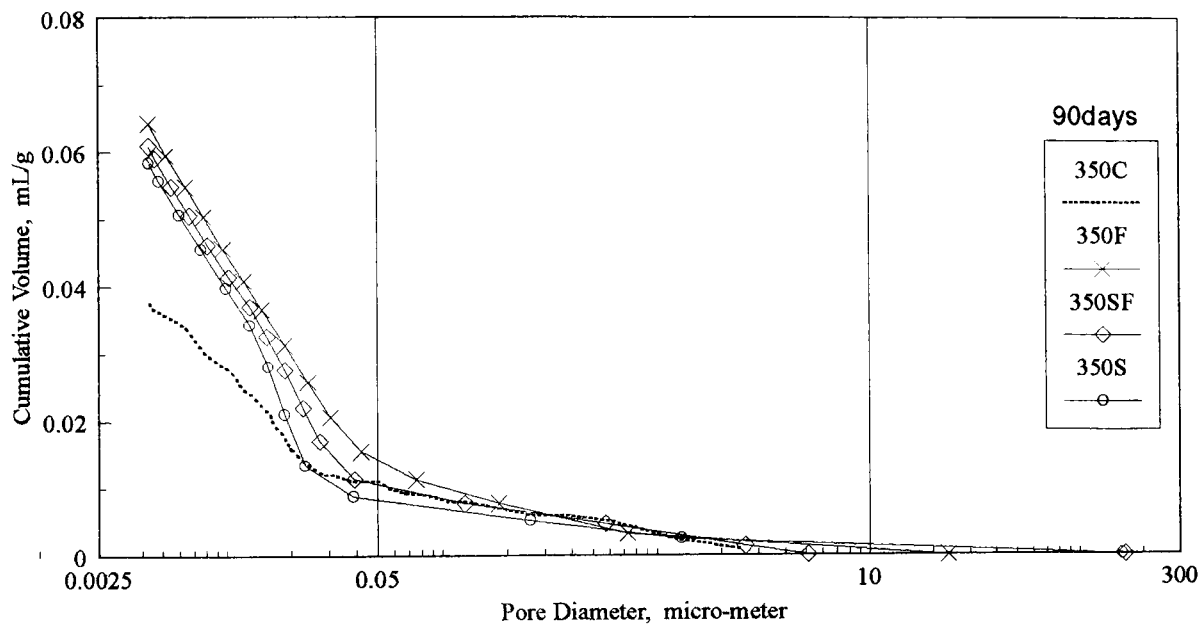
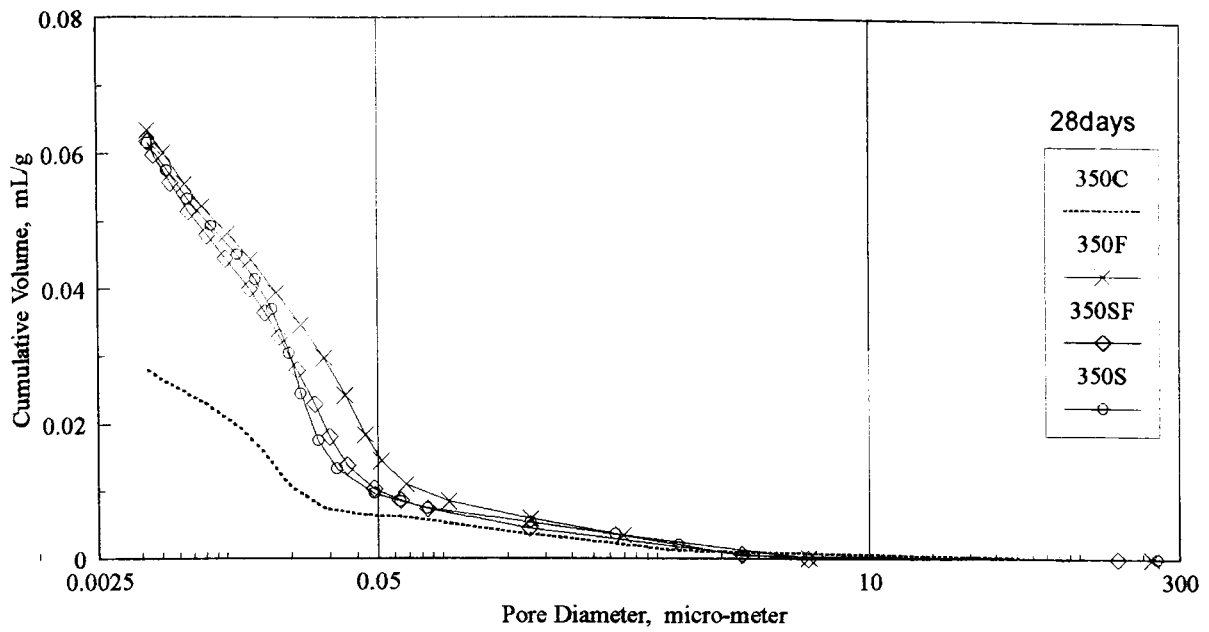


Figure 7-1 Cumulative pore volume curves for the 350 kg/m³ binder content OPC and HVFA concrete (Water curing)

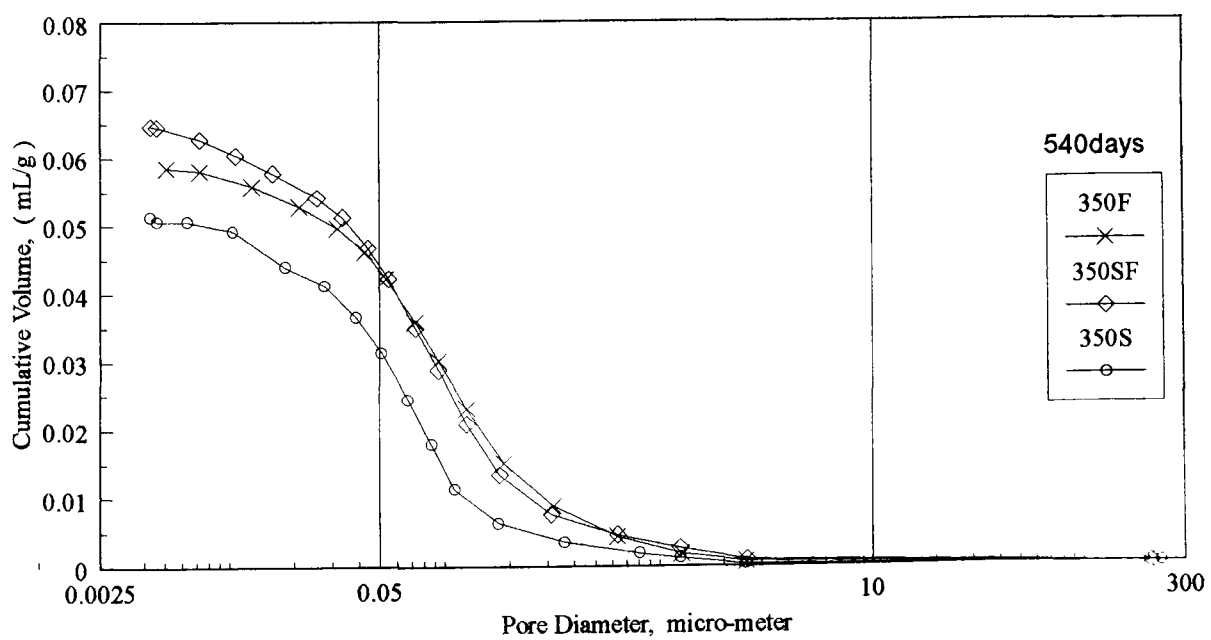
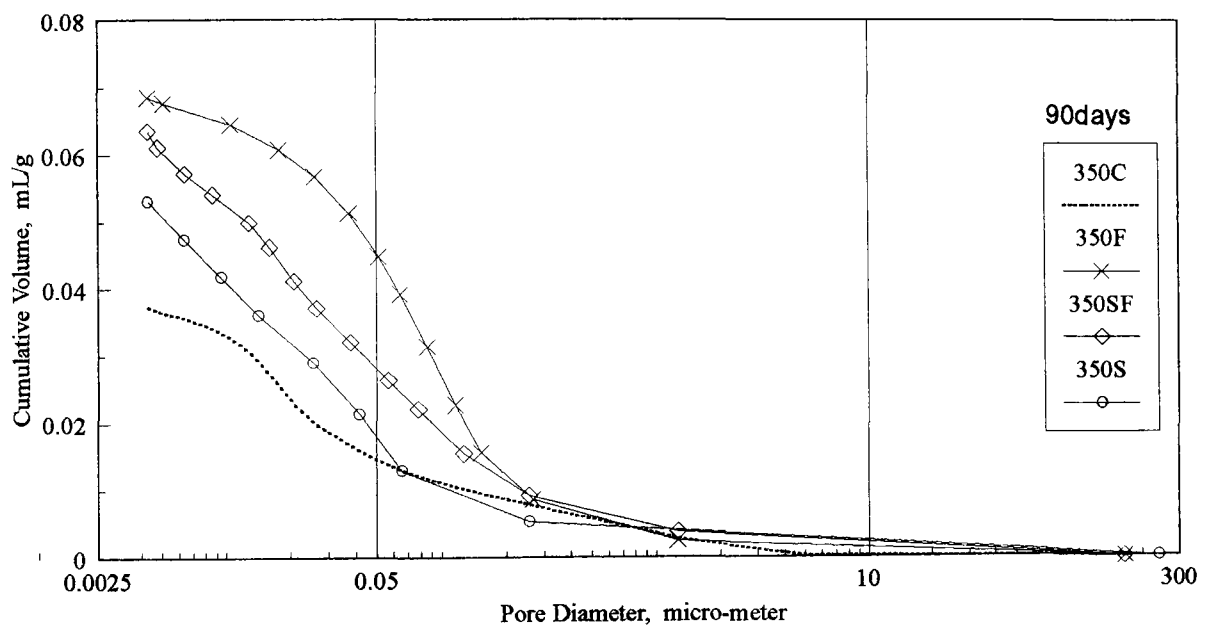
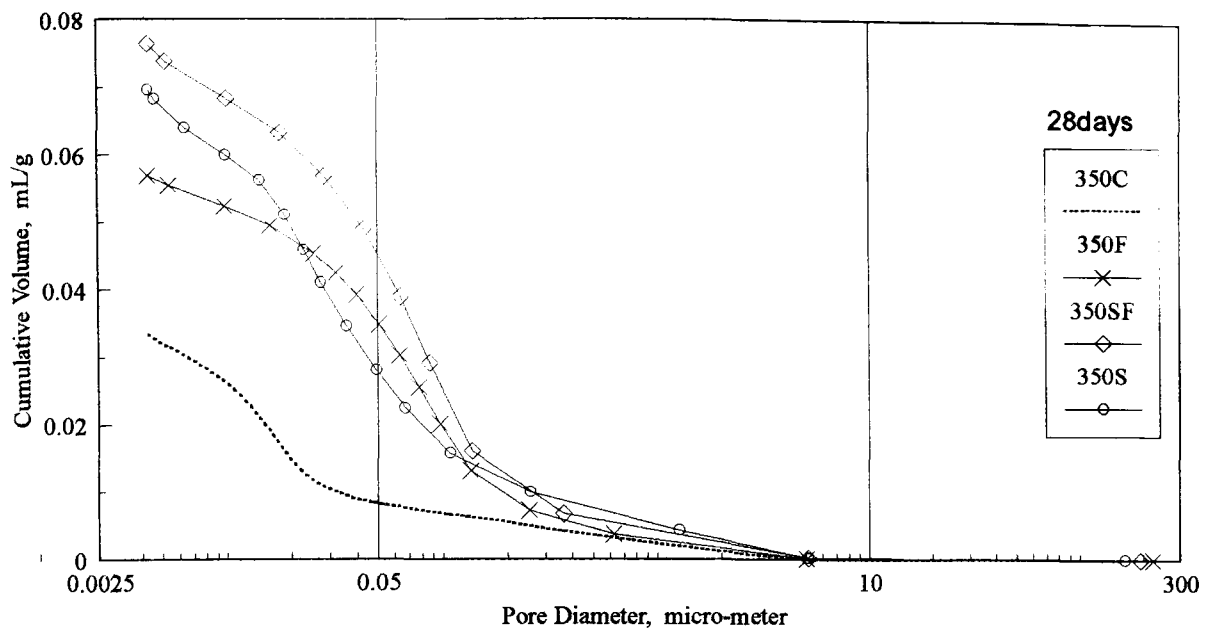


Figure 7-2 Cumulative pore volume curves for the 350 kg/m³ binder content OPC and HVFA concrete (Air curing)

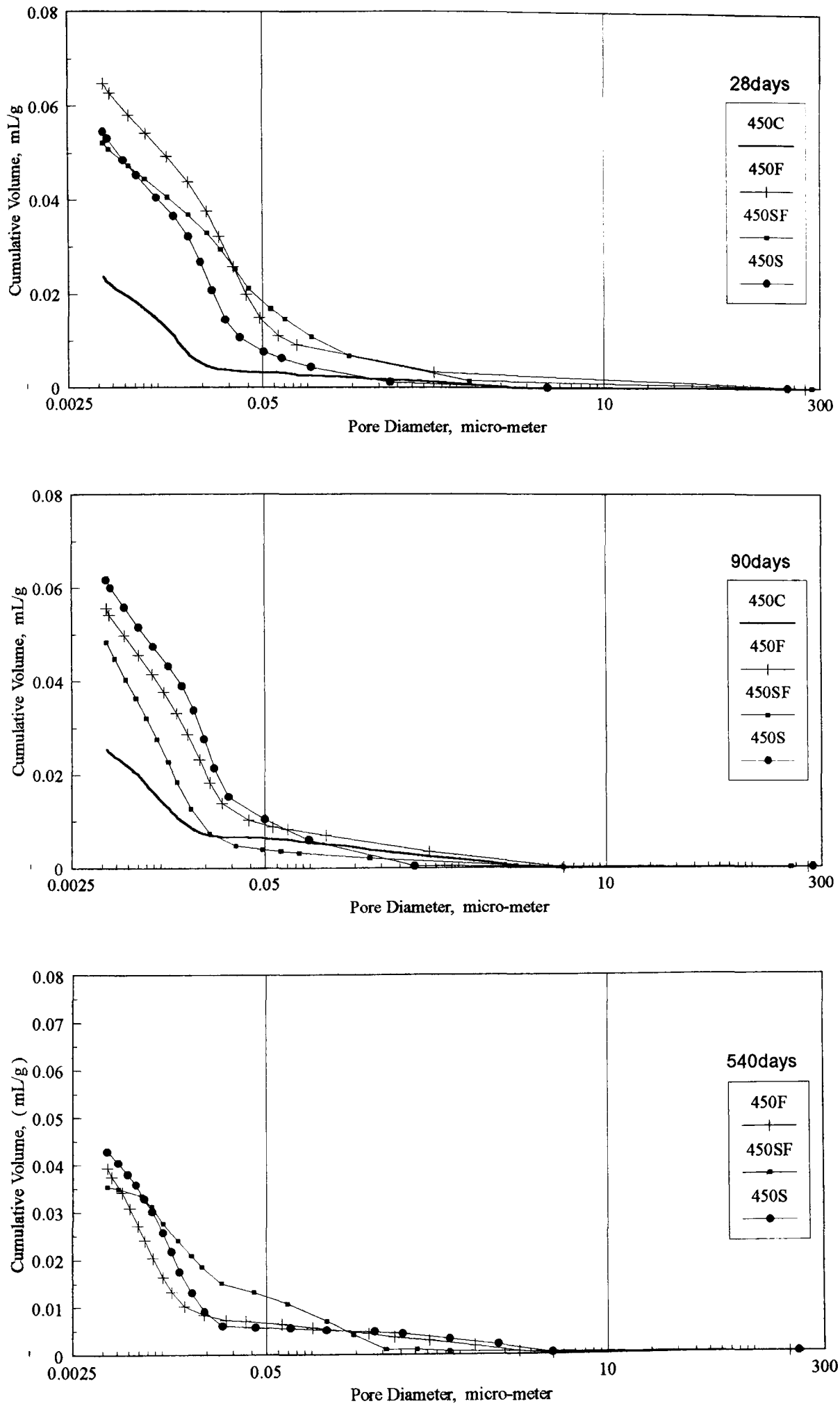


Figure 7-3 Cumulative pore volume curves for the 450 kg/m³ binder content OPC and HVFA concrete (Water curing)

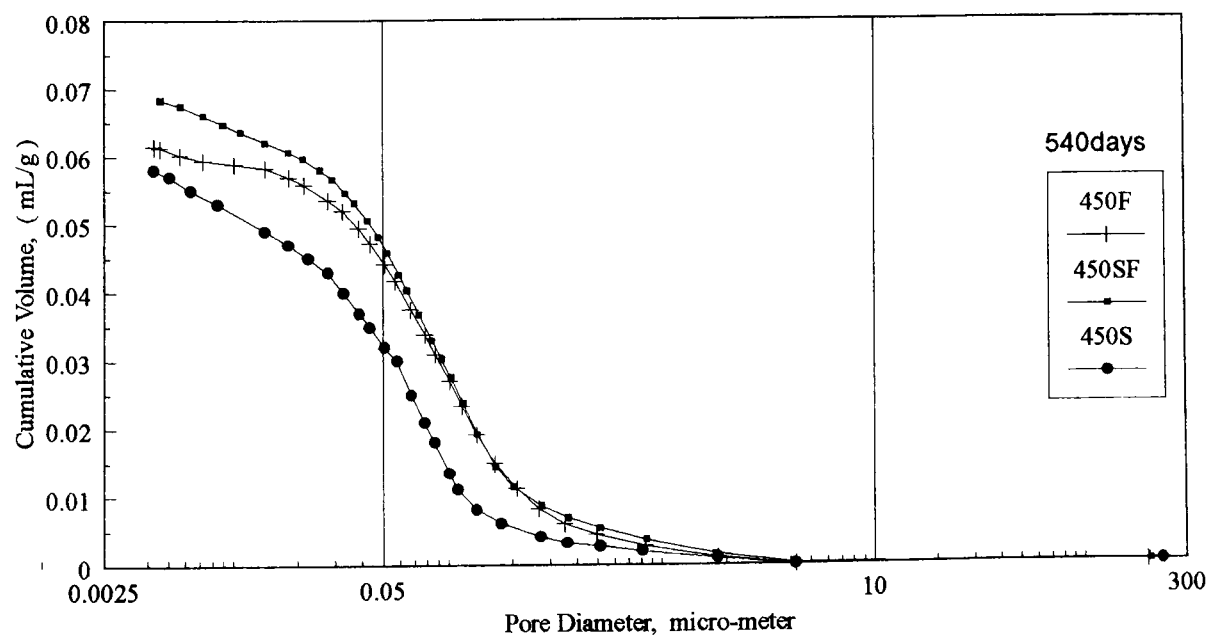
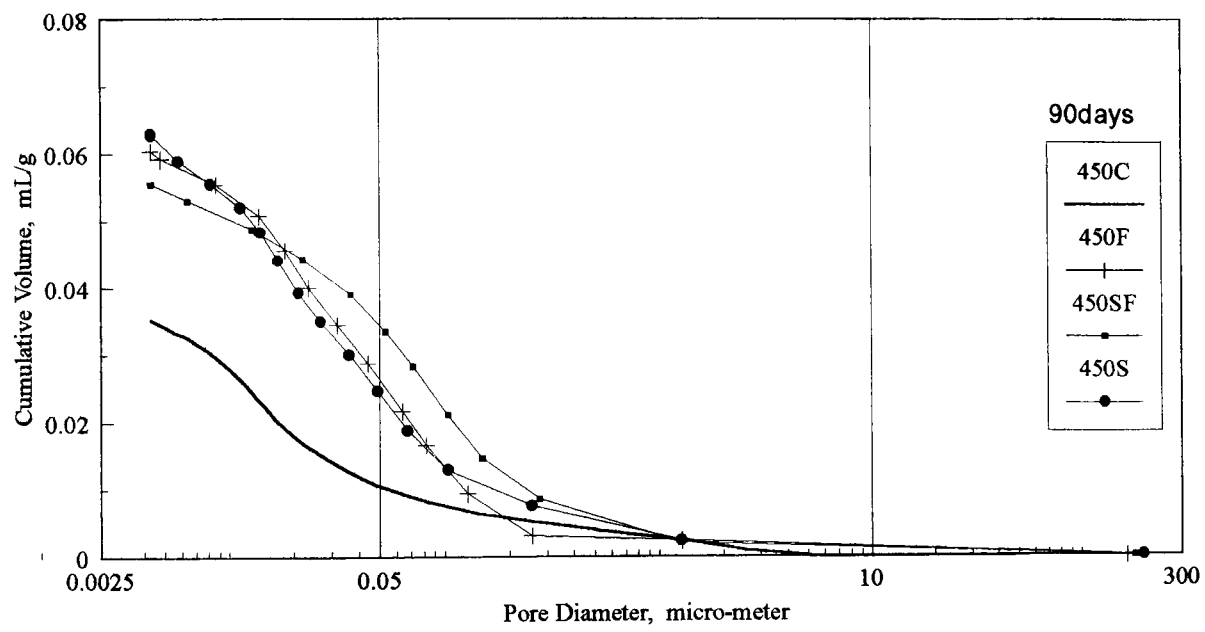
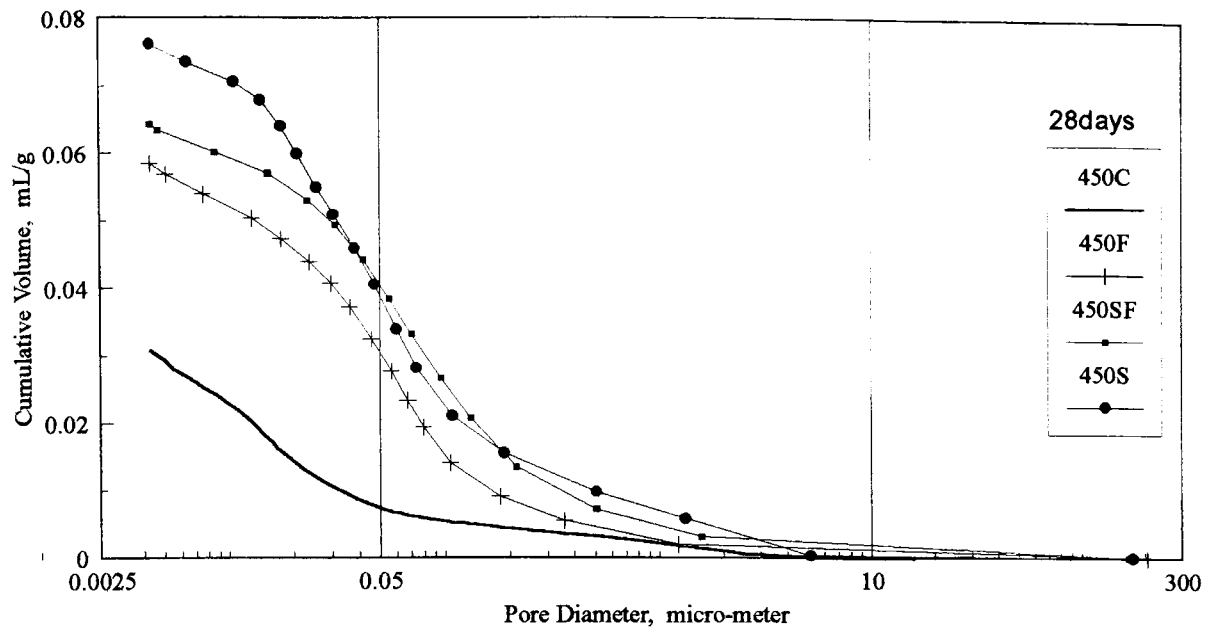


Figure 7-4 Cumulative pore volume curves for the 450 kg/m³ binder content OPC and HVFA concrete (Air curing)

**Table 7-1 Total accessible pore volume of OPC and HVFA concrete-Water curing
(Unit : mL/g)**

Days	28	90	540
350C	0.0280	0.0381	---
350F	0.0634	0.0642	0.0348
350SF	0.0617	0.0609	0.0473
350S	0.0616	0.0584	0.0470
450C	0.0237	0.0255	---
450F	0.0648	0.0556	0.0394
450SF	0.0522	0.0483	0.0354
450S	0.0546	0.0608	0.0428

**Table 7-2 Total accessible pore volume of OPC and HVFA concrete-Air curing
(Unit : mL/g)**

Days	28	90	540
350C	0.0334	0.0373	---
350F	0.0569	0.0685	0.0619
350SF	0.0760	0.0635	0.0647
350S	0.0696	0.0646	0.0513
450C	0.0309	0.0353	---
450F	0.0585	0.0604	0.0615
450SF	0.0643	0.0555	0.0687
450S	0.0708	0.0629	0.0581

**Table 7-3 The porosity of OPC and HVFA concrete-Water curing
(Unit : %)**

Days	28	90	540
350C	6.53	7.35	---
350F	13.65	12.82	7.16
350SF	12.45	11.75	10.20
350S	12.56	11.38	10.26
450C	5.36	6.00	---
450F	13.48	11.63	8.86
450SF	11.12	10.08	6.86
450S	11.51	12.16	9.23

**Table 7-4 The porosity of OPC and HVFA concrete-Air curing
(Unit : %)**

Days	28	90	540
350C	7.78	7.22	---
350F	11.95	13.51	12.55
350SF	15.24	12.61	14.15
350S	13.37	12.75	11.03
450C	6.94	7.64	---
450F	13.35	11.92	12.85
450SF	13.05	11.72	15.02
450S	14.48	12.78	11.75

As shown in the figures, total cumulative pore volumes are significantly affected by the HVFA concretes. It was quite obvious from the figures, the total volume of the geometrically continuous pores were higher for the HVFA concretes than the normal OPC concrete with various curing periods. However, the pore size distribution patterns appear to be different for the curing conditions and degree of hydration with ages.

From the results, total cumulative pore size volumes of all concretes tend, as expected, to decrease with increased hydration. At high degrees of hydration the curves tend to become concave in the case of all concretes under water curing condition. Meanwhile, the total accessible pore volume and porosity of OPC and HVFA concrete toward to the lower value were found.

Under water curing, the concrete made with 350SF appeared to have more or less the same cumulative pore volume of 350S, but the pore size distribution of this porosity is quite different ; the former had most of its porosity in the coarse size range, whereas that concrete of 350S is mostly in the fine size range. These variation of fine and coarse pores due to pozzolanic activity will be discussed in the next section.

At the end of 90 days, for all concretes under water curing, the total cumulative pore volumes are lower than 28 days. For the long term pore size distribution test at 540 days of all HVFA concretes under water curing, as expected, the total cumulative volumes of the geometrically continuous pore were low than at the ages of 28 days and 90 days. Meanwhile, the concrete made of 450SF had lowest percentage in porosity when compared to all of the HVFA concretes. This indicates that the amount of hydration products in 450SF were proportionately more than that other HVFA concretes. The presence of the silica fume in the HVFA concrete was thus instrumental in causing the beneficial effect observed on concrete strengths. This also explained the reason why the crushing pattern of the specimen containing fly ash or with both fly ash and silica fume was more ductile than that concrete without above mineral admixture.

The results also show that the use of air curing regime was a remarkable factor in determining the pore size distribution. These trends reflect a marked change in the total cumulative pore volume ; meanwhile, the percentage of porosity are increasing with continued air drying. Both the normal OPC and HVFA concretes showed higher accessible pore volumes compared to the corresponding water curing concretes. Irrespective of normal OPC concrete, at the age of 28 days, the concrete made of 350F had the total cumulative pore volumes lower than the other two HVFA concretes, Mix-350SF and Mix-350S. The concrete made of mixes containing fly ash as a partial replacement for both sand and cement , Mix-350S, Mix-450S had good ability to resist the loss of the potential strength in the long term by air dried condition.

From the results, at the end of 540 days the less the porosity of HVFA concrete in water curing, the more is the value in the air regime. This is in agreement with the preceding discussion in swelling and drying shrinkage of HVFA concretes. The concretes made of 350SF, 450SF showed significant reduction in total pore volume and, thus, had a good ability to resist swelling, but higher drying shrinkage strain were also found on both types of concrete.

7-2-2. Maximum continuous pore diameter of pore structure

The maximum $dv / d (\log d)$ and the threshold diameter of OPC and HVFA concrete under both types curing conditions are shown in Tables 7-5 and 7-6. The corresponding maximum $dv / d (\log d)$ against the threshold diameter on pore size distribution are illustrated in the Figs 7-5, 7-6, 7-7, and 7-8.

From the results, the differential pore volume plots clearly demonstrated the effect of HVFA concretes on the pore size distribution. At those ages under water curing, although the total cumulative pore volumes of the HVFA concrete were much higher than the normal OPC concrete, the differential pore volume showed a higher peak with a wider spread for the fine pores than that OPC concrete. At the age of 28 days concrete made of 450S had much more pores concentrated at pore diameter smaller than $0.023 \mu\text{m}$ in comparison with the OPC concrete under water curing.

Under similar conditions, irrespective of normal OPC concretes, the concrete made of 450S had cumulative pore volume lower than the other HVFA concretes, meanwhile, had most of its porosity spreading in the fine size range. The peaks of concrete mixed with cement alone replaced partial by fly ash, 350F and 450F, occur at a significantly larger pore diameter range than for the comparable concretes made with silica fume. The maximum pore diameters of the concrete 350F, 350SF and 350S were at 0.0406 μm , 0.0286 μm , and 0.0244 μm respectively. Concrete made of 450F, 450SF, and 450S, the maximum continuous pore diameter were at 0.0481 μm , 0.0327 μm , and 0.023 μm respectively. From the results, however, the “maximum continuous pore diameter” is a useful parameter in comprehending the concrete permeability. If permeability is directly related to the maximum continuous pore diameter, then the concretes of 350S and 450S would be the least permeable.

At the end of 90 days, again, the total cumulative pore volumes also were found to be lower in the concrete of 350S, and had much more than the other HVFA concretes. Surprisingly, concrete Mix-450SF had a lower cumulative pore volume, meanwhile, gave highest differential pore volume for the fine pores and lowest differential pore volumes for the coarse pores when compared to the normal OPC and all HVFA concretes. This indicates the presence of many pores in the fine pore range and a fewer number of pores in the coarse pore range for the concrete of 450SF in comparison with the concretes of 450S and 450F. Whereas, the concrete made of 450S had higher cumulative pore volumes than the other concretes, the differential pore volume is toward the bigger pore size distribution when compared to the concrete of 450SF. The maximum continuous diameter of the concrete Mix-450SF and Mix-450S were at 0.0107 μm and 0.0196 μm . These variations in the volume of fine pores in the concrete, although difficult to relate directly with concrete properties, are nevertheless reflected in the strengths of corresponding concretes. The addition of silica fume did, however, shift the distribution of pores toward the small sizes. For the long term test at 540 days, the $dv / d (\log d)$ curves for both types cementitious content concretes toward to the finer pore size distribution were found. Although the concrete made of 350F and 450F had lowest total cumulative pore volume when compared with the other HVFA concretes, the total coarse pores

volume had rather high. Reduction in the volume of large pore was observed with the progress of the pozzolanic reaction. High concrete strengths were generally associated with lower volume of large pores in the concrete. The distribution of pores moved toward to the finer diameter and this explained the phenomena of gradual increase in strength of concrete containing fly ash and silica fume, even though it had higher total pore volume than concrete without fly ash or silica fume.

From the Figs 7-6 and 7-8, the different pore plots clearly demonstrated the effect of air drying on the pore size distribution. All the concretes showed an increase in number of coarse pores accompanied by a decrease in number of fine pores. Irrespective of normal OPC concretes, the concrete made of 350F and 350SF had most of its porosity in the coarse size range compared to the concrete of 350S at the age of 28 days. The maximum continuous pore diameter of the concretes 350F, 350SF, and 350S were at 0.0853 μm , 0.0718 μm , and 0.0229 μm respectively. Although the total cumulative pore volume of the concrete 450S was much higher than the concretes made of 450SF and 450F, the differential pore volume had shown two peaks with a wider spread at the fine pores range. The maximum continuous pore diameter were at 0.0573 μm for Mix-450F, 0.0553 μm for Mix-450SF, and 0.0531 μm , 0.0219 μm for Mix-450S respectively. At the end of 90 days, the concrete made of 350F had a highest total cumulative pore volume and the differential pore volume and showed the maximum continuous pore diameter at 0.0991 μm , which is coarse pore range. The concrete 450S still had a lower cumulative pore volume than that of concretes 450SF and 450F, but, the differential pore volume had a peak concentrated at fine range. It is worth pointing out that the concrete made of 450SF had a higher cumulative pore volume as well as the differential pore volume had a peak in the coarse pores higher than 0.0751 μm , which located in the coarse pore range. For the long term test on the air curing of HVFA concretes, the $dv / d (\log d)$ curves for both types cementitious material content concretes were found toward to the coarse pore size distribution. The above results were found to be consistent with the discussion in engineering properties. In general, engineering properties of concrete is influence by the volume of all voids in concrete, capillary pores, gel pores, and entrained air, if present. From the result, it could be

inferred that, for hydration of concrete to continue, it is sufficient to prevent the loss of moisture from the concrete.

Table 7-5 The max. $dv/d(\log d)$ and threshold diameter of OPC and HVFA concrete-Water curing

Days	28		90		540	
Mix	Max. $dv/d-\log d$ (mL/g- μm)	Threshold diameter (μm)	Max. $dv/d-\log d$ (mL/g- μm)	Threshold diameter (μm)	Max. $dv/d-\log d$ (mL/g- μm)	Threshold diameter (μm)
350C	0.0592	0.0129	0.0621	0.0141	---	---
350F	0.0745	0.0406	0.0514	0.0223	0.0729	0.0081
350SF	0.0873	0.0286	0.0657	0.0206	*0.0706 **0.0708	0.0102 0.0073
350S	0.0913	0.0244	0.0914	0.0178	0.0866	0.0086
450C	0.0556	0.0162	0.0589	0.0129	---	---
450F	0.0988	0.0481	0.0790	0.0200	0.0677	0.0069
450SF	0.0651	0.0327	0.0725	0.0107	0.0412	0.0094
450S	0.0881	0.0230	0.0898	0.0196	0.0702	0.0116

Table 7-6 The max. $dv/d(\log d)$ and threshold diameter of OPC and HVFA concrete-Air curing

Days	28		90		540	
Mix	Max. $dv/d-\log d$ (mL/g- μm)	Threshold diameter (μm)	Max. $dv/d-\log d$ (mL/g- μm)	Threshold diameter (μm)	Max. $dv/d-\log d$ (mL/g- μm)	Threshold diameter (μm)
350C	0.0594	0.0128	0.0383	0.0170	---	---
350F	0.0596	0.0853	0.0669	0.0991	0.0536	0.0932
350SF	0.0522	0.0718	0.0440	0.0182	0.0603	0.1151
350S	0.0607	0.0229	*0.0501 **0.0439	0.0503 0.0156	0.0621	0.0781
450C	0.0352	0.0134	0.0363	0.0142	---	---
450F	0.0582	0.0573	*0.0464 **0.0500	0.0751 0.0193	0.0628	0.1160
450SF	0.0506	0.0553	0.0451	0.0863	0.0679	0.1173
450S	*0.0649 **0.0567	0.0531 0.0219	0.0514	0.0169	0.0703	0.0650

Remarks : * - Peak 1 and ** - Peak 2

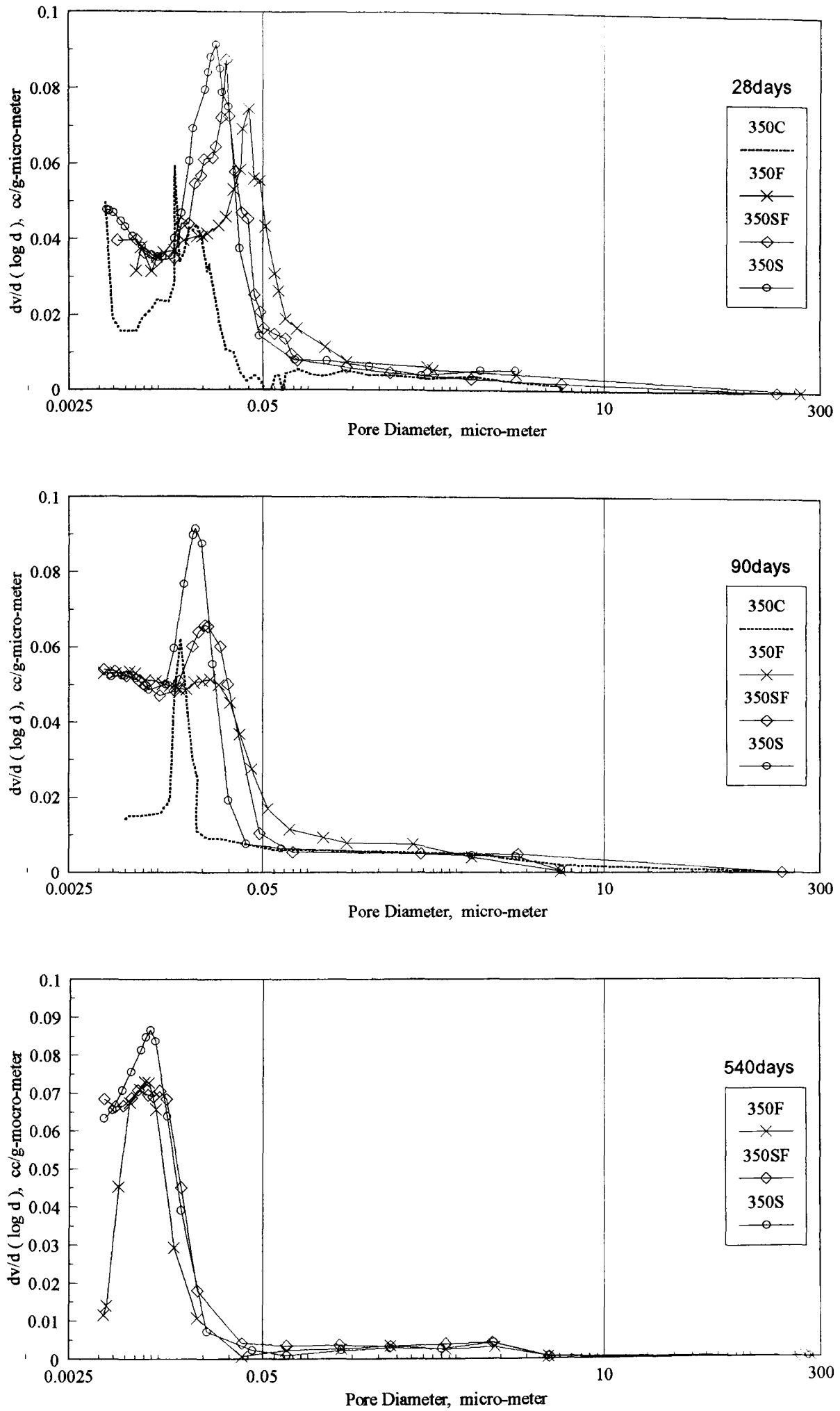


Figure 7-5 Differential pore volume curves for the 350 kg/m³ binder content OPC and HVFA concrete (Water curing)

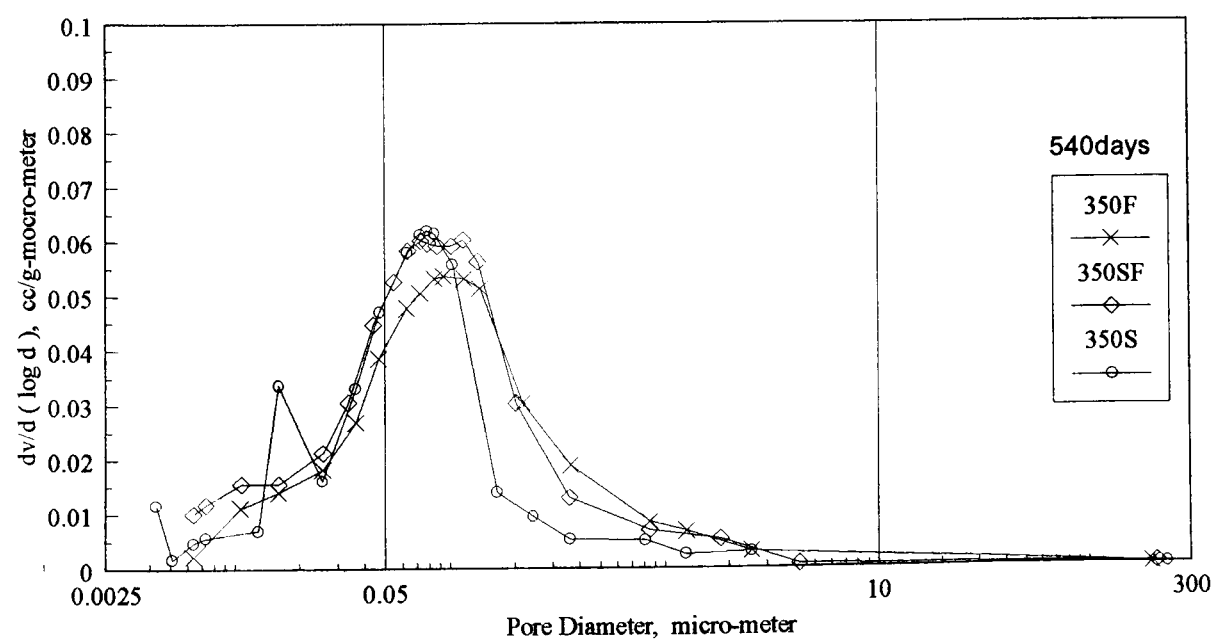
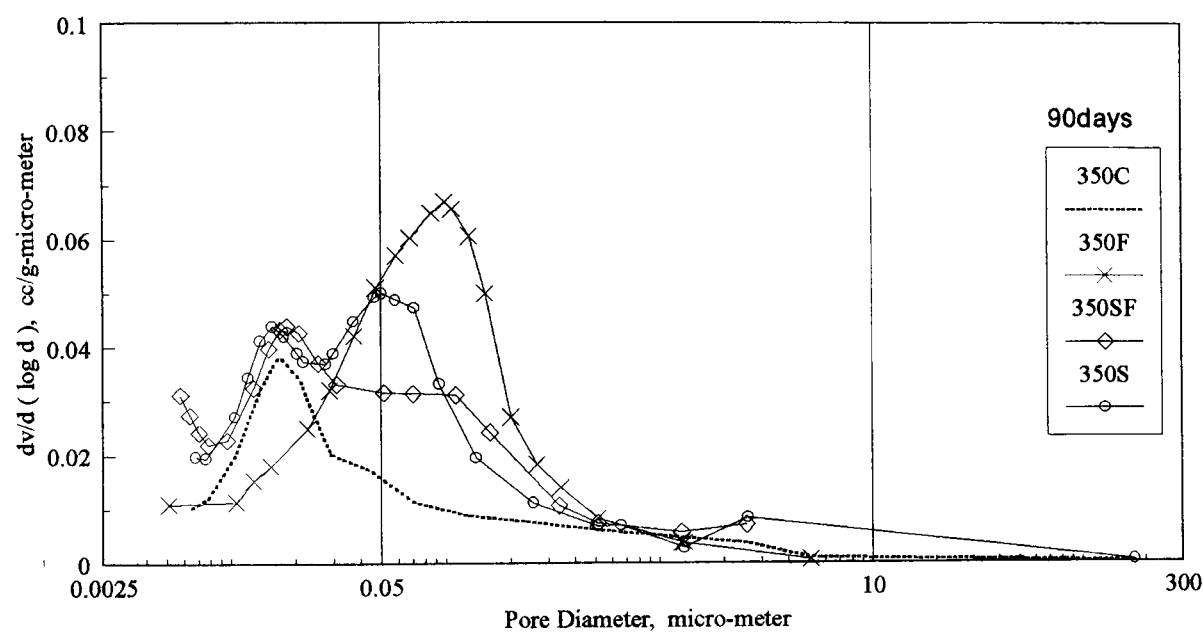
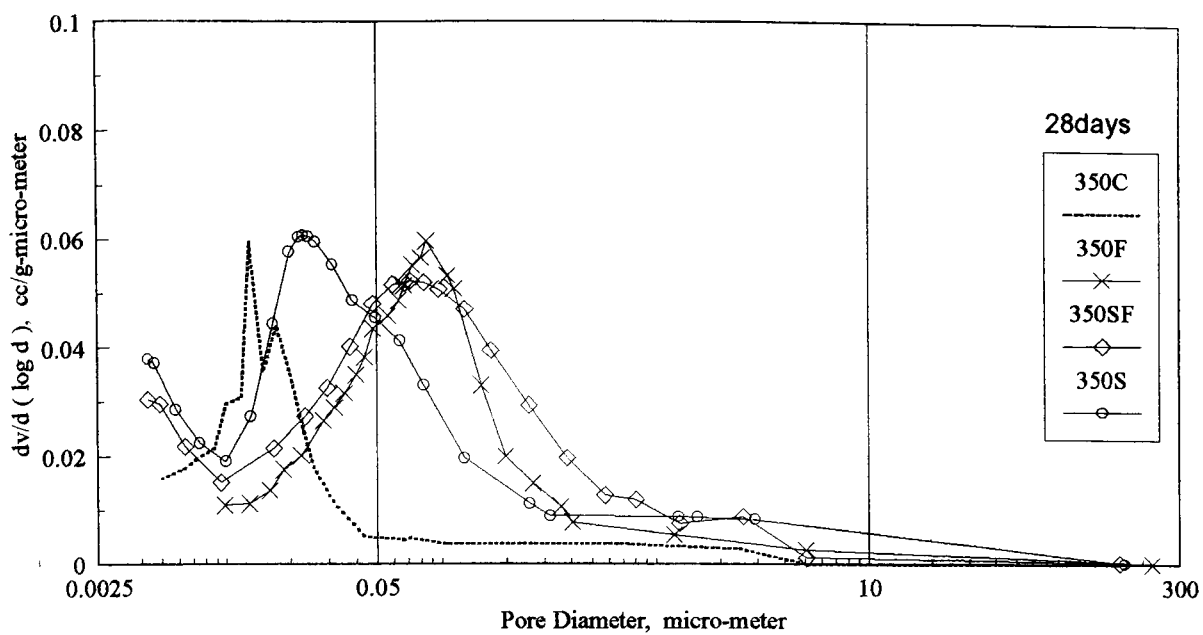


Figure 7-6 Differential pore volume curves for the 350 kg/m³ binder content OPC and HVFA concrete (Air curing)

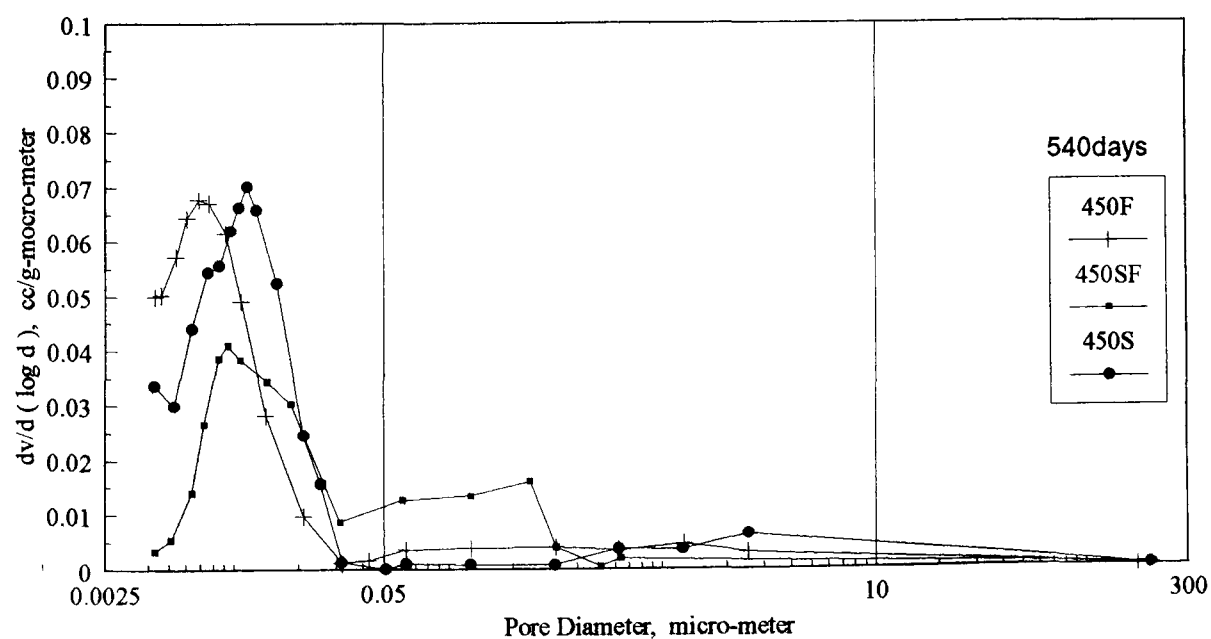
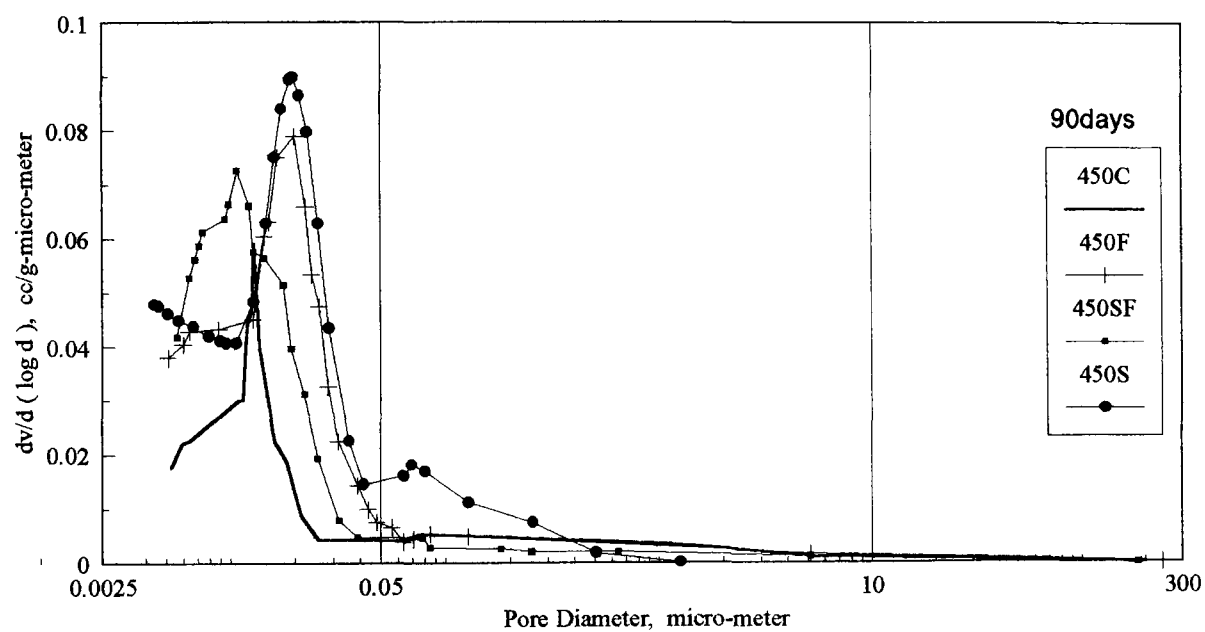
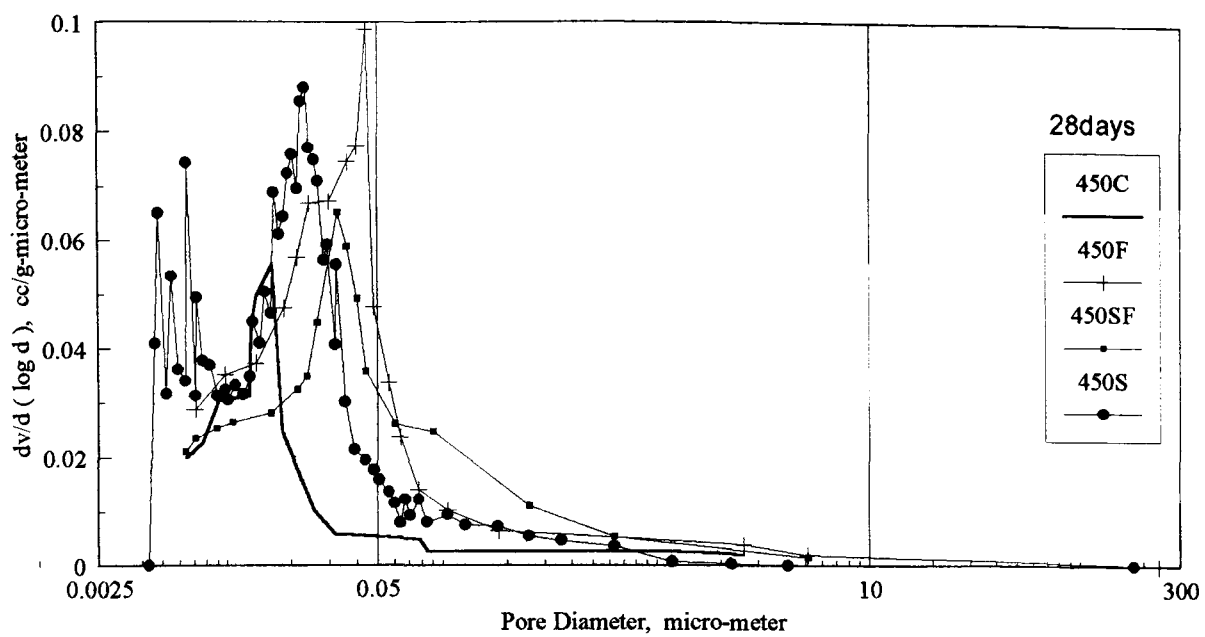


Figure 7-7 Differential pore volume curves for the 450 kg/m³ binder content OPC and HVFA concrete (Water curing)

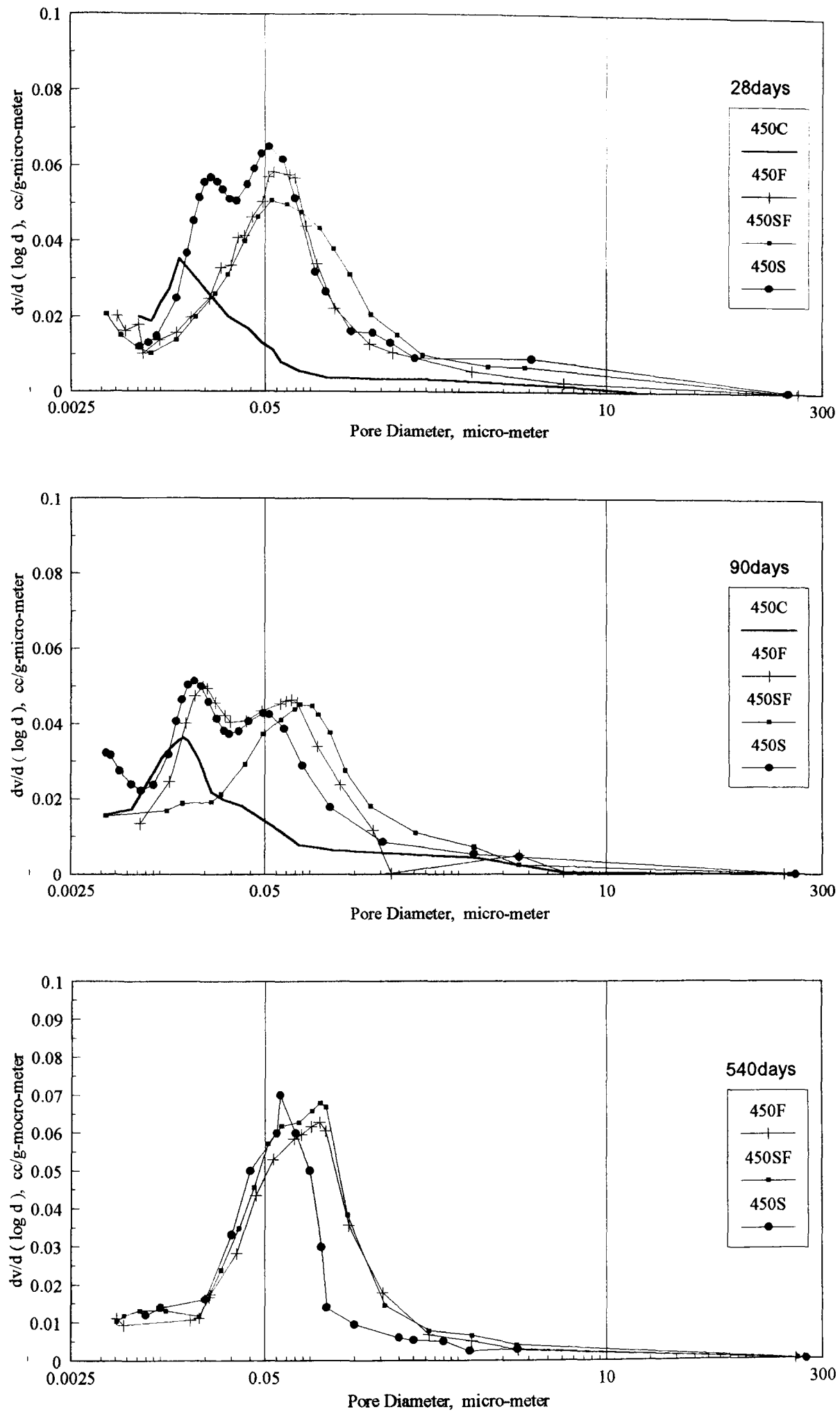


Figure 7-8 Differential pore volume curves for the 450 kg/m³ binder content OPC and HVFA concrete (Air curing)

7-2-3. Comparison with the total binder content on pore size distribution

In comparison with total binder content on all of concretes under both types of curing conditions are shown from Fig 7-9 to Fig 7-20. The results show that the total binder content does not seem to have much effect on the pore size distribution. Concretes made with 450 kg/m³ mixes were slightly lower cumulative pore volumes than that concretes 350 kg/m³ mixes under both types curing conditions. It is important pointing out that, although concrete made of 450S had higher cumulative pore volumes, the pore size distribution had similar trend 350S under water curing at 90 days. The maximum continuous pore diameter of both types of concrete approach to fine pore size range, which is 0.0178 μm for Mix-350S, 0.0196 μm for Mix-450S respectively. Similar results were found in air curing ; the maximum continuous pore diameter of Mix-450S had a finer pore size distribution at second peak than that of concrete of 350S.

It is interesting in the differential pore size plots, the concrete of both types of binder content under the same curing condition and age, had more or less a similar tendency in differential pore size curve. Porosity is a major factor in controlling strength and modulus of elasticity of concrete systems. As demonstrated in preceding discussion on engineering properties, the pulse velocity is controlled primarily by the dynamic modulus of elasticity of the concrete. Test concretes from all the mixtures with both types cementitious material contents had shown similar behaviours of pulse velocity under the same conditions. From the results, there is no doubt that the pulse velocity of concrete is also influenced by the volume of all pores in concrete.

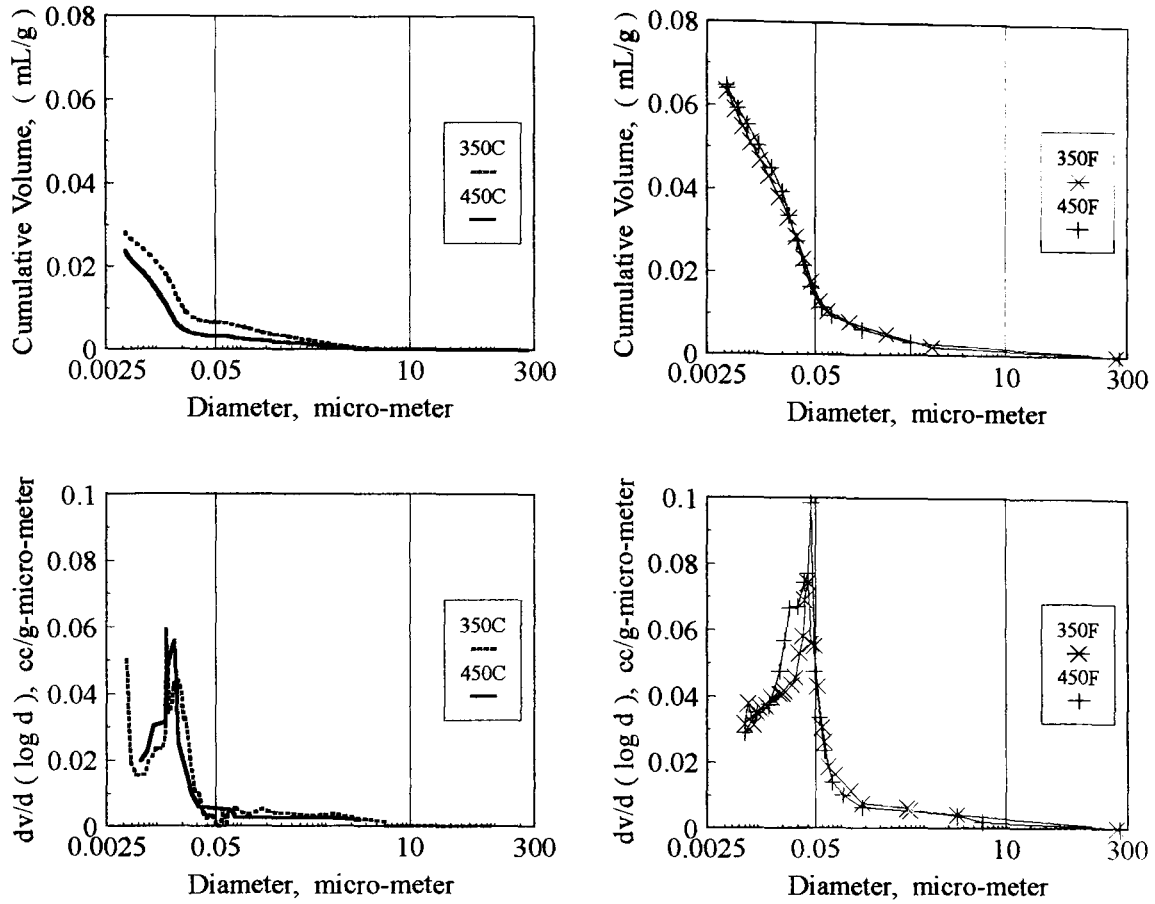


Figure 7-9 Cumulative and differential pore volume of 350C/450C, 350F/450F (Water curing 28 day)

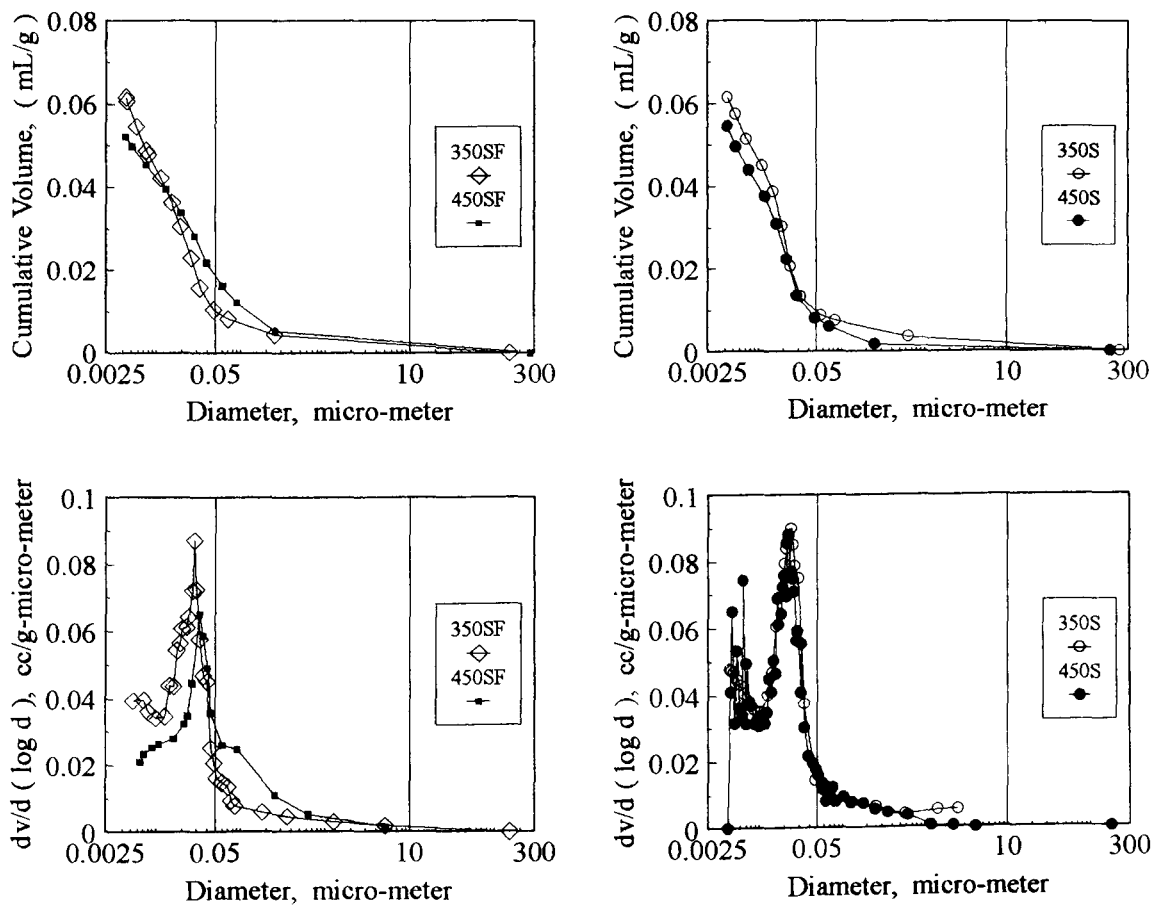


Figure 7-10 Cumulative and differential pore volume of 350SF/450SF, 350S/450S (Water curing 28 day)

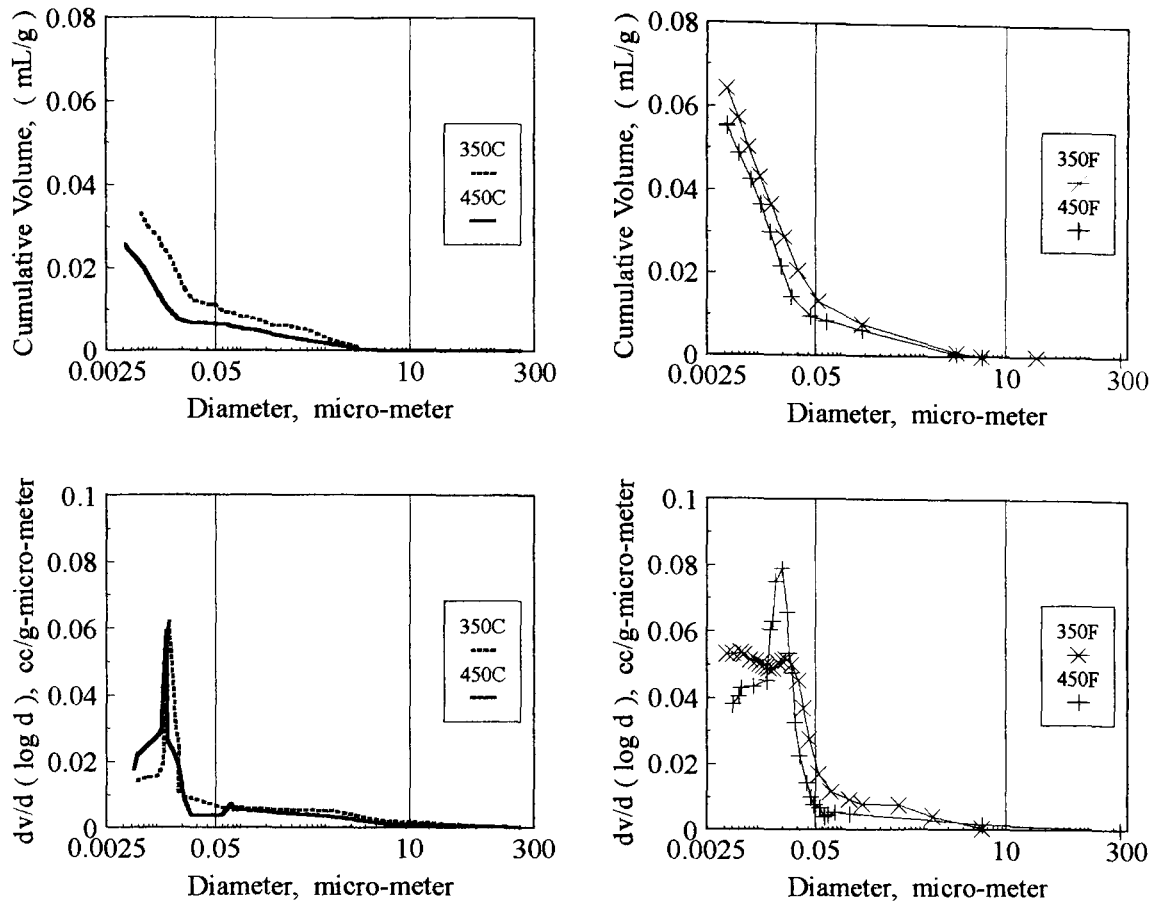


Figure 7-11 Cumulative and differential pore volume 350C/450C, 350F/450F (Water curing 90 day)

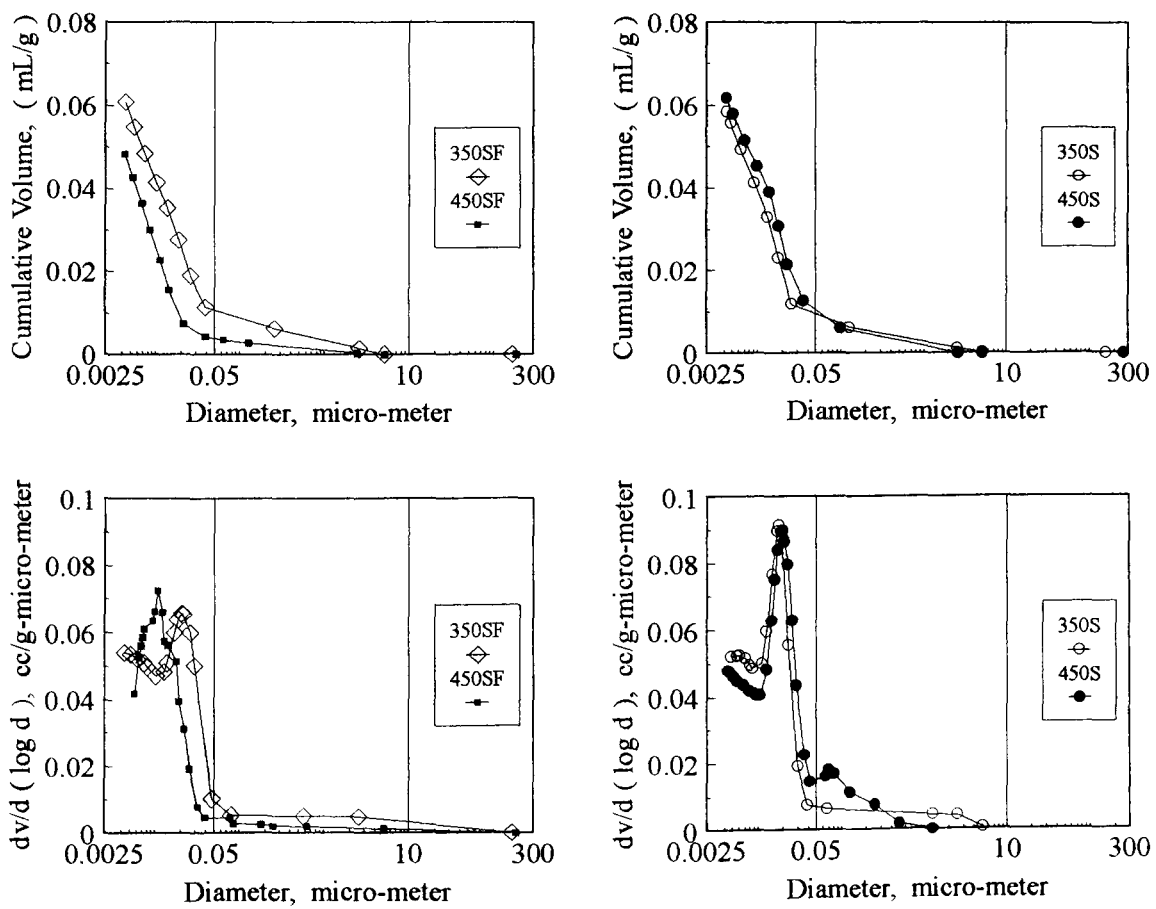


Figure 7-12 Cumulative and differential pore volume of 350SF/450SF, 350S/450S (Water curing 90 day)

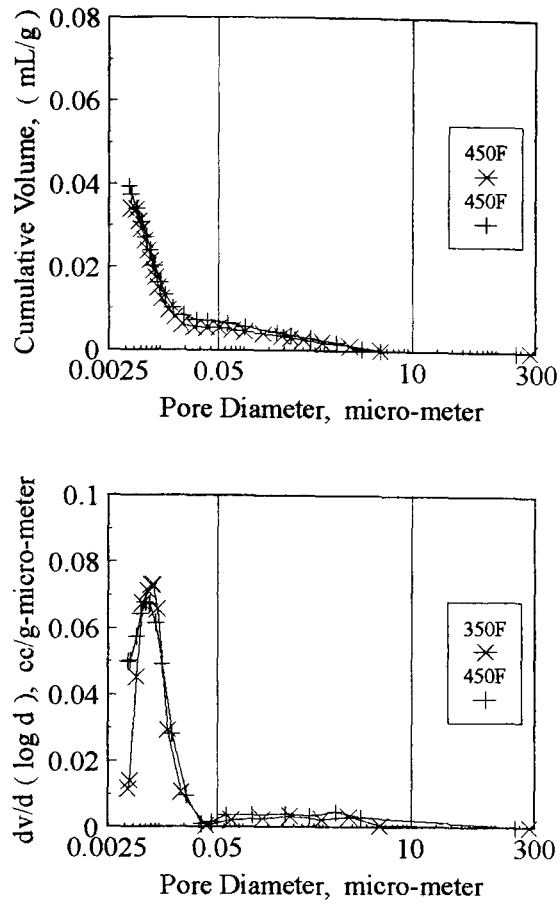


Figure 7-13 Cumulative and differential pore volume of 350F/450F (Water curing 540 day)

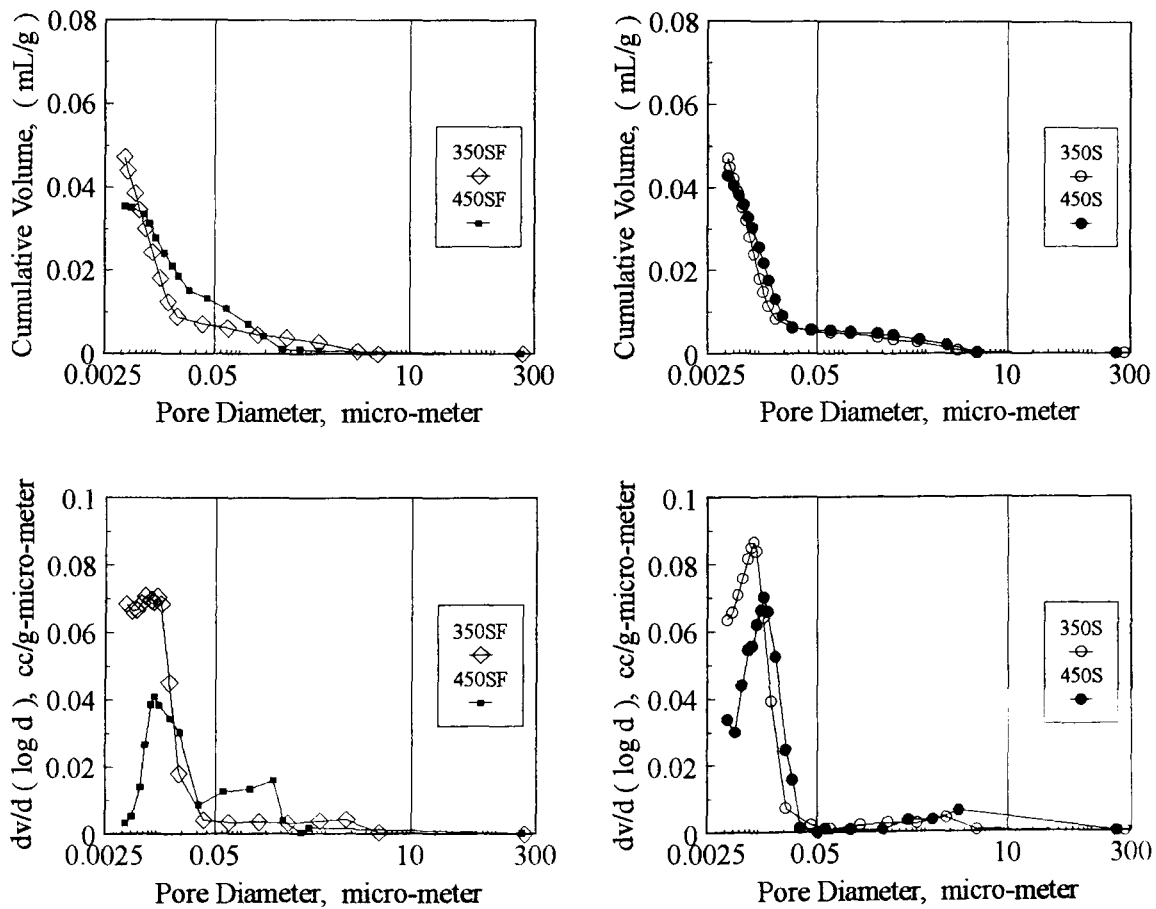


Figure 7-14 Cumulative and differential pore volume of 350SF/450SF, 350S/450S (Water curing 540 day)

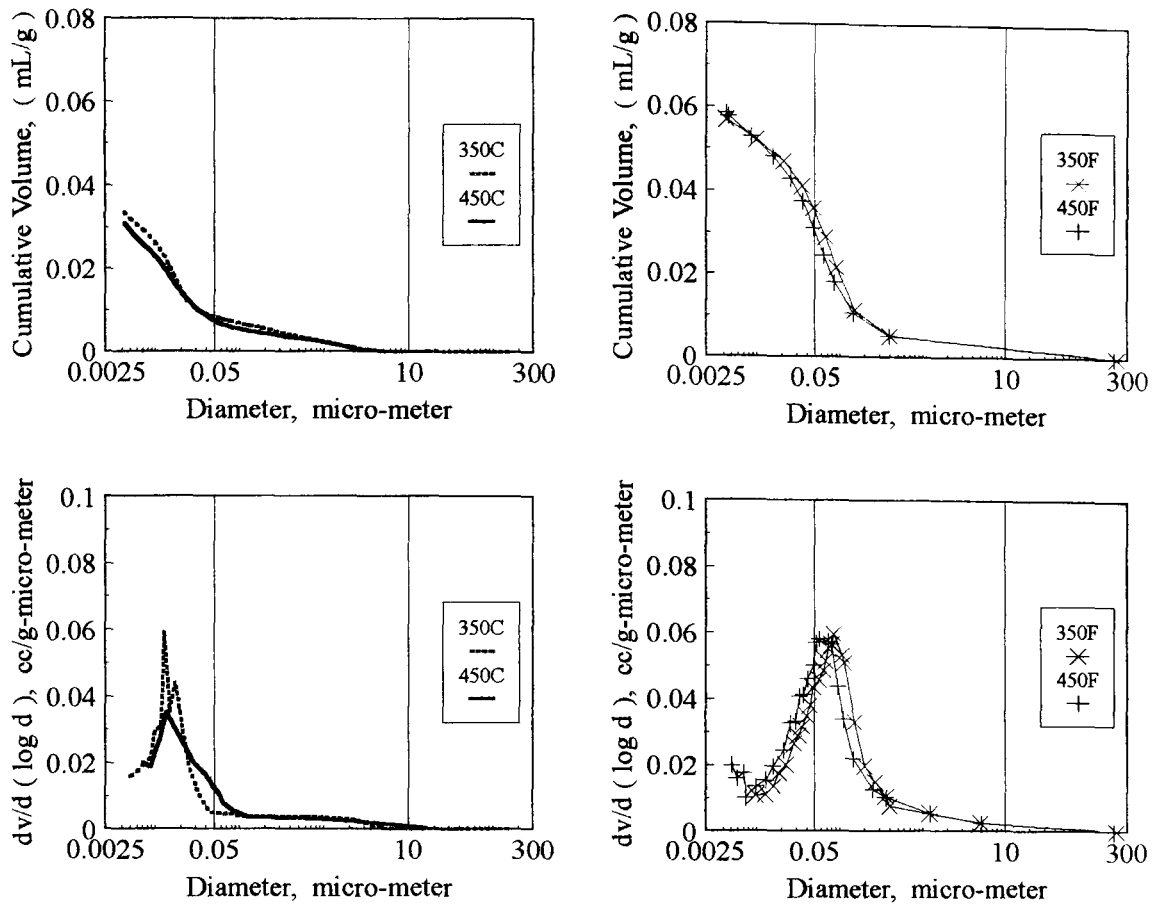


Figure 7-15 Cumulative and differential pore volume of 350C/450C, 350F/450F (Air curing 28 day)

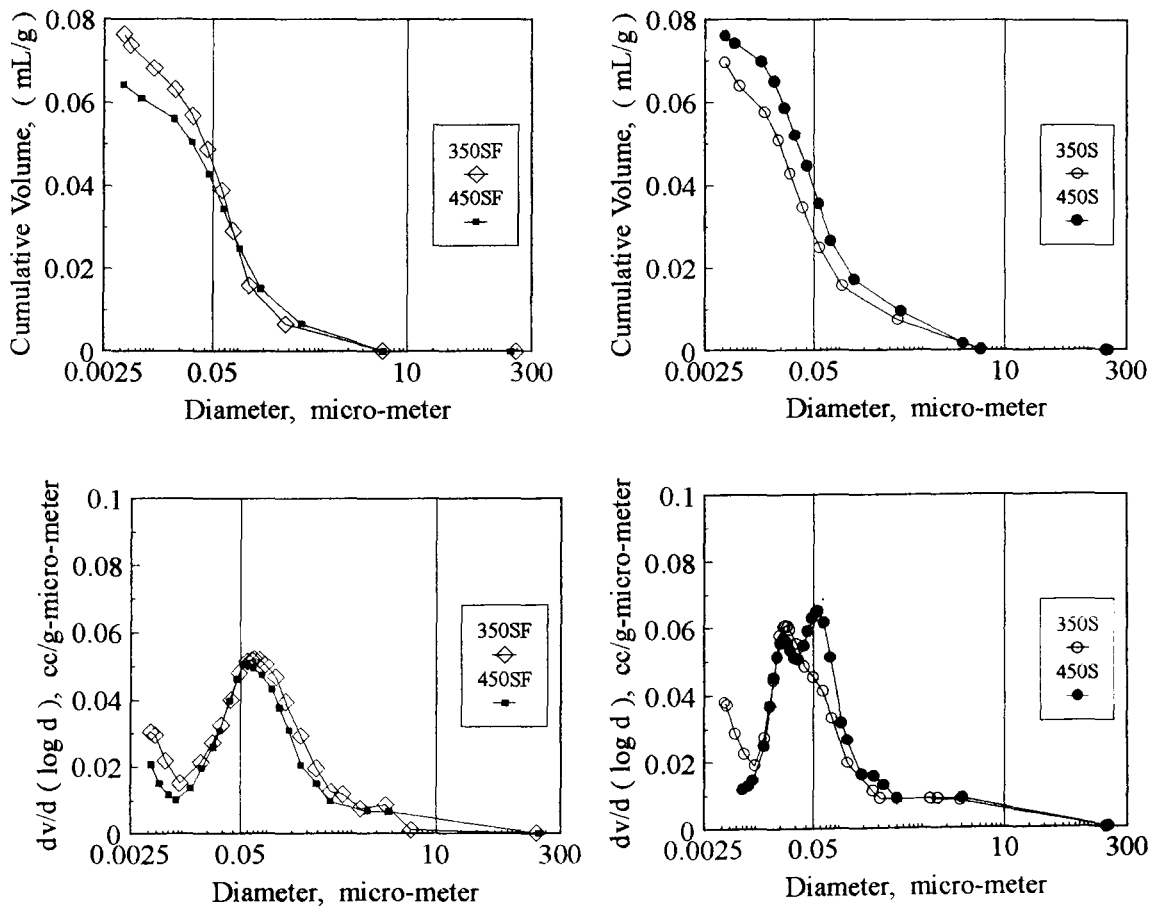


Figure 7-16 Cumulative and differential pore volume of 350SF/450SF, 350S/450S (Air curing 28 day)

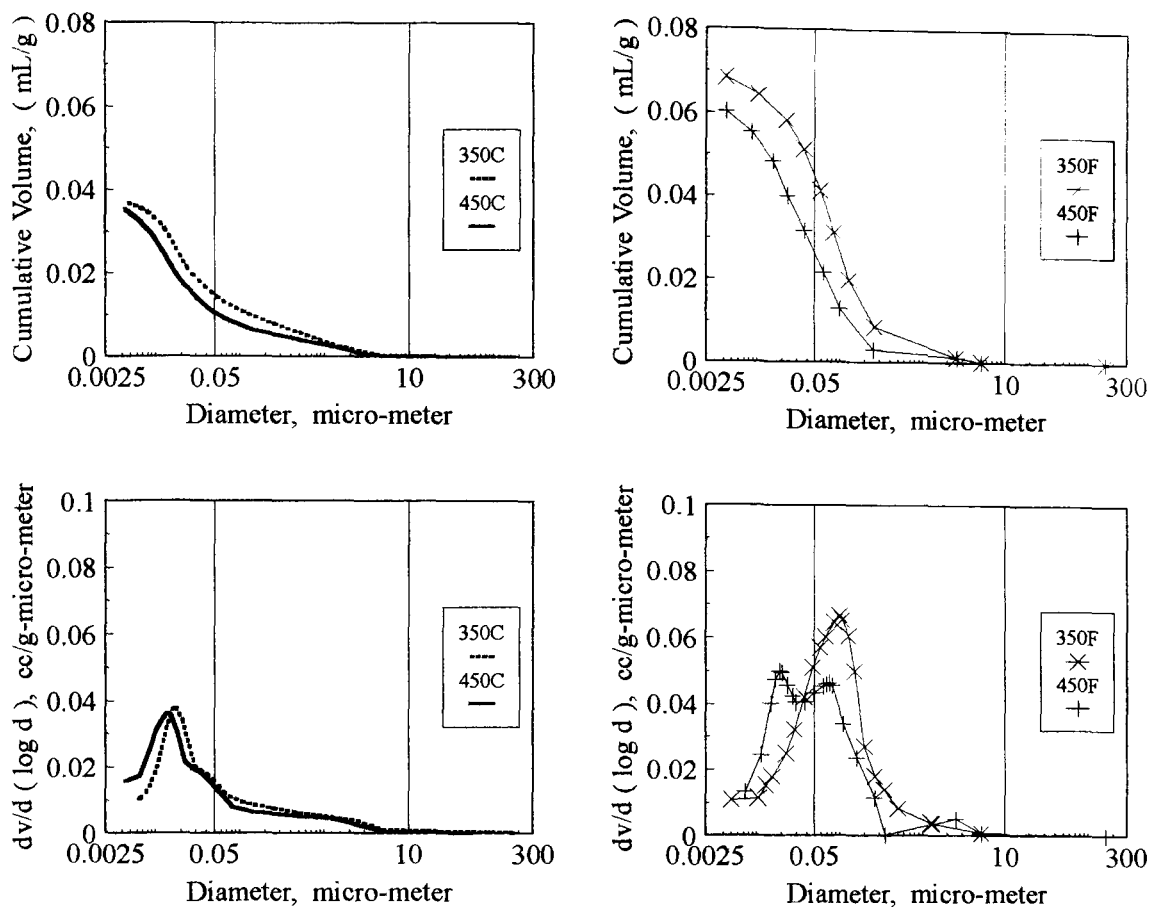


Figure 7-17 Cumulative and differential pore volume of 350C/450C, 350F/450F (Air curing 90 day)

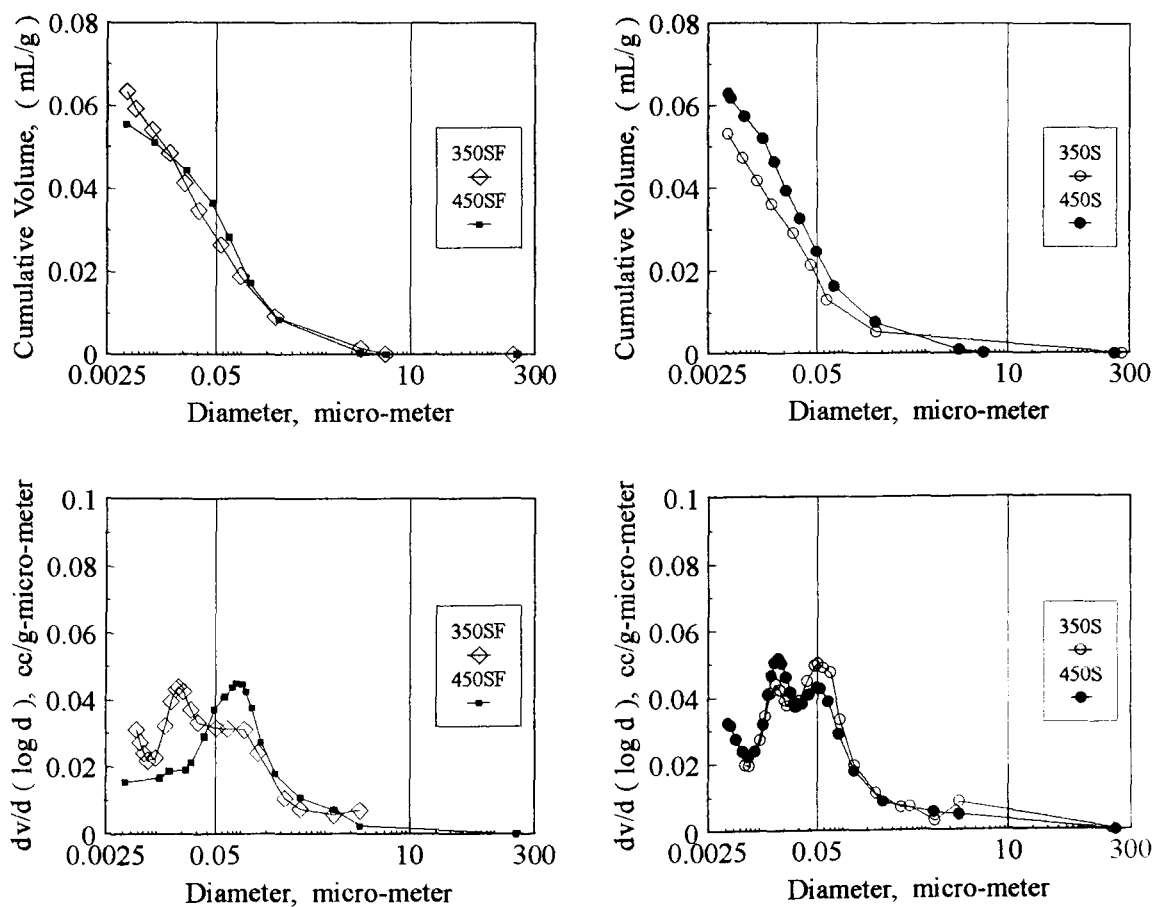


Figure 7-18 Cumulative and differential pore volume of 350SF/450SF, 350S/450S (Air curing 90 day)

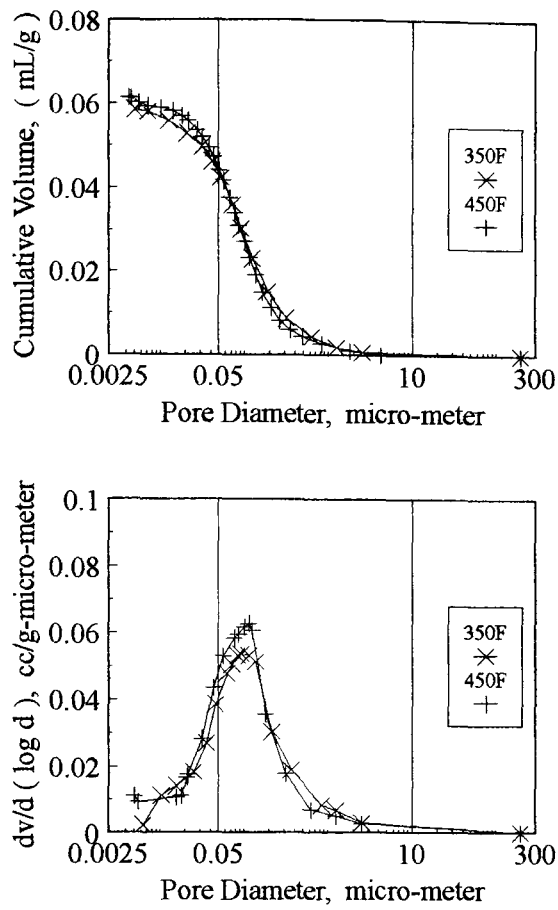


Figure 7-19 Cumulative and differential pore volume of 350F/450F (Air curing 540 day)

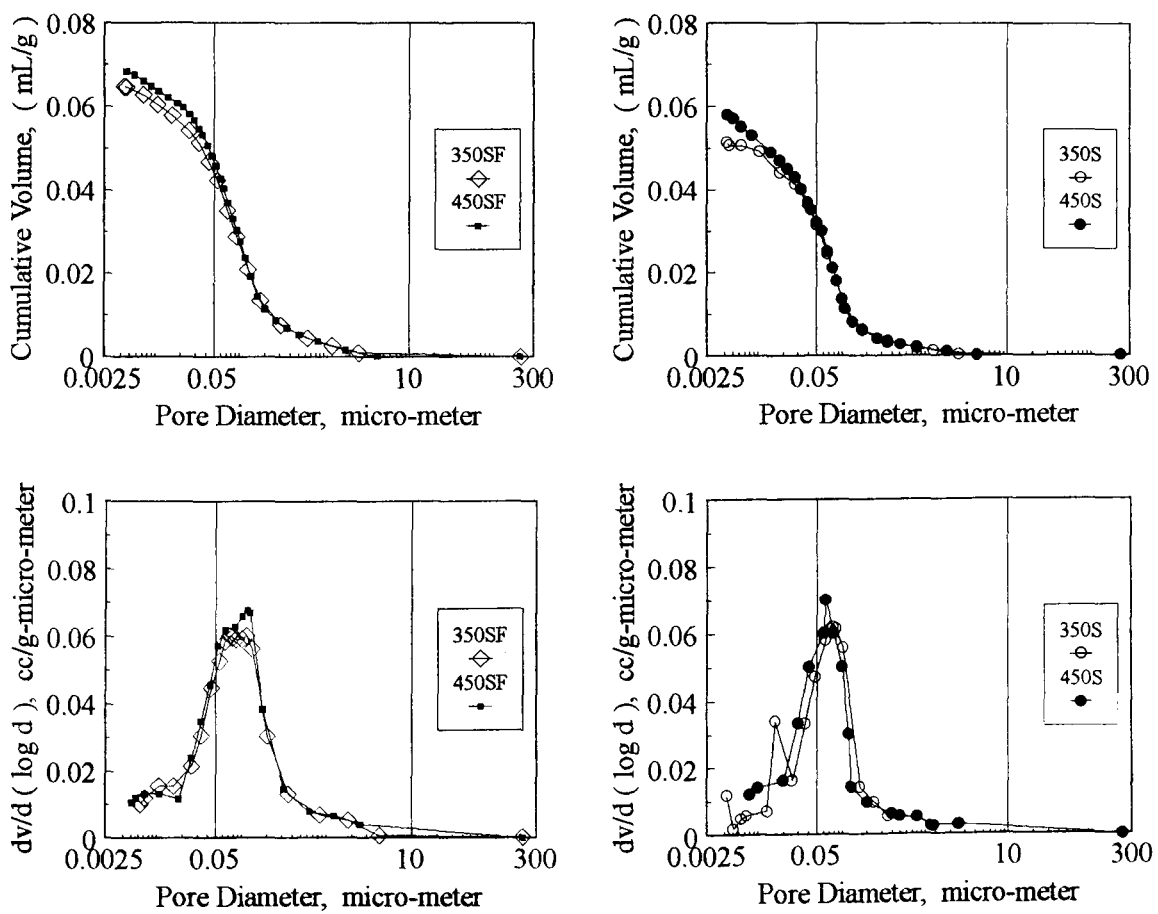


Figure 7-20 Cumulative and differential pore volume of 350SF/450SF, 350S/450S (Air curing 540 day)

7-2-4. Total, macro-pore and meso-pore volumes

As discussed in the preceding section, the pore structure will be divided into three parts following closely the division defined by IUPAC : macro-pores ($d > 500 \text{ \AA}$), meso-pores ($25 \text{ \AA} \sim 500 \text{ \AA}$), and micro-pores ($d < 25 \text{ \AA}$). The effect of different curing conditions on the total macro-pores , and meso-pores distribution of both types binder contents are presented in Tables 7-7 and 7-8.

The results show that all the concrete mixtures with continuous water curing exhibited a higher percentage meso-pores than the air drying concretes. Meanwhile, the use of air curing of all concretes a slight reduction in meso-pore, and macro-pore are just relatively increase with continued air drying.

Under water curing, however, the HVFA concretes had much greater meso-pores, when compared to the normal OPC concrete at the ages of 28 days and 90 days under the same conditions. The trends in the macro-pores are just the opposite. The larger percentage of macro-pores of normal OPC concrete reflects its “coarser” pore structure. It is reasonable to suppose that increase in meso-pores with increased curing age is the result of growth of hydration products during hydration reaction. On this table, it can be clearly seen that the concrete of 450SF the meso-pores range and much less in the macro-pores range at the age of 90 days. Meanwhile, at the end of 540 days, the concrete made of 350S and 450S had a highest percentage of meso-pores compared to the other HVFA concretes.

Macro-pore into meso-pore due to reduction of their pore size by the growth of hydration products into the available spaces between the unhydrated grains, which were initially filled with water [71].

Data from the results also showed that an increase in the accessible pore volume in the presence of concrete with air curing is associated with a decrease in the number of fine pores, and an increase in the number of coarse pores when compared to the wet specimens at the same conditions. This shift in pore structure is exhibited in the differential pore volume curves as were already shown in above Figs 7-2, 7-4, 7-6, and 7-8.

**Table 7-7 The macropore and mesopore on OPC and HVFA concrete-Water curing
(Unit : %)**

Range	> 0.05 μm			0.05 μm ~ 0.0025 μm		
	28	90	540	28	90	540
350C	22.86	28.78	---	77.14	71.22	---
350F	23.66	20.56	15.80	76.34	79.44	84.20
350SF	16.21	15.27	13.53	83.79	84.73	86.47
350S	15.05	13.01	11.06	84.95	86.99	88.94
450C	15.08	25.10	---	86.92	74.90	---
450F	21.45	16.37	17.26	78.55	83.63	82.74
450SF	34.29	8.07	15.31	65.71	91.93	84.69
450S	13.92	16.86	13.32	86.08	83.14	86.68

**Table 7-8 The macropore and mesopore on OPC and HVFA concrete-Air curing
(Unit : %)**

Range	> 0.05 μm			0.05 μm ~ 0.0025 μm		
	28	90	540	28	90	540
350C	24.55	38.61	---	75.45	61.39	---
350F	61.16	65.40	78.03	38.84	34.60	21.97
350SF	62.11	43.78	67.85	37.89	56.22	32.15
350S	37.93	31.26	61.21	62.07	68.74	38.79
450C	23.62	26.63	---	76.38	73.37	---
450F	51.45	42.38	71.87	48.55	57.62	28.13
450SF	62.05	60.36	67.69	37.95	39.64	32.31
450S	47.60	36.41	61.03	52.40	63.59	38.97

The pore size distribution in the presence of air curing concrete mixtures changed from a narrower to a wider distribution with a shift in meso-pore diameter toward to a macro-pore diameter. However, the variation in macro-pore, meso-pore indicated the air drying has a marked effect on the arrangement of these growing hydration products.

7-2-5. Some relations between the pore structure and compressive strength

The relationship between the compressive strength, f_c , and porosity of concrete, X , is by the power equation :

$$f_c = a X^b \text{ ----- (7-1)}$$

where f_c is the compressive strength in MPa, X is the porosity in %, and a and b are constants.

Although both mixes with 350 kg/m^3 and 450 kg/m^3 total binder content concretes had shown similar pore size distribution under the same conditions, the curing regime was the marked factor in determining the result of compressive strength, and the pore size distribution. In general, the water cured concretes showed higher values of compressive strength than those exposed to drying concretes ; it is suggested that separate equations be developed for each curing condition.

The relation between porosity and compressive strength for all concretes under different curing conditions is shown in Figs 7-21 and 7-22. The relationship is based on the data at 28 days, 90 days, and 18 months for all concretes under water and drying curing conditions. Regression analysis of the data shown in the figures produced the following relationships :

$$f_c = 243.7 X^{-0.67} \quad (\text{moist}) \quad (r = - 0.75) \text{ ----- (7-2)}$$

$$f_c = 505.8 X^{-0.95} \quad (\text{dry}) \quad (r = - 0.72) \text{ ----- (7-3)}$$

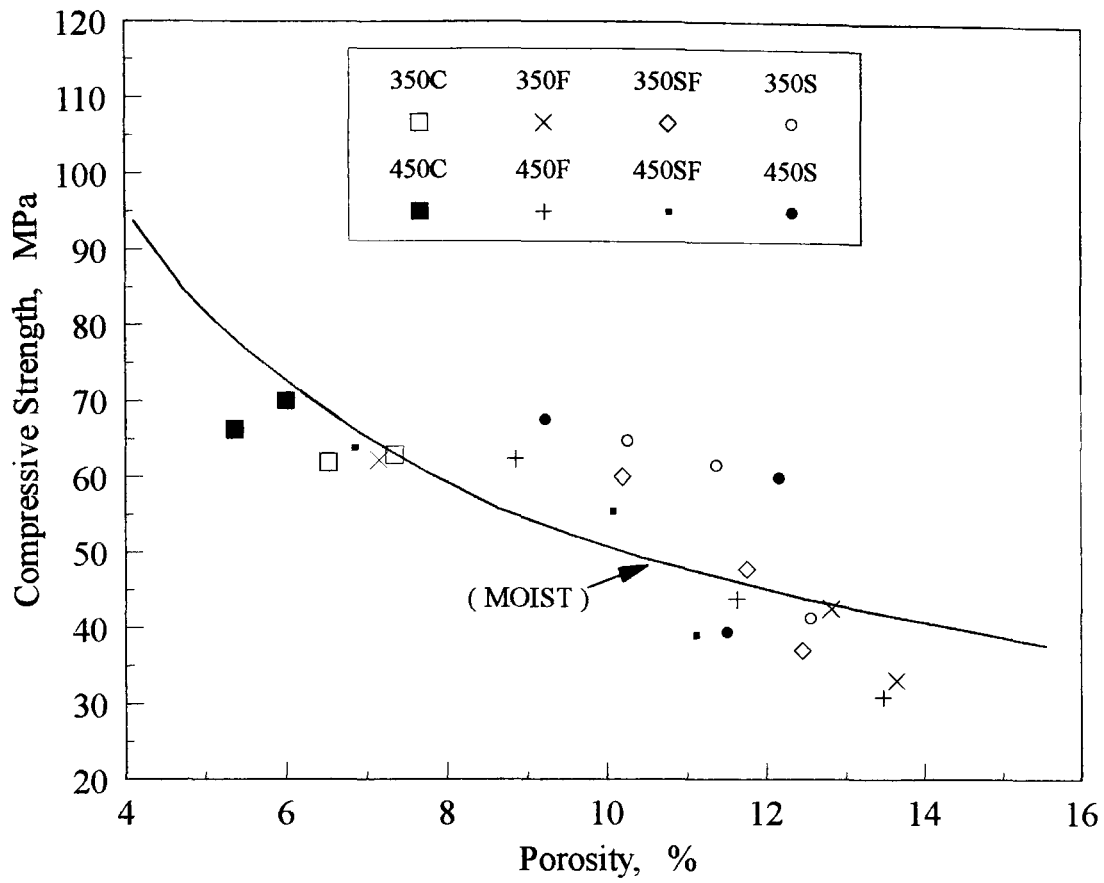


Figure 7-21 Relationship between compressive strength and porosity of OPC and HVFA concrete-Water curing

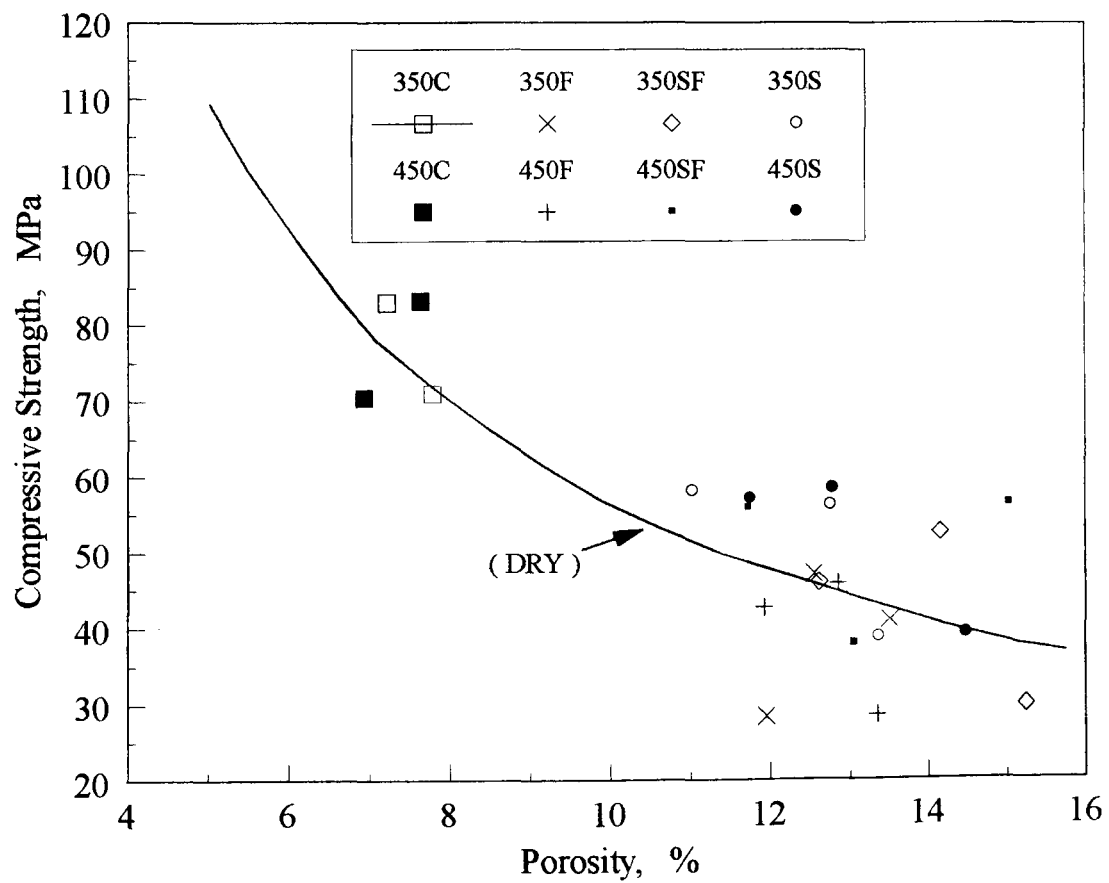


Figure 7-22 Relationship between compressive strength and porosity of OPC and HVFA concrete-Air curing

The correlation factor with the two equations is low. These data indicate a significant correlation between porosity and compressive strength in concretes at the 95 % confidence level. A single equation describing the two parameters can be used as given below, and is shown in Fig 7-23.

$$f_c = 288.4 X^{-0.74} \quad (\text{moist + dry}) \quad (r = -0.71) \text{ ----- (7-4)}$$

Again, the correlation factor between both parameters of equation is still low and the equation relating the two is approximately the same for the water and air drying curing concretes. All concretes have this same inverse dependency between strength and porosity. Many workers [91,116] have made attempts to correlate various mechanical properties with parameters related to pore structure, especially total porosity. In fact, the effect of the degree of hydration on macro-pore and meso-pore diameter obtained by Mercury Intrusion Porosimetry is shown in Tables 7-7 and 7-8. In most cases, very large changes occur in the diameter of the macro-pores and meso-pores. The variation in macro-pores and meso-pores indicate that curing condition and the degree of hydration have a marked effect on the arrangement of these growing hydration products [70,71]. Generally, at a given porosity, smaller pores lead a higher strength of the concrete. Regression analysis in Fig 7-24 shows that the coefficient of determination ($r = 0.90$), using meso-pore data in the relationship, is very high. The results infer that high strength / performance concretes are seen to be insensitive to the structure of the smaller pores, and are not to be associated with the total porosity. As can be seen in the preceding Tables 7-3, 7-4, porosity over the whole size range of pores has influence on concrete properties, yet it is difficult to get an exact assessment of pore size distribution because Mercury Intrusion Porosimetry measurement encompasses the whole size range and because it is difficult to interpret experimental data. Thus, comparisons of porosity should be made with care.

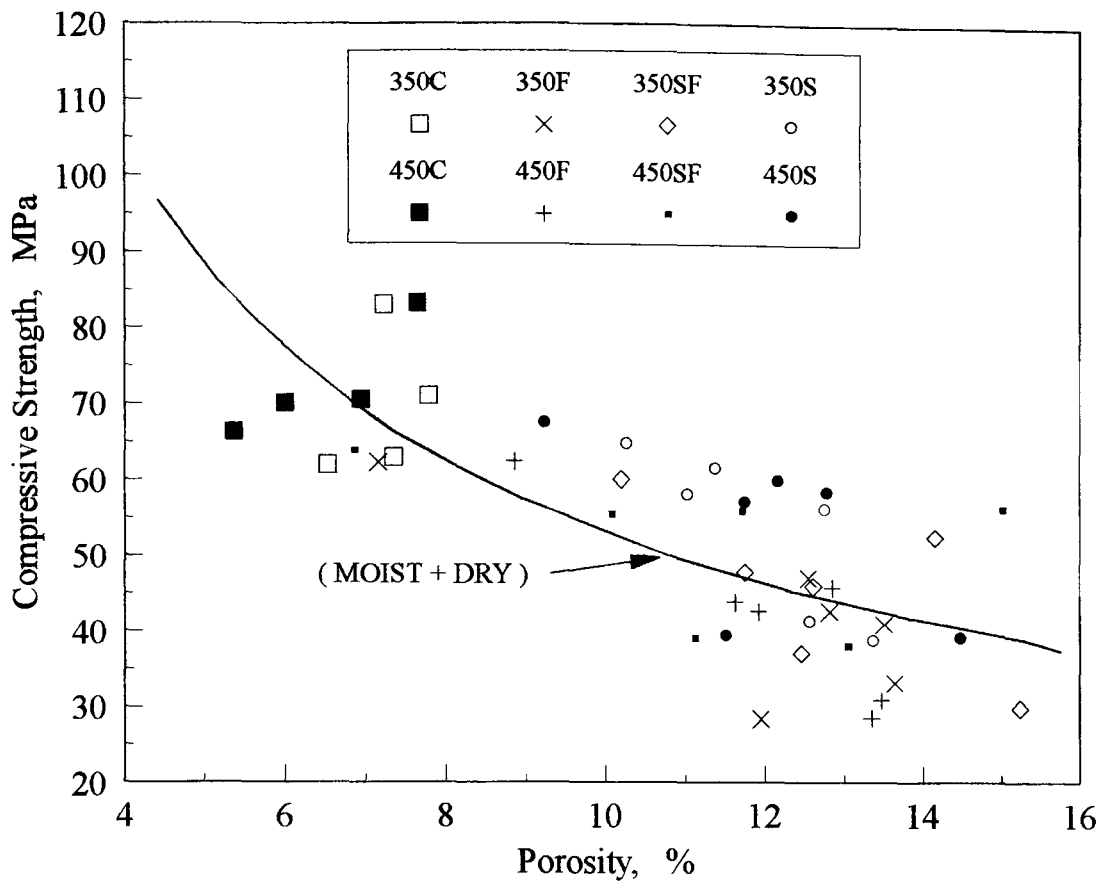


Figure 7-23 Relationship between compressive strength and porosity of OPC and HVFA concrete

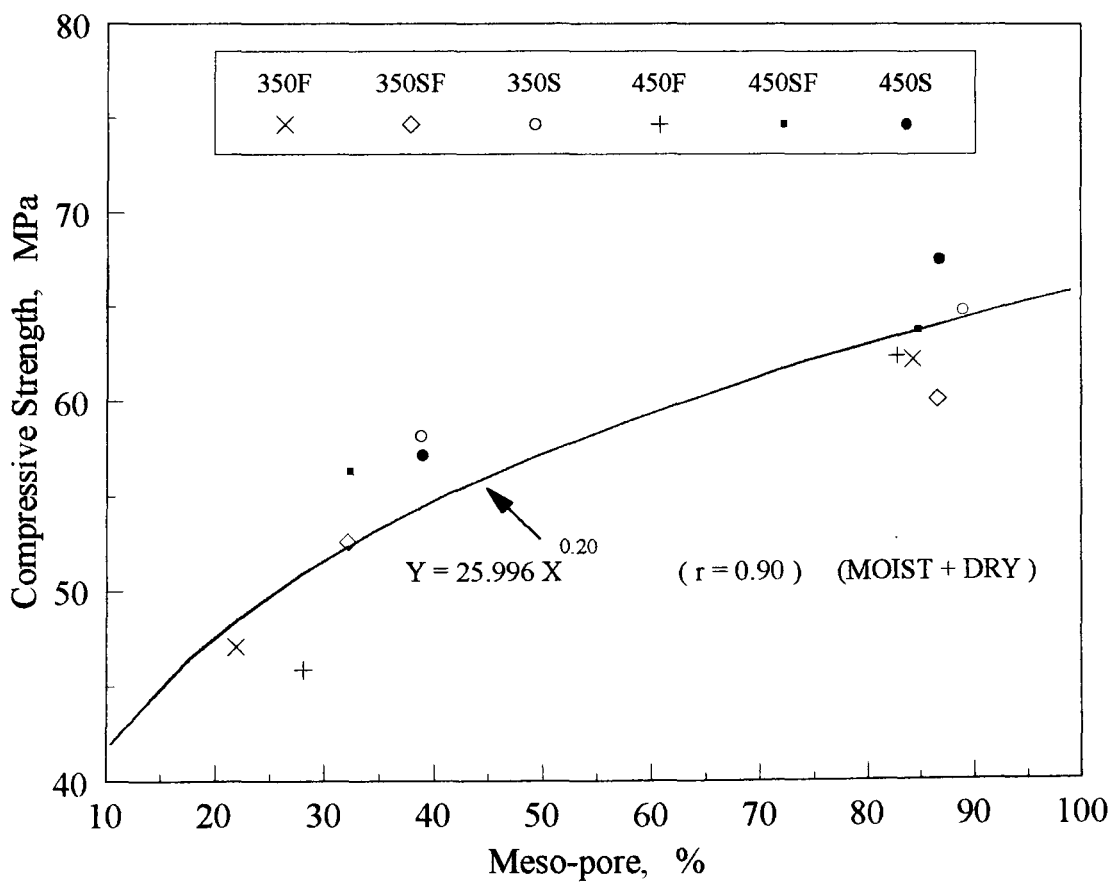


Figure 7-24 Relationship between compressive strength and meso-pore of HVFA concrete

7-3. PERMEABILITY OF HVFA CONCRETE

Permeability is one of the basic characteristics of concrete relating to its durability, and especially when concerned with its use in special applications such as in the isolation of water materials. If a concrete lacked impermeability, even though it theoretically has a high strength, it would not be acceptable in most cases since its durability would be at risk [94,117]. Moreover, permeability properties give considerable insight into the mechanisms of fluid and ionic transport through concrete. Relationships have been shown to exist between the air permeability and carbonation resistance and the initial surface absorption and abrasion resistance of concrete [118].

The permeability test is based on “The Leeds Permeability Cell” [112], which measures the coefficient of permeability by measurement of through flow of oxygen. Permeability tests were performed on 50 mm diameter 30 ~ 40 mm cores samples drilled from 100 × 100 × 500 mm prisms. The test specimens were subjected to different curing and tested at the age of 28 days, 90 days, and 18 months. For each curing three cored samples were used, the results are thus the average of three readings. Mix proportions and test procedure described in section 6-4-2. Variations in different replacement methods and total cementitious content also are investigated. The relationship between the compressive strength and permeability are also reported. A relation between the air permeability and porosity for HVFA concretes was found.

7-3-1. Effect of curing condition on air permeability

Under water curing with various curing periods, the data on the air permeability of HVFA concretes with both types of binder contents are given in Table 7-9 and illustrated in Figs 7-25 and 7-26.

**Table 7-9 High volume fly ash concrete permeability coefficient
(Unit : 10^{-16} m^2)**

Curing	Water curing				Air curing		
	28	90	180	540	28	90	540
350F	0.305	0.151	0.132	0.203	0.576	0.431	0.846
350SF	0.142	0.134	0.130	0.176	0.255	0.206	0.761
350S	0.126	0.127	0.121	0.163	0.234	0.160	0.454
450F	0.277	0.135	0.121	0.144	0.524	0.377	0.701
450SF	0.132	0.134	0.111	0.181	0.247	0.189	0.512
450S	0.117	0.102	0.101	0.194	0.217	0.160	0.437

Data from the results indicated that the coefficient of permeability was low in water cured specimens at early ages for all HVFA concretes. Between the ages of 28 days and six months, obviously, the presence of silica fume in mixes 350SF and 450SF helped mixes 350F and 450F to develop a denser internal structure and a lower permeability. Mixes 350S and 450S with large amounts of fly ash developed a much denser structure and low permeability from early ages. As already stated in section 5-5, the permeability of concrete is not only a simple function of its porosity, but depends also on the size, distribution, shape tortuosity, and continuity of the pores. The present investigation, from the preceding results of the pore size distribution in Table 7-7, suggested that the permeability is strongly controlled by an interconnecting network of capillary pores. At 28 days and 90 days under water curing, the concrete made with 450S had much lower macro-pores, compared to the same condition of concrete 450F. The reduction in amount of macro-pores with duration of specimens under water is correspondingly reflected in the permeability of concrete.

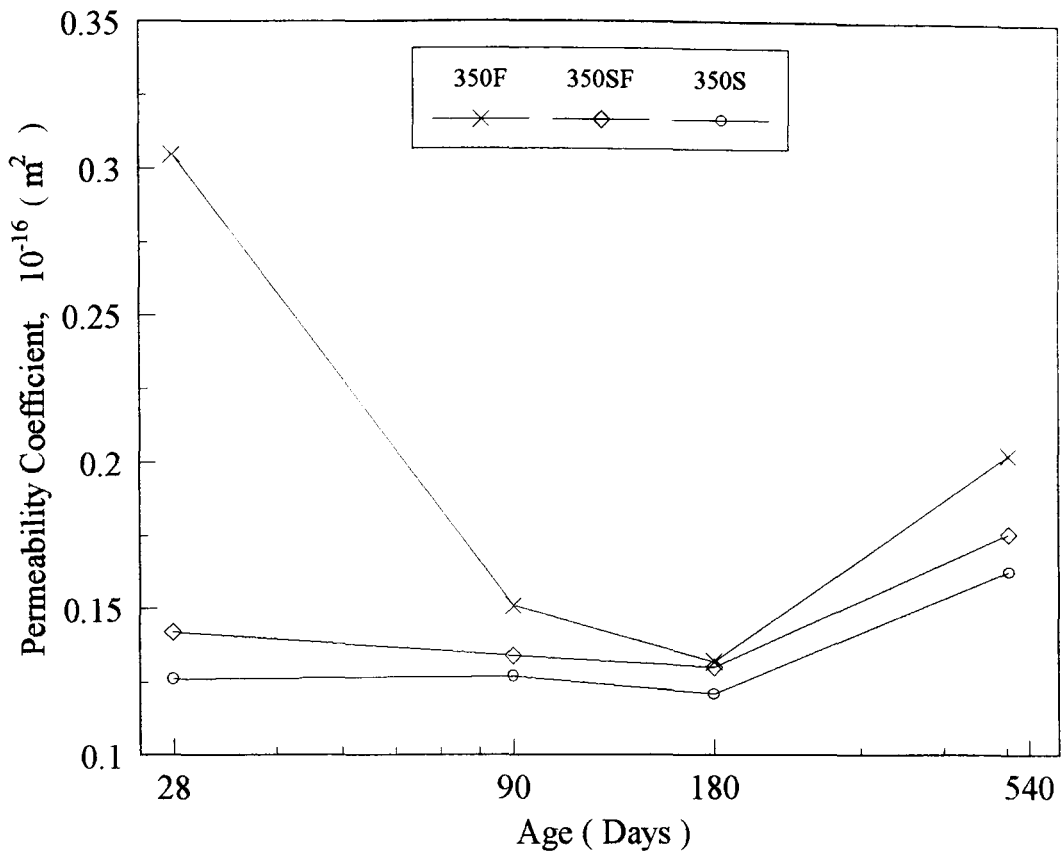


Figure 7-25 The permeability coefficient of HVFA concrete-water curing (350 kg/m³ mixes)

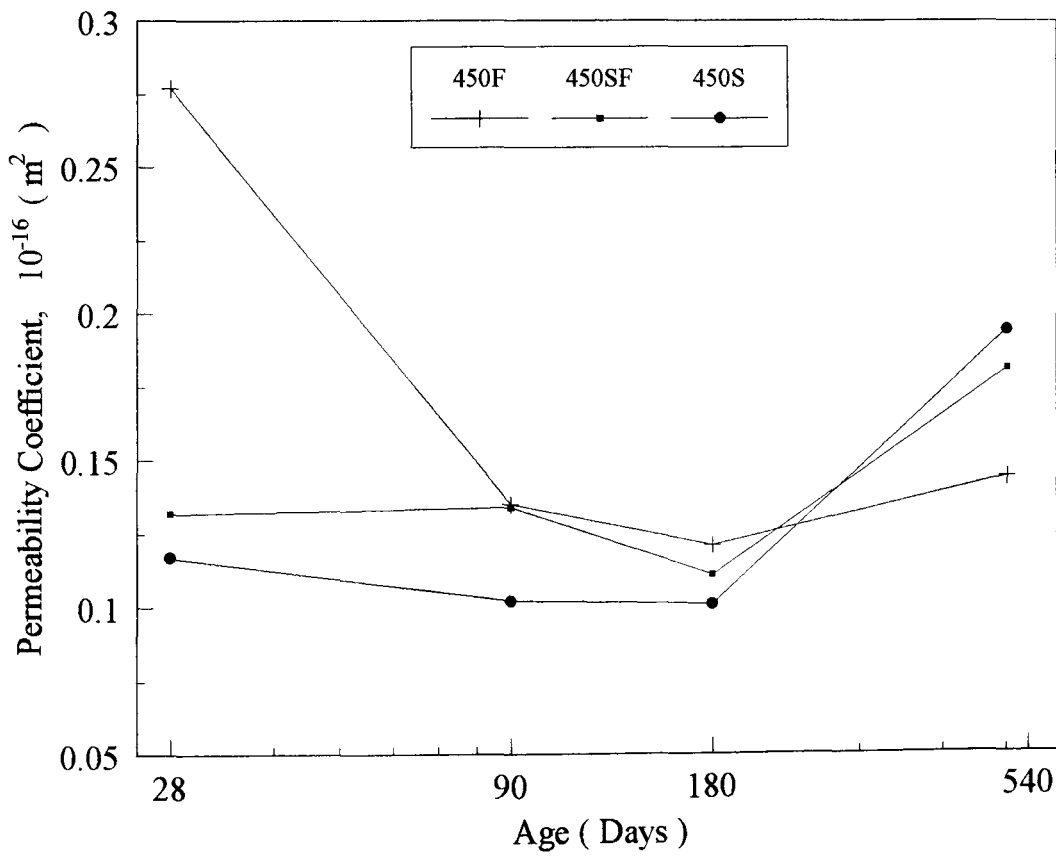


Figure 7-26 The permeability coefficient of HVFA concrete-water curing (450 kg/m³ mixes)

It is clear from those results that the permeability of the HVFA concrete was directly related to the pozzolanic reaction of fly ash and silica fume in concrete, which produces calcium silicate hydrate, tends to fill these unoccupied spaces to form a product with decreased permeability and which also results in improved strength [28]. These results were also found by Manmohan and Methta [37]. They showed that additions of pozzolanic and cementitious admixtures such as fly ash to portland cement were instrumental in causing pore refinement or transformation of large pores into fine pores - a process which had a far reaching influence on the permeability of the hardened cement concretes. Meanwhile, the use of fly ash to replace both cement and sand partially might have a good combination effect on permeability.

In general terms, it is possible to say that the higher the strength of the hardened cement concrete the lower its permeability - a state of affairs to be expected because strength is a function of the relative volume of gel in the space available to it [69]. Nevertheless, from the figures, the improvement in strength with ages of water curing seems not to be correspondingly reflected in the permeability of concrete. For the long term under water curing, the concretes exhibited slightly increasing coefficient of permeability at the age of 18 months when compared to the permeability with the same conditions at the age of six months. In comparing both porosity (Tables 7-7 and 7-8) and coefficient of permeability of concrete at the age of 504 days, the concrete made of 450F has a higher macro-pore volume but a lower coefficient of permeability. Whereas, for concrete made of 450S a lower percentage in macro-pores was found. The corresponding coefficient of permeability for the concrete made of 450S were high. It would be expected, as a first approximation, that a sample with a higher porosity also would have a large permeability. However, this generality does not take into consideration the possibility of and potential effects of differences in pore size distribution. Research data [9] indicate the sensitivity of high strength fly ash concrete to curing, especially for the most mature concrete. In a mature concrete, the permeability depends on size, shape, and concentration of the gel particles and on whether or not the capillaries have become discontinuous.

In the present investigation, the higher potential strength and the concomitant pozzolanic reactions of the HVFA concrete is true. This shift in

emphasis is accompanied by increasing permeability of all HVFA concretes at the end of 504 days even if the concrete is under moist curing. Considerable permeance had occurred at the end of 504 days, presumably due to the pre-oven dry condition (at 105 °C for 24 hours) may caused some damage to the microstructure. However, the variation in porosity indicats that higher temperature (105 °C) has a deal effect on the arrangement of these growing hydration products. Furthermore, the maturity is a function of the composition and properties of the cementitious material, curing temperature, and of the age of the concrete. The maturity of the concrete at later ages of the testing also influences the results of the permeability test [9]. This result is in agreement with the effects of heat curing on cement hydration observed by Goto et al [94]. They stated that the porosities of samples cured at 60 °C were lower than those cured at 27 °C and were related to higher permeability also in the former.

The relative rates of development of permeability of HVFA concretes cured in water and air curing at various ages are shown by the Table 7-10.

**Table 7-10 Influence of air curing on permeability
(Unit : %)**

Days	28		90		540	
	Water curing	Air curing	Water curing	Air curing	Water curing	Air curing
350F	100	189	100	285	100	417
350SF	100	180	100	154	100	432
350S	100	186	100	126	100	279
450F	100	189	100	279	100	589
450SF	100	187	100	141	100	283
450S	100	185	100	157	100	225

It is clear from these data that the permeability of the HVFA concrete was directly related to the moisture at any give time. All results also indicate that concrete curing in water is superior to that air drying curing. This advantage has also been observed for both strength development rate and dynamic modulus of elasticity of concrete.

The results indicate that the use of air curing of all HVFA concretes exhibited a marked increase of permeability with continued air drying, even though the concrete had higher strength. In general, the coefficient of permeability of concrete incorporating both fly ash and silica fume as partial replacement for cement performed lower than that concrete with cement alone replaced partially by fly ash.

The percentage increase of permeability coefficient with air cured specimens is about 86 % of average values for all HVFA concretes when compared with the moist cured specimens at the age of 28 days. At the age of 90 days, even at the higher measured strength, considerably higher permeability coefficient was found. The percentage increase on the coefficient of permeability for dry cured specimens in HVFA concretes are higher, ranged from 125 % to 489 % for both types of cementitious material contents when compared with the moist cured concretes at the age of 18 months. However, the more dense and strong the concrete, the lower is the value of its increase. The resistance of porous media to fluid is largely a function of capillary wall friction caused by fluid movement and is therefore affected by pore diameter, interconnectivity of the pore system, and tortuosity of individual pores [118]. It has been shown from the pore size distribution in Table 7-8 that air curing significantly increases macro-pore diameter and hence by implication effective pore diameter of concrete. Furthermore, drying the specimen increases its permeability, probably because shrinkage may rupture some of the gel between the capillaries and thus open new passage to air. The results of this study agree to Dhir and Byars [118,119,120] in their fly ash concrete investigation that air curing significantly increases large diameter porosity and hence by implication effective pore diameter of concrete.

In concrete systems, the values of the coefficient of permeability decrease very substantially with a decrease in the water / cement ratio. Specially, at a water / cement ratio of 0.75, the coefficient of permeability is typically 10^{-10} (m^2) and this would be considered to represent concrete with a high permeability. At a water / cement ratio of 0.45, the coefficient of permeability is typically 10^{-11} or 10^{-12} (m^2), permeability of an order of magnitude lower than the last value, considered to represent concrete with a very low permeability [69]. In the present investigation, all HVFA concretes' coefficient of permeability values were low, ranging from 0.144×10^{-16} to 0.846×10^{-16} (m^2) for both types of curing conditions at the end of 504 days measuring.

7-3-2. Permeability and strength development of high volume fly ash concrete

In Figs 7-27 and 7-28, the coefficients of permeability, P_{er} , are plotted against the corresponding compressive strength, f_c , of the data at the ages of 28 days, 90 days, 180 days, and 18 months for moist and dry cured specimens of both types of cementitious material content HVFA concretes. Regression analysis of the data shown in these figures produced the following relationships :

Water curing condition specimens

$$f_c = 23.71 P_{er}^{-0.25} \quad (28 \text{ days}) \quad (r = -0.93) \text{ ----- (7 - 5)}$$

$$f_c = 1.43 P_{er}^{-1.78} \quad (90 \text{ days}) \quad (r = -0.83) \text{ ----- (7 - 6)}$$

$$f_c = 5.48 P_{er}^{-1.09} \quad (180 \text{ days}) \quad (r = -0.96) \text{ ----- (7 - 7)}$$

$$f_c = 71.14 P_{er}^{-0.07} \quad (18 \text{ months}) \quad (r = 0.21) \text{ ----- (7 - 8)}$$

Air curing condition specimens

$$f_c = 843.6 P_{er}^{-2.25} \quad (28 \text{ days}) \quad (r = -0.83) \text{ ----- (7 - 9)}$$

$$f_c = 7004.4 P_{er}^{-2.36} \quad (18 \text{ months}) \quad (r = 0.86) \text{ ----- (7 - 10)}$$

where f_c is the compressive strength in MPa, and P_{er} is the coefficient of permeability in 10^{-16} (m^2).

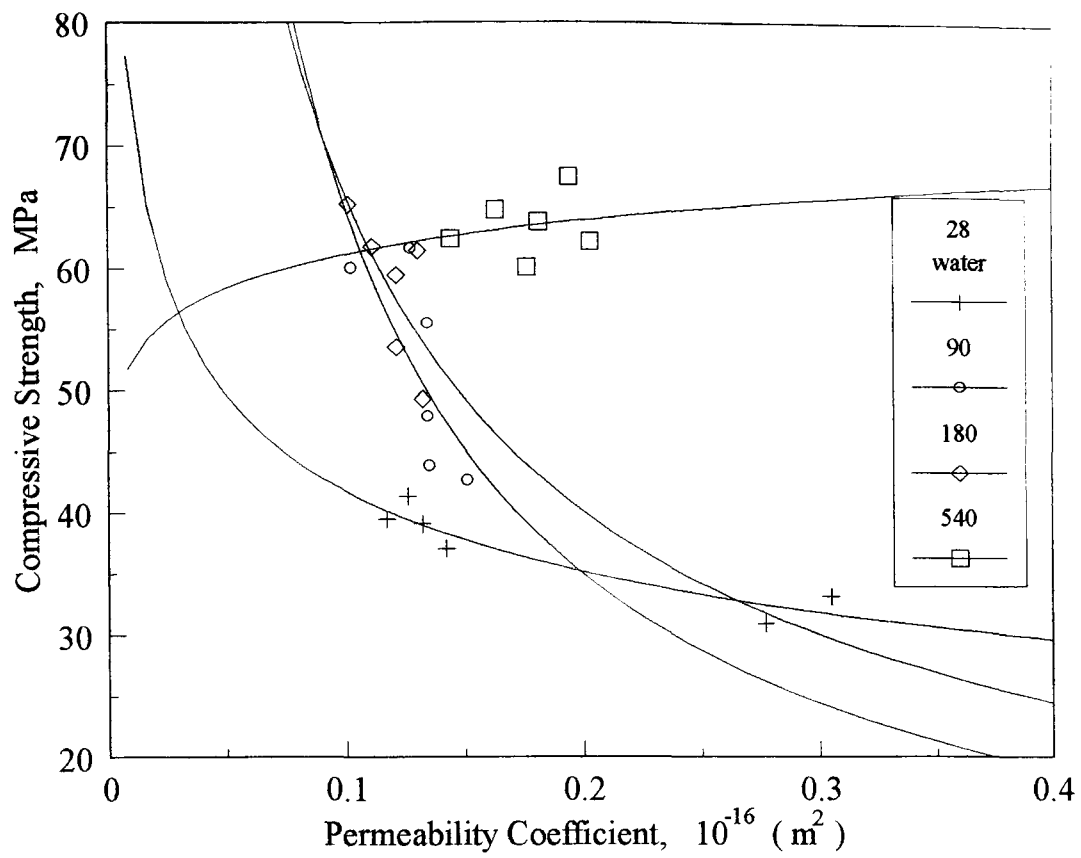


Figure 7-27 Relationship between permeability and compressive strength of HVFA concrete-water curing

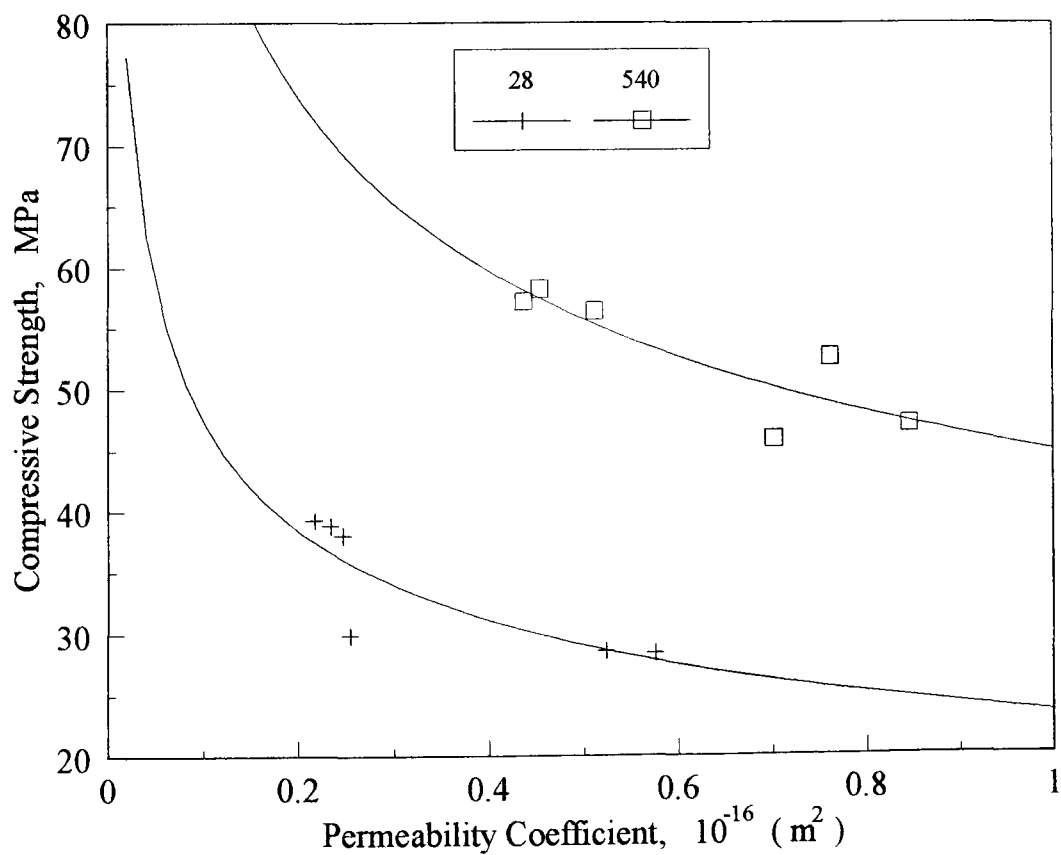


Figure 7-28 Relationship between permeability and compressive strength of HVFA concrete-air curing

It is obvious from the Fig 7-27, the higher degrees of hydration of HVFA concretes at the age of 540 days, the greater is the coefficient of permeability. In view of the positive correlation factor ($r = 0.21$) found in the equation relating to the concrete at 18 months with water curing, it is suggested that the correlation coefficient was very low. It is relieved that the compressive strength is still controlled by the porosity, the more the meso-pores of the concrete, the stronger is the compressive strength.

7-3-3. Permeability-porosity relation in high volume fly ash concrete

As already demonstrated, the strength development of concrete is not a simple function of its porosity, but depends also on the size and distribution of the pores. Thus, it follows that the permeability of hardened cement concrete is controlled by its capillary porosity.

The relationship between the coefficient of permeability, P_{er} , and meso-pore volume, M_{eso} , is generally by the following equation:

$$P_{er} = a M_{eso}^b \text{ ----- (7-11)}$$

where P_{er} is the coefficient of permeability of HVFA concrete in 10^{-16} m^2 , M_{eso} is the meso-pore volume of HVFA concrete in %, and a and b are constants.

The relationship between coefficient of permeability and the percentage of meso-pore for moist and dry cured specimens with both types of cementitious material content, at ages of 1 day to 18 months, is shown in Fig 7-29. Regression analysis of the data shown in the figure produced the following relationship :

$$P_{er} = 35.74 M_{eso}^{-1.23} \text{ (Moist + Dry) } (r = - 0.85) \text{ ---- (7-12)}$$

As shown in figure, there is a reasonable inverse correlation between the coefficient of permeability, P_{er} , and meso-pores, M_{eso} , of HVFA concrete which is curvilinear, in other words, the permeability coefficient of concrete decreases with an increase in the meso-pore volume. The relationship is observed to be influenced by

the air cured specimens. Although these correlation coefficients are somewhat low, there is a significant correlation at the 99 % confidence level between the coefficient of permeability and the meso-pores of HVFA concretes with both types of cementitious material contents under both curing conditions. Now, satisfactory explanation is apparent for this, however it is likely to be connected to the permeability of the hardened cement concrete when an adequate moist, and the degree of hydration, and hence lower coefficient of permeability was obtained.

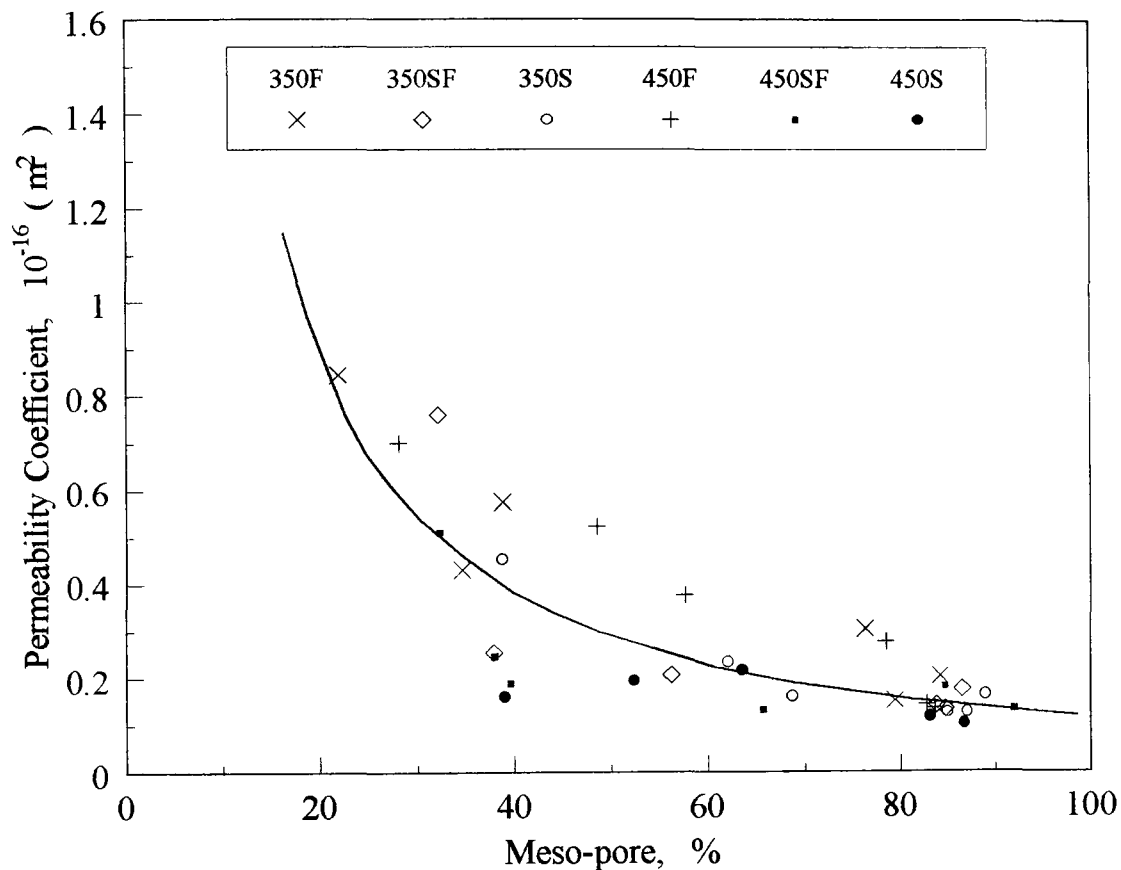


Figure 7-29 Relationship between permeability and meso-pores of HVFA concrete

7-4. WATER ABSORPTION OF HVFA CONCRETE

Absorption is an important concrete characteristic because it strongly influences the chemical stability, hardness, strength, and thermal properties of the concrete. Since the hardened cement concretes always contain more or less pores inside, practically all dry concretes are capable of absorbing water. The amount of the absorbed water depends primarily on the abundance and continuity of the pores in the concrete, whereas the rate of absorption depends on the size and continuity of these pores.

[121]. Other important factors, such as the curing history, water / cement ratio, aggregate characteristics, air content, cement type and fineness, and surface carbonation may also have an effect on absorption.

Absorption is usually measured by drying a specimen to a constant mass, immersing it in water, and measuring the increase in mass as a percentage of dry mass. In the present study, an absorption test on whole 75 mm × 100 mm core specimens as prescribed by BS 1881 : Part 122 : 1983, drying at 105 °C for 72 hours and immersion in water for 30 minutes, are determined. Each value represents the mean value for three specimens. All the specimens and performance procedure have been described in Chapter six. The test specimens were subjected to different curing and tested at the age of 28 days, 90 days, 180 days and 18 months.

In this section a detailed analysis of the water absorption on HVFA concretes will be discussed, and on its result will be described about the effect of different replacement method and curing regime on the characteristics of absorption. A relationship between the permeability of air and the percentage of water absorption for concrete was described.

7-4-1. Effect of curing condition and different replacement methods

Under water curing for various periods, the results of the water absorption of HVFA concretes with both types of cementitious material contents are shown in Table 7-11 and plotted in Figs 7-30 and 7-31. When compared at equal 28 day and 90 day strength for the wet-cured specimens the concretes made with 350SF, 450SF had greater water absorption, whereas for the Mix-350S and Mix-450S, with fly ash both as cement and sand replacement, had the lower water absorption. At the age of 180 days, the water absorption of all the HVFA concrete was reduced so that a lower value for both types of cementitious contents was measured. A more noticeable reduction for concrete 350SF and 450SF, relative to the corresponding 350F and 450F, was observed.

Table 7-11 High volume fly ash concrete water absorption (Unit : %)

Curing	Water curing				Air curing		
	28	90	180	540	28	180	540
350F	1.801	1.661	1.120	1.219	2.190	1.978	1.768
350SF	1.844	1.753	1.078	1.058	2.269	1.244	1.873
350S	1.020	0.963	0.807	0.977	1.317	1.240	1.809
450F	1.578	1.499	1.024	1.053	1.889	1.378	1.810
450SF	1.631	1.534	0.943	1.072	1.672	1.347	1.994
450S	1.015	0.961	0.784	1.082	1.293	1.149	1.809

For the long term wet curing, the water absorption of all HVFA concretes have appeared similar behaviour to that air permeability. The concretes exhibited slight increments in water absorption at the age of 18 months when compared to the age of six months with the same conditions. However, the higher potential strength and the consequent pozzolanic reaction of the concretes do exhibit good ability characteristics to resist water penetration.

In moist concretes, pores of different size are always occupied so that the absorption characteristics of HVFA concrete under water curing as well as drying condition varied depending on its pore volume and pore size distribution. From the preceding discussion on porosity, the meso-pore volumes of the concrete made of 350S are more than those of the concrete of 350SF and 350F. The result may reasonably suggest therefore that water does not easily move through the very small gel pores and that absorption is controlled by an interconnecting network of capillary pores [13]. Furthermore, as mentioned previous section, using fly ash to replace both cement and sand partially might have a combined effect of both separate replacements.

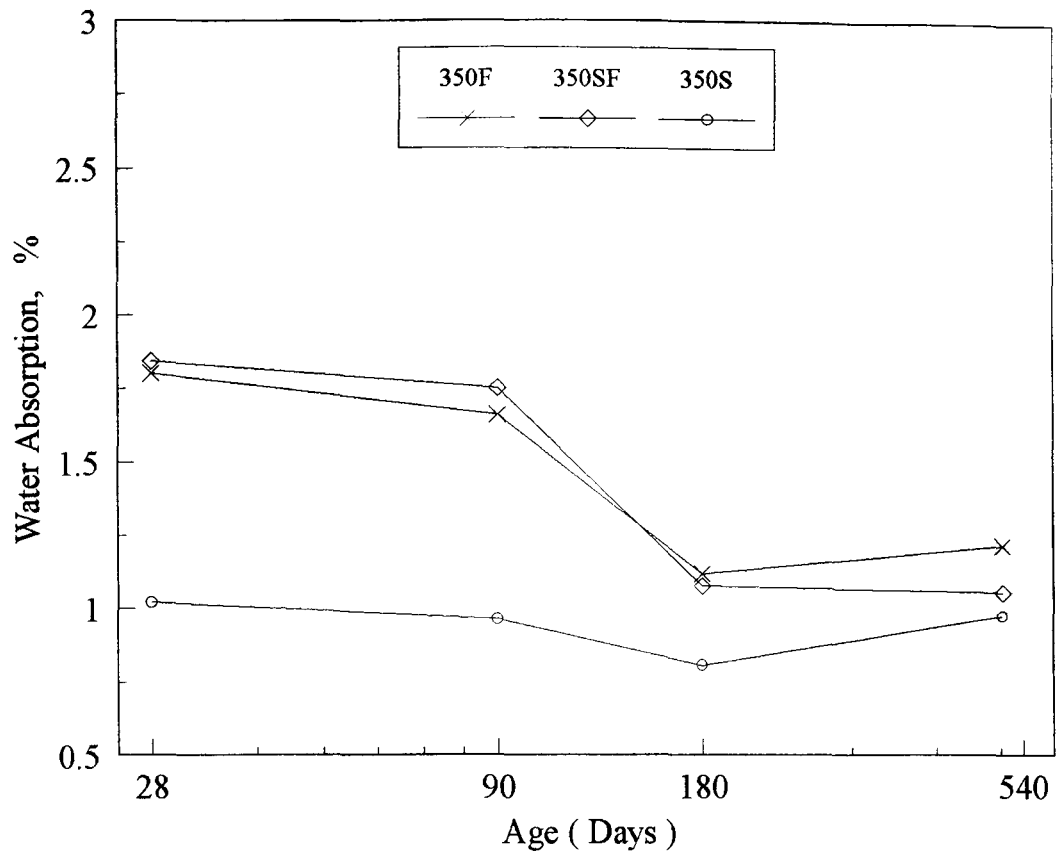


Figure 7-30 The water absorption of HVFA concrete-water curing (350 kg/m³ mixes)

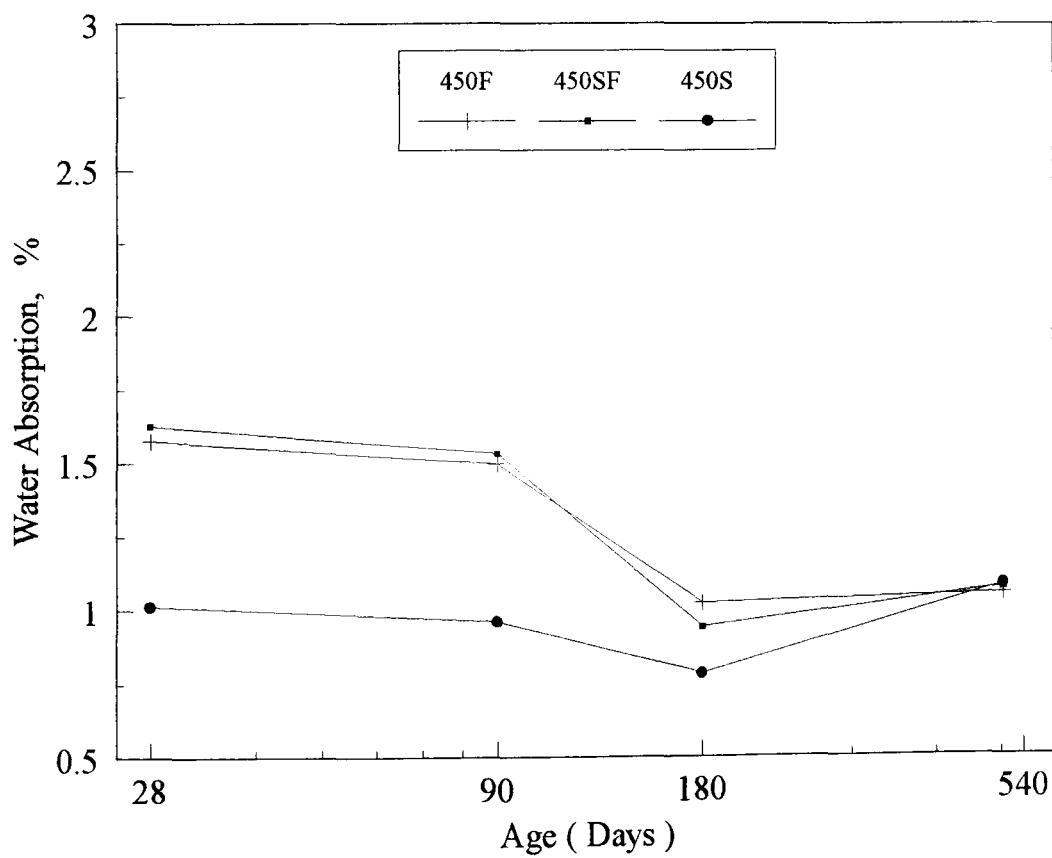


Figure 7-31 The water absorption of HVFA concrete-water curing (450 kg/m³ mixes)

Another important consequence of the concretes' 450 kg/m³ mixes, at the age of 18 months, was that the difference in water absorption was very small and consistent trends could be identified.

The relative rates of development of the water absorption of HVFA concretes cured in the water and air drying at various ages are shown in Table 7-12.

**Table 7-12 Influence of air curing on water absorption
(Unit : %)**

Days	28		180		540	
	Water curing	Air curing	Water curing	Air curing	Water curing	Air curing
350F	100	122	100	145	100	177
350SF	100	123	100	177	100	115
350S	100	129	100	185	100	154
450F	100	120	100	172	100	135
450SF	100	103	100	186	100	143
450S	100	127	100	167	100	147

The percentage increase of water absorption with air curing specimens is about 20 % of average values for all HVFA concretes when compared with the moist cured specimens at the age of 28 days. However, the percentage increased of water absorption increases with age of all mixtures in air curing specimens. The percentage increase of water absorption for all dry cured specimens ranged from 15 % to 77 % for both types of binder contents when compared with the moist cured specimens at the age of 18 months.

From the results, the curing regime had a much more significant effect on the water absorption than did the cementitious material, the concretes cured under dry conditions having a considerably greater water absorption [122]. These increases in the water absorption could be due to the change in microhardness and retrogression of the concretes due to air curing regime. For the most part, concrete after mixing

with water becomes a solid / fluid suspension and flowability gradually disappears as free water in concrete is gradually reduced. At the same time, the rigidity of the concrete becomes stronger and begins to develop its strength. The reduction of free water is caused by the formation of hydrates such as ettringite and C-S-H which need a large amount of water. The inner structure, due to the formation of hydrates, becomes a network which contributes to strength [13]. However, the pre-conditioning regime by air curing may cause a variety of change on internal parts of concrete. Changes in mechanical properties and porosity with time have been discussed previously for these system. The present investigation has suggested that this change in water absorption may be due to an accumulation of dense hydration products consisting of C-S-H, ettringite, $\text{Ca}(\text{OH})_2$, and hydrated aluminates at earlier periods around the unhydrated cementitious grains during air curing [123]. It is possible that the interaction of hydration products with fly ash or silica fume blends partially would cause increased loss of moisture and would be expected to lead to more extensive drying shrinkage cracking, which would be extended to form continuous channels around the unhydrated cementitious grains with time, thus allowing gel to imbibe more water. The increase of water absorption also helps to explain the lower strength, dynamic modulus of elasticity, and pulse velocity in the air cured concretes due to the combined effect of a higher permeability and water absorption.

7-4-2. Absorption-permeability relation of HVFA concrete

The relationship between absorption and the coefficient of permeability for both curing conditions and cementitious material contents, at the age of 504 days is shown in Fig 7-32. Regression analysis to establish the relationship between water absorption and the permeability coefficient from the data shown produced the following equation :

$$W_{\text{abs}} = 2.21 P_{\text{cr}}^{0.40} \quad (\text{moist + dry}) \quad (r = 0.94) \quad \text{-----} \quad (7-13)$$

Irrespective of the curing condition or type of cementitious content, the water absorption, W_{abs} , increases approximately with the cube root of its coefficient of permeability, P_{cr} . There is a reasonable curvilinear relationship between these two parameters, although somewhat scatters occur by air cured specimen. These data indicate a significant correlation at the 99 % confidence level between water absorption and air permeability of HVFA concretes at the later period.

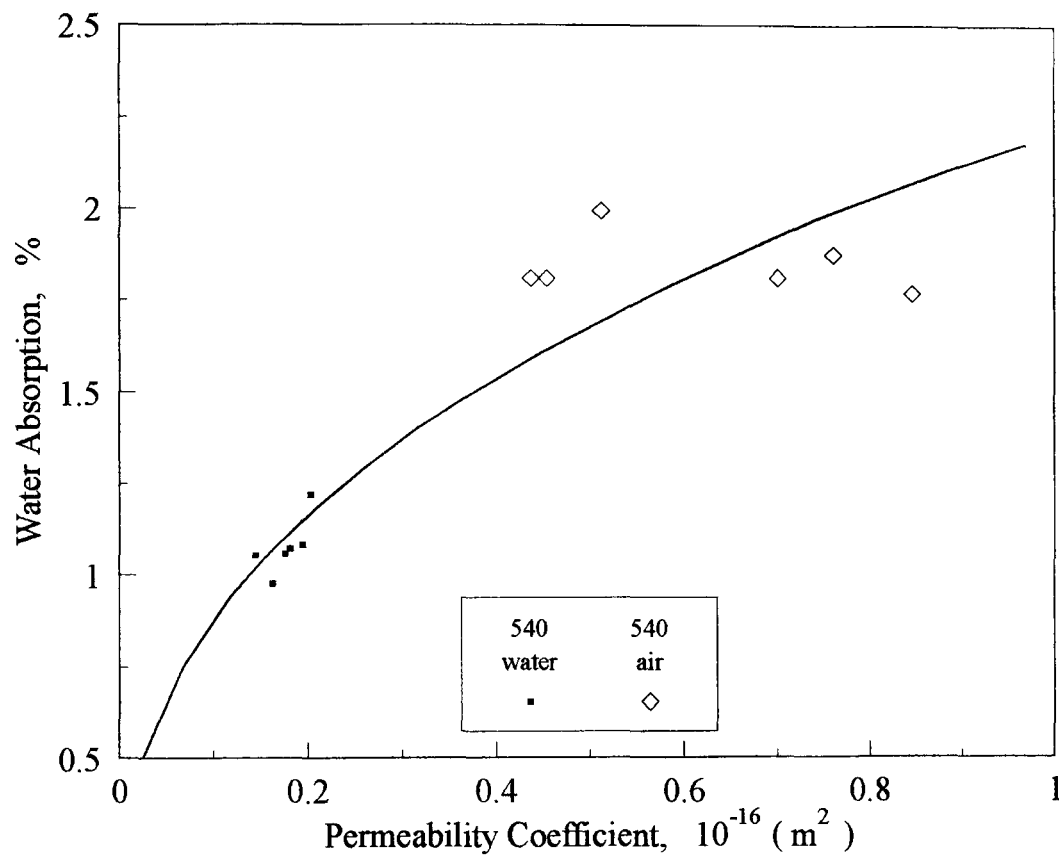


Figure 7-32 Relationship between permeability and water absorption of HVFA concrete

7-5. SOLID PHASE ANALYSIS : X-RAY POWDER DIFFRACTION

The crystal structure of different minerals always produces a characteristic diffraction pattern, whether that crystal is present in the pure state or as one constituent of a mixture of materials. This fact is the basis for the X-ray powder diffraction analysis.

The following section describes the X-ray diffraction to identify the crystalline phase and also to investigate the crystal structure of some of the phases. Routine qualitative scans of the various mixtures readily identified the predominant phases, calcium hydroxide, Ca(OH)_2 , and calcium silicate hydrate (C-S-H gel), together with evidence of unhydrated concrete minerals such as silicon dioxide (α -quartz), calcite (CaCO_3) and gypsum (C-S-H_2).

The test specimens were subjected to different curing conditions and analysed at the age of 28 days, 90 days, and 18 months. For comparison the hydrated powders of normal OPC and HVFA concretes are also included. These studies were done for the OPC and HVFA concretes made of 450 kg/m^3 mixes. All the samples were mixed and prepared as has been described in Chapter three and Chapter six

7-5-1. X-ray diffraction of normal OPC and HVFA concretes with water curing

The hydration products of normal OPC and HVFA concretes with and without silica fume under water curing with curing time are seen from the X-ray diffraction patterns in Figs 7-33, 7-34, 7-35 and Tables 7-13, 7-14, 7-15.

In the above figures all the X-ray diffractograms have been plotted with identical scales for both intensity (I) and 2θ , where θ is the Bragg's angle. Overall from the figures, a maximum intensity (100 %) peak corresponding to the α -quartz appears at 3.351 \AA for both OPC and HVFA concretes throughout the curing hydration period.

Unfortunately the C-S-H gel is poorly crystalline and amorphous to X-ray diffraction. Hence this technique is capable only of identifying the crystalline reaction products. Apart from the portlandite, Ca(OH)_2 , α -quartz (SiO_2), calcite (CaCO_3) and perhaps carboaluminate phase also appear in all samples independent of the different replacement methods. The α -quartz is believed to be from the aggregate used for compounding the concrete while, the calcite and carboaluminate phase might be as a result of the carbonation of portlandite during curing.

However, for all mixtures, the intensity of the X-ray reflections corresponding to the unhydrated compounds strongly decreased as a result of the hydration reaction under water curing regime.

Hydration products in the HVFA concretes were found to be different compared to that normal OPC concrete. As expected from the Fig 7-33, the concrete made of 450C with hydrated cement alone showed that the extent of hydration of calcium hydroxide (CH) (450C, *1, $d = 4.928 \text{ \AA}$, $I = 10$, *21, $d = 1.799 \text{ \AA}$, $I = 4$, *22, $d = 1.69 \text{ \AA}$, $I = 1$) exceeded those of concrete made of HVFA. Additionally, the amount of calcite phase in the OPC concrete is slightly higher than the concrete containing HVFA.

Up to three months curing further changes of the phase composition of the mixtures is detected by X-ray diffraction. It can be seen from Fig 7-34 that the diffraction peak of calcium hydroxide, Ca(OH)_2 , existing in the OPC concrete (450C, *1, $d = 4.928 \text{ \AA}$, $I = 8$) and in the HVFA samples (450F, *1, $d = 4.923 \text{ \AA}$, $I = 3$) (450SF, *1, $d = 4.928 \text{ \AA}$, $I = 1$) become low. The peaks of calcium hydroxide, Ca(OH)_2 , in Mix-450S completely disappear at 90 days. As shown by the above results with the addition of mineral admixture is able to hydrate further with time. When the hydration progresses the peaks of non-reactive phase decrease due to the activation of fly ash and silica fume with liberating calcium hydroxide, Ca(OH)_2 . Therefore, the calcium hydroxide is consumed at all ages of hydration [4].

The long term hydration reaction of X-ray diffraction pattern on HVFA concrete is shown in Fig 7-35. As expected, the hydration products of calcium

hydroxide, $\text{Ca}(\text{OH})_2$, completely disappears during 18 months for all HVFA concretes. Again, the presence of any pozzolanic material tends to consume any liberated calcium hydroxide as shown from the X-ray diffraction patterns.

**Table 7-13 X-ray diffraction of OPC and HVFA concrete-Water curing
(28 days of hydration)**

Hydrates products	450C	450F	450SF	450S
CH	peak1, $2\theta = 18.0$ $d = 4.928, I = 10$	peak1, $2\theta = 17.94$ $d = 4.944, I = 7$	peak1, $2\theta = 17.94$ $d = 4.944, I = 4$	peak1, $2\theta = 18.02$ $d = 4.923, I = 3$
	peak8, $2\theta = 28.66$ $d = 3.115, I = 2$	peak6, $2\theta = 28.6$ $d = 3.121, I = 1$		
	peak12, $2\theta = 34.06$ $d = 2.632, I = 10$	peak10, $2\theta = 34.02$ $d = 2.635, I = 4$	peak6, $2\theta = 34.0$ $d = 2.637, I = 3$	peak7, $2\theta = 34.1$ $d = 2.629, I = 3$
	peak19, $2\theta = 47.12$ $d = 1.929, I = 4$	peak17, $2\theta = 47.06$ $d = 1.931, I = 2$	peak13, $2\theta = 47.0$ $d = 1.933, I = 2$	peak13, $2\theta = 47.16$ $d = 1.927, I = 3$
	peak21, $2\theta = 50.74$ $d = 1.799, I = 4$	peak19, $2\theta = 50.76$ $d = 1.799, I = 2$	peak15, $2\theta = 50.6$ $d = 1.804, I = 2$	peak15, $2\theta = 50.64$ $d = 1.803, I = 2$
α -quartz	peak2, $2\theta = 20.82$ $d = 4.267, I = 16$	peak2, $2\theta = 20.78$ $d = 4.275, I = 23$	peak2, $2\theta = 20.74$ $d = 4.283, I = 27$	peak2, $2\theta = 20.82$ $d = 4.267, I = 31$
	peak5, $2\theta = 26.6$ $d = 3.351, I = 100$	peak4, $2\theta = 26.56$ $d = 3.356, I = 100$	peak4, $2\theta = 26.56$ $d = 3.356, I = 100$	peak3, $2\theta = 26.6$ $d = 3.351, I = 100$
	peak13, $2\theta = 36.52$ $d = 2.46, I = 10$	peak11, $2\theta = 36.44$ $d = 2.466, I = 17$	peak7, $2\theta = 36.48$ $d = 2.46, I = 6$	peak8, $2\theta = 36.52$ $d = 2.46, I = 16$
	peak14, $2\theta = 39.4$ $d = 2.287, I = 6$	peak12, $2\theta = 39.4$ $d = 2.287, I = 6$	peak8, $2\theta = 39.36$ $d = 2.289, I = 5$	peak9, $2\theta = 39.4$ $d = 2.287, I = 4$
	peak17, $2\theta = 42.42$ $d = 2.131, I = 5$	peak14, $2\theta = 42.38$ $d = 2.133, I = 8$	peak11, $2\theta = 42.38$ $d = 2.133, I = 5$	peak11, $2\theta = 42.42$ $d = 2.131, I = 13$
	peak18, $2\theta = 45.46$ $d = 1.995, I = 4$	peak16, $2\theta = 45.72$ $d = 1.984, I = 3$	peak16, $2\theta = 45.72$ $d = 1.984, I = 5$	peak12, $2\theta = 45.76$ $d = 1.983, I = 7$
	peak20, $2\theta = 50.08$ $d = 1.821, I = 10$	peak18, $2\theta = 50.04$ $d = 1.823, I = 14$	peak14, $2\theta = 50.08$ $d = 1.821, I = 18$	peak14, $2\theta = 50.1$ $d = 1.821, I = 25$
	peak23, $2\theta = 54.84$ $d = 1.674, I = 6$	peak20, $2\theta = 54.8$ $d = 1.675, I = 5$	peak16, $2\theta = 54.8$ $d = 1.675, I = 4$	peak16, $2\theta = 54.86$ $d = 1.673, I = 3$
	peak24, $2\theta = 59.9$ $d = 1.544, I = 8$	peak22, $2\theta = 59.88$ $d = 1.545, I = 8$	peak19, $2\theta = 59.88$ $d = 1.545, I = 8$	peak17, $2\theta = 59.92$ $d = 1.544, I = 8$
CaCO ₃	peak9, $2\theta = 29.32$ $d = 3.046, I = 3$	peak7, $2\theta = 29.32$ $d = 3.046, I = 2$		peak5, $2\theta = 29.42$ $d = 3.036, I = 2$

**Table 7-14 X-ray diffraction of OPC and HVFA concrete-Water curing
(90days of hydration)**

Hydrates products	450C	450F	450SF	450S
CH	peak1, $2\theta = 18.0$ $d = 4.928, I = 8$	peak1, $2\theta = 18.02$ $d = 4.923, I = 3$	peak1, $2\theta = 18.0$ $d = 4.928, I = 1$	---
	peak6, $2\theta = 28.62$ $d = 3.119, I = 1$	---	---	---
	peak8, $2\theta = 34.08$ $d = 2.631, I = 6$	peak5, $2\theta = 34.08$ $d = 2.631, I = 3$	peak6, $2\theta = 34.1$ $d = 2.629, I = 1$	---
	peak15, $2\theta = 47.08$ $d = 1.93, I = 2$	peak11, $2\theta = 47.12$ $d = 1.929, I = 1$	---	---
	peak17, $2\theta = 50.74$ $d = 1.799, I = 2$	peak17, $2\theta = 50.72$ $d = 1.8, I = 1$	peak13, $2\theta = 50.6$ $d = 1.804, I = 1$	---
α -quartz	peak2, $2\theta = 20.82$ $d = 4.267, I = 12$	peak2, $2\theta = 20.84$ $d = 4.262, I = 16$	peak2, $2\theta = 20.84$ $d = 4.262, I = 17$	peak1, $2\theta = 20.78$ $d = 4.275, I = 16$
	peak4, $2\theta = 26.6$ $d = 3.351, I = 100$	peak3, $2\theta = 26.62$ $d = 3.349, I = 100$	peak3, $2\theta = 26.64$ $d = 3.346, I = 100$	peak2, $2\theta = 26.58$ $d = 3.354, I = 100$
	peak9, $2\theta = 36.52$ $d = 2.46, I = 3$	peak6, $2\theta = 36.54$ $d = 2.459, I = 5$	peak7, $2\theta = 36.54$ $d = 2.459, I = 7$	peak4, $2\theta = 36.42$ $d = 2.467, I = 18$
	peak10, $2\theta = 39.44$ $d = 2.285, I = 3$	peak7, $2\theta = 39.44$ $d = 2.285, I = 3$	peak8, $2\theta = 39.44$ $d = 2.285, I = 5$	peak5, $2\theta = 39.4$ $d = 2.287, I = 4$
	peak13, $2\theta = 42.44$ $d = 2.13, I = 3$	peak9, $2\theta = 42.44$ $d = 2.13, I = 4$	peak10, $2\theta = 42.4$ $d = 2.132, I = 4$	peak7, $2\theta = 42.38$ $d = 2.133, I = 4$
	peak14, $2\theta = 45.76$ $d = 1.983, I = 2$	peak10, $2\theta = 45.74$ $d = 1.984, I = 3$	peak11, $2\theta = 45.78$ $d = 1.982, I = 3$	peak8, $2\theta = 45.72$ $d = 1.984, I = 2$
	peak16, $2\theta = 50.12$ $d = 1.82, I = 9$	peak12, $2\theta = 50.12$ $d = 1.82, I = 11$	peak12, $2\theta = 50.1$ $d = 1.821, I = 9$	peak9, $2\theta = 50.06$ $d = 1.822, I = 6$
	peak19, $2\theta = 59.92$ $d = 1.544, I = 6$	peak15, $2\theta = 59.92$ $d = 1.544, I = 8$	peak17, $2\theta = 59.96$ $d = 1.543, I = 15$	peak12, $2\theta = 59.88$ $d = 1.545, I = 4$

**Table 7-15 X-ray diffraction on HVFA concrete-Water curing
(18 months of hydration)**

Hydrates products	450F	450SF	450S
CH	---	---	---
α -quartz	peak2, $2\theta = 20.78$ $d = 4.275, I = 22$ peak3, $2\theta = 26.6$ $d = 3.351, I = 100$ peak8, $2\theta = 36.52$ $d = 2.46, I = 9$ peak9, $2\theta = 39.42$ $d = 2.286, I = 10$ peak11, $2\theta = 42.42$ $d = 2.131, I = 5$ peak12, $2\theta = 45.72$ $d = 1.984, I = 4$ peak13, $2\theta = 50.1$ $d = 1.821, I = 23$ peak17, $2\theta = 59.92$ $d = 1.544, I = 6$	peak1, $2\theta = 20.78$ $d = 4.275, I = 24$ peak3, $2\theta = 26.58$ $d = 3.354, I = 100$ peak8, $2\theta = 36.5$ $d = 2.462, I = 7$ peak10, $2\theta = 39.38$ $d = 2.288, I = 4$ peak13, $2\theta = 42.42$ $d = 2.131, I = 4$ peak14, $2\theta = 45.74$ $d = 1.984, I = 4$ peak15, $2\theta = 50.04$ $d = 1.823, I = 8$ peak18, $2\theta = 59.88$ $d = 1.545, I = 7$	peak1, $2\theta = 20.76$ $d = 4.279, I = 23$ peak2, $2\theta = 26.54$ $d = 3.359, I = 100$ peak10, $2\theta = 36.42$ $d = 2.467, I = 5$ peak11, $2\theta = 39.38$ $d = 2.288, I = 9$ peak15, $2\theta = 42.32$ $d = 2.136, I = 5$ peak16, $2\theta = 45.72$ $d = 1.984, I = 4$ peak18, $2\theta = 50.2$ $d = 1.823, I = 18$ peak20, $2\theta = 59.82$ $d = 1.546, I = 5$

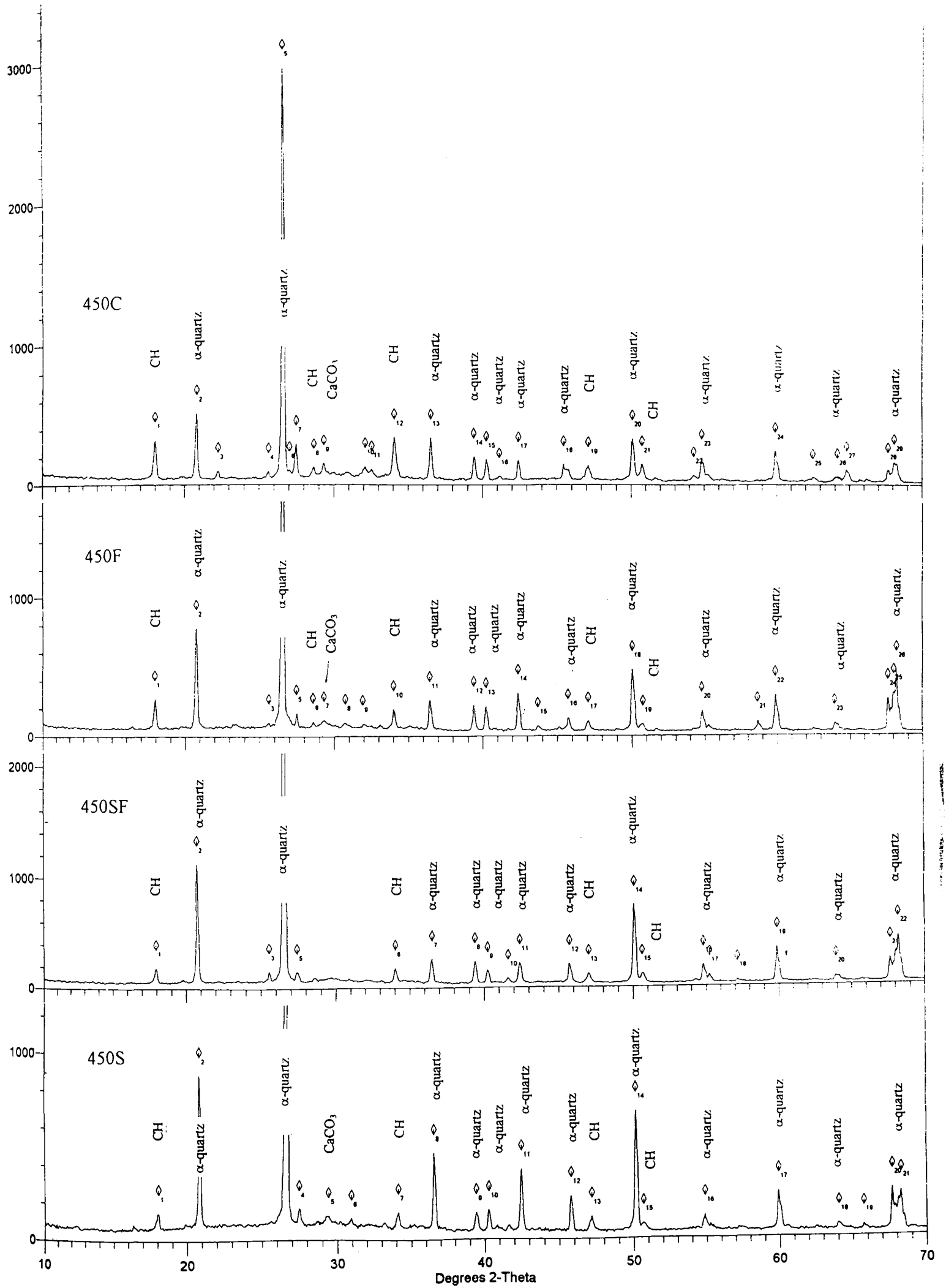


Figure 7-33 X-ray diffractograms for OPC and HVFA concrete-Water curing (28 days hydration)

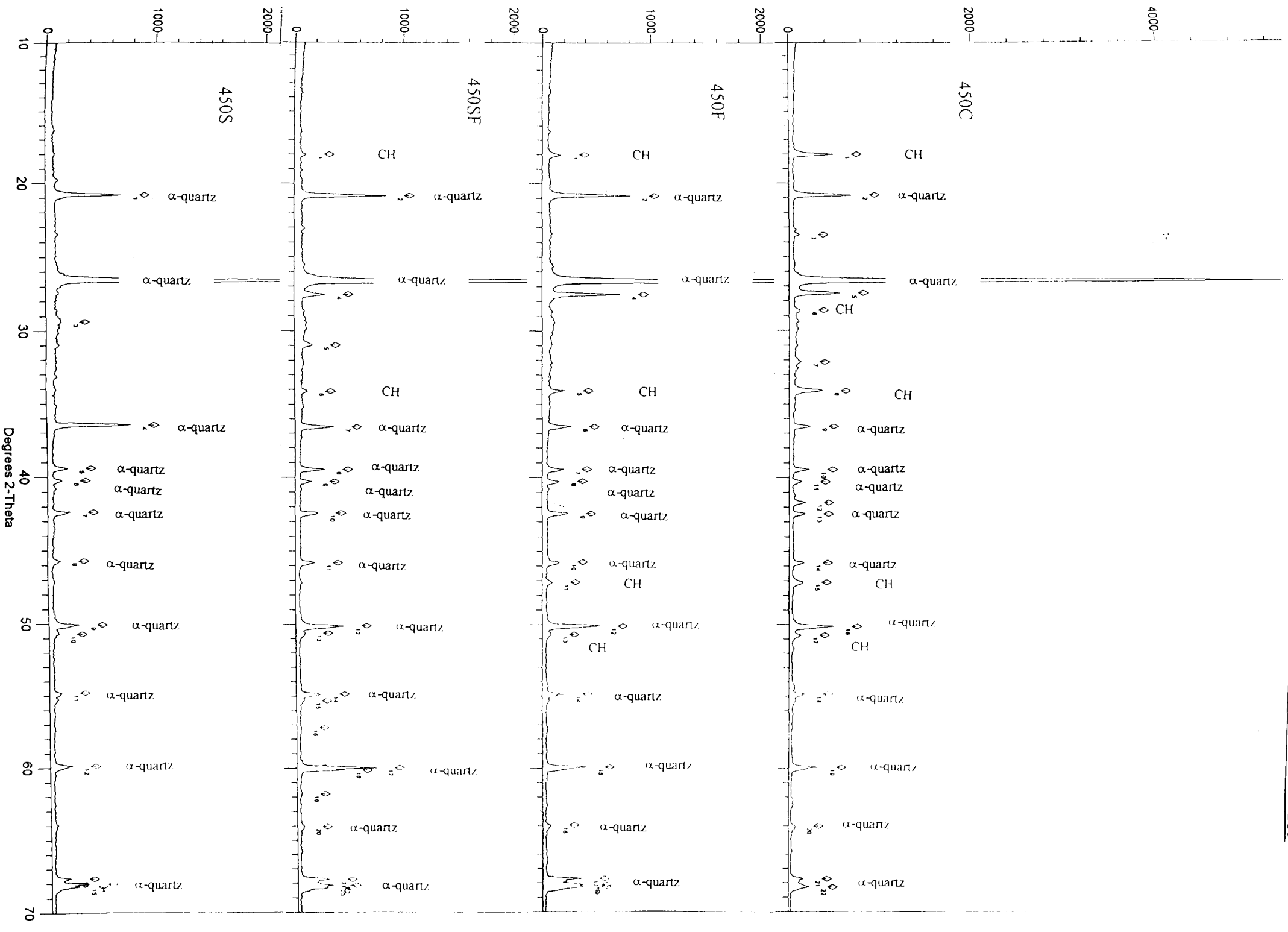


Figure 7-34 X-ray diffractograms for OPC and HVFA concrete-Water curing (90 days hydration)

7-5-2. Influence of air cured on X-ray diffraction

Under air curing, HVFA concretes with 450 kg/m³ mixes the X-ray diffraction patterns tested at the end of 18 months are shown in the Fig 7-36 and Table 7-16. The results show the remarkable influence of the air dried curing on hydration products which are responsible for mechanical change.

In all concrete mixtures, the intensity of the X-ray reflections corresponding to the unhydrated compounds strongly increased as a result of the hydration reaction. At the end of 18 months, in all of HVFA concretes, although both silica fume and fly ash are present, appreciable amounts of hydration products are formed and consequently the strength is lower than wet curing concretes. Meanwhile, a maximum intensity (100 %) peak corresponding to the α -quartz phase appears at $d = 4.271 \text{ \AA}$ for Mix-450S.

Much of the carboaluminate phase and high intensity peak were recorded by X-ray diffraction analysis on all HVFA concretes. CaCO_3 hydrates noticeably as is evidenced by the persistent presence of the peak at $42.36 2\theta$, $42.38 2\theta$, and $42.4 2\theta$ in Mix-450F, Mix-450SF, and Mix-450S respectively.

From the comparative analysis of Fig 7-36 marked differences can be seen in the degree of alteration caused by the carbonation. Although the combination of silica fume and fly ash formed the silicic acid gels, carbonation results in the formation of CaCO_3 through the intermediate formation of carboaluminate hydrates and by direct reaction between calcium hydroxide, Ca(OH)_2 , and CO_2 [103].

**Table 7-16 X-ray diffraction on HVFA concrete-Air curing
(18 months of hydration)**

Hydrates products	450F	450SF	450S
CH	peak1, $2\theta = 17.96$ $d = 4.939$, I = 6 peak6, $2\theta = 34$ $d = 2.637$, I = 5 peak12, $2\theta = 46.98$ $d = 1.934$, I = 2 peak14, $2\theta = 50.7$ $d = 1.801$, I = 2	peak1, $2\theta = 17.98$ $d = 4.934$, I = 4 peak6, $2\theta = 34.02$ $d = 2.635$, I = 6 peak12, $2\theta = 47.08$ $d = 1.93$, I = 2 peak14, $2\theta = 50.68$ $d = 1.801$, I = 2	peak3, $2\theta = 18.02$ $d = 4.923$, I = 3 peak9, $2\theta = 34.1$ $d = 2.629$, I = 4 peak17, $2\theta = 47.1$ $d = 1.929$, I = 2 ---
α -quartz	peak2, $2\theta = 20.78$ $d = 4.275$, I = 20 peak3, $2\theta = 26.56$ $d = 3.356$, I = 100 peak7, $2\theta = 36.46$ $d = 2.464$, I = 4 peak8, $2\theta = 39.4$ $d = 2.287$, I = 7 peak10, $2\theta = 42.36$ $d = 2.134$, I = 6 peak11, $2\theta = 45.68$ $d = 1.986$, I = 4 peak13, $2\theta = 50.06$ $d = 1.822$, I = 10 peak17, $2\theta = 59.84$ $d = 1.546$, I = 5	peak2, $2\theta = 20.8$ $d = 4.271$, I = 19 peak4, $2\theta = 26.56$ $d = 3.356$, I = 100 peak7, $2\theta = 36.52$ $d = 2.46$, I = 4 peak8, $2\theta = 39.4$ $d = 2.287$, I = 6 peak10, $2\theta = 42.38$ $d = 2.133$, I = 5 peak11, $2\theta = 45.78$ $d = 1.982$, I = 3 peak13, $2\theta = 50.06$ $d = 1.822$, I = 10 peak17, $2\theta = 59.9$ $d = 1.544$, I = 5	peak4, $2\theta = 20.8$ $d = 4.271$, I = 100 peak6, $2\theta = 26.56$ $d = 3.356$, I = 99 peak10, $2\theta = 36.44$ $d = 2.466$, I = 8 peak11, $2\theta = 39.4$ $d = 2.287$, I = 11 peak13, $2\theta = 42.4$ $d = 2.132$, I = 43 peak16, $2\theta = 45.74$ $d = 1.984$, I = 6 peak19, $2\theta = 50.08$ $d = 1.821$, I = 19 peak22, $2\theta = 59.88$ $d = 1.545$, I = 8
CaCO_3	peak4, $2\theta = 29.4$ $d = 3.038$, I = 5 peak10, $2\theta = 42.36$ $d = 2.134$, I = 6	peak5, $2\theta = 29.38$ $d = 3.04$, I = 5 peak10, $2\theta = 42.38$ $d = 2.133$, I = 5	peak7, $2\theta = 29.32$ $d = 3.046$, I = 8 peak13, $2\theta = 42.4$ $d = 2.132$, I = 43

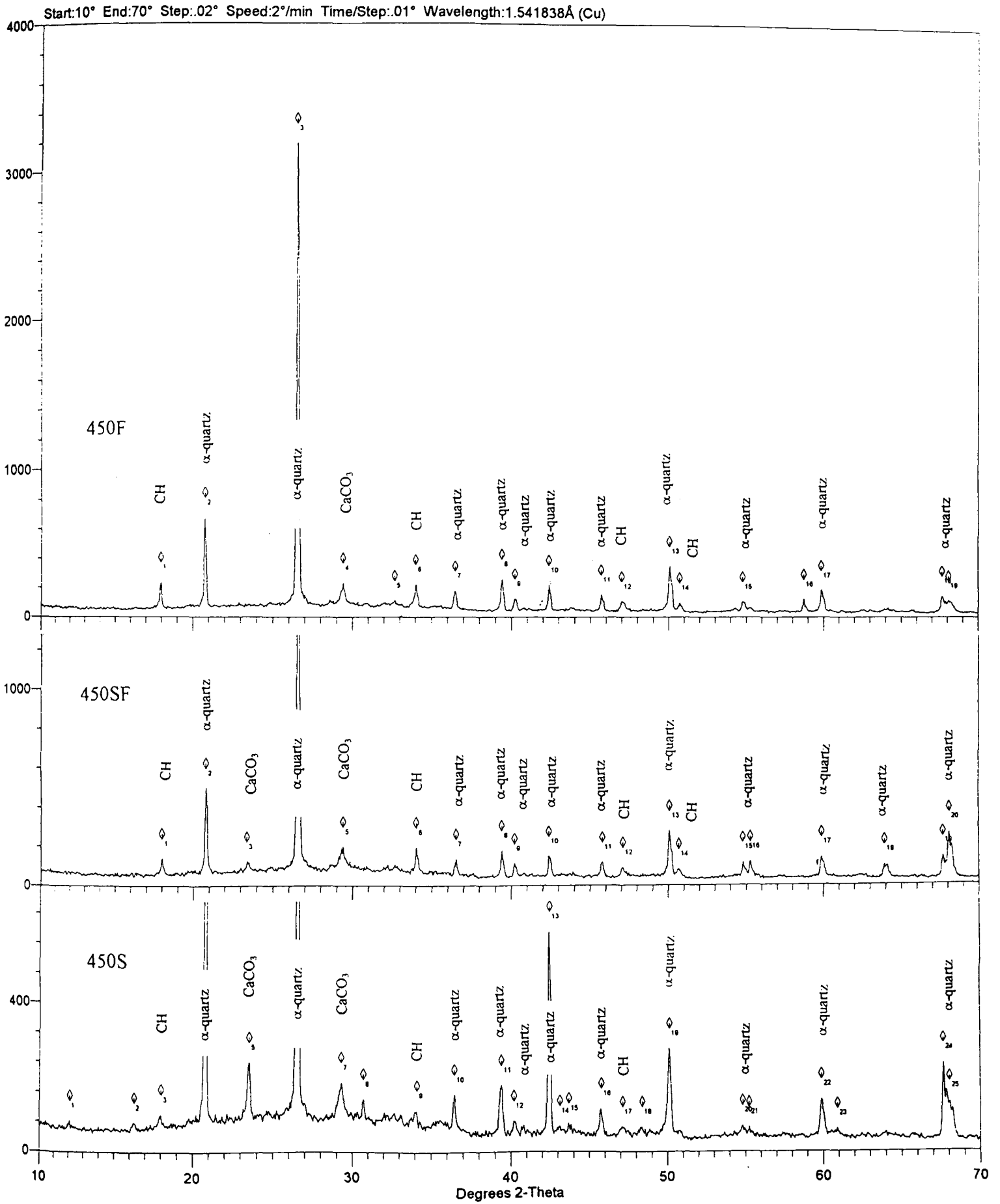


Figure 7-36 X-ray diffractograms for HVFA concrete-Air curing (18 months hydration)

7-6. CONCLUSION

From the results of the microstructure analyses on HVFA concretes, the following conclusions on the pore size distribution and hydrated products on OPC and HVFA concrete, and the mechanisms controlling the permeability and water absorption are presented.

1. The curing regime has shown a big influence on the microstructure development of HVFA concrete.
2. There exists an approximate indirect relationship between strength and pore size of hardened concretes.
3. Reduction in the volume of large pores was observed with the progress of the pozzolanic reaction. Higher concrete strengths were generally associated with lower volume of large pores in the concrete.
4. The addition of silica fume to the mix decreased the accessible pore volumes for HVFA concrete in comparison with the concrete without silica fume.
5. According to the air permeability and water absorption test, water-cured specimens are superior to the air-cured specimen. The coefficient of permeability of concrete incorporating high volume fly ash is very low. In any case, concretes made with 450 kg/m^3 cementitious material content gave impermeabilities, and hence water absorption, which are much lower than those obtained from concretes with 350 kg/m^3 cementitious content.
6. The higher potential strength of mature concrete are very sensitive to curing temperature (pre-oven dry, at 105°C , 24 hours) and degree of hydration.
7. The higher permeability and water absorption of air-cured HVFA concretes are explained by a poor dispersion of the precipitated hydration products during the hydration process.

8. The pronounced influence of the type of hydration products on the pore structure and on the strength of hardened concrete is caused by differences in the crystal structure.
9. A considerable amount of the non-reactive phase of α -quartz is due to the aggregate used in making the concrete.
10. Decrease in the levels of calcium hydroxide phase were seen with advancing water curing age in all the HVFA concretes, providing evidence for pozzolanic reactivity of the fly ash. Furthermore, the calcium hydroxide phase is completely consumed in HVFA at the age of 18 months.
11. Retrogression of HVFA concrete under air curing is associated with the formation of CaCO_3 from Ca(OH)_2 .

CHAPTER EIGHT

CONCLUSIONS AND RECOMMENDATIONS FOR FUTURE RESEARCH

8-1. OVERALL CONCLUSIONS

The conclusions drawn from this investigation are summarized at the end of each part, but the overall major conclusions derived from this study are given below.

1. The use of superplasticizer is compatible with HVFA concrete. Portland cement concrete mixes had a higher demand of HRWR than the HVFA concrete. The greater the binder content, the higher was the HRWR dosage required to maintain a constant consistency.
2. With HVFA concrete, increasing the total binder content brings little benefit in terms of strength development, pulse velocity, and pore size distribution. The concrete with the lower binder content had, however, a marginally higher pulse velocity. Using a low binder content is not only economical *per se*, but also leads to overcoming the undesirable effects of drying shrinkage.
3. Adequate curing is essential if HVFA concrete is to achieve its full potential. Further, the differences between specimens cured under wet conditions, and those exposed to prolonged drying are in general far more significant than differences between HVFA concretes made with different total binder content. The curing regime has a significant influence on the engineering properties and microstructure. With prolonged air drying up to 504 days, HVFA concretes exhibited a minimum loss of dynamic modulus and pulse velocity.
4. Although the early strength of concrete made with high volume fly ash was low, all HVFA concretes developed compressive strength at 28 days in the range 30 to

40 MPa, and 40 to 65 MPa at 90 days. The use of fly ash to replace both cement and sand simultaneously resulted in considerably higher strength values due to the decreased w/b ratio, and reduced loss of early strength. The presence of silica fume changes the strength of HVFA concrete due to the combined effect of accelerating hydration reactions with microstructural changes.

5. Based on strength development, the preference of using HVFA concrete is (1), the use of fly ash to replace both cement and sand simultaneously ; (2), made with both fly ash and silica fume ; (3), made by fly ash alone as cement replacement. Although low lime fly ash has a low reactivity, a proper design strategy can achieve economic and early strength requirements. The figure below shows such a strategy to produce HVFA concrete in order to conserve resources.

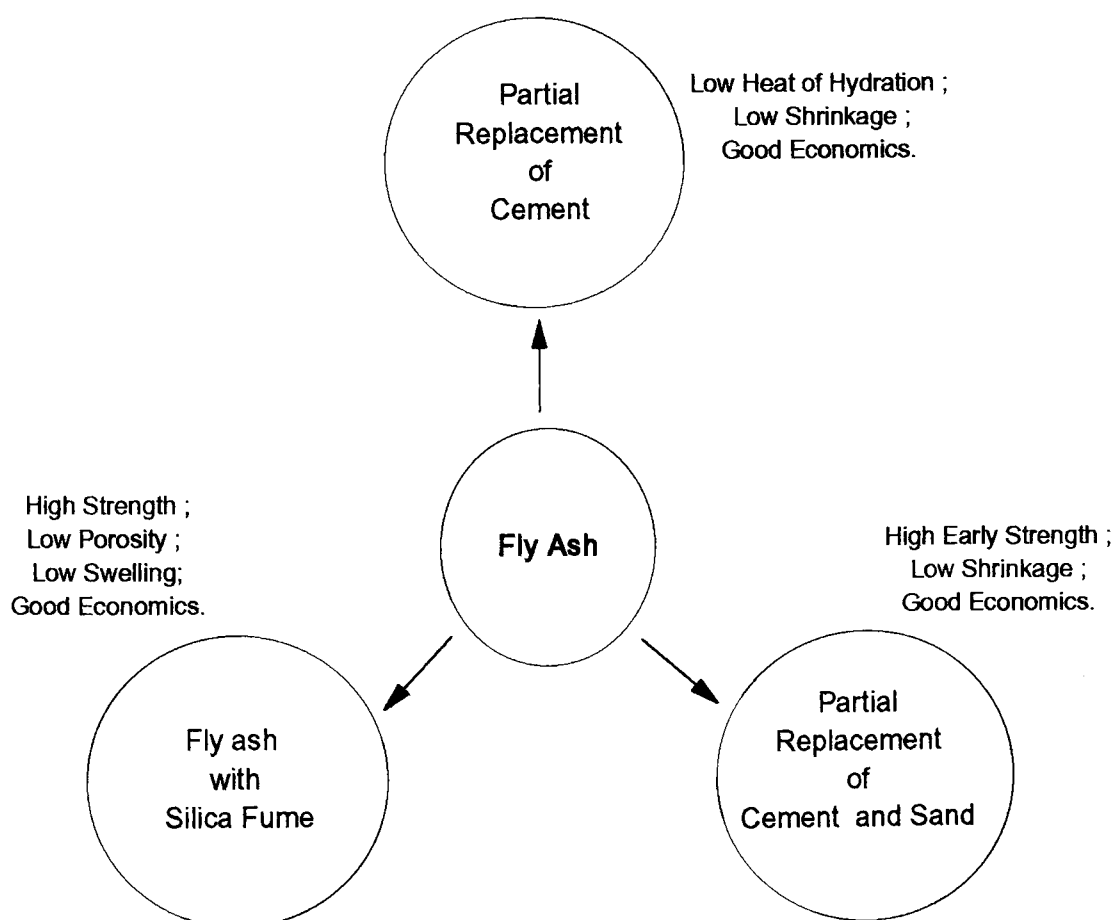


Figure 8-1 Strategies of using fly ash in HVFA concrete construction

6. The ettringite formed in the early stages of hydration accelerated swelling. This suggests that swelling begins at a lower critical degree of hydration. A considerably lower swelling was observed in the HVFA concrete containing silica fume, and this resulted in a concomitant decrease in the total accessible pore volume and porosity.
7. Low swelling of HVFA concrete results in higher drying shrinkage. The latter ranged from 550×10^{-6} to 640×10^{-6} m/m for all HVFA concretes at 504 days.
8. The dynamic modulus results were generally high, with values of the order of 55 GPa at 90 days for HVFA concrete with silica fume. Due to high pozzolanic activity, the percentage increment in dynamic modulus from 28 days to one year of HVFA concrete is about 3 ~ 4 times that of the normal OPC concrete. At the end of 18 months, the results are higher than the ACI Building Code 318-89 calculated values by about 50 % for the 450 kg/m^3 mixes.
9. The pulse velocity of HVFA concrete reached stable values by about six months. Both dynamic modulus and pulse velocity give good indication of the extent of deterioration of concrete affected by prolonged air drying. The average percentage loss of dynamic modulus or pulse velocity for all HVFA concretes was very low, about 3 %, when compared to the same concretes air cured for 28 days.
10. Concretes stored in air showed higher carbonation depths than those stored in water. Accompanying carbonation, HVFA concrete showed decomposition of hydration products, and as a result, concrete becomes porous.
11. The results from the air permeability and water absorption tests are, to some extent, related to the results from the pore size distribution test. Both these tests thus seem suitable for predicting changes in the pore size of concrete systems. The HVFA concrete with wet curing showed low water absorption and permeability coefficient. The latter ranged from 0.117×10^{-16} to $0.305 \times 10^{-16} \text{ m}^2$ for HVFA concrete cured for 28 days, and from 0.102×10^{-16} to $0.151 \times 10^{-16} \text{ m}^2$ for HVFA concrete cured for 90 days.

12. The results show that porosity is a major factor in controlling the engineering behaviour of HVFA concrete. There exists an approximative indirect relationship between strength and pore size of hardened concretes.
13. X-ray diffraction studies made it possible to gain a better understanding of the microstructural changes induced by these procedures. The formation of predominant ettringite / gypsum leads to swelling / drying shrinkage. It was shown that an increase in curing leads to a change in the microstructure of C-S-H hydrates. Decrease in the levels of calcium hydroxide (CH) was seen with advancing curing age in all the HVFA concretes, providing evidence for pozzolanic reactivity of the fly ashes.

8-2. RECOMMENDATIONS FOR FUTURE WORK

During this study several interesting points have come up, which could not be investigated because of the limitations of time. For further work in this direction, the author makes the following suggestions.

1. An examination of potential accelerators to increase early-age strength development is required.
2. Further investigation of other fly ashes in HVFA concrete is necessary to determine the optimum parameters in terms of mix proportions, admixture type and dosage.
3. To extend the use of HVFA in commercial applications the influence on their properties of extreme curing conditions such as high or low temperature and low moisture availability should be investigated.
4. Studies of long-term creep under different curing conditions will be very useful.
5. The use of fly ash to replace both cement and sand has improved early strength. It is necessary to investigate the effect of different exposure regimes such as,

sodium chloride solution and sulphate solution, and evaluate the long-term durability characteristics of HVFA concrete.

References

1. Bland, C. H. and Sharp, J. H., "A Conduction Calorimetric Study of Gasifier Slag-Portland Cement Blends", *Cement Concrete Research*, 1991, 21, pp 359-367.
2. Bland, C. H., Sharp, J. H. and Barker, A. P., "Electron Probe Microanalysis of Gasifier Slag Cement Pastes", *Advances in Cement Research*, 1991 / 92, 4, No. 16, Oct., pp. 159-166.
3. Bland, C. H., Sharp, J. H. and Osborne, G. J., "Small-scale Durability Study of Gasifier Slag-Portland Cement Blends", *Advances in Cement Research*, 1994, 6, No. 21, Jan., pp. 37-43.
4. Bland, C. H. and Sharp, J. H., "The Chemistry of Portland Cement-Gasifier Slag Interactions", *Advances in Cement Research*, 1990, 3, No. 11, July., pp. 91-98.
5. Papadakis, V. G., Fardis, M. N. and Vayenas, C. G., "Hydration and Carbonation of Pozzolanic Cements", *ACI Materials Journal* Vol. 89, No. 2 March-April 1992, pp. 119-130.
6. Swamy, R. N., "Fly Ash Concrete Potential without Misuse", *Materials and Structures*, No. 23, 1990, pp. 397-411.
7. Malhotra, V. M., "Superplasticizer Fly Ash Concrete for Structural Applications", *ACI Concrete International*, Vol. 8, No. 12, December 1986, pp. 28-31.
8. *Proceedings American Concrete Institute, Index, Vols. 26-45, 1929-1949, Synopsis*, pp. 34.
9. Berry, E. E., Malhotra, V. M. and Carette, G. G., "Investigation of High Volume Fly Ash Concrete Systems", Prepared by Radian Canada Inc. Mississauga, Ontario, Canada and Canada Centre for Mineral and Energy Technology (CANMET), Ottawa, Ontario, Canada, Final Report, October 1993.

10. Swamy, R. N., "Fly Ash Utilisation in Concrete Construction", Second International Conference on Ash Technology and Marketing, Barbican Centre, London, September 16th-21st 1984, pp. 359-367.
11. Kokubu, M., "Fly Ash and Fly Ash Cement", Proceeding of the Fifth International Symposium of the Chemistry of Cement, Tokyo, 1968, The Cement Association of Japan Part IV, pp. 75-102.
12. Mehta, P. K., "Pozzolanic and Cementitious By-products as Mineral Admixture for Concrete - A Critical Review", First International Conference on The Use of Fly Ash, Silica Fume, Slag and Other Mineral By- Products in Concrete, July 31-August 5 1983, pp. 1- 46.
13. Mindess, S. and Young, J. F., "Concrete", Prentice-Hall, Inc. Englewood Cliffs, New Jersey, 1981.
14. Malhotra, V. M., "High-Performance Structural Concrete Incorporating Large Percentages of Fly Ash", Invited Paper for Presentation at the Fifth International Colloquium on Concrete in Developing Countries, and for publication in the proceedings, January 3-6, 1994, Cairo, Egypt.
15. Jähren, P., "Use of Silica Fume in Concrete", First International Conference on The Use of Fly Ash, Silica Fume, Slag and Other Mineral By - Products in Concrete, July 31 - August 5 1983, pp. 625-642.
16. Lamond, J. F., "Twenty Five Years Experience Using Fly Ash in Concrete", First International Conference on The Use of Fly Ash, Silica Fume, Slag and Other Mineral By - Products in Concrete, Canada, July 31 - August 5 1983, pp. 47-69.
17. Guillaume, L., "Pozzolanic Activity of Fly Ash in Portland Cement and Slag Cement", Silicate Inds., Vol. 28, No. 6, 1963, pp. 297-300.
18. Bache, H. H., Idorn, G. M., Nepper-Christensen, P. and Nielson, J., "Morphology of Calcium Hydroxide in Cement Paste", Symposium on Structure of Portland Cement Paste and Concrete, 1966, pp. 154-174.

19. Kokubu, M. and Yamada, J., "Fly Ash Cements", The VI International Congress on The Chemistry of Cement, Moscow, September 1974, pp. 1-47.
20. Clifton, J. R., Brown, P. W. and Geoffery Frohusdorff, "Reactivity of Fly Ashes with Cement", Cement Research Progress, 1977, pp. 321-341.
21. Swamy, R. N., Sami, A. R. Ali. and Theodorakopoulos, D.D., "Early Strength Fly Ash Concrete for Structural Applications", ACI Journal, September - October 1983, pp. 414-4213.
22. Tikalsky, P. J., Carrasquillo, P. M. and Carrasquillo, R. L., "Strength and Durability Considerations Affecting Mix Proportioning of Concrete Containing Fly Ash", ACI Materials Journal, November - December 1988, pp. 501-511.
23. Olek, J. and Diamond, S., "Proportioning of Constant Paste Composition Fly Ash Concrete Mixes", ACI Materials Journal, March - April 1989, pp. 159-166.
24. Berry, E. E. and Malhotra, V. M., "Fly Ash for Use in Concrete - A Critical Review", ACI Journal, March - April 1980, pp. 59-73.
25. Hopkins, C. J. and Cabrera, J. G., "The Influence of Pulverised Fuel Ash on the Workability of Concrete", Second International Conference on Ash Technology and Marketing, Barbican Centre, London, September 16th - 24th 1984, pp. 393-397.
26. Sturup, V. R., Hooton, R. R. and Clendenning, T. G., "Durability of Fly Ash Concrete", First International Conference on The Use of Fly Ash, Silica Fume, Slag and Other Mineral By - Products in Concrete, July 31 - August 5 1983, pp. 71-86.
27. Langley, W. S., Carette, G. G. and Malhotra, V. M., "Strength Development and Temperature Rise in Large Concrete Blocks Containing High Volumes of Low - Calcium (ASTM Class F) Fly Ash", ACI Materials Journal, July - August 1992, pp. 362-368.

28. Stodola, P. R., "Performance of Fly Ash in Hardened Concrete", *Concrete International*, December 1983, pp. 64-65.
29. Cripwell, J. B., Brooks, J. J. and Wainwright, P. J., "Time Dependent Properties of Concrete Containing Pulverised Fuel Ash and a Superplasticizer", *Second International Conference on Ash Technology and Marketing*, Barbican Centre, London, September 16th - 21st 1984, pp. 313-320.
30. Thomas Michael, D. A and Matthews, J. D., "Performance of Fly Ash Concrete in UK Structures", *ACI Material Journal*, Vol. 90, No. 6, Nov. - Dec. 1993, pp. 586-593.
31. Mohammed Maslehuddin, Abdulaziz I. Al-Mana, Mohammed Shamim, and Huseyin Saricimen, "Effect of Sand Replacement on the Early-Age Strength Gain and long-term Corrosion - Resisting Characteristics of Fly Ash Concrete", *ACI Materials Journal*, January - February 1989, pp. 58-62.
32. Bamforth, P. B., "In Situ Measurement of the Effect of Partial Portland Cement Replacement Using Either Fly Ash or Ground Granulated Blast Furnace Slag on the Performance of Mass Concrete", *Proc. Instn. Civil Engineers*, Vol. 69,, Part 2, Sept. 1980, pp. 777-800.
33. Ross, A. D., "Some Problems in Concrete Construction", *Magazine Concrete Research*, Vol. 12, No. 38, 1960, pp. 27-34.
34. Alexander, K. M., Wardlaw, J. and Ivanusec, I., "A 4 : 1 Range in Concrete Creep when Cement SO₃ Content, Curing Temperature and Fly ash Content are varied", *Cement Concrete Research*, Vol. 16, No. 2, Mar. - Apr. 1986, pp. 173-180.
35. Tikalsky, P. J. and Carrasquillo, R. L., "Influence of Fly Ash on the Sulphate Resistance of Concrete", *ACI Materials Journal*, Vol. 89, No. 1, Jan. - Feb. 1992, pp. 69-75.

36. Rezansoff, T. and Stott, D., "Durability of Concrete Containing Chloride Based Accelerating Admixtures", *Canadian Journal of Civil Engineering*, Vol. 17, 1990 pp. 102-111.
37. Manmohan, D. and Mehta, P. K., "Influence of Pozzolanic, Slag, and Chemical Admixtures on Pore Size Distribution and Permeability of Hardened Cement Paste", *Cement, Concrete, and Aggregates*, Vol. 3, No. 1, 1981, pp. 63-67.
38. Mehta, P. K., "Effect of Fly Ash Composition on Sulphate Resistance of Cement", *ACI Journal, Proceedings* Vol. 83, No. 6, November - December 1986, pp. 994-1000.
39. Tikalsky, P. J. and Carrasquillo, R. L., "Fly Ash Evaluation and Selection for use in Sulphate Resistance Concrete", *ACI Materials Journal*, Vol. 90, No. 6, Nov. - Dec. 1993, pp. 545-551.
40. C Plowman, CEGB Harrogate, "The Chemistry of PFA in Concrete - A Review of Current Knowledge", *Second International Conference on Ash Technology and Marketing*, Barbican Centre, London, Sept. 16th - 21st 1984, pp. 437-443.
41. Swamy, R. N. and Al-Asali, M. M., "Engineering Properties of Concrete Affected by Alkali Silica Reaction", *ACI Materials Journal*, September - October 1988, pp. 367-375.
42. Swamy, R. N. and Al-Asali, M. M., "Expansion of Concrete Due to Alkali-Silica Reaction", *ACI Materials Journal*, January - February 1988, pp. 33-40.
43. Georges, C., Alain B., Chevrier, R. L. and Malhotra, V. M., "Mechanical Properties of Concrete Incorporating High Volumes of Fly Ash from Sources in the US", *ACI Material Journal*, Vol. 90, No. 6, Nov. - Dec. 1993, pp. 535-544.
44. Bilodeau, A. and Malhotra, V. M., "High-Performance Concrete Incorporating Large Volumes of ASTM Class F Fly Ash", Published in the Second Edition of "Advances in Concrete Technology", issued in 1994 by CANMT, Ottawa, Canada, pp. 508-523.

45. Alasali M. M. and Malhotra V, M., "Role of Concrete Incorporating High Volumes of Fly Ash in Controlling Expansion due to Alkali-Aggregate Reaction", *ACI Materials Journal*, Vol. 88 No. 2 March - April 1991, pp. 159-163.
46. Buttler, F. G., Decter, M. H. and Smith, G. R., "Studies on the Desiccation and Carbonation of Systems Containing Portland Cement and Fly Ash", First International Conference on The Use of Fly Ash, Silica Fume, Slag and Other Mineral By-Products in Concrete, Canada July 31 - August 5 1983, pp. 367-380.
47. Browne, R. D., "Ash Concrete - Its Engineering Performance", Second International Conference on Ash Technology and Marketing, Barbican Centre, London, September 16th - 21st 1984, pp. 295-301.
48. Haque, M. N. and Kawamura, M., "Carbonation and Chloride - Induced Corrosion of Reinforcement in Fly Ash Concrete", *ACI Materials Journal*, Vol. 89, No. 1, Jan. - Feb. 1992, pp. 41-48.
49. Swamy, R. N. and Tanikawa, S., "Control of Steel Corrosion in Chloride Contaminated Concrete Through Aron Wall Surface Coating", *Durability of Concrete*, Second International Conference, Montreal, ACI SP-126, Canada, 1991, pp. 371-392.
50. Dhir, R. K., Jones, M. R. and Seneviratne, A. M. G., "Diffusion of Chloride into Concrete, Influence of PFA Quality", *Cement and Concrete Research*, Vol. 21, No. 6, November 1991, pp. 1092-1102.
51. Haque, M. N., Kayyali, O. A. and Gopalan, M. K., "Fly Ash Reduces Harmful Chloride Ions in Concrete", *ACI Materials Journal*, Vol. 89, No. 3, May - June 1992, pp. 238-241.
52. Mehta, P. K. and GjØrv, O. E., "Properties of Portland Cement Concrete Containing Fly Ash and Condensed Silica Fume", *Cement and Concrete Research*, Vol. 12, 1982, pp. 587-595.

53. Grutzeck, M. W., Scott, A. and Roy, D. M., "Mechanism of Hydration of Condensed Silica Fume in Calcium Hydroxide Solutions", First International Conference on The Use of Fly Ash, Silica Fume, Slag and Other Mineral By - Products in Concrete, Canada, July 31 - August 5 1983, pp. 643-652.
54. Xiaofeng, C., Shanglong, G., David, D. and Steven, L. M., "Role of Silica Fume in Compressive Strength of Cement Paste, Mortar, and Concrete", ACI Materials Journal, Vol. 89, No. 4, July - August 1992, pp. 375-387.
55. GjØrv, O. E., "Durability of Concrete Containing Condensed Silica Fume", First International Conference on The Use of Fly Ash, Silica Fume, Slag and Other Mineral By- Products in Concrete, Canada, July 31-August 5 1983, pp. 695-709.
56. Sellevold, E. J. and Radjy, F. F., "Condensed Silica Fume in Concrete ; Water Demand and Strength Development", First International Conference on The Use of Fly Ash, Silica Fume, Slag and Other Mineral By - Products in Concrete, Canada, July 31 - August 5 1983, pp. 677-694.
57. Collins, T. M., "Proportioning High-Strength Concrete to Control Creep and Shrinkage", ACI Materials Journal, Vol. 86, No. 6, November - December 1989, pp. 576-577.
58. Swamy, R. N., "Design for Durability and Strength Through the Use of Fly Ash and Slag in Concrete", unpublised, March 1997.
59. Swamy, R. N. and Mahmud, H. B., "Mix Proportions and Strength characteristics of Concrete Containing 50% Low-Calcium Fly ash", Proc. 2nd International Conference Fly Ash, Slag, Silica Fume and Natural Pozzolnas in Concrete, 1986, pp. 413-432.
60. Langley, W. S., Carrette, G. G. and Malhotra V. M., "Structural Concrete Incorporating High Volumes of ASTM Class F Fly Ash", ACI Material Journals, Vol. 86. No. 5 September - October 1989, pp. 507-514.

61. Giaccio, G. M. and Malhotra, V. M., "Concrete Incorporating High Volumes of ASTM Class f Fly Ash", *Cement, Concrete and Aggregates, CCAGDP*, Vol. 10, No. 2 Winter, 1988, pp. 88-95.
62. Aimin, Xu. and Sarkar, S. L., "Microstructural Development in High Volume Fly Ash Cement System", *Journal of Material in Civil Engineering*, Vol. 6, N0. 1, February 1994, pp. 117-137.
63. Sivasundaram, Carette, G. G. and Malhotra, V. M., "Mechanical Properties, Creep, and Resistance to Diffusion of Chloride Ions of Concretes Incorporating High Volumes of ASTM Class F Fly Ash From Seven Different Sources", *ACI Materials Journal*, Vol. 88, No. 4, July - August 1991, pp. 407-416.
64. "Measurement of Hardened Concrete Carbonation Depth", *RILEM Draft Recommendation CPC-18, Materials and Structures, Research and Testing*, RILEM, Paris. Vol. 17. No. 102, 1984, pp. 437-440.
65. Garette and Malhotra, V. M., "Early-Age Strength Development of Concrete Incorporating Fly Ash and Condensed Silica Fume", *First International Conference on The Use of Fly Ash, Silica Fume, Slag and Other Mineral By - Products in Concrete, Canada, July 31 - August 5 1983*, pp. 765-784.
66. Goldman, A. and Bentur, A., "Bond Effects in High Strength Silica Fume Concretes", *ACI Material Journal*, V. 86, No. 5, Sept. - Oct. 1989, pp. 440-447.
67. Cohen, M. D., "Theories of Expansion in Sulfoaluminate-Type Expansive Cement ; Schools of Thoughts", *Cement and Concrete Research*, Vol. 13, No. 6, Nov. 1983, pp. 809-818.
68. Kesler, C. E., "Control of Shrinkage, Creep and Temperature Volume Changes Through Variations of Material Properties", *State of Art Report, Technical Committee No. 25 : Creep, Shrinkage, and Temperature Effects, ASCE-IABSE Joint Committee on Planning and Design of Tall Building, 15 January 1972*, pp. 1-11.

69. Neville, A. M., "Properties of Concrete", Fourth Edition, 1995.
70. Bentur, A., "The Pore Structure of Hydrated Cementitious Compounds of Different Chemical Composition", *Journal of The American Ceramic Society*, Vol. 63, July - August 1980, pp. 381-386.
71. Bentur, A., "Effect of Curing Temperature on the Pore Structure of Tricalcium Silicate Pastes", *Journal of Colloid and Interface Science*, Vol. 74, No. 2, April 1980, pp. 549-560.
72. Haque, M. N., Langan, B. W. and Ward, M. A., "High Fly Ash Concretes", *ACI Journal* January - February 1984, pp. 54-59.
73. Detwiler, R. J. and Mehta, P. K., "Chemical and Physical Effect of Silica Fume on the Mechanical Behaviour of Concrete", *ACI Material Journal*, Vol. 86, No. 6, November - December 1989, pp. 609-614.
74. Baalbaki, W., Aïtcin, P. C. and Ballivy, G., "On Predicting Modulus of Elasticity in High Strength Concrete", *ACI Material Journal*, Vol. 89, No. 5, Sept.- Oct. 1992, pp. 517-520.
75. Kameswara Rao, Swamy, R. N. and Mangat, P. S., "Mechanical Behaviour of Concrete as a Composite Material", *Matériaux Et Constructions*, Vol. 7, No. 40 pp. 265-271.
76. Hobbs, D. W., "The Dependence of the Bulk Modulus, Young's Modulus, Creep, Shrinkage and Thermal Expansion of Concrete upon Aggregate Volume Concentration", *Matériaux Et Constructions*, Vol. 4, No. 20, 1971, pp. 107-114.
77. Lobo, C. and Cohen, M. D., "Effect of Silica Fume on Expansion Characteristics of Expansive Cement Pastes", *ACI Material Journal*, Vol. 89, No. 5, Sept.- Oct. 1992, pp. 481-490.

78. Popovics, S., Rose, J. L. and Popovics, J. S., "The Behaviour of Ultrasonic Pulses in Concrete", *Cement and Concrete Research*, Vol. 20, 1990, pp. 259-270.
79. Litvan, G. G. and Meyer, A., "Carbonation of Granulated Blast Furnace Slag Cement Concrete During Twenty Years of Field Exposure", *Fly Ash, Silica Fume, Slag, and Natural Pozzolans in Concrete*, SP-91, American Concrete Institute, Detroit, 1986, pp. 1445-1462.
80. Kokubu, M. and Nagataki, S., "Carbonation of Concrete with Fly Ash and Corrosion of Reinforcement in 20 Years Tests", *Fly Ash, Silica Fume, Slag and Natural Pozzolans in Concrete-Proceeding of the Third International Conference*, SP-114, Vol. 1, American Concrete Institute, Detroit, 1989, pp. 315-329.
81. Ewerstson, C. and Prtersson, P. E., "The Influence of Curing Conditions on The Permeability and Durability of Concrete Results from a Field Exposure Test", *Cement and Concrete Research*, Vol. 23, 1993, pp. 683-692.
82. Malami, C., Batis, G., Nouloumbi, H. and Kaloidas, V., "Influence of Pozzolanic and Hydraulic Cement Additions on Carbonation and Corrosion of Reinforced Mortar Specimens", *Proceeding of International Conference held at the University of Sheffield, 24-28 July 1994*, Edited by R. N. Swamy, Vol. 2 pp. 668-682.
83. Nagataki, S., Ohga, H. and Kim, E. M., "Effect of Curing Condition on the Carbonation of Concrete with Fly Ash and the Corrosion of Reinforcement in long-term Tests", *Fly Ash, Silica Fume, Slag and Natural Pozzolans in Concrete*, SP-91, American Concrete Institute, Detroit, 1986, pp. 1445-1462.
84. Afridi, M. U. K., Chaudhary, Z. U., Ohama, Y., Demura, K. and Iqbal, M. Z., "Carbonation Resistance of Powdered and Aqueous Polymer-Modified Mortars and Effects of Carbonation on Their Pore Structures", *Proceedings of*

- International Conference held at the University of Sheffield, 24-28 July 1994, Edited by R. N. Swamy, Vol. 2 pp. 974-987.
85. Dalgleish, B. J., Pratt, P. L. and Moss, R. I., "Preparation Techniques and the microscopical Examination of the Portland Cement Paste and C_3S ", *Cement and Concrete Research*, Vol. 10, No. 5, 1980, pp. 665-676.
86. Dent Glasser, L. S., Lachowski, E. E., Mohan, K. and Taylor, H. F. W., "A Multi-Method Study of C_3S hydration", *Cement and Concrete Research*, Vol. 8, No. 6, 1978, pp. 733-740.
87. Berger, R. L. and McGregor, T. D., "Influence of Admixture on the Morphology of Calcium Hydroxide Formed During Tricalcium Silicate Hydration", *Cement and Concrete Research*, Vol. 2, No. 1, 1972, pp. 43-56.
88. Bentur, A., Berger, R. L., Lawrence, F. V., Milestone, N. B., Mindess, S. and Young, J. F., "Creep and Drying Shrinkage of Calcium Silicate Pastes III. A Hypothesis of Irreversible Strains", *Cement and Concrete Research*, Vol. 9, No. 1, 1979, pp. 83-96.
89. Roy, D. M., Gouda, G. R. and Bobrowsky, A., "Very High Strength Cement Pastes Prepared by Hot - Pressing and Other High - pressure Techniques", *Cement Concrete Research*, Vol. 2 No. 3, 1972, pp. 349-366.
90. Rössler, M. and Odler, I., "Investigation on the Relationship between Porosity Structure and Strength of Hydrated Portland Cement Pastes I. Effect of Porosity", *Cement Concrete Research*, Vol. 15 No. 2, 1985, pp 320-330.
91. Watson, K. L., "A Simple Relationship between the Compressive Strength and Porosity of Hydrated Portland Cement", *Cement Concrete Research*, Vol. 11, 1981, pp. 473-476.
92. Feldman, R. F. and Beaudoin, J. J., "Microstructure and Strength of Hydrated Cement", *Cement and Concrete Research*, Vol. 16, 1976, pp. 389-400.

93. Sersale, R., Cioffi, R., Frigione, G. and Zenone, F., "Relationship between Gypsum Content, Porosity, and Strength of Cement", *Cement and Concrete Research*, Vol. 21, No. 1, 1991, pp. 120-126.
94. Goto, S. and Roy, D. M., "The Effect of W / C Ratio and Curing Temperature on the Permeability of Hardened Cement Paste", *Cement and Concrete Research*, Vol. 11, 1981, pp. 575-579.
95. Kung, J. H., "Drying Shrinkage and Microstructure of Hydrated Calcium Silicate", Ph.D. Thesis, University of Illinois, 1978.
96. Young, J. F., "Drying Shrinkage of Plain Concrete", unpublished, 1981.
97. Darmawan, L., Richard, L. B. and Young, J. F., "Simple Method for Measuring Water Permeability of Concrete", *ACI Materials Journal*, Vol. 86, No. 5, September - October 1989, pp. 433-439.
98. Lea, F. M., "The Chemistry of Cement and Concrete", 1956, Second Edition.
99. Kantro, D. L., Weise, C. H. and Brunauer, S., "Symposium on Structure of Portland Cement Paste and Concrete", Highway Research Board Special Report 1966.
100. Diamon, M., Abo-el-enein, S. A., Hosaka, G., Goto, S. and Kondo, R., "Pore Structure of Calcium Silicate Hydrate in Hydrated Tricalcium Silicate", *Journal of The American Ceramic Society*, Vol. 60, Mar. - Apr. 1977, pp. 110-114.
101. Winslow, D. N. and Diamond, S., "Specific Surface Of Hardened Portland Cement Pastes as Determined by Small-Angle X-ray scattering", *Journal of The American Ceramic Society*, Vol. 57, No. 5 May 1974, pp. 193-197.
102. Jennings, H. M. and Pratt, P. L., "On the Hydration of Portland Cement", *Proceeding of British Ceramic Society*, 1979, pp. 179-193.

103. Hansen, T. C., Radjy, F. and Sellevold, E. J., "Cement Paste and Concrete", Building Materials Laboratory, The Technical University of Denmark, 1973, pp. 233-268.
104. Lachowski, E. E., Mohan, K., Taylor, H. F. W. and Moore, A. E., "Analytical Electron Microscopy of Cement Pastes. II. Pastes of Portland Cement and Clinkers", Journal of the American ceramic Society, vol. 63, 1980, pp. 447-452.
105. Lachowski, E. E., "Trimethylsilylation as a Tool for the Study of Cement Pastes", Cement and Concrete Research, Vol. 9, No. 3, 1979, pp. 337-342.
106. Parrott, L. J. and Taylor, M. G., "A Development of the Molybdate Complexing Method For the Analysis of Silicate Mixtures", Cement and Concrete Research, Vol. 9, No. 4, 1979, pp. 483-488.
107. Bentur, A. and Young, J. F., "Simplified method of Determining the Polysilicate Content in Cementitious Pastes Using Trimethylsilyl Derivatives", Cement and Concrete Research, Vol. 11, No. 2, 1981, pp. 287-290.
108. Chatterji, S., "Drying Shrinkage of Cement Paste and Concrete : A Reappraisal of the Measurement Technique and its Significance", Cement and Concrete Research, Vol. 6, No. 1, 1976, pp. 145-148.
109. Cook, R. A. and Hover, K. C., "Mercury Porosimetry of Cement-Based Materials and Associated Correction Factors", ACI Materials Journal, Vol. 90, No. 2, 1993, pp. 152-161.
110. Shi, D. and Winslow, D. N., "Contact angle and Damage During Mercury Intrusion into Cement Paste", Cement and Concrete Research, Vol. 15, 1985, pp. 645-654.
111. Winslow, D. N. and Diamond, S., "A Mercury Porosimetry Study of the Evolution of Porosity in Portland Cement", Journal of Materials, Vol. 5, No. 3, September 1970, pp. 564-585.

112. Cabrera, J. G. and Lynsdale, C. J., "A new Gas Permeameter for Measuring the Permeability of Mortar and Concrete", *Magazine of Concrete Research*, Vol. 40, No. 144, September 1988, pp. 177-182.
113. British Standards Institution, "Method for Determination of Water Absorption", BS 1881 : Part 122 : 1983.
114. Cullity, B. D., "Elements of X - ray Diffraction", Second Edition, 1978.
115. Marsh, B. K., Day, R. L. and Bonner, D. G., "Pore Structure Characteristics Affecting the Permeability of Cement Paste Containing Fly Ash", *Cement and Concrete Research*, Vol. 15, 1985, pp. 1027-1038.
116. Roy, D. M. and Gouda, G. R., "Porosity-Strength Relation Cementitious Materials with Very High Strengths", *Journal of The American Ceramic Society - Discussion and Notes* Vol. 56, No. 10, May 1973, pp. 449-550.
117. Jose Anagel Lechuga Albala and Sebastla Alegre Rossello, "Concrete Impermeability Study", *Second International Conference on Ash Technology and Marketing*, Barbican Centre, London, September 1984, pp. 387-389.
118. Dhir, R. K. and Byars, E. A., "Pulverised Fuel Ash Concrete: Intrinsic Permeability", *ACI Material Journal*, Vol. 90, No. 6, Nov. - Dec. 1993, pp. 571-580.
119. Dhir, R. K. and Byars, E. A., "Pulverised Fuel Ash Concrete: Near Surface Absorption Properties", *Magazine of Concrete Research*, Vol. 43, No. 157, Dec. 1991, pp. 219-231.
120. Dhir, R. K. and Byars, E. A., "Pulverised Fuel Ash Concrete: Permeation Properties of Cover to Steel Reinforcement", *Cement and Concrete Research*, Vol. 23, No. 3, 1993, pp. 554-556.
121. Popovics, S., "Concrete-Making Materials", Hemisphere Publishing Corporation, First Edition, 1979, pp. 167-192.

122. Nixon, P. J., Hardcastle, J. and Ben-Bassat M., "The effect of differences in the composition of Portland Cement on the Properties of Hardened Concrete", *Magazine of Concrete Research*, Vol. 42, No. 151, Jun. 1990, pp. 59-66.
123. Feldman, R. F., "Significance of Porosity Measurements on Blended Cement Performance", *First International Conference on The Use of Fly Ash, Silica Fume, Slag and Other Mineral By - Products in Concrete Canada*, July 31 - August 5 1983, pp. 415-433.